Alcohol and micronutrient-induced regulation of Aβ load and Tau hyperphosphorylation through modulation of mitochondrial fusion/fission pathways

Grace Ugochi Okoro

Department of Applied Sciences,

University of the West of England, Bristol.

June 2019

A thesis submitted in partial fulfilment of the requirements of the University of the West of England, Bristol for the degree of Doctor of Philosophy.

ACKNOWLEDGEMENTS

This thesis and the entire research could not have been achieved without my faith, my family, friends and supervisory team. I would like acknowledge and thank them for their help and support.

Firstly, I would like to deeply thank my director of studies, Prof Myra Conway for her tremendous support, encouragement, firmness and belief in me. Your work ethic and hard work have over these years inspired me to be a better researcher. Thank you for cheering me on when the going got though and encouraging me all the way. Thank you for the prompt feedbacks and regular meetings.

I must also thank my second supervisors, Dr Vinood Patel and Dr Bahareh Vahabi for your support and ethanol expertise, your contributions have made this possible.

A big thank you to members of Team Conway, past and present- Tom, Matt, Chris, Fred, Mai, Marcela, Jasmine, Ivo and all the masters and undergraduate students I had the pleasure of working with for making the ride smoother. Thank you to the technical team at CRIB, UWE, Bristol who helped in numerous ways-Dave Corry for training me to use the confocal microscope.

I would like to immensely thank my husband, Francis for the enormous sacrifices you made to ensure that I get all the support needed to complete the PhD and my daughters Ruby and Lily to letting mummy do some work even when you want to be cuddled 24/7.

Finally, I would like to thank my friends- Mrs Grace Oni, Lise, Marian for all the impromptu babysitting helps. Emmanuel for your constant advice and mentorship which were very useful, Paul Deane for listening to all my rants and many more (the list would be endless) who have been supportive in their own unique ways.

ABSTRACT

Introduction and aims: Alzheimer's disease (AD) has for decades been associated with increased accumulation of brain amyloid β peptides (Aβ) and phosphorylated tau. Unfortunately, targeted therapy to Aβ in particular has not been successful resulting in a diversified approach to understanding the disease pathology. Mitochondrial dysfunction is among a range of cellular and molecular processes postulated to contribute to AD, which could be a target for lifestyle factors such as alcohol and micronutrients. Ethanol-mediated neurotoxicity and its contribution to AD has in part been associated with increased oxidative stress and Aβ levels. However, conflicting reports debate whether moderate levels offer protection whereas heavy alcohol consumption accelerate cognitive decline. Similarly, micronutrient, which are essential requirements for proper growth and development can become neurotoxic when taken or when accumulated in excess. Toxic levels of Zinc (Zn) and Manganese (Mn), the focus in this thesis have both been associated with neurotoxicity and implicated in AD. To address if different levels of alcohol evoke a switch from neuroprotection to neurotoxicity and the neurotoxic impact of excessive Zn and Mn, we investigated the contribution of ethanol, Zn, Mn-induced neurotoxicity in regulating protein aggregation, Aβ, p-tau accumulation. We hypothesize using the SH-SY5Y neuronal cell model, ethanol, Zn and Mn-induced regulation of protein aggregation, Aβ, p-tau accumulation is mediated by a dysregulation of mitochondrial function and fusion/fission dynamics.

Methods: Using Western blot analysis, antioxidant proteins, fusion/fission proteins, autophagy and apoptotic markers, ERK/AKT kinases, Aβ and p-tau were assessed. Mitochondrial membrane potential (MMP) was analyzed using the JC-1 MMP assay and SOD activity using enzyme activity assay. Confocal microscopy of live cells was used to determine changes in mitochondrial morphology while fixed cells were assessed for LC3 levels. Mitochondrial respiration and function were assessed using the Seahorse Mitostress Assay.

Results: In response to toxic ethanol exposure, SH-SY5Y cells show an increase in ROS, a targeted antioxidant response, dysregulated mitochondrial dynamics and function indicated by a significant increase in fission protein, Drp1, fragmented mitochondria while decreasing fusion proteins, Opa1 and Mfn1 and decrease in mitochondrial membrane potential, low basal mitochondrial respiration and low mitochondrial ATP production. This results in shift towards autophagy/mitophagy, a switch between cell survival and toxicity linking to ERK activation and mTORC1 suppression that leads to increased apoptosis and cell death. Despite protein aggregation and Aβ increase with toxic ethanol exposure, levels of p-tau showed a dramatic decrease indicating that ethanol regulation of AD supports Aβ production rather than p-tau increase. Similar response was observed following toxic Mn and Zn levels, however cells exposed to toxic levels of Zn undergo a possible alternative pathway which is non-apoptotic.

Discussion: Together these findings have identified new and novel mechanisms by which ethanol, Zn and Mn affects mitophagy and mitochondrial fusion/fission integrity through increased ROS generation and MMP dissipation and consequent cell survival pathway response impact modulation of Aβ and p-tau, offering insight into how these pathways become dysregulated under conditions that are associated with AD pathology.

PRESENTATIONS AND PUBLISHED WORKS

Oral presentations

'Alcohol, Micronutrients and my body: Good? Not so good? Plain bad?' Postgraduate research forum 2017, University of the West of England.

Alcohol increases beta-amyloid (Aβ) load through redox-mediated dysregulation of mitochondrial dynamics, Gordon Research Seminar and Conference, Spain.

Poster presentation

Ethanol/micronutrient-induced neurotoxicity dysregulates neuronal mitochondrial dynamics, EMBO FEBS, 2017, Italy.

Publications

Okoro, G, Patel, V.B., Vahabi, B., and Conway, M.E (2019). Alcohol regulates Aβ load and Tau hyperphosphorylation through modulation of mitochondrial fusion/fission pathway (awaiting publication).

Table of Contents

Table of Figures

ABBREVIATIONS

4EBP1 Eukaryotic translation initiation factor 4E-binding protein 1

AD Alzheimer's disease

ADH alcohol dehydrogenase

Akt Protein Kinase B

ALDH acetaldehyde dehydrogenase

AMPK 5' adenosine monophosphate-activated protein kinase

APLP1 Aβ precursor-like protein

APP amyloid precursor protein

Aβ amyloid-beta peptides

BACE1 β-site APP cleavage enzyme

BSA Bovine serum albumin

CsA Cyclosporine A

CTF C-terminal fragment

CypD Cyclophilin D

DMEM Dulbeco Modified Eagle Media

DNA Deoxyribonucleic acid

ECAR extracellular acidification rate

EDTA Ethylenediaminetetraacetic acid

ERK Extracellular Signal-regulated Kinase

EtOH ethanol

GPx Glutathione preoxidase

GRX Glutaredoxin

GSH Glutathione

GSR Glutathione reductase

H_2O_2 Hydrogen peroxide

IMM inner mitochondrial membrane Drp1 Dynamin-related protein

MAPK Mitogen-activated protein kinase

MCI mild cognitive impairment

MMP mitochondrial membrane potential

MMSE mini-mental state exam

Mn Manganese

MPT mitochondrial permeability transition

MPTP mitochondrial permeability transition pore adenosine triphosphate ATP

mtDNA mitochondrial DNA

mTOR Mammalian target of rapamycin

NaCl Sodium chloride

NADH Nicotinamide adenine dinucleotide

Nrf2 Nuclear factor erythroid 2–related factor 2

OCR oxygen consumption rate ethyl alcohol EtOH

OMM Outer mitochondrial membrane

PBS Phosphate buffered Saline

PI3K phosphatidylinositol 3-kinase

PI3K Phosphoinositide 3-kinases

PINK1 PTEN-induced putative kinase 1

PSEN1/2 presenilin-1/2

PTEN Phosphatase ad tensin homolog

ROS reactive oxygen species

RTK receptor tyrosine kinases

S6K Ribosomal protein S6 kinase *beta-1*

SAM S-adenosyl methionine

SDS Sodium Dodecyl Sulphate

SE Standard Error

SOD Superoxide dismutase

TBST Tris-buffered saline and Tween-20

TEMED Tetramethylethylenediamine

TREM2 Triggering receptor expressed on myeloid cells 2

TRPM transient receptor potential melastatin

TRX thioredoxin

VDAC voltage-dependent anion channel

WKS Wernicke-Korsakoff syndrome

Zn Zinc

α7nAChR α7 nicotinic acetylcholine receptor

Chapter 1

1.0- INTRODUCTION

1.1- ALZHEIMER'S DISEASE

Alzheimer's disease (AD) is the most common type of dementia accounting for 60- 80% of diagnosed dementia cases (Neugroschl and Wang, 2011). The incidence of this disease has increased from 36 million in 2010 to a reported 50 million worldwide in 2018 (World Alzheimer's Report, 2010 and 2018) and affects mostly people aged 65 and above. There are however, cases of an earlier onset which presents in the 40s or 50s (Alzheimer's Association, 2015) and is mostly associated with a genetic predisposition. The rare early-onset AD has been linked with mutations in the amyloid precursor protein (APP), presenilin-1 (PSEN1) and presenilin-2 (PSEN2) genes, with the late-onset AD associated with an apoE variation as a major risk factor (Chouraki and Seshadri, 2014). Apolipoprotein E (ApoE) functions as a cholesterol carrier involved in the transport of lipids and brain injury repair. ApoE allele polymorphism especially in individuals carrying the ε4 allele have been associated with the strongest risk factor for AD (Liu et al., 2013). Studies have suggested that ApoE play an important role in the modulation of Aβ metabolism, aggregation and deposition with the ε4 allele being less efficient in Aβ clearance due its weaker affinity for Aβ binding compared to the ε2 & 3 alleles thereby mediating an overall gain of toxic function and loss of neuroprotective function in AD pathology (Kim et al., 2009). Therefore, age of onset and genetic factors, which represent only 1-5 % of cases, are the only known correlations with the progression of the disease. While there is the hereditary form as a result of the mutation of any of the above mentioned genes, there is also the sporadic form whose aetiology remains unknown. What is however known is that in post-mortem brains, patients present with amyloid plaques (amyloid beta- Aβ), neurofibrillary tangles

(hyperphosphorylated tau protein), severe neuronal loss and brain shrinkage (Figure 1.1).

1.1.1 AMYLOID AND TAU HYPOTHESIS IN ALZHEIMER'S DISEASE

The idea that the accumulation of Aβ peptide could be the causative factor for AD put forward by (Glenner and Wong, 1984) have been met with scepticism and over time, there have been evidences for and against this hypothesis. In support of the amyloid hypothesis are that all AD patients manifest glial and neuritic cytopathology as a result of progressive deposition of Aβ, apoE4 allele increase AD risk and decrease Aβ clearance resulting in Aβ aggregation and neuropathologies typical of AD, missense mutation of presenilin1&2, a common feature of early-onset AD increases the production of hydrophobic Aβ42/43 peptides which self-aggregate causing downstream AD pathology (Mori *et al.,* 1992, Hardy and Selkoe,2002, Selkoe and Hardy, 2016, Han et al., 2017). Despite these evidences, there are findings that appear to undermine the amyloid hypothesis such as decreased correlation between amyloid plaque burden and the degree of cognitive impairment as evidenced in mouse model (Kim *et al.,* 2007), amyloid imaging reporting the accumulation of Aβ in healthy brain and few amyloid deposits in AD brains suggesting neurodegeneration and neuronal cell loss occurs through a process independent of Aβ. There are suggestions that it is the accumulation of APP C-terminal fragment that causes phosphorylated tau accumulation and neuronal impairment (Tamayev *et al.,* 2012) with neuropathological studies suggesting neurofibrillary tangles formation may preceed amyloid plaques (Schonheit et al, 2004). Also recently considered is the inability of numerous clinical trials of anti-amyloid agents to meet their pre-specified endpoints (Mehta et al., 2017). Despite the linkage of APP with AD pathophysiology, understanding its physiological role is important in ascertaining whether a loss of function is contributory to AD pathology. Under normal physiological conditions, APP mediates developmental axonal pruning following sensory loss, neurite outgrowth, synaptogenesis and acts as a cell adhesion molecule (Marik et al., 2016). APP is cleaved by α-secretase to give rise to soluble APP (sAPPα) which play a neuroprotective role of promoting memory retention and maintaining synaptic plasticity (Zhang *et al.,* 2011). With aging or under

pathological conditions, β-site APP cleavage enzyme BACE1, the major β-secretase in the brain cleave APP yielding a large secretory APP- β (sAPPβ) and an intracellular C-terminal fragment CTF99 which is cleaved by the γ-secretase producing an APP intracellular domain (AICD), p3 and Aβ. The hydrophobic nature of Aβ peptides confer on them an intrinsic ability to self-assembly forming aggregates and different conformations like the monomeric and oligomeric forms. The monomeric forms have also been reported to bind to plasma membrane where they form an aggregate and are taken up into endocytic vesicles (Jin et al., 2016). Additionally, the oligomeric forms have been reported as capable of directly inserting into plasma membranes where they form pore-like structures that are selectively permeable to calcium causing a disruption in calcium homeostasis which leads to synaptic degeneration, memory loss and intracellular Aβ accumulation through its binding to the α7 nicotinic acetylcholine receptor (α7nAChR) (reviewed in Kayed and Lasagna-Reeves, 2013).

The tau hypothesis proposes that the abnormal phosphorylation of tau results in generation of paired helical filaments and neurofibrillary tangles (Ittner and Gotz, 2011). Tau is a natively unfolded, soluble, microtubule-associated protein of mature neurons which facilitate stabilisation of axonal microtubules, polymerisation and assembly. On its own, tau protein normally show little tendency for aggregation and have been described as being preferentially located at neuronal axons where it undergoes posttranslational modifications such as glycosylation, phosphorylation, oxidation, glycation and cross-linking which contribute to its microtubule stabilizing attribute with tau phosphorylation being the most widely studied. Tau phosphorylation sites involve those that can be modified by proline directed kinases such as GSK3, tau protein kinase II (cdk5), MAP kinase, JNK and those modified by non-proline directed kinases such as protein kinase A, C, calmodulin kinase II. This process regulates its binding to microtubules acting as the major regulatory mechanism of tau function (Avila et al., 2004). The binding affinity of tau to microtubules, major neuronal transport system places tau as a central focus in the facilitation of molecular movements within the axon (Kopeikina et al., 2012). In normal physiological conditions, tau function is maintained by a balance between the

activities of these kinases and tau-directed phosphatases - PP2A and PP1. Under pathological conditions such as AD, it is proposed that a shift in balance elicits tau hyperphosphorylation, resulting in decreased affinity between tau and the microtubules thus affecting its function as a stabilizer with GSK3 majorly implicated. It is also proposed that an accumulation of misfolded hyperphosphorylated tau leads to the formation of toxic oligomeric neurofibrillary tangle suggested to be as a result of a loss of function and gain of toxic function of tau (Pirscoveanu et al., 2017, Bejanin *et al.,* 2017). In frontotemporal dementia, another neurodegenerative condition, tau mutations and an impairment of its microtubule-stabilising capacity leads to tau aggregate formation and an increase in the mutated and hyperphosphorylated form over normal tau (Yamada *et al.,* 2015), correlating well with disease progression and cognitive decline (Rademakers et al., 2004). To enable ease of description for disease process progression, the Braak staging of AD-related neurofibrillary pathology was performed on neuronal sections and largely involved scoring the topographic expansion of lesions consisting of hyperphosphorylated tau protein, neurofibrillary tangles and neurophil threads deposited within specific neurons at specific sites (Braak et al., 2006). Furthermore it is thought that tau aggregate formation in cells is enhanced by the extracellular domain of APP which act as a receptor enabling tau fibril incorporation into cells (Takahashi *et al.,* 2015) suggested to be through 5' adenosine monophosphate-activated protein kinase **(**AMPK) at Ser422 happening late in the disease process (Mairet-Coello *et al.,* 2013) revealing that although the accumulation of Aβ is considered the starting point of AD, tau hyper-phosphorylation mediates the processes that lead to disease progression (Figure 1.2). Hyper-phosphorylated tau accumulates in neuronal cells and disrupts neuronal function, reducing mitochondrial respiration and membrane potential (Eckert *et al.,* 2010).

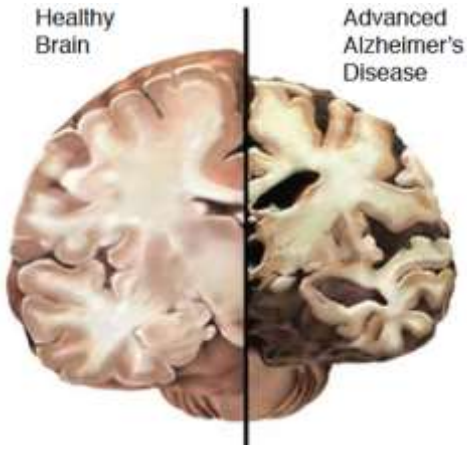

Figure 1.1- Representation of a healthy brain compared to an AD brain. The general neuronal loss and shrinkage distinguishing healthy brain from AD brain with the smaller size of the AD brain is also accompanied by atrophied grooves and folds at the outer layer and larger ventricles (Kidd, 2008).

These findings led to the development of two so-called fundamental hypotheses thought to underpin the pathogenesis of AD, (1) the amyloid hypothesis and (2) the tau hypothesis.

Overall despite the evidence in support of these hypotheses, drugs targeted towards amelioration of Aβ aggregation have not been effective, therefore the need for more focus on therapies targeted at tau aggregation and accumulation as evidence from AD mouse models expressing human APP suggest that a reduction in endogenous tau levels prevented Aβ–induced memory impairment (Roberson *et al.,* 2007).

1.1.2- OTHER AD RISK FACTORS

Individuals carrying the Apo ε4 allele have been reported to be at increased risk for AD compared to their counterparts carrying Apo ε3 allele and is linked to age-related cognitive decline (Liu *et al.,* 2013). ApoE isoforms have been suggested to regulate Aβ aggregation and tau-mediated neurodegeneration (Shi *et al.,* 2017) with impairment in ApoE function implicated in Aβ clearance (Robert *et al.,* 2017).

Triggering receptor expressed on myeloid cells 2 (TREM) expressed on microglial membrane and resultant neuroinflammatory response have been

reported to promote tau-dependent neurodegeneration. Experiments with ApoE lacking mice and TREM2 deficiency showed reduced neuroinflammation thereby protecting against neuronal cell damage (Leyns *et al.,* 2017, Ulland *et al.,* 2017).

1.1.3- ALZHEIMER'S DISEASE: CURRENT THINKING

Beyond the traditional and most commonly held views about the aetiology of AD (Aβ cascade and phosphorylated tau), recent research now involves a diversification in approach to better understand the mechanism that underlies the disease manifestation. This has been necessitated by recent failures of anti-amyloidogenic trials supporting the stance that the pathomechanism recognised to trigger familial AD does not necessarily mean a direct correlation to sporadic cases. Although there are increasing number of AD drugs in trial phases, the trials have been marked with continuous failures with the CREAD 1 & 2 (a Roche-sponsored clinical research study of drugs targeted at plaques and other AD proteins) at phase III trial stage being discontinued very recently (https://www.biospace.com/article/a-long-line-of-failures-roche-drops-alzheimer-s-drug-trials/). Although Aβ generation and processing is a prominent feature of AD, it is not exclusive. As reviewed by Wang *et al.,* (2017), it is currently proposed that there are associations and links between the abnormalities at systemic levels and Aβ production/metabolism and that the manifestation of these abnormalities underlie the disease process. The interactions between the brain and the peripheral body systems have a huge role to play in the changes associated with the progression of AD (Kozlov *et al.,* 2017).

Several scientific experiments to challenge the status quo have put forward the postulation that based on current knowledge; there are a range of cellular and molecular processes that contribute to the pathology of AD. These processes include cell cycle events, alterations in lipid metabolism, tau biochemistry, autophagy, protein misfolding, and neurotransmitter metabolism, mitochondrial dysfunction, vascular dysfunction and inflammatory processes (Behl and Ziegler, 2017).

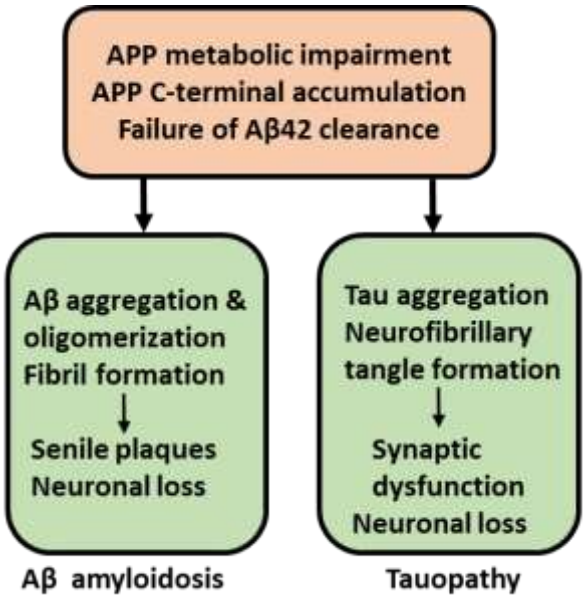

Figure 1.2- Proposed order of major pathogenic processes leading to AD. Impairment of APP metabolism and accumulation of APP c-terminal fragments trigger tau pathology leading up to disease progression, neuronal loss and cognitive function decline (Adapted from Kametani and Hasegawa, 2018).

1.1.4- DYSFUNCTIONAL MITOCHONDRIA: NEW AD TARGET

The mitochondrion, an important organelle and a pivotal point when considering the free radical theory of aging have been proposed to play an important role in AD pathology because it is both the main source of energy production and reactive oxygen species (ROS) generation in cells (Grimm and Eckert, 2017). There is a growing body of experimental evidence reflecting a disturbance of neuronal mitochondrial bioenergetics/dynamics and transportation/distribution during aging and oxidative stress conditions (Amadoro *et al.,* 2014). As a result, deficient antioxidant defense mechanisms and a simultaneous increase in oxidative stress contribute to cell death (Rebrin *et al.,* 2007, Pandya *et al.,* 2013).

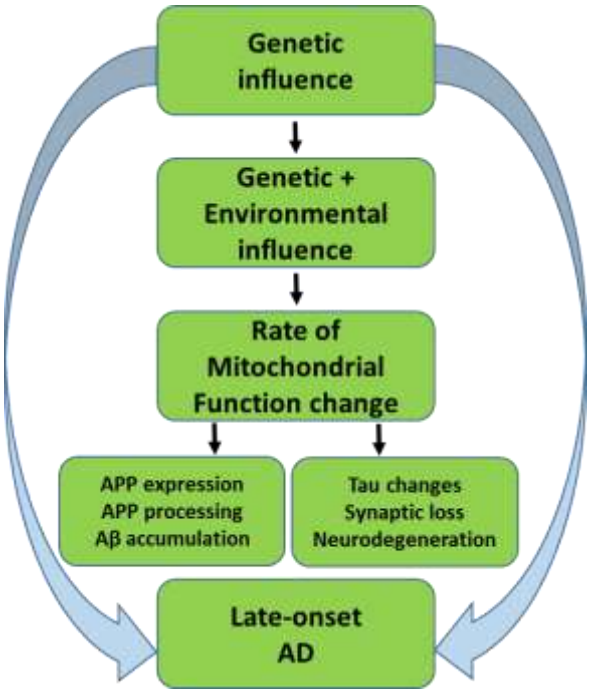

Figure 1.3- Proposed mitochondrial cascade hypothesis. This hypothesis maintain mitochondrial function is genetically determined and decline with the aging process. A threshold of mitochondrial decline over time is surpassed which triggers AD associated symptoms such as APP expression, processing and Aβ accumulation all eventually contributing to late-onset AD. Adapted from Swerdlow et al., 2014.

A mitochondrial cascade hypothesis has been postulated implicating this organelle as a target for late-onset sporadic AD (Figure 1.3). The hypothesis infers firstly that individual baseline mitochondrial function, which includes rate of ROS and mitochondrial damage accumulation, is genetically determined with more maternal contribution due to pattern of mitochondrial DNA inheritance. Secondly, in addition to genetic input, environmental factors such as alcohol and toxic metals also contribute to mitochondrial changes associated with the aging process and lastly, an individual's baseline mitochondrial function and function change rate will influence their sequence of AD onset by affecting APP expression, processing and Aβ accumulation (Swerdlow *et al.,* 2014). Linking AD to mitochondrial function lends support to the suggestion that there is a general decline in mitochondrial function as aging progresses and that adequate or inadequate compensation determines the manifestation of symptoms (Navarro and Boveris, 2007). Recent studies suggest that Aβ plaque formation precedes clinical AD manifestation

supposedly up to a decade (Jack *et al.,* 2011). Mitochondrial cascade and Aβ accumulation hypothesis propose that as aging-dependent mitochondrial decline starts, bioenergetics is stimulated to enable compensation in neurons leading to a rise in Aβ production and accumulation, which coincides with the asymptomatic phase of compensated brain aging. Following further mitochondrial decline as brain aging continues, bioenergetic compensation is no longer sustained for leading to a decline in Aβ accumulation and AD symptom manifestation (Swerdlow, 2014).

1.2- MITOCHONDRIAL FISSION/FUSION

Under normal physiological conditions, mitochondrial homeostasis is maintained through the regulation of the mitochondrial quality control mechanism-fission/fusion dynamics, mitochondrial biogenesis and mitophagy. The fission/fusion dynamics is a tightly regulated and important mechanism for maintaining mitochondrial quality control. In mitochondrial fission, the organelle components are split into 2 daughter mitochondria whereas the merging of 2 daughter mitochondria is fusion. In the event of increased fission, there is fragmentation characterised by small round-shape mitochondria that are poorly connected while in fusion, mitochondria is characterised by elongated and high connectivity (Shirihai *et al.,* 2015). Mitochondrial fission is regulated by the GTPase protein Drp1 (Onyango *et al.,* 2016) while mitofusins Mfn1 & 2 control mitochondrial fusion at the outer mitochondrial membrane (OMM) level and Opa1 at the inner mitochondrial membrane (IMM) level (Tilokani *et al.,* 2018). The fission-mediating Drp1 act similar to dynamin by assemblying into spirals around the neck of endosomes constricting lipid tubules and twisting following GTP cleavage. This assembly at division sites around the OMM drives the fission process and involves actin filaments and microtubules. Fusion on the other hand is mediated by the C-terminal coiled regions of Mfn 1 and Mfn2 which bring about a tethering between mitochondria through the formation of heterotypic or homotypic complexes between adjacent mitochondria (Suen et al., 2008). Dysregulation of this pathway is associated with various pathophysiology with mitochondrial fission linked to mitochondrial dysfunction, increased oxidative stress and cell death (Zemirli *et al.,* 2018). Increased expression of Drp1 and mitochondrial fragmentation, loss

of mitochondrial membrane potential (MMP) and ATP production, increased oxidative stress are all associated with AD (Wang *et al.,* 2009) which overtime overpowers the mitochondrial fusion-mediated repair leading to selective mitochondrial degradation-mitophagy (Martinou and Youle, 2011). Using double-labeling immunofluorescence and immunoprecipitation analysis in AD brain and 3xTg.AD mouse, Drp1 have been shown to interact with major AD hallmarks, Aβ and phosphorylated tau. Increased mitochondrial fission and interaction of fission protein Drp1 with Aβ and phosphorylated tau which leads to an increase in mitochondrial fragmentation and a decrease in mitochondrial fusion have been reported in AD neuronal cells (Manczak and Reddy, 2012). Mitochondrial biogenesis and degradation is another key regulator of mitochondrial dynamics. Both processes are stimulated and regulated by several factors with the stress response playing a major role in its regulation. Kinases such as AMPK, mTOR kinases and the transcription factor Nrf2 are involved in mitobiogenesis. In response to stress, mitobiogenesis is increased to compensate for and restore the effect of an increase in the degradation of damaged mitochondria or for an overall improvement in mitochondrial function (Zong *et al.,* 2002, Dorn *et al.,* 2015).

In addition to their role in energy metabolism of the cell, the mitochondria also play a role in the regulation of apoptosis upstream of caspase activation. This physiologic phenomenon can be mediated via the modulation of calcium Ca^{2+} signalling and intrinsic signals such as DNA damage, kinase inhibition ischemia and oxidative stress (Jeong and Seol, 2008). The Bcl-2 family members and Bax protein, the two widely studied apoptosis-mediating factors upon receiving cell death stimuli translocate to the mitochondria from the cytosol where they induce the release of apoptogenic mitochondrial proteins such as cytochrome c (cyt c). p53 and TR3 are transcriptional activators respond to DNA damage by targeting the mitochondria. p53 activate caspases through apoptotic protease-activating factor Apaf-1/caspase 9 pathway independent of cyt c release whereas TR3 triggers the release of cyt c. Apaf-1 protein is hydrolysed in the cytosol resulting in a conformational change that allows it to bind cyt c at the same time undergoing oligomerisation. Apaf-1 oligomerisation results in the exposure of its caspase-recruitment domain (CARD) allowing it to bind procaspase-9 resulting in subsequent release of

active caspase-9 which activate other downstream caspases such as caspase-3, 7 and 7 (Parone et al., 2002). As cyt c is released, the mitochondria fragments into smaller units. Inhibiting this fission process inhibits the release of cyt c thereby delaying cell death (Suen et al., 2008)

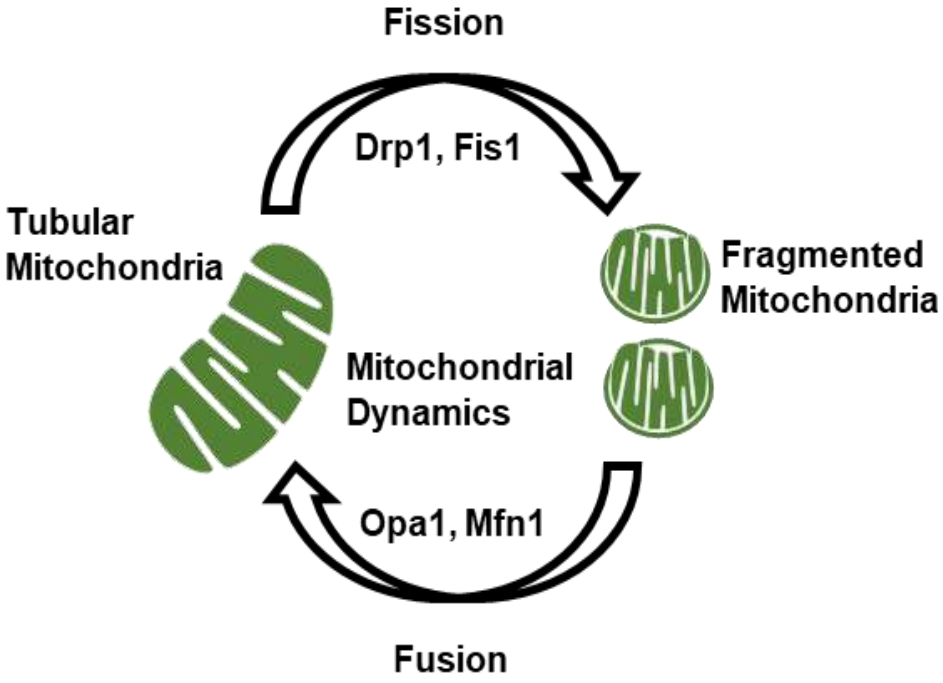

Figure 1.4- Mitochondrial dynamics. Under physiological conditions, mitochondrial dynamics homeostasis is maintained by constant fusion and fission events. In stress conditions, fission results in small rounded mitochondria and fusion form elongated tubular networks (Adapted from Balog et al., 2016).

The removal of damaged mitochondria is enhanced by fission as this process reduces the mitochondrial size and cause a loss of membrane potential while also differentiating dysfunctional parts of the mitochondrial network enabling its removal (Lemasters, 2014). Mitophagy, a selective form of autophagy involves the selective engulfment of damaged/dysfunctional mitochondria by autophagosomes for degradation and recycling. ROS generation has been implicated as a trigger for mitophagy activation (Kim *et al.,* 2007). In mitophagy,

PTEN-induced putative kinase 1 (PINK1), which accumulates on damaged OMM recruits parkin which ubiquinates OMM proteins resulting in p62-LC3 interaction which triggers autophagosomal clearance of damaged mitochondria (Onyango *et al.,* 2016). Studies have reported impaired mitophagy in AD leading to accumulation of dysfunctional mitochondria alongside an increase in oxidative stress (Ashrafi and Schwarz, 2015).

An additional aspect that can undergo changes in response to oxidative stress is the mitochondrial membrane potential (MMP). The mitochondrial permeability transition pore (MPTP) is an inner mitochondrial membrane channel known to open following high levels of calcium in the mitochondrial matrix leading to the collapse of MMP and swelling of mitochondrial matrix (Elrod and Molkentin, 2013) and comprise of the voltage-dependent anion channel (VDAC), ANT and Cyclophilin D (Cyp D). A loss of MMP impacts ATP production (Martinez-Reyes *et al.,* 2016). Cyp D has been implicated as the most critical regulator of MPTP, playing a protective role in cell apoptosis and necrotic death. (Schinzel *et al.,* 2005). Cyclosporine A (CsA), generally used as an immunosuppressant desensitizes the MPTP has the ability to bind and inhibit Cyp D (Giorgio *et al.,* 2010). In human studies, CsA has been shown to normalize dysfunctional mitochondria and reduce apoptotic frequency in patients with skeletal muscle diseases (Merlini *et al.,* 2008). Nevertheless, on its own CsA at a concentration of 1 to 10µM, CsA has been shown to significantly increase ROS intracellularly (Chen *et al.,* 2002). CsA was included in this study especially in mitochondrial dynamics and function investigation, to harness its protective potential from ethanol, zinc and manganese-induced oxidative stress.

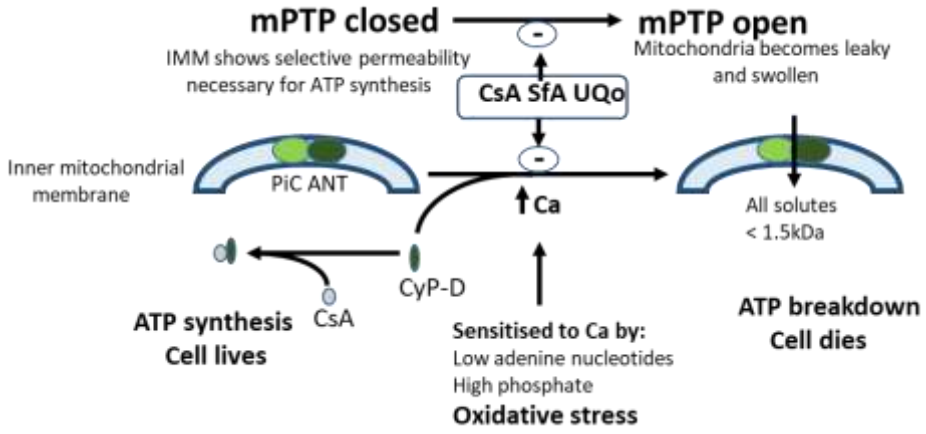

Figure 1.5- Cyclophilin D regulation and the mitochondrial permeability transition pore (MPTP). Several components of the IMM and OMM combine to make up the MPTP. All solutes ≤1.5 kDa cross the IMM giving rise to organelle swelling and rupture, a key factor in necrotic cell death. The negative MMP cause calcium efflux into the mitochondrial matrix. ROS increases MPTP opening while ATP inhibits the pore formation. CypD inhibition using CsA will cause an increase in ATP synthesis and prevent cell death. PiC- mitochondrial phosphate carrier, ANT- adenine nucleotide translocase, sfA- sanglifehrin A, UQo- ubiquinone (Adapted from Halestrap and Pasdois, 2009).

1.3- ETHANOL METABOLISM AND ROS GENERATION

Alcohol is a widely consumed substance with numerous profound effects on the body particularly the nervous system (Imam 2010). Alcohol metabolism occurs via by two main pathways, the oxidative and non-oxidative pathway (Figure 1.6). The oxidative pathway of alcohol metabolism is catalysed by alcohol dehydrogenase (ADH), cytochrome P450 2E1 and catalase in the cytosol, peroxisome and microsomes respectively (Zakhari, 2006).

The oxidative pathway of alcohol metabolism involve ADH oxidizing alcohol to acetaldehyde, a toxic product in the cytosol accompanied by NAD^+ reduction to NADH. Acetaldehyde is oxidised to acetate in the mitochondria with NAD^+ reduction to NADH catalysed by acetaldehyde dehydrogenase (ALDH) (Cederbaum, 2012). During sustained alcohol consumption at high levels, the cytosolic route of alcohol metabolism is increased but only to a limited extent therefore increase in CYP2E1-mediated alcohol oxidation is activated for enhanced alcohol clearance giving rise to the production of ROS and NAD^+ reduction to NADH. Increase NADH/NAD^+ ratio in the cytosol and mitochondria

leads to the perturbation of carbohydrate, protein, lipid metabolism via protein carbonylation and lipid peroxidation, mitochondrial permeability transition (MPT) and gene expression modulation, cell death, ROS and acetate formation (Zakhari, 2013). Mitochondrial permeability transition and mitochondrial membrane potential are affected following ethanol metabolism causing specific pores to open, resulting in swelling and eventual apoptosis (Alano *et al.,* 2004). In acute alcohol ingestion, there is an increase in brain acetate uptake as an alternative energy source (Volkow *et al.,* 2013).

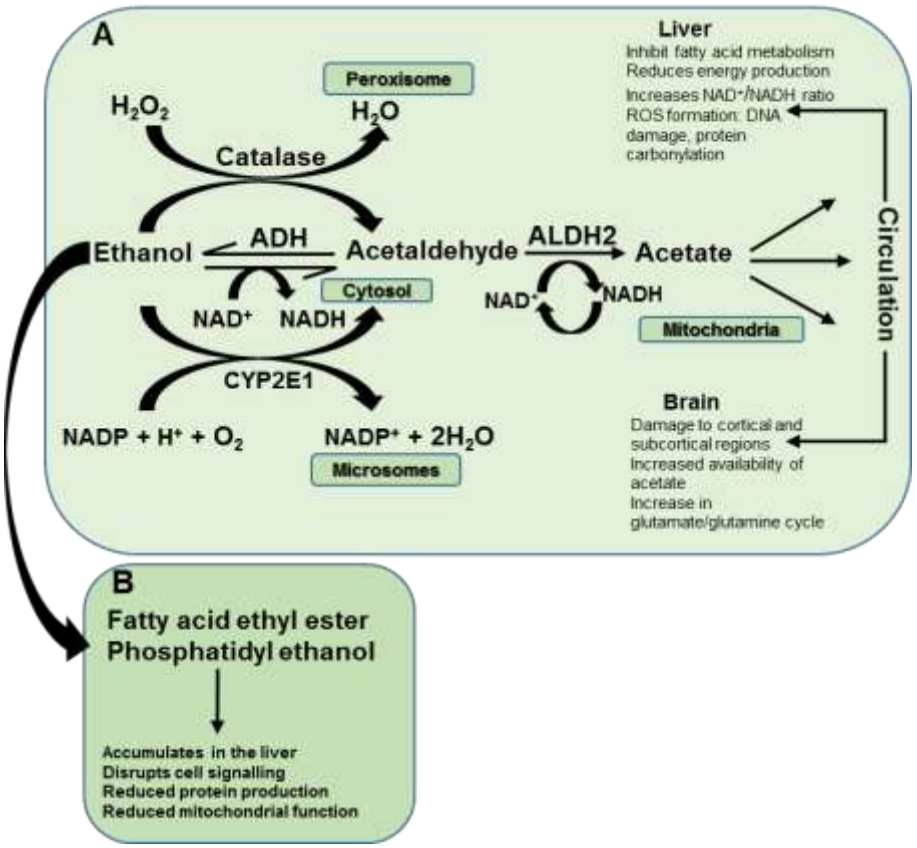

Figure 1.6- Oxidative and non-oxidative pathway of alcohol metabolism. The oxidative pathway is catalysed by ADH, CYP2E1 and catalase in the cytosol, microsomes and peroxisome respectively. Acetaldehyde is oxidised by ALDH to acetate accompanied by an increased NADH/NAD^+ ratio (A). The non-oxidative pathway is considered as minor under normal conditions and gives rise to the products, FAEE and phosphatidyl ethanol both of which accumulates in the liver and disrupts cell signalling due to their poor metabolism (B) (Cederbaum, 2012, Zakhari, 2013).

Also associated with chronic alcoholism is inflammation, vitamin malabsorption, altered methionine metabolism, glutathione depletion, DNA damage and cognitive defect. Methionine is activated to S-adenosyl methionine (SAM), which donates its methyl group and is converted to S-adenosylhomocysteine which is hydrolysed to homocysteine and reduced to glutathione (GSH) through the transsulfuration pathway. Alcoholic liver injury induces alteration in methionine metabolism resulting from decreased transmethylation and transsulfuration depleting GSH thereby increasing oxidative stress (Figure 1.7). The non-oxidative pathway is not very prominent under normal conditions but gives rise to fatty acid ethyl ester and phosphatidyl ethanol which can accumulate in the liver disrupting cell signalling (Nassir and Ibdah, 2014).

Although the main intracellular source of ROS is the mitochondrial ETC, ethanol metabolism also promotes ROS generation and oxidative stress from enzymatic activation of CYP2E1 and NADPH oxidases, resulting in mitochondrial function impairment further aggravating ROS generation and oxidative stress with a resultant vicious cycle that activate MPT and increase cell susceptibility to apoptotic signals. In more recent studies, mitochondrial dysfunction have been explored as an AD target and because ethanol metabolism increase ROS generation and mitochondrial dysfunction, therefore this thesis focus on the impact of ethanol, Zn and Mn on ROS signalling, its impact on mitochondrial dynamics and function in SH-SY5Y neuronal cells.

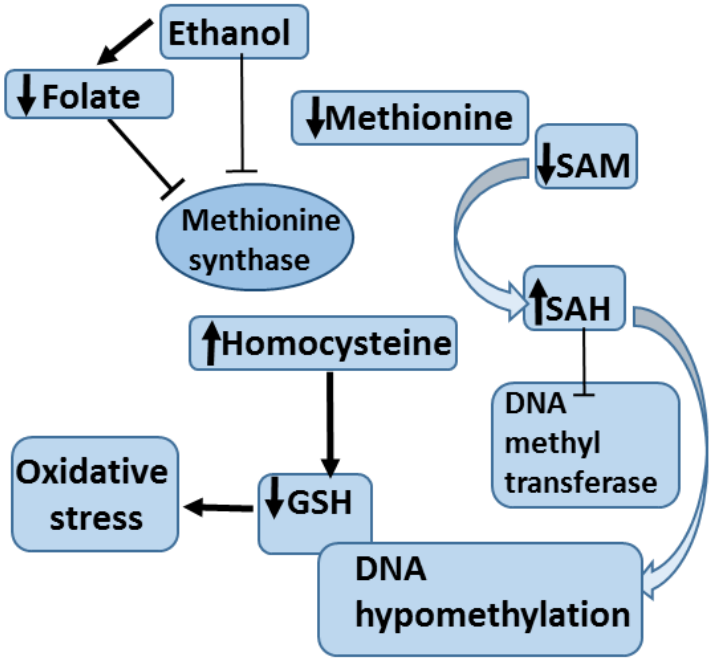

Figure 1.7- Chronic alcoholism alters methionine metabolism. Chronic drinking reduces folate level and inhibit methionine synthase. This gives rise to DNA hypo methylation as a result of DNA methyl transferase inhibition and oxidative stress from GSH depletion.

1.3.1- ETHANOL AND MITOCHONDRIAL DYNAMICS/ BIOENERGETICS

Ethanol metabolism generate ROS and diminish the cell's antioxidant system, resulting in mtDNA damage, mitochondrial function impairment, further ROS generation perpetuating a vicious cycle (Hoek *et al.,* 2002).

Oxidative stress as a major factor has been shown to elicit differing response from the fusion/fission pathway implying an association between ethanol-induced ROS generation and mitochondrial dynamics disruption. ROS have been shown to mediate dysregulation of mitochondrial fission and fusion as seen in cerebellar granule neurons where ROS generation resulted in extensive mitochondrial fusion thereby increasing Mfn2 expression and protecting the cells from apoptotic death (Jahani-Asl *et al.,* 2007).

Similarly ethanol-induced disruption of mitochondrial dynamics and function in ARPE-19 epithelial cell line indicated by dose dependent increase in mitochondrial fission via activation of DRP1 and proteolytic cleavage of OPA1 (Bonet-Ponce *et al.,* 2015), there are however limited studies on the effect of ethanol on fusion/fission dynamics especially in SH-SY5Y neuronal cells.

1.3.2- ETHANOL AND THE RAS/ERK SIGNALLING PATHWAYS

ROS acts as a signalling molecule that induces activation of the RAS/ERK pathway to enhance cell survival in oxidative stress conditions. The schematic diagram (Figure 1.8) highlights kinases of these pathways important cellular role such as cell growth, differentiation, survival and death (Ravingerova *et al.,* 2003) with protein synthesis, autophagy and apoptosis similarly activated by binding of growth factors to PI3K receptors leading up to Akt and mTOR activation (Abraham and O'Neill, 2014).

Ethanol exposure to cells elicits a series of effects on intracellular signalling pathways enabling neuroadaptation to repeated ethanol exposure. Several studies have highlighted how ethanol alter signalling pathways involving different kinases among which are ERK, MAPK, AKT, MTORC1 and S6K (Ron and Messing, 2013). These pathways are important for cell survival following oxidative stress conditions. Acute exposure to 100 mM ethanol in cortical cell culture was shown to inhibit phospho-ERK activation with similar effects in the cortex, hippocampus and cerebellum of the brain (Chandler and Sutton, 2005). Similarly, AKT phosphorylation have been reported in the medial prefrontal cortex of rats exposed to acute ethanol (Neznanova *et al.,* 2009) and in juvenile rats following a 48-hr ethanol exposure (Yang *et al.,* 2017). In PC-12 neuronal cells, acute ethanol exposure increase AKT phosphorylation (Liu *et al.,* 2017) suggesting that the ERK/AKT pathways mediates the ethanol-induced neurotoxicity and in a bid to activate survival mechanisms. mTORC1 signalling pathway responds differently to ethanol exposure in a cell-specific manner but largely function as a protective mechanism in oxidative stress conditions. Phosphorylation of mTORC1 and its substrates S6K and 4EBP1 have been reported in the nucleus accumbens of mice with excessive ethanol consumption history (Neasta *et al.,* 2010, Beckley *et al.,* 2016). The inhibitory action of ethanol on mTOR has been described as ethanol being similar to pharmacologic mTOR inhibitors, however, there is only a partial inhibition of mTOR signalling following ethanol administration in B-cell lymphoma in comparison to complete inhibition by INK128, an active-site mTOR inhibitor (Mazan-Manmczarz *et al.,* 2015).

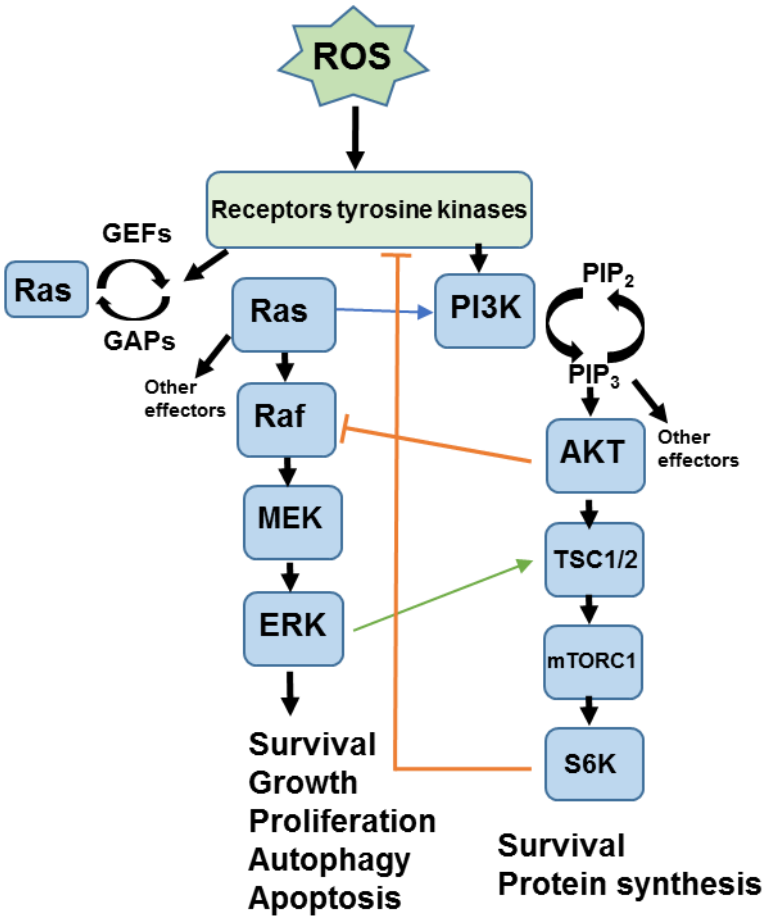

Figure 1.8- Activation of PI3K/MAPK pathways. Both pathways are interconnected leading to activation or inhibition at different points under certain conditions. PI3K-coupled receptors were activated by Ras, receptor tyrosine kinases (RTK) direct binding and ROS transduces signal to different downstream effectors-AKT, mTORC1, S6K, activating pro-cell survival or death downstream effects such as autophagy, apoptosis, protein synthesis and cell proliferation (Adapted from Lei and Kazlauskas, 2009).

1.3.3- ETHANOL-INDUCED NEUROTOXICITY

The Central Nervous System (CNS) requires and consumes high amounts of oxygen, has lower levels of antioxidant enzymes and is more susceptible to oxidative stress, therefore require strict ROS homeostasis (Cohen-Kerem and Koren, 2003). Excessive alcohol consumption has many detrimental

neurological effects which include increased oxidative stress, mitochondrial dysfunction and cell death (Reddy *et al.,* 2013). The impact of ethanol on its targets produce both acute and chronic toxic effects resulting from its metabolism, with acetaldehyde, one toxic metabolite particularly implicated in non-specific protein and DNA modifications (Wallner and Olsen,2008). Ethanol interact with and potentiates γ-aminobutyric acid $(GABA)_A$ and glycine receptors GlyR while inhibiting glutamate and N-methyl-D-aspartate (NMDA) receptors in neurons and synapses throughout the brain depending on the exposure level, resulting in suppression of neuronal synaptic communication giving rise to the intoxication symptoms that ensue and in some cases withdrawal anxiety-like behaviour (Abrahao et al., 2017).

At different regions of the brain, varying effects are observed most especially affecting cognitive function and morphology (Fadda and Rosetti, 1998). Ethanol neurotoxicity results in general brain shrinkage, significant reduction in white matter (Kril *et al.,* 1997) diminished brain volume and remarkable cell loss (Pitel *et al.,* 2012). The frontal lobe is characterised by cortical atrophy, ventricular enlargement, meningeal thickening accompanying cell loss and hippocampal bilateral volume deficits evidenced from microscopic analysis (Moselhy *et al.,* 2001). Studies have shown that ethanol also affects the maturation of neurons by impacting on their differentiation. It does this by altering the membrane proteins and cytoskeleton involved in synapse maturation as well as inducing neuronal apoptosis (Guadagnoli *et al.,* 2016). Ethanol exposure to the hypothalamic region of rat foetal brain was shown to increase cellular apoptosis. Ethanol activates microglia together with cytokine release resulting in neuroinflammation which enhance apoptosis due to an increase in microglial-derived factors (Boyadjieva and Sarkar, 2013). Neuroinflammation following microglial activation mediate ROS generation which play a signalling role influencing cell survival by the activation of the gene expression kinase pathways (Rojo *et al.,* 2014). Ethanol metabolism also target astrocytes, oligodendrocytes and synaptic terminals within the nervous system impacting functions such as neuronal survival and cell migration (de la Monte and Krill, 2014).

There have been suggestions over the years to the protective effect of low and moderate alcohol consumption on cognitive function. While some studies suggest neuroprotective effects (Zuccala *et al.,* 2001, Galanis *et al.,* 2000), others show no significant benefit at all (Huang *et al.,* 2002) resulting in a rather inconclusive perception. Several studies have engaged differing approaches to define alcohol levels considered low, moderate or excessive with some relating this to blood alcohol level (Getachew *et al.,* 2018). In human drinkers, 8 or more alcoholic drinks per week have been considered heavy or excessive drinking while 1-7 drinks per week is considered mild to moderate drinking (Heymann *et al.,* 2016). This is considered as 1-<7 units per week (light), 14-21 units per week (moderate) and > 30 units per week (heavy/excessive) drinking (Topiwala *et al.,* 2017). Experimental studies in SH-SY5Y cells have considered 500 mM ethanol exposure as relatively high hence represent heavy or excessive alcohol exposure with 10 mM considered low alcohol level (Getachew *et al.,* 2018, Ramlochansingh *et al.,* 2011). In human endothelial cells, 17.1 mM ethanol concentration was considered low level exposure (Grenett *et al.,* 2000).

1.3.4- ETHANOL, MCI AND ALZHEIMER'S DISEASE

Ethanol consumption has been associated with a wide range alcohol related brain damage with Wernicke-Korsakoff syndrome (WKS) representing an extreme case. (Venkataraman *et al.,* 2017). WKS occur from a combination of chronic alcoholism and thiamine deficiency (Day *et al.,* 2013) and is shown via MRI to cause lesions in the mammillary bodies and periventricular areas and volume deficits of the hippocampus, thalamus, cerebellum and pons (Zahr *et al.,* 2009). The pathobiology of this syndrome is however different from that of AD as thiamine administration is a potent treatment strategy in the acute phase of WKS (Day *et al.,* 2013).

Although AD is associated with age-related cognitive decline, not all memory complaints are presumed to be indicative of AD as some are associated with the normal aging process. There is however a staging of mild cognitive impairment (MCI) where an individual is cognitively impaired memory-wise

relative to age expectation but do not meet the criteria for clinically-determined AD (Kelley and Petterson, 2007). There is an effort to develop a tool for accurately predicting progression from MCI to AD. However, female MCI patients with abnormal CST tau levels, lower mini-mental state exam (MMSE) score, hypertension, atrophy of the medial temporal lobe and hippocampus had a high risk of progressing to AD (Li *et al.,* 2016).

Mild to moderate alcohol consumption have been linked to a decreased risk of dementia and other cognitive impairments and heavy alcohol use associated with increased risk of dementia and severe cognitive impairments (Rehm *et al.,* 2019). A population-based study over a 43-year period have shown no difference between non-drinkers and light drinkers with respect to dementia predisposition. On the other hand, heavy drinking has been associated with an increase in the predisposition to dementia risk with a stronger link to spirit consumption relative to wine (Handing *et al.,* 2015). A cohort study of 360 patients over 19 years have shown that heavy drinkers had a faster decline in cognitive abilities as evidenced by a deteriorating MMSE score compared to the abstainers or moderate drinking counterparts with hard liquor associated with a faster decline rate (Heymann *et al.,* 2016). MCI patients with moderate alcohol consumption have been reported to present a lower rate of AD progression, with moderate wine consumption showing an even significantly lower rate of disease progression compared to abstainers (Solfrizzi *et al.,* 2007). MCI patients who were light drinkers were shown to have better MMSE scores (Xu *et al.,* 2009) and moderate drinking in AD patients reported to slow cognitive decline rate (Heymann *et al.,* 2016), however a cohort study have reported that even at moderate alcohol consumption, hippocampal atrophy results (Topiwala *et al.,* 2017).

Using animal models, moderate ethanol consumption (10 and 50 mM) has been shown to have a potential for protection from Aβ toxicity while improving memory and cognitive functions in 3xTgAD mice (Munoz *et al.,* 2014). In the 3xTgAD mice, ethanol binding to fibrillary Aβ caused a destabilisation of Aβ oligomers into monomers thereby preventing neuronal membrane disruption and increased intracellular calcium concentration which would have otherwise occurred with resulting synaptic failure (Munoz *et al.,* 2014). An *in vitro* study

of 10 mM ethanol exposure to Aβ decreased its toxicity by disrupting the critical salt bridge between residues Asp 23 and Lys 28, an important step for Aβ dimerization which correlates with Aβ toxicity (Ormeno *et al.,* 2013). 'Moderate ethanol preconditioning' phenomena (a case of prolonged moderate alcohol intake) with 20-30 mM ethanol in hippocampal slice culture was shown to prevent Aβ-induced neurodegeneration by suppressing pro-inflammatory mediators and increasing the molecular chaperone hsp70 (Belmadani *et al.,* 2004).

Neuroinflammation, a characteristic feature of alcohol consumption is closely associated with aggravated amyloid pathology (Karuppagounder *et al.,* 2009). Emerging experimental evidence not only suggests a link between AD progression and neuroinflammation, but propose that neuroinflammation is a potential event that drives AD pathogenesis (Heppner *et al.,* 2015). Activation of microglial cells are differentially perpetuated by different forms of Aβ leading to inflammatory cytokine release pushing further aggregation of Aβ required for plaque formation. This is a self-driven cycle that leads on to neurodegeneration and cell death (Heurtaux *et al.,* 2010, Wu *et al.,* 2000). Alcohol directly or indirectly contributes to this cycle by stimulating TLR2/4 production causing a greater amount of inflammatory cytokine release (Venkataraman *et al.,* 2017).

1.3.5- AUTOPHAGY AND MITOPHAGY

Autophagy and mitophagy are regulated through crosstalk between key signalling pathways governed by the mammalian target for rapamycin (mTORC1) and the Ras/Erk pathway. Autophagy is a self-degrading process that play a housekeeping role geared towards clearing damaged organelles, intracellular pathogen and removal of misfolded or aggregated proteins. This process is either selective or non-selective in the removal of specific organelles. The three forms of autophagy- macro, micro and chaperone-mediated autophagy (CMA) all function to promote degradation of cytosolic contents at the lysosome (Glick et al., 2010). In macro-autophagy, the content to be degraded are delivered through the autophagosome, a membrane-bound vesicle which binds to a lysosome forming an autolysosome and directly engulfed by the lysosome in micro-autophagy and delivered to the lysosome

bound to a chaperone such as Hsc-70 in CMA. The autophagy process begins with phagophores expansion to engulf cytosolic cargo sequestrating them in a double-membraned autophagosome which fuses with the lysosome which releases lysosomal acid proteases which degrade the autolysosomal conent. The resultant by-products such as amino acids are transported into the cytoplasm where they are re-used to build macromolecules making autophagy a cell recycle factory promoting energy efficiency of the cell (Axe et al., 2008). At the molecular level, phagophore formation is regulated by the activity of Atg1 kinase complex with Atg 13/17 alongside Vps34 and Beclin followed by Atg5-Atg12 conjugation, phagophores multimerisation and interaction with Atg16L, LC3 processing and insertion into the membrane of extending phagophores, capture of targets for degration and fusion of the autophagosome with lysosome leading to protease-mediated degradation. This pathway is regulated by signalling pathways such as stress signalling kinases in the cells like JNK-1 and the mTOR kinase. The mTOR kinase mediates autophagy via the inhibition of ATG1/Ulk-1/2 when pahagophore formation is at its earliest phase while JNK-1 mediates autophagy process by phosphorylation Bcl-2 and enhancing Beclin-1 ability to bind with VPS34 (Wei et al., 2008). Autophagy induction is also mediated by hypoxia, nutrient starvation and low cytosolic ATP levels and inhibited by increased growth factor signalling. In neuronal cells, there is a hypothesis that biosynthesis of autophagosomes are normally maintained at a low level despites changes in nutrient availability due to the neuron's ability to maintain normal neuronal function using several energy sources (Nixon et al., 2005). A counter hypothesis proposes that the low level of basal autophagy is due t the neuron's efficiency is clearing formed autophagosomes by fusing them with the lysosome (Boland et al., 2008). In AD, autophagy is seen as playing a dual role of benefits and detriments. In a healthy central nervous sytem, there is an efficient clearance of Aβ peptide as it is produced maintaining balance however in AD brain there is increased level of aggregation of Aβ peptide due to a disturbance of the autophagosome-lysosomal pathway where there is deficient lysosomal clearance and accumulation of incompletely digested proteins (Bordi et al., 2016). AD mouse model exposed to rapamycin, generated an increase in autophagy which led to reduced Aβ accumulation,

improved cognitive abilities and caused a decline in AD progression (Zhang et al., 2017). Conversely, there is an argument that overstimulation of autophagy overpowers the clearing capacity of the lysosome causing an accumulation of Aβ-containing autophagosomes in neurones resulting in intracellular toxicity (Liang and Jia, 2014).

Mitophagy a selective form of mitochondrial autophagy have been implicated in the pathogenesis of AD (Kerr et al., 2017) and as discussed in section (1.2), disruption of mitochondrial dynamics has been implicated in several neurodegenerative diseases resulting in severe neurological dysfunction due to inactivation or mutation of the major fusion/fission proteins (Berthelot *et al.,* 2016). However, neither the role of ethanol induced mitophagy nor the underpinning mechanisms have been studied in neuronal cells relative to Aβ and tau expression, key markers of AD pathology.

1.4- MICRONUTRIENTS IN THE NERVOUS SYSTEM: IMPACT OF ZN AND MN IRREGULARITY

Micronutrients are one of the major groups of nutrients required by the body in small amounts necessary for proper growth and development. They include vitamins, minerals and trace elements such as manganese (Mn), zinc (Zn), iron (Fe), selenium (Se), molybdenum (Mo), cobalt (Co), chromium (Cr) and iodine (I). This thesis is focused on Zn and Mn and the mechanism associated with AD pathology. In brain and CNS development, inadequate micronutrient supply results in negative structural and functional impact (Gonzalez and Visentin, 2016).

In neurodevelopment, Zn is required for both prenatal and postnatal development and is required for gene expression, cell growth, differentiation and metabolism (Jackson *et al.,* 2008). Zn also serves as a regulatory factor for different enzymes while contributing to cognitive neurodevelopment (Salgueiro *et al.,* 2002, McCall *et al.,* 2000). Mn is required for carbohydrate and lipid metabolism, improved immune function and as metalloenzymes necessary for different metabolic processes in the body (Avila *et al.,* 2013, Li and Yang, 2018).

Although Zn has a beneficial role to play, in excess it is toxic and detrimental to cell wellbeing affecting metabolic functions in the body (Igic *et al.,* 2002). Similarly, in excessive amounts, Mn toxicity in the brain, lung, and liver has been reported, with accumulation in brain tissue resulting in a Parkinson's disease-like disorder commonly reported (Crossgrove and Zheng, 2004). Excessive Zn and Mn have been implicated in AD (Tong *et al.,* 2014, Religa *et al.,* 2006). High plasma Mn have been linked to high plasma Aβ-peptides with invitro studies showing an increase of Aβ following excessive Mn exposure (Tong *et al.,* 2014) and a two-fold increase level of Zn in AD brain compared to control counterpart (Religa *et al.,* 2006). What is not known is the role of Zn/Mn-induced dysregulation of mitochondrial dynamics on AD pathology. Here, the impact of micronutrients Zn and Mn on neurotoxicity, mitochondrial function and homeostasis will be studied.

1.4.1- ZINC-INDUCED NEUROTOXICITY

Zn is abundantly required in the body for cell development and as a functional component of several proteins (McDonald, 2000). Zn, an essential trace element is important for different biological processes playing a variety of roles which can be categorised as structural, catalytic and regulatory functions (Kambe et al., 2015). Zn fingers play an important role in DNA replication and transcription, acting as a structural ion in transcription factors helping them bind to DNA sequences in an accurate manner (LatifWani et al., 2017). Zn also acts as a regulatory signalling ion mediating the transfer of information intracellularly and in-between cells (Maret, 2013). Additionally Zn is a part of a large number of enzymes with carbonic anhydrase II being the first metalloenzymes to be discovered. Zn is located at the catalytic site of many enzymes where it interact with substrate molecules during chemical reactions and also play a role in the stabilisation of tertiary protein structure (McCall et al., 2000).

In the brain, the estimated Zn concentration is 150 µM with the majority (about 80%) bound to proteins. Post-synaptic release of Zn from the synaptic vesicles give rise to a range of 10-100 µM free ions (Bozym *et al.,* 2006). Intracellularly, free unbound zinc ranges from nanomolar to a few micromolar which is

regarded as non-toxic (Frederickson *et al.,* 2005). In adult rat brain also, the intracellular physiologic concentration of zinc has been reported to be approximately 150 µM and extracellular concentration less than 1 µM (Takeda *et al.,* 2010, Takeda *et al.,* 2001). In cortical neurons, exogenously applied 300 µM Zn have been reported to elicit a dose-dependent generalised neuronal injury (Yokoyama *et al.,* 1986).

In glutamatergic neuronal cells, under normal physiological conditions, zinc, exists alongside glutamate in presynaptic vesicles. Under pathological conditions, vesicular zinc is released to the synaptic cleft alongside glutamate in excess and gain entrance into post synaptic neurons through NMDA and AMPA/kainate receptors and voltage-gated calcium channels (Martinez-Galan *et al.,* 2003, Morris and Levenson, 2012). This post-synaptic accumulation of excessive free zinc acts as a signal that triggers glutamergic excitotoxicity thereby exacerbating cell toxicity (Zatta *et al.,* 2003).

Table 1.1- Zn distribution in various parts of the human body

Body Location	% distribution
Skeletal Muscle	57
Liver	5
Bone	29
Brain	1.5
Heart	0.4
Skin	6
Kidney	0.7

A number of molecular mechanisms have been suggested to mediate Zn-induced neurotoxicity including mitochondrial dysfunction and neuronal signalling. This is suggested to be elicited by increased ROS production resulting in the opening of the permeability transition pore thereby disrupting mitochondrial enzymes and respiration (Sensi *et al.,* 2003). An acute elevation (increase from 0.001-0.1 mM Zn for 24 h) of Zn in cholinergic neuroblastoma cells resulted in reversible pyruvate dehydrogenase activity inhibition. When cells were exposed to higher Zn (0.15-0.2 mM) for 24 h, pyruvate dehydrogenase activity inhibition was irreversible (Ronowska *et al.,* 2007)

further contributing to an increase in ROS production. Zn has been shown to increase the expression of superoxide dismutase and heme-oxygenase, enzymes associated with increased oxidative stress leading to dopaminergic neurodegeneration (Singh *et al.,* 2011). Various alterations in gene expression of metal-related genes (metallothioneins, Zn transporter), ER stress- related genes and the *Arc* gene have been implicated in Zn-induced neurodegeneration (Kawahara *et al.,* 2013). Zn-mediated intracellular calcium ion metabolism in neurons is suggested to play a role in Zn-induced neurotoxicity and eventual apoptosis (Mizuno and Kahawara, 2013).

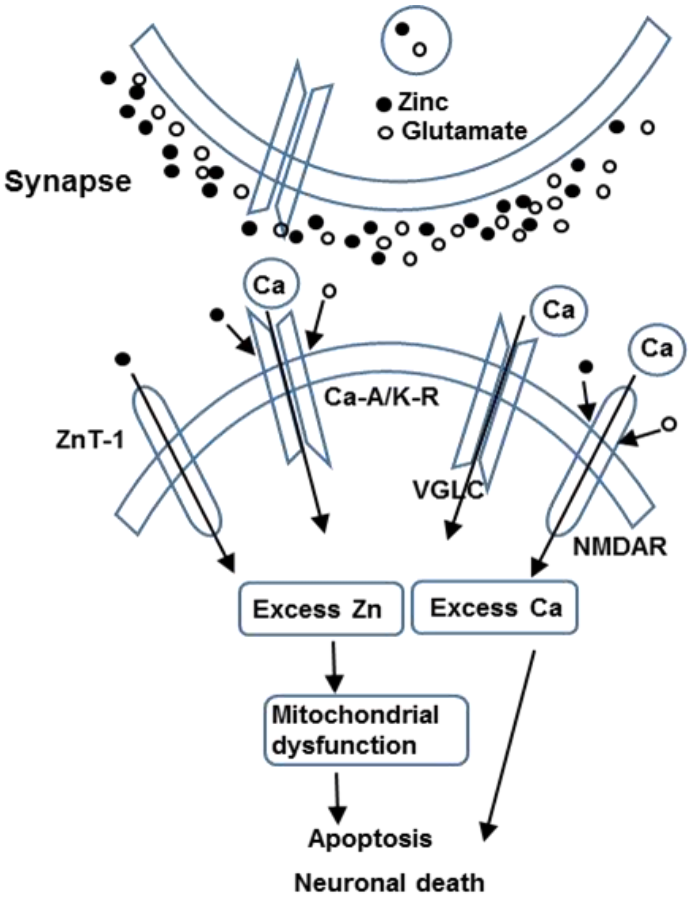

Figure 1.9- Mechanism of Zn-induced neurotoxicity. High Zn concentrations are secreted from pre-synaptic neuronal vesicles alongside excessive glutamate enhancing the expression of Ca-A/K-R which mediates the translocation of Zn into surrounding neurons where it inhibit mitochondrial respiration, deplete energy production while increasing ROS production. This increases Ca^{2+} levels, thus leading up to activation of the apoptotic pathway and eventual neuronal cell death (Adapted from Kawahara *et al.,* 2014).

1.4.2- ZINC AND ALZHEIMER'S DISEASE

Abnormal deposition and accumulation of Aβ together with its tendency to form insoluble aggregates that promote neurotoxicity is regarded as a key hallmark of AD, therefore factors promoting this are regarded as contributory to AD pathogenesis (Kawahara *et al.,* 2014). Zn concentration > 300 nM have been reported to enhance Aβ aggregation and the binding of APP to extracellular matrix (Bush *et al.,* 1994). The study of post-mortem hippocampal tissue from AD patients revealed synaptic vesicles contained three times the amount of free Zn found in the hippocampus compared to non-AD matched control suggesting that Zn plays a role in enhancing Aβ oligomer-induced toxicity in AD (Szutowicz *et al.,* 2017). A similarity between the post-mortem analysis of human AD brains and the mitochondrial compartments of post-synaptic cholinergic neuronal cells exposed to Zn treatment have been reported where similar patterns of inhibition of mitochondrial enzymes- isocitric acid dehydrogenase, pyruvate dehydrogenase, aconitase and α-ketoglutaric acid dehydrogenase precede loss of neurotransmitter functions and structural damage (Bubber *et al.,* 2005, Ronowska *et al.,* 2007). There has been a wide study of biometal-induced Aβ aggregation in AD with copper and Zn being the prominent participants. Zn has been shown to have a greater influence in the aggregation process, enhancing Aβ aggregation even in small quantities due to Zn ion rapid exchange between Aβ peptides (Mattheou *et al.,* 2016, Sharma *et al.,* 2013). Interactions between Zn and APP, Aβ, metallothioneins, GSK3B and tau proteins and the resultant ROS generation, mitochondrial dysfunction, energy deficit, protein aggregation have been widely studied in AD pathogenesis and linked to Zn dyshomeostasis. However, the impact of Zn on fusion/fission dynamics and how this impacts Zn-induced mitochondrial dysfunction and contribute to protein aggregation, Aβ and phosphorylated tau production.

Zn has been reported to form a component of the Aβ plaque where it catalyses oxidative stress through ROS generation (Stelmashook *et al.,* 2014). Despite the findings on Zn interaction with Aβ, its definitive role in AD pathology is not fully clear. As Zn binds to Aβ, it inhibits its proteolytic cleavage while also

inhibiting the activity of the ɣ-secretase enzyme necessary for Aβ generation suggesting a paradoxical role of preventing Aβ generation and degradation (Ayton *et al.,* 2013). Zn also interacts with the tau-protein enhancing its aggregation, phosphorylation and the formation of neurofibrillary tangles that impair cognitive functions (Craddock *et al.,* 2012). The paradoxical identity of Zn has been reported through its response to stress as both inhibitory and via promotion of stress response. Zn promotes oxidative stress when it is in concentrations outside the physiological range, either in excess or deficient amount. This it does by altering mitochondrial respiration thereby increasing the amount of ROS generated (Sensi *et al.,* 2003, Dineley *et al.,* 2003). Zn has been shown to protect sulfhydryl groups against oxidation and reduce thiol reactivity suggesting an antioxidant role. Its role in the conformational changes to Aβ has been proposed to protect Aβ from interacting with oxidising metals which could lead to further peroxide formation (Powell, 2000, Gibbs *et al.,* 1985, Cuagungco *et al.,* 2000).

1.4.3- IMPACT OF ZINC ON MITOCHONDRIAL FUNCTION, BIOENERGETICS AND THE FUSION/FISSION PATHWAY

In the mitochondria of cholinergic neuronal cells, only 1% of the total zinc pool is found in the mitochondria with the cytosol contains a higher concentration of Zn. Exposure to 100-300 µM Zn of neuronal cells resulted in intra-mitochondrial Zn accumulation, shown to be mediated by the activation of AMPA/kainate receptors, with a subsequent loss in MMP. This accumulation led to long persisting Zn-triggered ROS generation and failure of several mitochondrial functions even after Zn exposure has been terminated (Sensi *et al.,* 2000, Ronowska *et al.,* 2007) suggesting the mitochondria is a key target for Zn-induced neurotoxicity. Further evidence show that an increase in intracellular free Zn concentration subsequently results in disruption of mitochondrial functions and energy deficits thereby leading to depolarisation of the neurons affected. Mitochondrial exposure to excessive Zn (> 250 µM Zn) has been reported to also cause an irreversible inhibition of specific mitochondrial enzymes such as isocitrate $NADP^+$ dehydrogenase and aconitase through a direct reaction with the enzyme's –SH groups (Ronowska *et al.,* 2010). Similar enzymes involved in acetyl CoA metabolism found in the

cytoplasmic compartment were shown to remain unaffected by high zinc concentrations strongly indicating that excessive free Zn-induced neurotoxicity targets the mitochondria specifically (Ronowska *et al.,* 2007).

Studies have shown a swelling of the mitochondria associated with the movement of high concentrations of Zn into the mitochondria from the cytosolic pool. Under basal conditions, isolated neuronal mitochondria exposed to submicromolar levels of Zn (40 pmol- 400 nmol per mg of protein) result in the opening of the inner mitochondrial membrane channel (MPTP), an increase in oxygen consumption and decrease in ROS generation. However, an increase in Zn concentration (40-400 nmol/mg) resulted in a partial loss in MMP linked to inhibition of the electron transport and MPTP opening, increase in ROS formation and decrease in oxygen consumption (Sensi *et al.,* 2003). In HepG2 cells, Zn challenge diminished ATP production as a result of delayed ADP conversion to ATP, also a follow-on from the perturbation of enzymes involved in the ETC and TCA cycle. There is a suggestion also that ATP production dysregulation results from a decrease in the expression of mitochondrial aconitase. This is linked to zinc's disruption of the Fe-S cluster in mitochondrial aconitase, a key enzyme required for the production of ATP thereby diminishing its production. (Lemire *et al.,* 2008).

In epithelial cells and INS1-832/13 β-cell line, exposure to hydrogen peroxide caused the activation of the transient receptor potential melastatin (TRPM)-2 channel, allowing the influx of Ca^{2+}. This influx led to the release of lysosomal Zn thereby resulting in an uptake of Zn into the mitochondria promoting Drp1 recruitment and an increase in mitochondrial fission (Li *et al.,* 2017, Abuarab *et al.,* 2017). This thesis seek to investigate the impact of excessive Zn exposure on mitochondrial fusion/fission dynamics SH-SY5Y neuronal cells.

1.4.4- ZINC AND METABOLIC SIGNALLING PATHWAYS

The movement of Zn across cell membrane (as illustrated in Figure 1.10) is mediated by a family of ZIP channels and ZnT transporters. While the ZIP channels mediate Zn influx from extracellular space into intracellular compartments, ZnT transporters mediate Zn efflux (Nimmanon *et al.,* 2017). ZIP channel subfamilies exist from ZIP1-14, however in different cells, there

are specific ZIP channels responsible for the intercompartmental movement of Zn. In DT40 cells, the ZIP9 facilitates Zn influx while ZIP6, 7, 10 is involves in Zn influx in breast cancer cell lines (Nimmanon *et al.,* 2017, Taylor *et al.,* 2008, Taniguchi *et al.,* 2013). Zn neurotoxicity results in the activation of various neuronal signalling molecules such as ERK 1/2 (Seo *et al.,* 2001). Activation of Ras an upstream regulator of ERK phosphorylation has been linked to oxidative cell death in neuronal cells (Du *et al.,* 2002). The Zn-sensing receptor has been evidenced as a link between extracellular Zn and the intracellular release of calcium which then leads to the phosphorylation of ERK1/2.

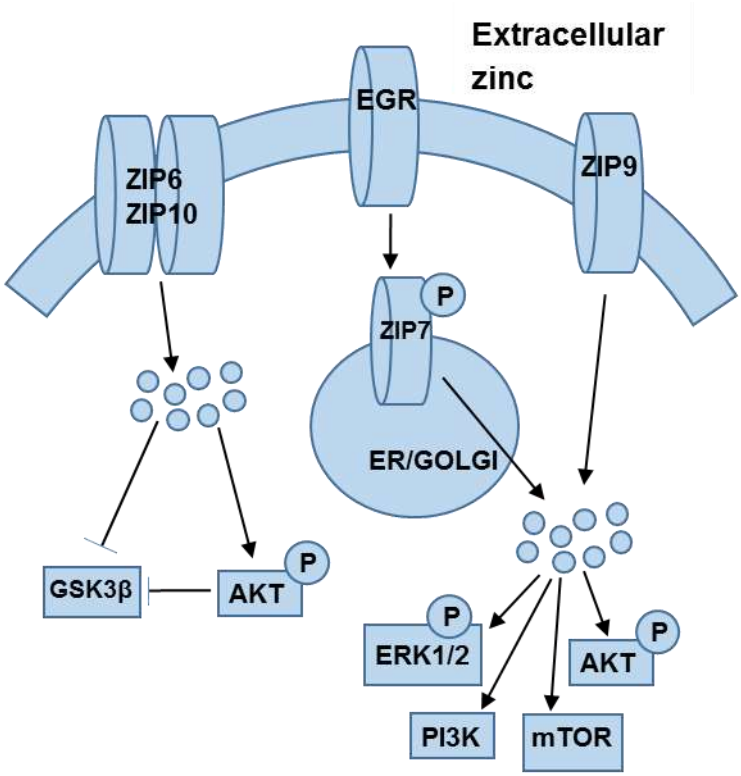

Figure 1.10- Schematics showing ZIP6/10, ZIP7 and ZIP9-mediated activation pathways. In cancer cells, stimulation of EGFR results in ZIP7 phosphorylation which in turn result in Zn release from the ER/Golgi thereby activating the kinases of Akt, ERK1/2. In MCF-7 cells, CK-mediated phosphorylation of ZIP7 release Zn from intracellular stores activating ERK1/2, PI3k- AKT and mTOR signalling pathways. In DT40 cells, ZIP9-induced increase in intracellular Zn concentration activates AKT and ERK1/2 (Taylor et al., 2008).

An alteration of this receptor has been shown to inhibit ERK1/2 phosphorylation suggesting a strong dependence of this process on extracellular Zn (Azriel-Tamir *et al.,* 2004). Similar study reported extracellular

Zn in rat neuronal cells gives rise to ERK1/2 activation which has also been implicated as the mechanism that mediated Zn-induced neurotoxicity (He and Aizenman, 2010). The Zn transporter ZIP9 responsible for increase in the levels of intracellular Zn play an important role in Akt and ERK phosphorylation. Results show that this phosphorylation is facilitated by the presence of intracellular Zn (Taniguchi *et al.,* 2013). Zn has been shown to possess an antidepressant-like property linked to the phosphorylation of mTOR and p70S6K (Szewczyk *et al.,* 2015). The deficiency of Zn however, has been linked to an impairment in ERK1/2 phosphorylation leading to several alterations in brain development and behavioural deficiencies (Nuttal and Oteiza, 2012). This study investigated Zn-induced activation of the ERK/AKT metabolic signalling pathway.

1.5- MANGANESE-INDUCED NEUROTOXICITY

Although Mn is an essential nutrient, there is the need to maintain a homeostatic Mn level to prevent either deficiency or excess. Mn deficiency results in growth impairment, defects in the skeletal system, dysregulated glucose tolerance, oxidative stress and mitochondrial dysfunction (Li and Yang, 2018). Excessive exposure of Mn to cells on the other hand stimulates apoptosis, neurological and motor disorders, oxidative stress and mitochondrial dysfunction (Smith *et al.,* 2017).

When Mn is accumulated in the basal ganglia, there is the manifestation of cognitive and motor impairments resembling manifestations of Parkinson's disease, known as manganism (Peres *et al.,* 2016). This manifestation of motor impairment has been the focus of investigations regarding the connection between Mn overexposure and its cognitive effects. More recently, there is an increase in attention to the cognitive deficit arising from Mn neurotoxicity and its contribution to neurodegenerative disorders following decades of exposure (Weiss, 2010). It is hypothesized that this accumulation at the basal ganglia in astrocytes result in inflammation of the region giving rise to nitric-oxide induced neuronal injury (Liu *et al.,* 2006). Chronic exposure to Mn is implicated in neurotoxicity and impairment of neurodevelopment at critical stages with sensitivity to Mn toxicity being cell-dependent (Hernandez *et al.,* 2011). Elevated Mn level have been shown to trigger oxidative stress

thereby inducing mitochondrial dysfunction that results from excessive production of ROS. This leads to loss of mitochondrial inner membrane potential, opening of the mitochondrial transition pores, mitochondrial swelling and the impairment of oxidative phosphorylation, which results in decreased ATP synthesis (Gavin *et al.,* 1999, Milatovic *et al.,* 2009). The impact of Mn neurotoxicity is suggested to be partly mediated through deregulation of neurotransmitters. This results in excitotoxicity and cell death, however, the underlying mechanism is not understood (Quintanar, 2008). Excessive exposure of neuronal cells to Mn-induced oxidative stress and dopaminergic neurodegeneration as shown by dopamine depletion and downregulation of its transporters. This effect was suggested to trigger motor dysfunction and neuronal loss, pointing to a possible interaction between oxidative stress and the resulting neurodegeneration in the substantia nigra (Deng *et al.,* 2015).

Like Zn, excessive accumulation of Mn in the mitochondria inactivate enzymes such as aconitase thereby impairing oxidative phosphorylation and causing further oxidant production. This effect has been reported to inhibit complex II activity of the electron transport chain promoting ROS generation and MMP disruption (Galvani *et al.,* 1995, Gavin *et al.,* 1992 and Milatovic *et al.,* 2007, Smith *et al.,* 2017). Oxidative stress resulting from excessive exposure to Mn has been linked to apoptotic cell death. Predominantly expressed is caspase-3 cleavage dependent apoptotic pathway. PC12 cells exposed to excessive Mn demonstrated an increased apoptotic rate which is directly linked to oxidant production levels. Treatment of the cells with antioxidants prevented apoptotic events indicating the role of oxidants in Mn-induced apoptosis (Deng *et al.,* 2015, Chtourou *et al.,* 2014).

1.5.1- MANGANESE AND ALZHEIMER'S DISEASE

Manganese homeostasis (increased and decreased levels) is considered to play an important role in the pathogenesis of neurodegenerative diseases. Meta-analysis of serum Mn levels in AD and MCI patients reveal a significant decrease in the levels of serum Mn levels in AD and MCI patients compared to healthy control subjects indicating that Mn deficiency is a risk factor for the pathology of AD (Du *et al.,* 2017). Mn is regarded to potentially play a dual role

in its link with AD pathology. There is evidence of changes in the expression of the Mn-dependent antioxidant SOD2 in lymphocytes of AD patients, with amyloid pathology enhanced in MnSOD enzyme deficiency. Overexpression of this enzyme slowed down the formation of plaques, enhanced plaque degradation and Aβ resistance (Dumont *et al.,* 2009).

However, a study involving 40 elderly adults with different cognitive levels of cognitive abilities showed a significant correlation between blood Mn levels and cognitive rating, a simultaneous increase in Mn and Aβ levels and *in vitro* evidence to support an increase in Aβ levels following Mn treatment (Tong *et al.,* 2014). Further evidence from analysis of Mn concentration in plasma and CSF of AD patients reveal a significantly higher concentration of Mn in AD plasma versus the control subjects with an inverse outcome in CSF. Mn concentrations were lower in CSF of AD patients than in the control subjects (Gerhardsson *et al.,* 2008).

Neuropsychological dysfunction has been reported in primates chronically exposed to Mn. In this study Mn-exposed monkeys demonstrate an upregulation of Aβ plaques deposition in the frontal cortex, increased mRNA expression of Aβ precursor-like protein (APLP1) and changes to the paired associate learning- a tool for diagnosis of preclinical AD (Schneider *et al.,* 2013, Guilarte, 2013). Nuclear magnetic resonance was used to show a weak Mn ion binding to the N-terminal of Aβ (1-40) suggesting an AD Mn metal chemistry and a potential implication in the disease pathogenesis (Wallin *et al.,* 2016).

1.5.2- IMPACT OF MANGANESE ON MITOCHONDRIAL FUNCTION, BIOENERGETICS AND THE FUSION/FISSION PATHWAY

Mn has been shown to easily accumulate in neuronal mitochondria but has a very slow efflux rate and as a result causes Mn-induced neurotoxicity which disrupts mitochondrial functions and dynamics (Prakash *et al.,* 2017). Like Zn, Mn exposure has been implicated in the inhibition of the activities of mitochondrial enzymes aconitase and MnSOD and mitochondrial respiration (Anantharaman *et al.,* 2006, Zheng *et al.,* 1998). In addition to its disruptive effects on mitochondrial enzymes, there is also a disruption of the

mitochondrial electron transport chain, mutation of the mitochondrial genome thereby enhancing free radical production (Brown *et al.,* 1999).

In a study where SH-SY5Y cells were exposed to Mn over a range of 0 – 100 µM to mimic human brain Mn content at baseline (≤ 10 µM) and at toxic concentration exposure (≤ 50 µM), it was evidenced that following toxic exposure range, there was an increase in hydrogen peroxide production, SOD2 activity and a decrease in oxygen consumption rate (Fernandes *et al.,* 2017). Likewise, exposure of primary astrocytic cells to 100 µM Mn for 24 h showed a significant decrease in basal mitochondrial respiration and oxygen consumption rate compared to untreated cells. There was also a simultaneous decrease in mitochondrial ATP production, non-mitochondrial respiration and a decline in glycolytic function measured by the extracellular acidification rate (ECAR). Indicative of impaired mitochondrial function and biogenesis, human astrocytic U373 cells exposed to 50.46 µM Mn for 24 h shows reduced mitochondrial mass and increase in circularity signifying enhanced mitochondrial fission (Sarkar *et al.,* 2018).

Mn exposure (750 µM) to C6 neuronal cells for 24 h has been shown to affect mitochondrial dynamics. Results show an increase in expression of the fission protein Drp1 and a decrease in Opa1 fusion protein. Co-treatment with CsA, an MPTP opening inhibitor protected the cells from Mn-induced mitochondrial disruption (Alaimo *et al.,* 2014). Further studies on Gli36 astrocytic cells also demonstrates Mn-induced deregulation of the fusion/fission proteins Opa-1, Mfn-2 and Drp-1 expression, mitochondrial network disruption and increased fragmentation of neuronal mitochondria (Alaimo *et al.,* 2013). PC12 cells exposed to Mn demonstrates a significant decline in Mfn2 expression closely associated with caspase-3 activation. Overexpression of Mfn2 attenuated Mn-induced apoptosis, however, inhibition of apoptosis does not rescue the downregulation of Mfn2 indicating Mfn2 loss as an early event following excessive Mn exposure (Liu *et al.,* 2017).

1.5.3- MANGANESE AND MAPK/mTORC1 SIGNALLING

Results from several *invitro* studies have demonstrated that Mn exposure impact the MAPK/AKT/mTORC1 pathways. Several studies demonstrate that Mn exposure increases inflammatory mediators which have an effect of inducing an increase in MAPK activity. In activated glia cells, ERK activation is achieved following Mn exposure due to the activation of kinases upstream of MAPK (Crittenden and Filipov, 2011). Exposure to 500 µM Mn in microglial cells have also been shown to increase phosphorylation of Erk and Akt while activating iNOS inflammatory mediator expression indicating Erk/Akt pathway activation following Mn exposure acts as a survival mechanism (Bae *et al.,* 2006).

Exposure of U87 glioblastoma cells to 100 µM Mn an increase in phosphorylation of mTOR with the mTOR protein level remaining unchanged. However, at a concentration of 400 µM, there is a decline in mTOR phosphorylation (Puli *et al.,* 2006). Chronic Mn exposure has been shown to increase basal mTOR and phosphorylated mTOR expression (Srivastava *et al.,* 2016).*In vivo* experiment involving developing rat striatum exposed to Mn show an activation of the MAPK/Erk/Akt pathways. In the *in vivo* study, striatal and hippocampal slices exposed to 10-1000 µM Mn show a significant increase in ERK phosphorylation with the *in vivo* study showing a further increase in phosphorylation of Akt (Peres *et al.,* 2013, Cordova *et al.,* 2012). There is also evidence from *in vivo* studies indicating Mn exposure from fertilisation reflect persistent activation of the ERK pathway (Pinsino *et al.,* 2011).

Considering conflicting reports and debate regarding neuroprotective role of moderate alcohol intake, this study will determine if different levels of alcohol evoke a switch from neuroprotection to neurotoxicity. Despite the association of excessive ethanol, Zn and Mn exposure with AD hallmarks- Aβ and phosphorylated tau, there is the need to understand the role of mitophagy and the mitochondrial fission/fusion dynamics mechanism and cell survival pathway response in modulating the expression of these key AD hallmarks

1.6- RESEARCH HYPOTHESES

Hypothesis: Ethanol, zinc and manganese-induced neurotoxicity impairs mitochondrial function through disruption of the fusion/fission dynamics

Chapter 2

2.0- MATERIALS AND METHODS

2.1- MATERIALS

SH-SY5Y neuroblastoma cell line was purchased from ATCC (Manassas, VA). Antibodies to superoxide dismutase SOD 1 (ab16831), glutaredoxin GRX 1 (ab187507), thioredoxin TRX 1 (ab57675), 4- hydroxynonenal (4-HNE) (ab46545), SQSTM1/ p62 (ab56416), actin (ab8226), Nrf2 (ab62352), glutathione peroxidase GPx (ab108427), glutathione reductase GSR (ab124995), Hsp60 (ab59458), Opa1 (ab42364), Mfn1 (ab57602), Drp1 (ab56788), Bax (ab182733), Bcl2 (ab692), Akt (ab8805), phospho-Akt T308 (ab8933), Erk 1/2 (ab196883), phospho-Erk Thr202/Tyr204(ab214362), mTOR (ab134903), phospho-mTOR S2481(ab137133), p70S6K (ab9366), phospho-S6K T229 (ab59208), phospho-tau S396 (ab109390), beta-amyloid 1-42 (ab12267), glutamate dehydrogenase GDH (ab154027), alcohol dehydrogenase ADH1B (175515), rabbit raised antibody to aldehyde dehydrogenase ALDH2 (70917), malondialdehyde (MDA), 1x 2, 4-dinitrophenylhydrazine (DNPH) solution, 1x derivatization solution, standard protein with DNP residues, 2x extraction buffer, 5000x primary anti-DNP antibody (rabbit), 5000x HRP conjugated secondary antibody (goat anti-rabbit) all part of the oxidized protein western blot kit (ab178020) were purchased from Abcam (Cambridge, UK). MAP LC3β Antibody (G-9) was purchased from Santa Cruz Biotechnology, Heidelberg, Germany and Phospho-p70 S6 Kinase (Thr389) Antibody was purchased from Cell Signalling Technology, Leiden, Netherlands. Goat raised antibody to rabbit IgG and horse raised antibody to mouse IgG were purchased from Vector Labs (Peterborough, UK). Rabbit raised antibody to divalent metal transporter DMT-1 (AB S983) was purchased from Millipore, UK. Amersham hybond ECL polyvinylidene fluoride (PDVF) membrane, Amersham hyper film ECL were purchased from GE HealthCare Life Sciences (UK) and phosphate buffered saline (PBS) tablets was purchased from Oxoid (Hampshire, UK). Bovine

serum albumin (BSA) was purchased from Gemini Bio Products (USA) and triton X-100, β-mecarptoethanol, bromophenol blue dye, coomasie blue G dye, Amido black dye, TWEEN 20, Tris, TEMED, thiobarbituric acid, hydrogen peroxide, potassium bromate, pure ethyl alcohol, 30 % acrylamide, ammonium per sulphate (APS) were purchased from Sigma-Aldrich (Dorset, UK). Foetal bovine serum (FBS), Dulbecco's minimum essential medium (DMEM), Tris-Glycine SDS-PAGE gel, 0.25 % Trypsin- EDTA, NuPAGE MES SDS running buffer (20x) were purchased from Life Technologies (Carlsbad, CA). Cyclophilin D monoclonal antibody clone E11AE12BD4 (10458653), Glacial Acetic Acid, sodium hydroxide, methanol, sodium chloride, glycine, sodium dodecyl sulphate (SDS), EDTA, EGTA, trichloroacetic acid were purchased from Fisher Scientific (Loughborough, UK). Marvel was locally purchased.

2.2- METHODS

2.2.1- TISSUE CULTURE

SH-SY5Y cells were maintained at 60-80% confluence in antibiotics-free Gibco Dulbecco's modified eagle medium containing 10% FBS and 1X L-glutamine at 37°C and 5% CO_2. The cells were sub-cultured every 48 hours. At 70 – 80% confluence the cells were rinsed with 3 mL sterile PBS, PBS was then removed and discarded. The adherent cells were detached from the bottom of the flask by adding 2.5 mL of 0.25 % EDTA-Trypsin, incubated at 37°C for 5 minutes. The trypsin was neutralised by adding 2.5 mL of DMEM, transferred into a 14 mL eppendorf tube and centrifuged at 1,300 rpm for 5 minutes. The supernatant was decanted, and the cell pellet resuspended in DMEM and transferred into new T75 flasks or transferred onto the improved Neubauer chamber for cell counting.

2.2.2- CELL DIFFERENTIATION

SH-SY5Y cells were differentiated by incubating the cells in 10 μM retinoic acid for 7 days. In a T75 culture flask, 5 x 10^6 cells were seeded overnight followed by treatment with 10 μM retinoic acid in 3 % FBS DMEM for 48 h. Subsequent incubation with fresh 10 μM retinoic acid in 3 % FBS DMEM for 48 h was

carried out twice, followed by an overnight incubation of cells in 3 % FBS DMEM prior to cell treatments.

2.2.3- ETHANOL, ZINC AND MANGANESE CELL TREATMENTS

SH-SY5Y cells were treated with 250 mM, 500 mM ethanol, 150 µM, 300 µM zinc and 200 µM, 400 µM manganese, respectively. Depending on the proposed experiment, cells are co-treated with 2.5 mM NAC, 2.5 mM GSH, 1 µM cyclosporine A.

Table 2.2- Treatment solutions

Treatments	Stock concentration	Stock concentration protocol	Working conc. protocol
40 µM H_2O_2	100 mM H_2O_2	51 µL 30 % w/v H_2O_2 in 5 mL media	4 µL stock in 10 mL media
250 mM EtOH	100 % EtOH		14.6 µL stock in 10 mL media
500 mM EtOH	100 % EtOH		29.2 µL stock in 10 mL media
150 µM Zn	200 mM	0.057g Zn sulphate in 2 mL media	7.5 µL stock in 10 mL media
300 µM Zn	200 mM	0.057g Zn sulphate in 2 mL media	15 µL stock in 10 mL media
200 µM Mn	200 mM	0.039g Mn chloride in 2 mL media	10 µL stock in 10 mL media
400 µM Mn	200 mM	0.039g Mn chloride in 2 mL media	20 µL stock in 10 mL media

2.2.4- PROTEIN EXTRACTION USING RIPA BUFFER

Cells grown in a T75 flasks at 70 – 80% confluence had the culture media aspirated, washed twice with sterile PBS and incubated with 2 mL of trypsin at 37°C for 5 minutes. Detached cells were washed twice with sterile PBS, the cell pellet was resuspended in 80 µL of RIPA (10 mM TRIS, 150 mM NaCl, 1

mM EDTA, 1 mM EGTA) buffer (4285 µL RIPA, 714 µL protease inhibitor and 50 µL Triton X), and allowed to sit on ice for 30 minutes. One mL syringes and G23/25 needles were used to break cells. The suspension was centrifuged at 15,000 rpm at 4°C for 10 minutes. The protein concentration of the supernatant was quantified using the Amido black assay (Section 2.2.3), Bicinchoninic acid (BCA) (Section 2.2.4) protein concentration assay or Bradford (Section 2.2.5) protein determination assay or stored at -20°C until required.

2.2.5- PROTEIN ESTIMATION USING THE AMIDO BLACK ASSAY

Protein standard solutions (1, 2.5, 5, 7.5 and 10 µg) were prepared from a 1 mg/ mL BSA solution using ultrapure water (Table 2.1). Unknown samples were diluted (½, 1/5, 1/10, 1/20) accordingly. Once samples were prepared, 30 µL 1 M Tris-HCl buffer was added to each standard and test sample.

Table 2.1 Amido Black Standard Solutions

BSA (µg/µL)	BSA (µL)	Ultrapure Water (µL)
0	0	270
1	10	260
2.5	25	245
5	50	220
7.5	75	195
10	100	170

To each tube, 60 µL of 60% TCA was added and samples were vortexed and incubated at room temperature for 5 minutes. The Buchner flask and whatman membrane were prepared with the whatman membrane washed thrice with 6 % TCA. Each sample was added onto the individual square of the Whatman membrane. The membrane was rinsed intermittently between every 4 to 5 samples with 6 % TCA. The membrane was stained using the amido black dye solution (0.1% amido black 10B sodium salt, 45% methanol, 10% acetic acid) for 2 minutes, washed with water for 30 seconds and destained with a destaining solution (90% methanol, 2% glacial acetic acid, water) for 1 minute. This cycle of washing and destaining was repeated 3X. The membrane was cut into the individual squares containing the protein standards and samples,

eluted with an eluent buffer (25 mM NaOH, 0.5 mM EDTA and 50%ethanol), vortexed and allowed to standard for 30 minutes. Into each well of a 96-well plate, 200 µL of the elution buffer was added in duplicate and the change in absorbance measured at 620 nm wavelength.

2.2.6- PROTEIN ESTIMATION USING THE BICINCHONINIC ACID (BCA) ASSAY

The BCA protein assay working reagent was prepared according to the manufacturer's instructions by adding 50 parts of the BCA solution to 1 part of 4 % copper (II) sulphate solution. In a 96 well plate, 25 µL each of BSA standard solutions 2, 4, 6, 8, 10 µg, blank and samples were added in triplicate followed by 200 µL of BCA working solution and plate was incubated at 37°C for 30 minutes in the dark and then the absorbance was measured at 562 nm.

2.2.7- PROTEIN ESTIMATION USING THE BRADFORD ASSAY

The Bradford working reagent was prepared from 1.5 % stock solution (330 mg Coomasie blue G, 66.6 mL phosphoric acid, 33.3 mL ethanol), 1.9 % ethanol, 4 % phosphoric acid made up to 100 mL water. Standard protein solutions of 0.2, 0.4, 0.6, 0.8, 1.0, 1.2 µg/ µL, blank and diluted samples were added in triplicate to a 96-well plate followed by 200 µL of the Bradford working reagent. The change in absorbance was recorded at 620 nm with the fluostar spectrophotometer and unknown sample protein concentration calculated from a standard calibration plot.

2.2.8- CELL VIABILITY ASSAY

In a 96-well plate, 50,000 cells are seeded overnight in triplicate. The cells were treated with 100 µM H_2O_2, 125, 250, 500, 1000 mM ethanol, 200, 400, 800, 1600 µM zinc and 200, 400, 800, 1600 µM manganese, respectively with control cells incubated with media only and incubated for 24, 48 and 72 hours, in a sealed plate and incubated at 37°C and 5% CO_2. The cell treatment solution is replaced by 100 µL of media and 20 µL of the CellTitre Aqueous One Solution Reagent (containing tetrazolium compound [3-(4,5-dimethylthiazol-2-yl)-5-(3-carboxymethoxyphenyl)-2-(4-sulfophenyl)-2H-tetrazolium, inner salt; MTS and an electron coupling reagent (phenazine

ethosulfate; PES) was added. This was followed by incubation for 90 minutes at 37°C and 5% CO_2 in the dark. The change in absorbance was measured at 490 nm. The assay blank well contained 100 µL of media and 20 µL of the CellTitre Aqueous One Solution Reagent with no cells. The change in absorbance was monitored at 490 nm.

2.2.9- 1D SDS-PAGE

Reduced protein samples (20 µg) were prepared by adding 6.25 µL of 4X loading buffer (150 mM Tris-HCl pH 8.5, 0.175 mM phenol red, 0.51 mM EDTA, 0.2 mM blue G250, 2% LDS, 10% glycerol) and 1 µL of 5% β- mecarpto-ethanol , adjusting the volume to 25 µL in an eppendorf tube and heated at 95°C for 10 minutes. Each protein sample (20 µL) was loaded onto a 4-12% SDS-PAGE gel (1.5 M Tris-HCl pH 8.8, 0.5 M Tris-HCl pH 6.8, 30% acrylamide, 10% SDS, TEMED, 1% APS) with a protein ladder. Using the running buffer (250 mM Tris-HCl, 1.9 M Glycine, 1 % SDS, pH 8.3), the proteins were separated at 120 V and 175 V for 20 minutes and 60 minutes, respectively. Proteins were transferred onto a PVDF membrane for 16 hours at 65 V and 500 mA in transfer buffer (250 mM Tris, 1.9 M Glycine, 1 % SDS, pH 8.3) at 4°C. The membrane was washed 4 times for 5 minutes each with 1X TBST (20 mM Tris-HCl, 150 mM NaCl, 1%Tween, pH 7.5), blocked with 5 % Marvel for 1 hour and probed with primary antibody (anti-SOD, GRX, TRX, Nrf2 depending on the requirement for individual experiment) in 5 % Marvel overnight at 4°C. The membrane was washed four times for 5 minutes each and blocked with secondary antibody (Goat raised antibody to rabbit IgG or horse raised antibody to mouse IgG) for 1 hour at room temperature in the dark. The membrane was imaged following exposure to chemiluminescent HRP substrate using the Odyssey Imager from Li-Cor Biosciences according to the manufacturer's instructions.

2.2.10- GEL ELECTROPHORESIS OF PROTEINS MODIFIED THROUGH PROTEIN CARBONYLATION

The cells were treated with 100 µM H_2O_2, 250 and 500 mM ethanol, 150 and 300 µM zinc, 200 and 400 µM manganese, respectively for 3 and 6 hours at 37°C and 5 % CO_2, harvested using 0.25 %Trypsin-EDTA and washed twice

in PBS. Protein extraction was completed according to the manufacturer's instruction. Protein was incubated with manufacturer's 2x extraction buffer (up to 1x) on ice for 20 minutes followed by centrifugation at 15,000 x g for 20 minutes at 4°C and the supernatant transferred into a fresh tube. The sample protein concentration was quantified using the Amido black assay (Section 2.2.3). The protein was separated on a 4-12 % SDS, derivatised using 1x DNPH solution, incubated at room temperature for 15 minutes and neutralised before loading onto a Tris-Glycine gel according to the manufacturer's instruction. Modified proteins were separated at 150 V for 90 minutes. The membrane was washed using 1x PBST (PBS, pH 7.5 containing 0.05 % Tween) as opposed to the TBST used for other Western blot procedures.

2.2.11- JC1-MITOCHONDRIAL MEMBRANE POTENTIAL ASSAY

In a clear bottomed, dark sided 96-well plate 15,000 SH-SY5Y cells were seeded and allowed to attach overnight. The cells were (according to the kit manufacturer's instruction) washed once with 1x dilution buffer, stained with 20 µM JC-1 dye in 1x dilution buffer and incubated for 10 minutes at 37º C. The cells were washed twice in 1x dilution buffer solution after incubation with the dye before adding each treatment (100 µM H_2O_2, 250 and 500 mM ethanol, 150 and 300 µM zinc, 200 or 400 µM manganese, respectively). These were prepared in supplemented buffer (1x dilution buffer supplemented with 10% FBS) and incubated for 3, 6 and 24 hours after which the fluorescence was monitored at an excitation wavelength of 535/475 nm for aggregate only and aggregate plus monomer and 590/530 nm emission wavelength. FCCP 100 µM treatment for 4 hours is used as a positive control for the assay.

2.2.12- RHODAMINE 123 MITOCHONDRIAL MEMBRANE POTENTIAL ASSAY

Using a 12-well plate, 500,000 SH-SY5Y cells were seeded overnight. The cells were treated with 100 µM H_2O_2, 250 and 500 mM ethanol, 150 and 300 µM zinc, 200 and 400 µM manganese, respectively for 3 and 6 hours. An hour prior to the treatment end point, 6 µL of 2500 µg/mL Rhodamine 123 dye was added to each well with 3 mL DMEM. This was mixed thoroughly with culture

medium and incubated at 37º C for 1 hour. The media was removed into respective labelled tubes and the cells were washed with 1 mL ice cold PBS. Trypsin was added to the cells and the detached cells transferred into the previously labelled tubes. Each of the wells were rinsed with 1 % FBS DMEM to harvest all remaining cells and the suspension centrifuged at 500 g for 5 minutes. The supernatant was discarded, the cell pellets washed once in 1 mL ice cold PBS and resuspended in 500 µL of ice cold PBS containing 2 % FBS. The cells were analysed using the flow cytometer at the FL2 channel for Rhodamine 123 dye.

2.2.13- PROTEOSTAT AGGREGATION ASSAY

All reagents were brought to room temperature and vials centrifuged at 16,000 rpm for 5 seconds. Using a clear bottom dark sided 96-well plate, Proteostat positive and negative control were prepared according to the manufacturer's instruction. The protein standard solutions (0, 0.20, 0.39, 0.78, 1.56, 3.13, 6.25 and 12.5% aggregate, respectively) were mixed on a rotating rocker for 30 minutes and briefly centrifuged before use. Working detection reagent was prepared by mixing 10 µL stock detection reagent, 20 µL 10X assay buffer and 170 µL DMSO together in the dark according to manufacturer's instruction. To each well was added 2 µL of diluted detection reagent and 98 µL each of positive and negative control solutions, standard solutions and protein extract from 100 µM H_2O_2, 250 and 500 mM ethanol, 150 and 300 µM zinc, 200 and 400 µM manganese cell treatments respectively. The microplate was incubated in the dark for 15 minutes at room temperature and fluorescent signal was measured using the microplate reader at an excitation and emission filter setting of 550 nm and 600 nm, respectively.

2.2.14- DCFDA ROS ASSAY

In each well, 25,000 SH-SY5Y cells were seeded overnight. The cells were treated with 100 µL of 40 µM H_2O_2, 150 µM and 300 µM zinc sulphate, 200 µM and 400 µM manganese chloride, 250 mM and 500 mM ethanol, respectively for 6 and 24 hours using a phenol red free media. To each reactant, 100 µL of 2X 30 µM DCFDA solution was added and incubated in the dark at 37º C for

45 minutes. The fluorescent intensity was measured using a fluorescence plate reader at excitation of 485 nm and emission of 535 nm.

2.2.15- IMMUNOCYTOCHEMISTRY

Coverslips were sprayed with a generous amount of ethanol in the cell culture hood and left for 30 minutes to dry. The coverslips were transferred onto each well of a 12-well plate, and treated with 0.1% poly-L-lysine for 20 minutes. Coverslips were washed thrice and allowed to dry. SH-SY5Y cells were seeded (50, 000) on each coverslip and incubated for 48-72 hours to allow cells reach 70-80% confluence. Cells were treated with 500 mM ethanol, 300 µM zinc and control cells incubated with media for 24 hours. Following treatment, cells were washed twice with PBS and fixed with 0.25% glutaraldehyde for 20 minutes. Cells were incubated in PBS, 100 mM glycine and 10% FBS for 5 minutes each, washed twice with PBS, incubated with Triton X-100 for 20 minutes, washed twice with PBS, washed 4 times for 10 minutes each with 1mg/ mL sodium borahydride, washed twice with PBS and incubated overnight with 3% BSA at 4°C. Cells were washed twice with PBS and incubated with anti-LC3 (1:250) in the dark for an hour and anti-mouse secondary antibody (1:250) for another hour. Cells are washed twice with PBS and mounted with DAPI mounting medium, ready for imaging with the Leica confocal microscope.

Live cell modification: Cells (50,000) were seeded on a chamber slide to achieve 70-80% confluence, treated for 24 hours with 500 mM ethanol, 300 µM zinc and 400 µM manganese with control cells incubated in media. The cells are stained with 1 µM Mitotracker red for 20 minutes and 500 nM Lysotracker green for 15 minutes. The stains are replaced with phenol red free media and imaged using the Leica confocal microscope.

2.2.16- CELL FRACTIONATION

Cells treated with 250 mM and 500 mM ethanol for 24 hours were washed twice in ice cold PBS, scraped and centrifuged in an eppendorf at 4°C, 900 g for 5 minutes. The supernatant was discarded, and the pellet was resuspended

in ice-cold 1 M TRIS buffer (200 µL), sonicated and incubated on ice for 30 minutes. The lysate was centrifuged at 900 g, 4°C, for 5 minutes, the pellet is resuspended in RIPA buffer containing SDS and 0.01 % triton x-100. The supernatant was transferred into a new tube and centrifuged at 20,000 g 4°C, for 30 minutes. The resulting supernatant (cytosolic fraction) was collected while the pellet (membrane fraction) was washed with extraction buffer and then resuspended in 10 mM MES-buffered saline, incubated in ice for 1 h and centrifuged at 4°C, 20,000 g for 30 minutes and then stored at -20°C for subsequent analysis.

2.2.17- SOD ENZYME ACTIVITY ASSAY

This procedure was carried out according to the manufacturer's instructions (Fridovich, 1985). In brief, 9 x 10^6 differentiated SH-SY5Y cells were seeded overnight, treated with 250 and 500 mM ethanol, 150 and 300 µM zinc, 200 and 400 µM manganese, respectively for 24 h. Cells were harvested using a scraper in 500 µL of cold PBS, centrifuged for 10 minutes at 2,000 g, 4°C and the supernatant discarded. The cells were washed again in 1 mL PBS and centrifuged for 10 minutes at 2,000 g and 4°C. Cells were lysed using a freeze-thaw method of incubating cells at -20°C for 20 minutes and 37°C for 10 minutes thrice. Cells were sonicated in an ice bath to aid lysis and centrifuged at 4°C, 10,000 g for 15 minutes. The supernatant was diluted with 100 µL PBS. Sample solutions and blanks were added to each well as described in the table below:

Table 2.2- SOD enzyme assay protocol

	Sample (µL)	Blank 1 (µL)	Blank 2 (µL)	Blank 3 (µL)
Sample solution	20		20	
Double distilled water		20		20
WST working solution	200	200	200	200
Enzyme working solution	20	20		
Dilution buffer			20	20

The solutions were mixed thoroughly and the plate was incubated at 37°C for 20 minutes. The absorbance was monitored at 450 nm using the fluostar microplate reader. The following equation was used to calculate the SOD activity:

SOD activity (inhibition rate %) = {[(Ablank 1 - Ablank 3) – (Asample - Ablank 2)]/ (Ablank 1 - Ablank3)} x 100.

2.2.18- SEAHORSE ASSAY CELL TITRATION

Several parameters reflecting mitochondrial function were analysed using the Seahorse XFe Analyzer (Seahorse Biosciences, Massachusetts, USA). Several optimisation experiments were carried out to achieve optimal baseline readings and then the mitostress assay was carried out according to the Seahorse MitoStress Test Manual. SH-SY5Y cells were seeded at different densities into a Seahorse XF24 microplate in triplicate using recommended seeding density from the seahorse website database. The cells were seeded in 100 µL DMEM and incubated at 37°C, 5% CO_2 for 5-6 hours to adhere to the bottom of the plate, then topped up with 400 µL of DMEM and incubated overnight. The Seahorse XFe 24 analyser was warmed overnight and the assay cartridge soaked in 1 mL per well of XF calibrant overnight in a CO_2 -free incubator at 37°C. Using the XF 24- well plate, wells A1, B4, C3 and D6 are media only blank well with no cells. After approximately 24 hours, the XF media for the assay was prepared by supplementing the media with 10 mM glucose, 2 mM glutamine and 1 mM pyruvate. The pH of the media was adjusted to 7.4 using 0.1 M NaOH and the media was warmed up. An hour prior to the experiment, the cells are washed twice with the prepared XF media, where 500 µL of media was added and the plate incubated in CO_2 -free incubator at 37°C for at least 45 minutes before the start of the experiment. During incubation the software was prepared as per the manufacturer's instructions. When prompted the sensor cartridge with the calibrant plate is loaded onto the analyser tray to be calibrated and equilibrated. Subsequently, the cell culture microplate was loaded, tray door closed, and the assay started. Following the protocols already set up in the software, oxygen consumption

rate (OCR) and extracellular cell acidification rate (ECAR) readings for each well were taken and recorded.

2.2.19- THE MITOSTRESS TEST

Following the optimization experiments, the mitostress assay was carried out to determine the cell's mitochondrial responses to different treatments. This assay involved the measurement of the OCR of cells as a key parameter. After the injection of compounds (1 µM FCCP, 1 µM oligomycin and 0.5 µM antimycin A / rotenone mix) that are the modulators of the electron transport chain, parameters like the basal respiration, ATP production, proton leak, maximal respiration, spare respiratory capacity and non-mitochondrial respiration were measured/calculated. Differentiated SH-SY5Y cells were seeded overnight, the cells were treated with 250 mM ethanol, 250 mM ethanol and 1 µM CsA, 500 mM ethanol, 500 mM ethanol and 1 µM CsA, 150 µM zinc, 150 µM zinc and 1 µM CsA, 300 µM zinc, 300 µM zinc and 1 µM CsA, 200 µM manganese, 200 µM manganese and 1 µM CsA , 400 µM manganese, 400 µM manganese and 1 µM CsA, respectively and control cells incubated in seahorse media for 24 h and the mitostress assay performed on the cells following treatment.

An hour prior to the experiment, the cells are washed twice with the prepared XF media, in each well is added 500 µL media and the plate incubated in CO_2 -free incubator at 37°C for at least 45 minutes before the start of the experiment. During this incubation, the assay software was prepared according to the manufacturer's instruction. The cartridge ports A, B and C were loaded with 56 µL of 1 µM oligomycin, 62 µL of 1 µM FCCP and 69 µL of 0.5 µM Rotenone/ antimycin A respectively. When prompted the sensor cartridge with the calibrant plate is loaded onto the analyser tray to be calibrated and equilibrated. Subsequently, the cell culture microplate was loaded, tray door closed, and the assay initiated. Following the set protocols the OCR and metabolic profile for each well was assessed and recorded. The protein concentration from each well was also determined and result normalised using crystal violet.

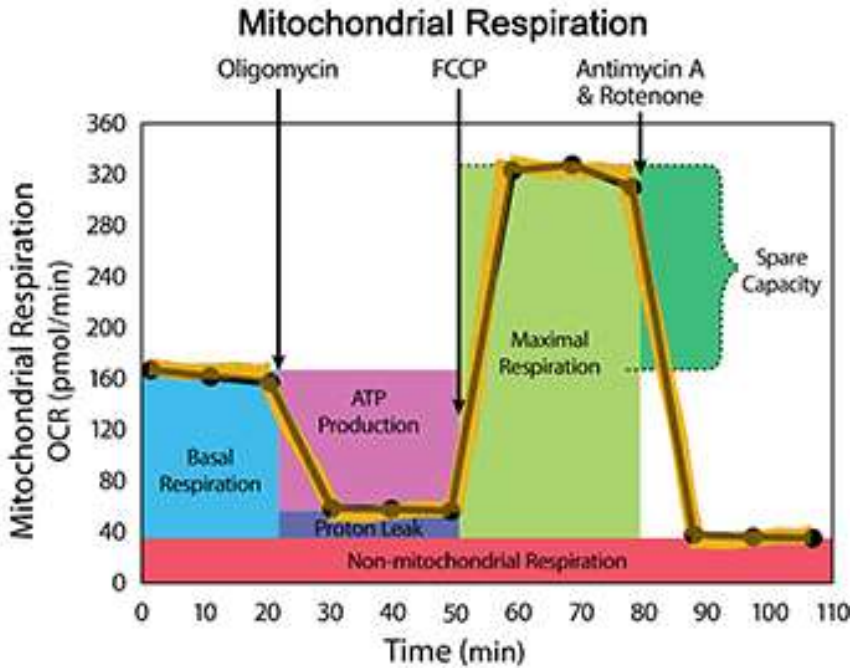

Figure 2.1- Diagram showing the typical metabolic profile of cells when studying mitochondrial function using the Seahorse MitoStress test assay (taken from Seahorse Biosciences MitoStress Test manual).

2.2.20- PROTEIN NORMALISATION

OCR readings were normalised against protein concentration. Here, cells were washed in PBS, and then lysed in 30 µL of RIPA buffer (Millipore, UK) for 30 minutes for 4°C. The protein concentration was determined for each well using 5 µL of lysate/BSA standard loaded in duplicate using Bradford reagent (Section 2.2.5).

2.2.21- SEAHORSE DATA ANALYSIS

The data file was analysed using the Seahorse Wave 2.0 software, which allows for normalization of OCR values against protein concentration of each well (or other means) and the removal of outlying values (determined by the standard deviation). The analysed data was then saved as a new Excel file. which is opened in MitoStress Report Generator. The assay parameters are automatically calculated and reported by the Muulti-File XF Report Generator. The table below explains the equations used to calculate each assay parameter.

Table 2.3- XF Cell Mito Stress Test Parameter Equations

Parameter value	Equation
Non-mitochondrial Oxygen Consumption	**Minimum rate measurement after Rotenone/antimycin A injection**
Basal Respiration	**(Last rate measurement before first injection) – (Non-Mitochondrial Respiration Rate)**
Maximal Respiration	**(Maximum rate measurement after FCCP injection) – (Non-Mitochondrial Respiration)**
H+ (Proton) Leak	**Minimum rate measurement after Oligomycin injection) – (Non-Mitochondrial Respiration**
ATP Production	**(Last rate measurement before Oligomycin injection) – (Minimum rate measurement after Oligomycin injection)**
Spare Respiratory Capacity	**(Maximal Respiration) – (Basal Respiration)**

2.2.22- STATISTICAL ANALYSIS

Densitometry data was calculated using value from the Li-Cor Odyssey imager and estimated as a fold increase relative to loading control-GAPDH/ β-actin. Statistical analysis was conducted using Graph Pad Prism 7.0 software. Data analysis were performed with one-way analysis of variance (ANOVA), Turkey's test for post-hoc analysis and two-way ANOVA test for the MTS assay.

Chapter 3

Dysregulated mitochondrial function/association with AD pathology in ethanol-induced oxidative stress

Contents

3.1- INTRODUCTION

With ageing, there is an increased susceptibility to alcohol-related injury (Moos *et al*., 2009), and alcohol-related cognitive impairment, largely associated with alcohol dependency and misuse (National Institute for Health and Care Excellence 2015). Ethanol can easily cross the blood brain barrier therefore prolonged exposure can cause an increase in reactive oxygen species (ROS), which leads to a series of deleterious events including increased lipid peroxidation, protein modification and DNA damage, which collectively activates a neuroinflammatory response leading to cell death (Comporti *et al.,* 2010). Whilst heavy alcohol consumption, together with reports of heavy smoking, and a positive apoE allele has been associated with earlier onset AD (up to 10 years earlier) (Harwood *et al*., 2010), moderate alcohol consumption have been reported to play a protective role. Experimental studies in SH-SY5Y cells have considered 500 mM ethanol exposure as relatively high hence represent heavy or excessive alcohol exposure with 10 mM considered low alcohol level (Getachew *et al.,* 2018, Ramlochansingh *et al.,* 2011) hence the choice of ethanol concentration used in this study. Although the mechanisms have not been elucidated, transgenic Aβ mouse models exposed to ethanol have reported increased levels of amyloid precursor protein (APP), beta-site APP cleaving enzyme 1 (BACE 1) and increased Aβ production indicating a link between ethanol consumption and AD pathology (Kim *et al.,* 2011).

In alcohol-related brain injury the regions most affected are the frontal temporal and hippocampal areas, the latter identified as the origin of AD onset (Lindberg *et al.,* 2012). In cells, a key target includes the mitochondrion, as it is the site for ethanol detoxification and a key source of ROS and mitophagy, both of which have been linked with ethanol-induced toxicity (Bonet-Ponce *et al.,* 2014). Mitophagy functions to maintain homeostasis, where mitochondria undergo constant fusion and fission throughout the cell cycle in response to changes in the redox environment and energy needs (Pi *et al.,* 2013). It is a form of selective autophagy and is considered a protective mechanism to avoid toxic accumulation of damaged mitochondria. Mitochondrial dynamics are

tightly regulated through mitochondrial fission proteins (dynamin-related protein 1 (Drp1), optic atrophy 1 (OPA1) or the pro-apoptotic Bcl-2 family member Bax) and mitochondrial fusion proteins (Uo *et al.,* 2009). Autophagy and mitophagy are regulated through crosstalk between key signalling pathways governed by the mammalian target for rapamycin (mTORC1) and the Ras/Erk pathway. Disruption of mitochondrial dynamics has been implicated in several neurodegenerative diseases resulting in severe neurological dysfunction due to inactivation or mutation of the major fusion/fission proteins (Berthelot *et al.,* 2016). However, the role of ethanol induced mitophagy nor the underpinning mechanisms have not been studied in neuronal cells relative to Aβ and tau expression, key markers of AD pathology.

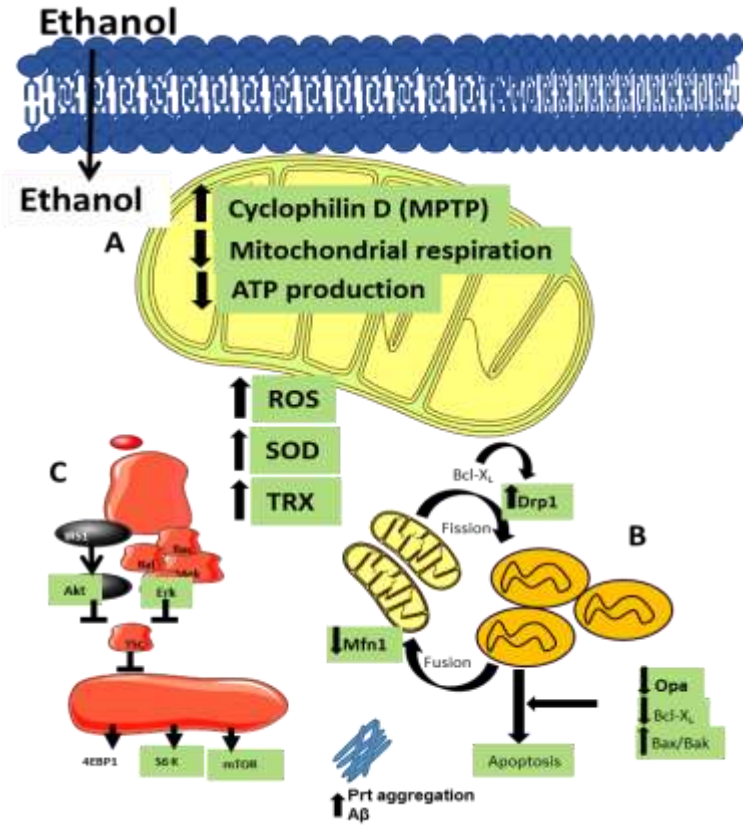

Figure 3.1-Pathways impacted by ethanol-induced neurotoxicity. Exposure of neuronal cells to toxic ethanol levels impair mitochondrial function, modulates the cell's antioxidant system and elicits response from the metabolic signalling pathways.

The schematic diagram (Figure 3.1) above highlights the processes and pathways impacted by chronic amount of ethanol. Exposure of SH-SY5Y neuronal cells to toxic amount of ethanol induce significant mitochondrial dysfunction as reflected by increased cyclophilin D, a mitochondrial protein closely related to mitochondrial permeability transition pore, thereby decreasing membrane potential. As a result, there is increased ROS generation with activation of antioxidant response. The levels of SOD and TRX proteins were raised to combat oxidative stress with mitochondrial respiration and ATP production both impaired (**A**). There is a disruption of the mitochondrial fission/fusion dynamics, with increased autophagy and apoptosis (**B**), through dysregulation of the Ras/ERK and PI3k/AKT/mTOR pathway ultimately leading to increase in protein aggregation and Aβ build-up (**C**).

3.2- AIMS AND OBJECTIVES

Hypothesis: Ethanol-induced neurotoxicity contribute to AD pathology through impairment of mitochondrial function and disrupted fusion/fission dynamics.

Specific aim 1: Investigate the impact of ethanol-induced oxidative stress on the redox status of SH-SY5Y neuronal cells.

Specific aim 2: Determine the effect of ethanol on neuronal cell mitophagy (fusion/fission dynamics) and protein aggregation.

Specific aim 3: Evaluate the impact of dysregulated mitochondrial function on Ras/ERK metabolic signaling pathway.

Specific aim 4: To understand the role of cyclosporine A in regulating mitophagy following ethanol-induced neurotoxicity.

Specific aim 5: Determine if ethanol-induced toxicity contribute to AD pathology in SH-SY5Y neuronal cell model.

3.3- RESULTS

3.3.1- ETHANOL DECREASES SH-SY5Y CELL VIABILITY, INCREASES ROS FORMATION AND MODULATES THE CELL ANTIOXIDANT SYSTEM

Exposure of SH-SY5Y neuronal cells to moderate and high ethanol (EtOH) concentrations caused a loss in cell viability and an increased production of ROS (Figure 3.2). SH-SY5Y cell viability was significantly decreased in a concentration (125-1000 mM) and time dependent manner (6 h, $p \leq 0.0001$ for all EtOH concentrations, 24 h, $p = 0.0046$, ≤ 0.0001 and ≤ 0.0001 for 250 mM, 500 mM and 1 M concentrations respectively and 48 h, $p \leq 0.001$ and $p \leq 0.0001$ for 500 mM and 1 M EtOH concentrations, Figure 3.2A). To better understand the mechanism underlying the cytotoxic effects of EtOH in SH-SY5Y cells, ROS generation following EtOH exposure was investigated. SH-SY5Y cells were labelled with DCFDA which forms a highly fluorescent compound DCF in response to ROS oxidation. A significant increase in DCF intensity was measured in a dose dependent manner after 6- and 24-hour EtOH exposure. There was a significant increase in cells exposed to 500 mM EtOH for 6 h and cells exposed to 250 mm 500 mM EtOH for 24 h ($p = 0.0403$ and $p = 0.0012$, ≤ 0.0001 respectively, Figure 3.2B). In response to EtOH-induced toxicity, there was significant increase in SOD levels following exposure to 500 mM EtOH for 24 h, no significant change to GRX levels and significant increase in TRX levels in cells exposed to 250 mM EtOH for 24 h ($p=0.0268$ and $p=0.0071$ respectively, Figure 3.3A & C) with 40 µM H_2O_2 used as oxidative stress-inducing positive control. SOD activity, which plays an important role in ROS metabolism was also measured. At 3 h EtOH exposure, there was a significant increase in SOD activity following 250 and 500 mM EtOH concentrations and a significant decrease from 500 mM exposure for 24 h ($p=0.0019$, 0.0063 and $p=0.0215$ respectively, Figure 3.4A & B)

The results suggest that the SOD and TRX systems rather than the GRX protect the cells from ethanol-induced neurotoxicity and SOD activity is increased as a coping mechanism to combat the induced oxidative stress in acute condition but is eventually overwhelmed with persistent exposure to EtOH.

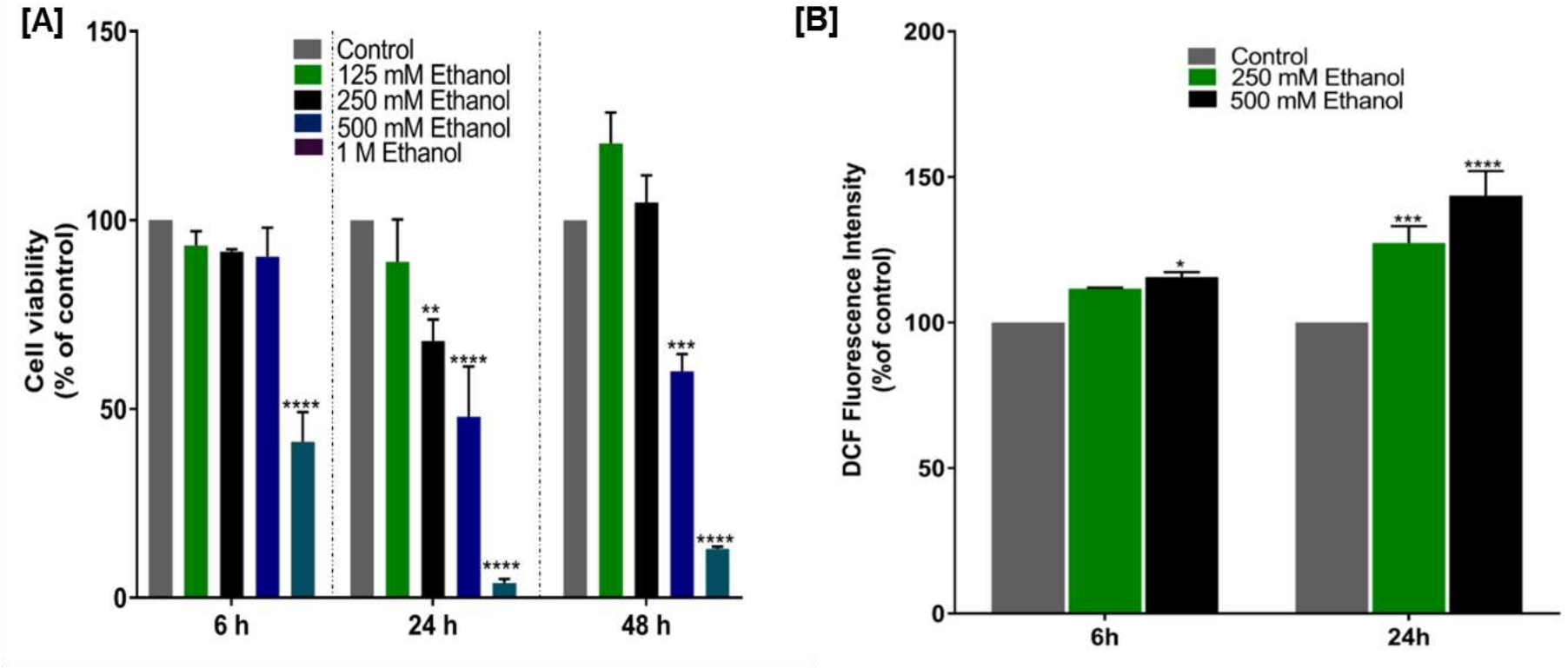

Figure 3.2: Loss of cell viability and an increase in ROS in SH-SY5Y cells in response to ethanol toxicity. Cell viability/metabolic activity and intracellular ROS generation in ethanol treated SH-SY5Y cells determined by MTS reduction and DCFDA fluorescent dye staining, respectively. **Panel A:** Cells were treated with 125-1000 mM ethanol, relative to control cells and incubated for 6 h, 24 h and 48 h, respectively. Cell viability was assessed using the MTS assay and the change in absorbance measured at 500 nm. **Panel B:** Cells were treated with 250 mM and 500 mM ethanol, respectively, relative to control cells for 6 and 24 h. Intracellular ROS was assessed using DCFDA and DCF fluorescent intensity at 500 nm. Data are expressed as mean ± SEM of 3 independent experiments. *p ≤ 0.05, **p ≤ 0.01, ***p ≤ 0.001, ****p ≤ 0.0001 relative to control.

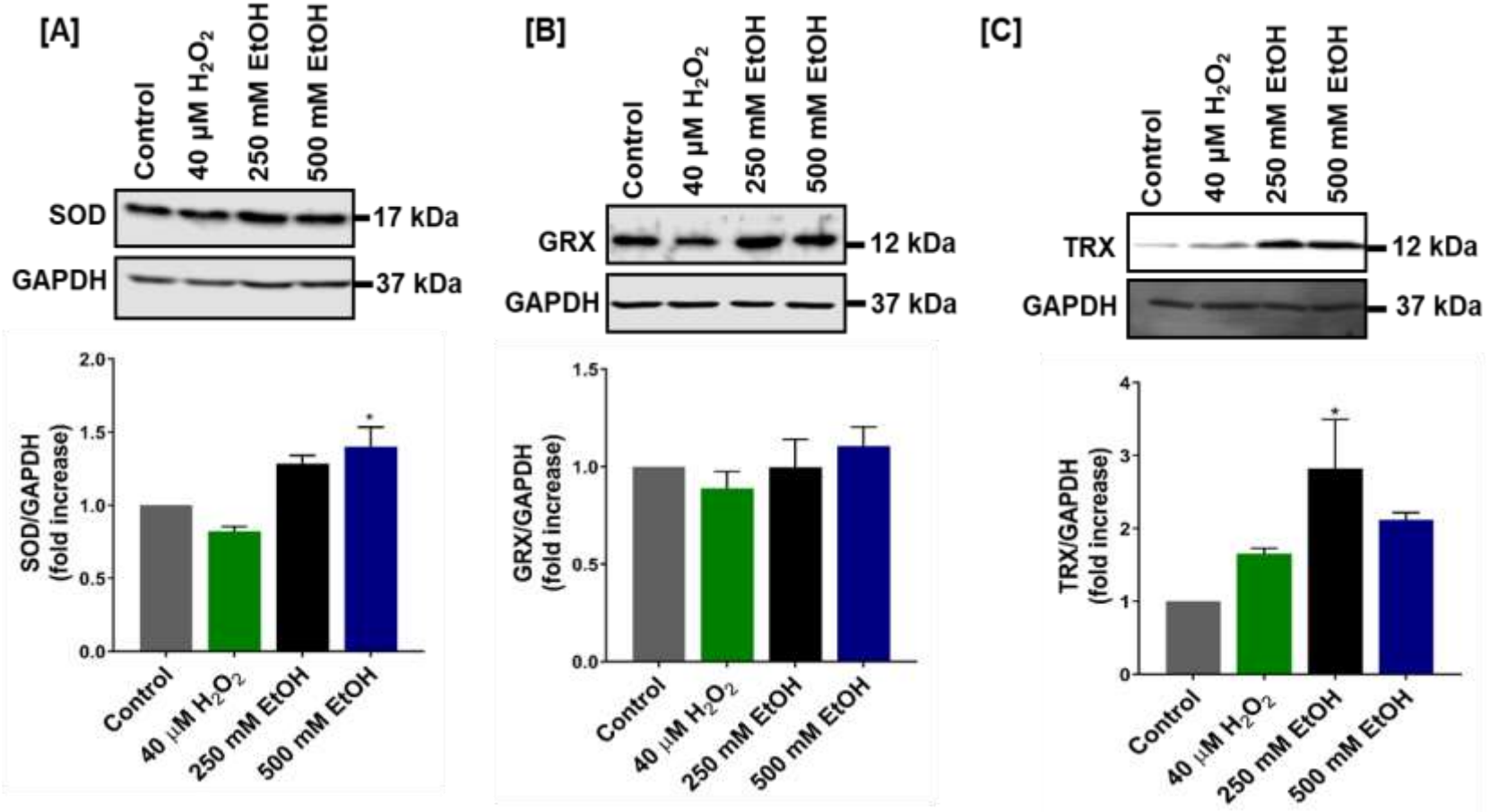

Figure 3.3- Differential protein expression of SOD, GRX and TRX in ethanol treated SH-SY5Y neuronal cells. Cells were treated as indicated relative to control cells for 24 h. SOD, GRX and TRX protein expression were determined by Western blot analysis. Immunoblot of **Panel A:** SOD, **Panel B:** GRX**, Panel C**: TRX and their respective GAPDH expression. Data was normalized to respective GAPDH and expressed as mean ± SEM of 3 independent experiments. *p ≤ 0.05 compared to control.

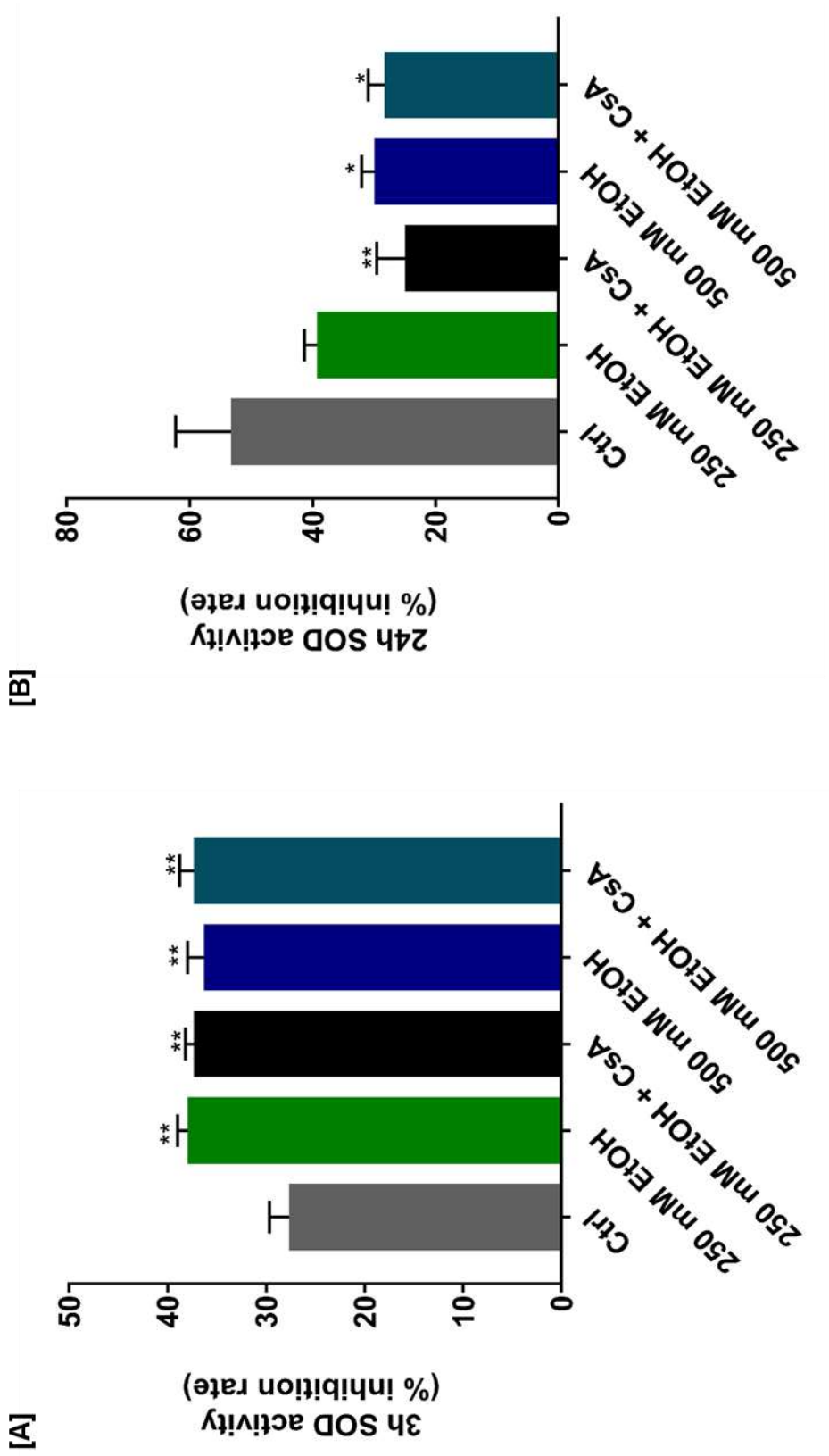

Figure 3.4. SOD activity in ethanol treated SH-SY5Y neuronal cells. Cells were treated as indicated relative to control cells and assayed for SOD activity using the SOD enzyme activity assay kit. **Panel A:** SOD activity in response to varied ethanol concentrations and CsA cotreatments incubated for 3 h and **Panel B:** SOD activity in response to varied ethanol concentrations and CsA cotreatments incubated for 24 h. Data are expressed as mean ± SEM of 3 independent experiments. *$p \leq 0.05$ and **$p \leq 0.01$ compared to control.

3.3.2- ALTERED MITOCHONDRIAL MEMBRANE POTENTIAL AND BIOENERGETICS IN ETHANOL-TREATED SH-SY5Y CELLS

In response to EtOH treatment, mitochondrial membrane potential (MMP) was measured using the fluorogenic dye JC-1. A significant reduction of MMP was observed following EtOH treatment at 500 mM (p= 0.0130, Figure 3.5A), with no significant change or recovery effect observed following ethanol-CsA cotreatment.

The effect of EtOH on mitochondrial bioenergetics using the Agilent seahorse XFe24 analyzer was determined. SH-SY5Y neuronal cells were treated with 250 mM and 500 mM EtOH and control cells treated with 10 % FBS DMEM for 24 hours prior to performing the Mito Stress assay. This assay measures OCR, basal mitochondrial respiration, proton leak, spare respiratory capacity and ATP production (Figure 3.5 C, D and E). In a concentration-dependent manner, varying effect of EtOH treatment was observed with 250 mM ETOH treatment causing an increase and 500 mM ETOH treatment causing a decrease in basal mitochondrial respiration and oxygen consumption. There was a significant increase in basal mitochondrial respiration following 250 mM EtOH treatment ($p \leq 0.0001$) and significant decrease following 500 mM EtOH ($p=0.0008$). The same pattern was observed in proton leak ($p=0.0054$ and 0.0446), spare respiratory capacity ($p=0.0007$ and ≤ 0.0001) and ATP production ($p \leq 0.0001$and ≤ 0.0001) respectively (Figure 3.5 C, D and E).

The expression of the mitochondrial matrix marker cyclophilin D was significantly increased in response to 250 mM EtOH treatment ($p=0.0088$, Figure 3.6A) suggesting also a possible disruption of calcium metabolism with no significant change following 40 µM H_2O_2 treatment used as a positive control for oxidative stress. The mitochondrial chaperone Hsp60 level following 250 mM EtOH treatment was significantly decreased ($p=0.0392$, Figure 3.6B).

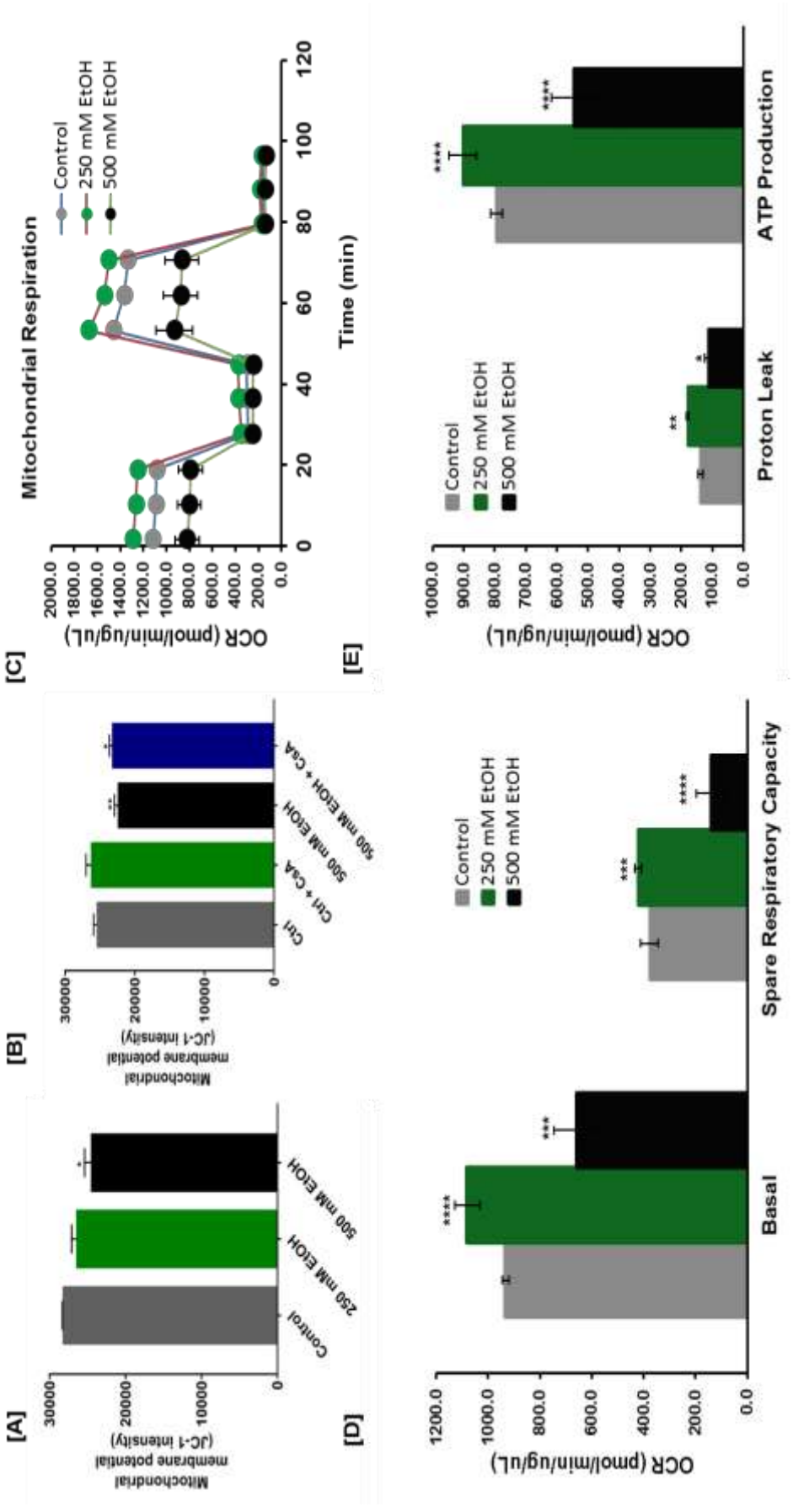

Figure 3.5- Ethanol exposure decreased mitochondrial membrane potential and altered mitochondrial respiration in SH-SY5Y cells. Cells were treated as indicated relative to control cells for 24 h. **Panel A and B:** JC-1 assay measuring MMP. **Panel C:** Seahorse Mito Stress Test measuring oxygen consumption rate (OCR), **Panel D:** basal mitochondrial respiration and spare respiratory capacity, **Panel E:** mitochondrial proton leak and ATP production. Data are expressed as mean ± SEM of 3 independent experiments. *p ≤ 0.05, **p ≤ 0.01, ***p ≤ 0.001, ****p ≤ 0.0001 compared to control.

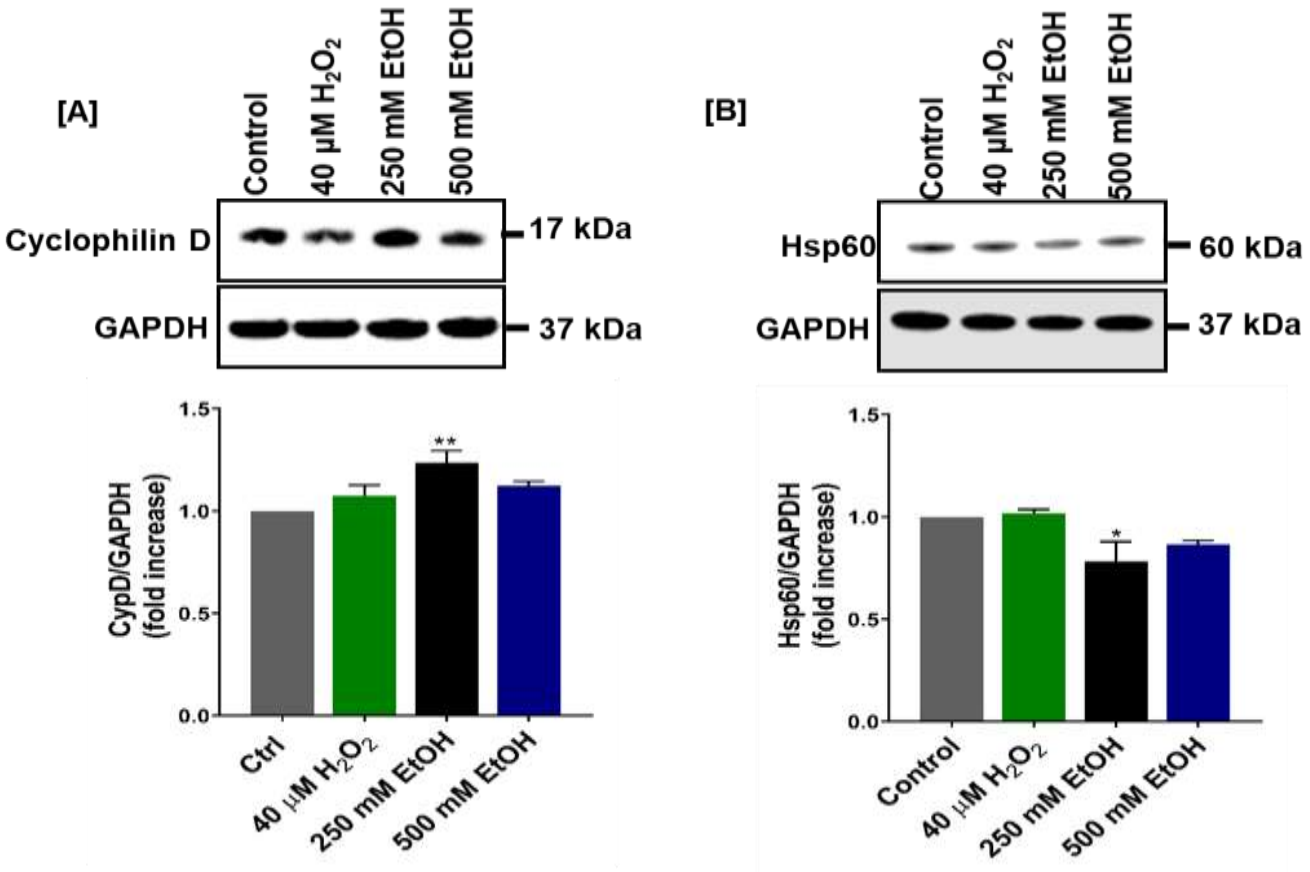

Figure 3.6. Expression of mitochondrial proteins Cyclophilin D and Hsp60 in ethanol treated SH-SY5Y neuronal cells. Cells were treated as indicated relative to control cells for 24 h. Cyclophilin D/ Hsp60 protein expression was determined by Western blot analysis. Data is expressed relative to GAPDH and control. **Panel A:** Representative Immunoblot, and densitometric analysis of Cyclophilin D relative to GAPDH expression. **Panel B:** Representative Immunoblot and densitometric analysis of Hsp60 relative to GAPDH expression. Data are expressed as mean ± SEM of 3 independent experiments. *p ≤ 0.05, **p ≤ 0.01 compared to control.

3.3.3- ETHANOL-INDUCED MITOCHONDRIAL DYNAMICS DISRUPTION

Cyclosporine A, an inhibitor of cyclophilin D responsible for MPTP opening and function was used as co-treatment the EtOH treated cells to determine whether it plays a protective role with reference to EtOH-induced neurotoxicity. Furthermore, the mitochondrial fusion/fission cycle plays an important intracellular role in maintaining neuronal cell homeostasis. To determine the effect of EtOH on mitochondrial dynamic complexes, the fission/fusion pathway protein levels were examined. The protein levels of dynamin-like GTPases Drp1, OPA1 and MFN1 were determined by Western blot analysis.

As shown in Figure 3.7A, EtOH exposure increased fission, as shown by a significant increase seen in Drp1 in response to 250 mM EtOH ($p=0.0061$) with no recovery effect observed by 250 mM EtOH + CsA co-treatment. Cells exposed to 1 µM CsA showed significant increase ($p=0.0243$). The level of the fusion protein, MFN1, was decreased on exposure to 500 mM EtOH. Cells treated with 1 µM CsA only showed significant increase ($p=0.0033$) suggesting its tendency to promote mitochondrial fission while cells co-treated with 500 mM EtOH and CsA showed a significant increase suggesting a likely recovery effect ($p=0.0284$, Figure 3.7C). Similarly, OPA1, was decreased on exposure to 500 mM EtOH. Cells treated with both 250 mM EtOH + CsA and 500 mM EtOH + CsA showed a significant increase suggesting a likely recovery effect ($p=0.0047$ and $p=0.0362$, Figure 3.7B).

Morphological changes in mitochondria were also observed in cells exposed to 500 mM EtOH as monitored by the mitochondrial dye Mito Tracker. Following 24 h treatment, cells become rounded with punctate structure typical of mitochondrial fission (Figure 3.7D) .

In response to 500 mM EtOH, there was significant increase in the apoptotic marker Bax ($p=0.0470$), however a significant decrease in Bax levels from 250 mM EtOH and 250 mM EtOH + CsA treatments ($p= 0.0111$ and $p=0.0267$ respectively, Figure 3.8A). Interestingly, anti-apoptotic marker Bcl2 protein levels did not show any significant change (Figure 3.8B).

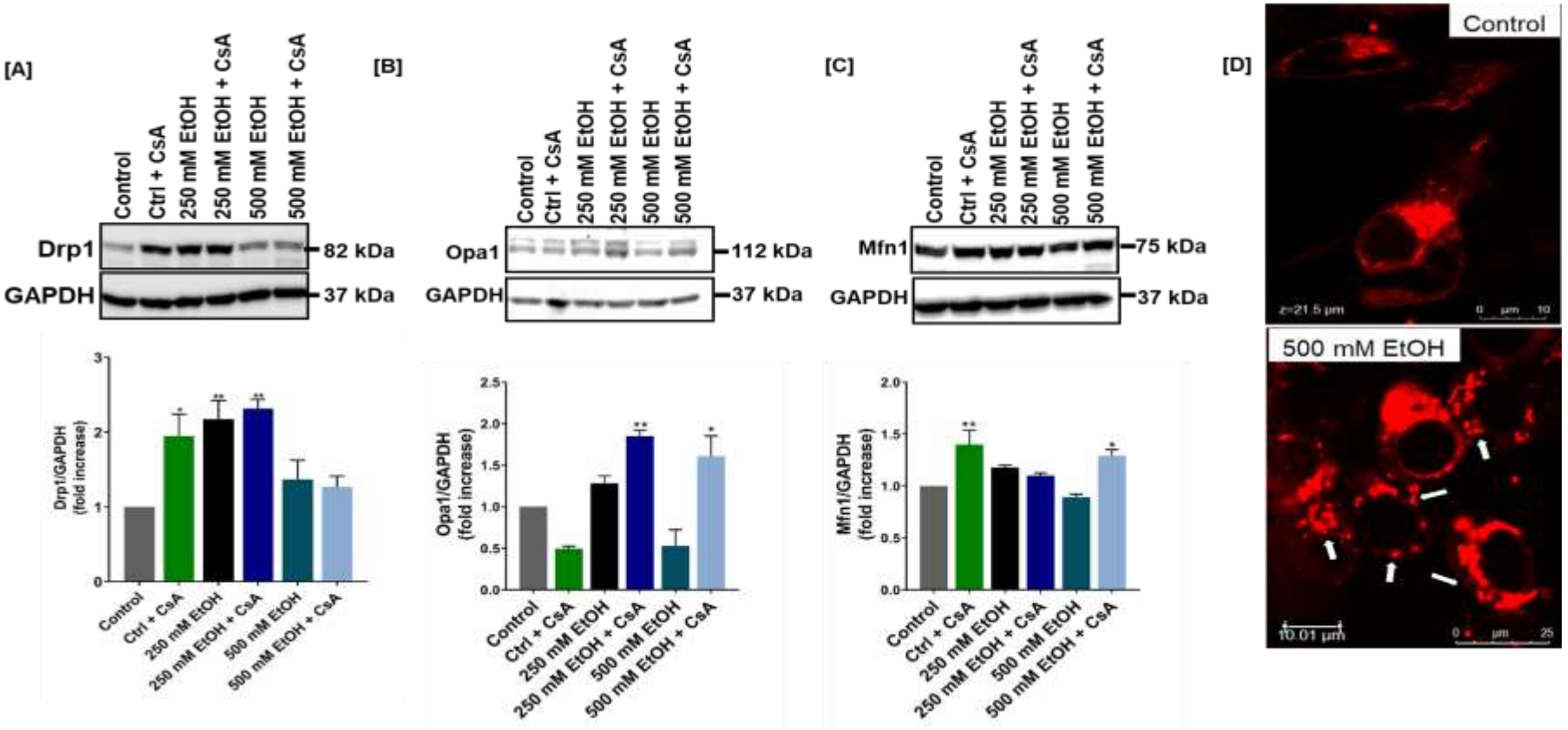

Figure 3.7. Differential expression of mitochondrial fission protein Drp1 and fusion proteins Opa1 and Mfn1 in ethanol treated SH-SY5Y neuronal cells. Cells were treated as indicated relative to control cells for 24 h. Protein expression was determined by Western blot analysis. Data is expressed relative to GAPDH and control samples**. Panel A:** Representative Immunoblot and densitometric analysis of Drp1 **Panel B:** Opa1 **Panel C:** Mfn1 relative to GAPDH expression. **Panel D:** Confocal analysis of Mitotracker red in control relative to ethanol treated cells. Arrows indicate a fragmented and rounded mitochondria typical of mitochondrial fission. Data are expressed as mean ± SEM of 3 independent experiments (n=3). *p ≤ 0.05, **p ≤ 0.01 compared to control.

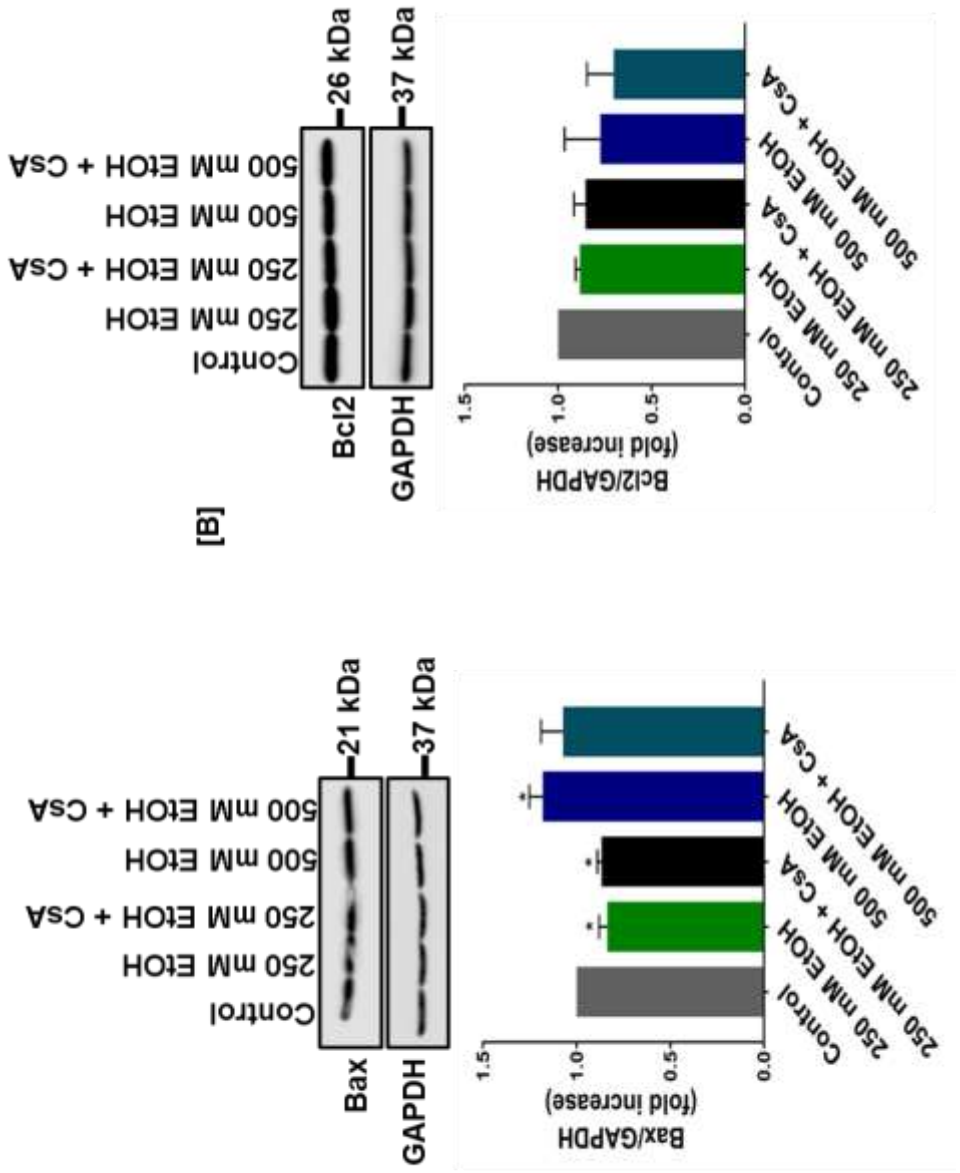

Figure 3.8- Apoptotic markers Bax and Bcl2 in ethanol treated SH-SY5Y neuronal cells. Cells were treated as indicated relative to control cells for 24 h. Protein expression was determined by Western blot analysis. Data is expressed relative to GAPDH and control samples. **Panel A:** Representative Western blot and densitometric analysis of Bax relative to GAPDH expression **Panel B:** Representative Western blot and densitometric analysis of Bcl2 relative to GAPDH expression. Data are expressed as mean ± SEM of 3 independent experiments. *p ≤ 0.05. compared to control.

3.3.4- ETHANOL TREATMENT ELICITS AUTOPHAGY IN SH-SY5Y CELLS

Cells maintain homeostasis by recycling damaged organelles through the process of autophagy. To maintain cell homeostasis, autophagy is activated to allow for recycling of damaged cell organelles. This process is an adapted mechanism for cell survival. In this study, it has been shown that exposing SH-SY5Y cells to EtOH caused an increase in autophagy evidenced by an increase in LC3I/II and p62. Results showed a significant increase in the conversion of LC3-I to its lipid-conjugated autophagosome-bound form LC3-II in both EtOH treatments (Figure 3.9A, $p=\leq 0.0001$). The levels of p62, the protein delivering ubiquinated autophagic cargo to the autophagosomes by interacting with LC3 was also increased at 500 mM EtOH treatment (Figure 3.9B).

Immunofluorescence confocal microscopy was also used to detect LC3 following EtOH exposure showing an increased LC3 staining in cells exposed to EtOH treatment after 24 h (Figure 3.9C). The autophagic machinery is sometimes specifically targeted to a single organelle and this was determined by confocal imaging of EtOH-treated cells stained with Mitotracker Red and Lysotracker green. Results showed possible co-localization of Mitotracker Red and Lysotracker green (Figure 3.10) and a completely disrupted and fragmented mitochondria in response to EtOH treatment.

This is suggestive of autophagy/mitophagy playing a role in mediating EtOH-induced neurotoxicity. The activation of both pathways is indicative of the cell's response mechanism of initiating a process targeted at getting rid of dysfunctional and damaged organelle.

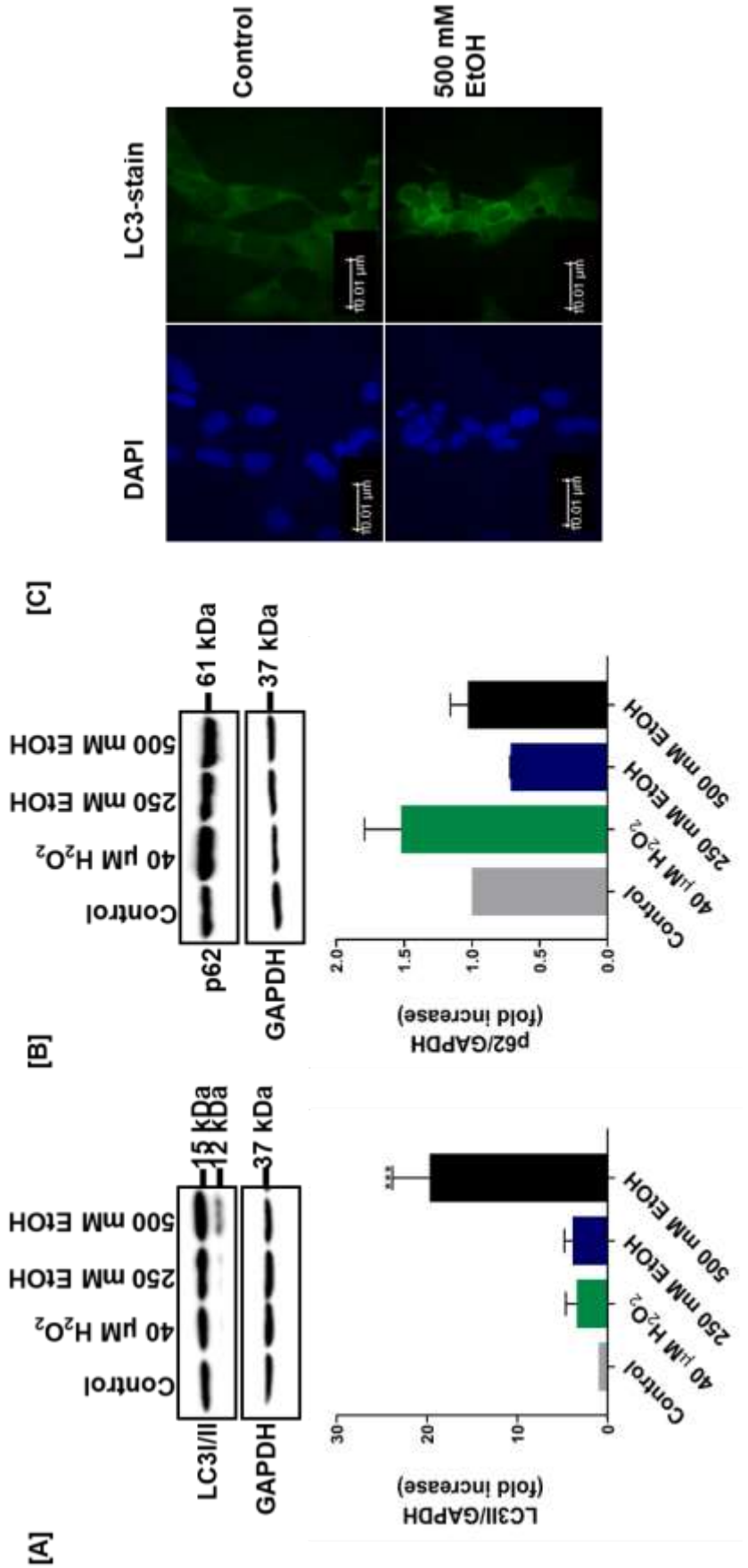

Figure 3.9- Autophagy is increased in ethanol treated SH-SY5Y neuronal cells. Cells were treated as indicated relative to control cells for 24 h. Protein expression was determined by Western blot analysis. Data is expressed relative to GAPDH and control samples. **Panel A:** Representative Western blot and densitometric analysis of LC3I/II relative to GAPDH expression **Panel B:** Representative Western blot and densitometric analysis of p62 relative to GAPDH expression. **Panel C:** Using confocal microscopy LC3 expression was increased in EtOH treated samples relative to controls. Arrow show membrane versus nuclear staining of the autophagy marker LC3. Cells treated with 500 mM EtOH show an accumulation of LC3 in the nucleus. Data are expressed as mean ± SEM of 3 independent experiments. ***p ≤ 0.001 compared to control.

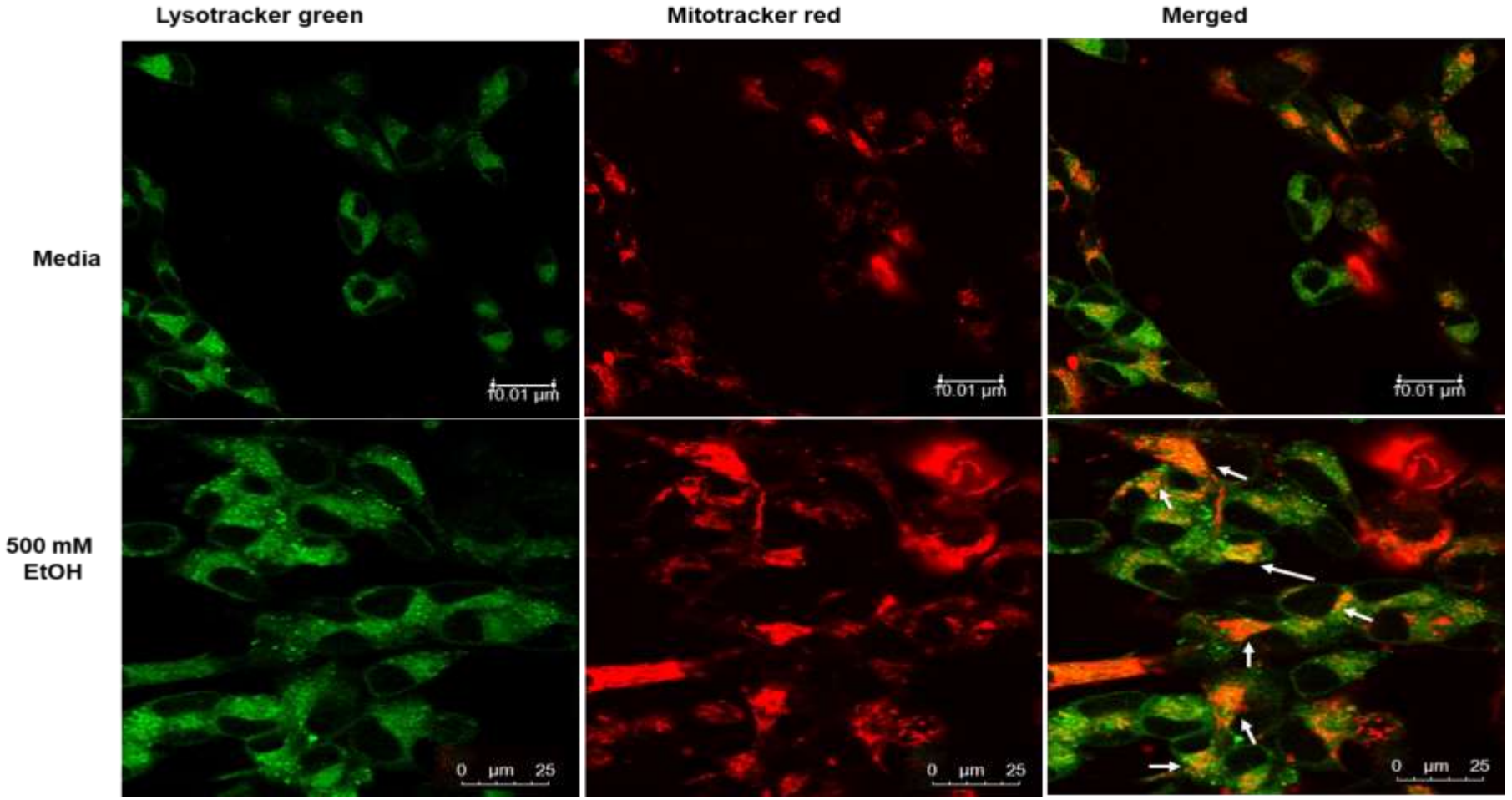

Figure 3.10- Representative confocal images of MitoTracker Red (MTR) and LysoTracker green (LTG) in SH-SY5Y cells treated with or without 500 mM EtOH for 24 h. The morphology of the mitochondria in response to 500 mM EtOH exposure was visualised using the MTR dye. Arrows show colocalisation between MTR and LTR indicative of mitophagy.

3.3.5- ETHANOL EXPOSURE ACTIVATES THE RAS/ERK AND PI3K/AKT, MTORC1/S6K PATHWAYS IN SH-SY5Y NEURONAL CELLS

The Ras/ERK and PI3K/Akt/mTORC1 pathways are involved in various cell signalling events such as cell survival and death, play a role in maintaining neuronal plasticity and this pathway has been implicated in the pathogenesis of many human diseases. Receptors to several growth factors are linked to the Ras/ERK and PI3K/Akt signalling pathways. For instance, the mTORC1 complex, an important regulator of growth and metabolism is regulated by the Ras/Erk signalling pathway. In this study, to understand the potential pathways involved in autophagy-induced cell death the effect of EtOH exposure on the inter-related pathways- PI3K/Akt and mTORC1/p70S6K axis and the Ras/ERK, pathways was determined using Western blot analysis.

The activation of Erk, Akt, mTORC1 and S6k indicated by the ratio of phosphorylation of Erk at Thr202/Tyr204, Akt at T308, S6K at T229 and mTOR at S2481 respectively against the total Erk, Akt, mTOR and S6K values were determined. Result showed significant increase in activation of Akt in response to 500 mM EtOH, 250 mM and 500 mM EtOH-CsA cotreated cells ($p= 0.0177$, $p= 0.0194$, $p= 0.0464$, Figure 3.11B) and significant increase in activation of mTOR in 500 mM EtOH and 500 mM EtOH-CsA cotreated cells ($p=0.0294$, $p= 0.0003$, Figure 3.11C) and no significant changes to p-S6K and Erk activation. (Figure 3.11A & D).

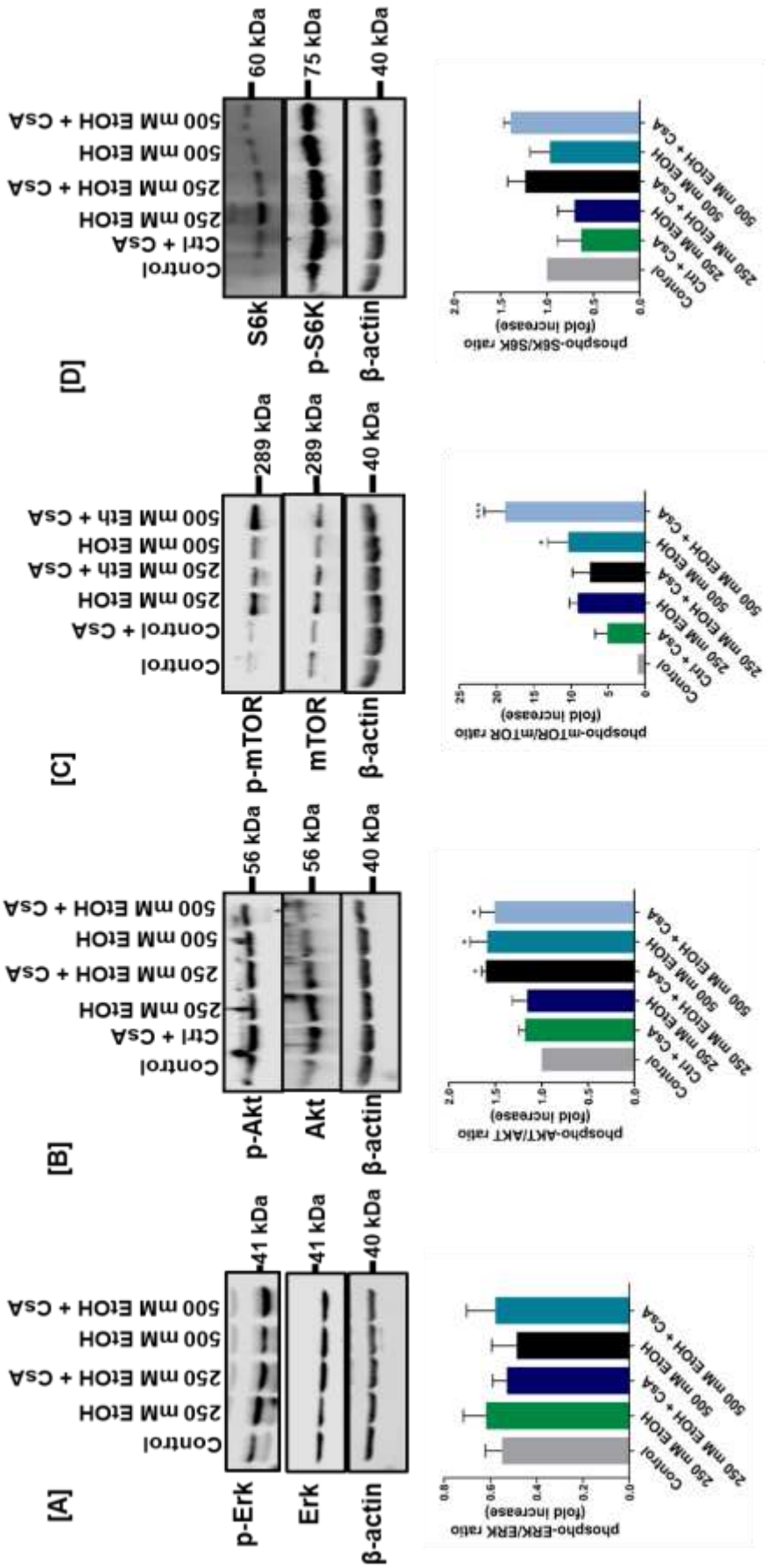

Figure 3.11. Phosphorylation of the Ras/Erk and P13K/Akt/mTOR signalling pathways are regulated by ethanol in SH-SY5Y neuronal cells. Cells were treated as indicated relative to control cells for 24 h. Protein expression was determined by Western blot analysis. **Panel A:** Representative Western blot and densitometric analysis of pErk/ Erk ratio relative to actin expression **Panel B:** Representative Western blot and densitometric analysis of pAkt/ Akt ratio relative to actin expression. **Panel C:** Representative Western blot and densitometric analysis of p-mTOR/mTOR ratio relative to actin expression. **Panel D:** Representative Western blot and densitometric analysis of p-S6K/S6K ratio relative to actin expression Data are expressed as mean ± SEM of 3 independent experiments (n=3). *p ≤ 0.05, ***p ≤ 0.001 compared to control.

3.3.6- IMPACT OF ETHANOL ON METABOLIC PROTEINS BCATM AND GDH

The BCATm and GDH are both enzymes responsible for branched chain amino acids (BCAA) and glutamate catabolism. GDH is part of a protein complex formed by BCATm and BCKDC responsible for BCAA oxidation and cycling of nitrogen (Islam *et al.,* 2010). As a result of the participation of these enzymes in BCAA metabolism and its potential involvement in AD pathology we investigated the impact of EtOH on BCATm and GDH expression.

There was a significant increase in BCATm protein in cells were exposed to 250 mM and 500 mM EtOH for 24 h (p= 0.0371 and p= 0.0003, Figure 3.12A) with 40 µM H_2O_2 used as oxidative stress positive control significantly decreased (p= 0.0228). However, there was a decrease in GDH levels in cells exposed to 40 µM H_2O_2 (p= <0.0001) and 500 mM EtOH treatment for 24 h (p=0.0104, Figure 3.12B). This data suggests the key proteins involved in BCAA metabolism are regulated by EtOH exposure.

3.3.7- ETHANOL INCREASES PROTEIN AGGREGATION WHILE INCREASING Aβ LOAD

Protein misfolding is a hallmark of several neurodegenerative disorders including Alzheimer's disease. As a result of its association with increased oxidative stress, we investigated the impact of EtOH treatment on total cell protein aggregation. There was a significant increase in aggregated protein following 250 mM EtOH treatment (p= 0.0168, Figure 3.13A) with similar effect when cells cotreated with CsA (p=0.0236, Figure 3.13A). At 500 mM EtOH concentration, significant increase in aggregated proteins was sustained and similarly with CsA co-treatment (p= 0.0003 and 0.0018, Figure 3.13A).

Finally, an increase in the expression of Aβ was observed in 1 µM CsA, 250 and 500 mM EtOH treated cells (p= 0.0001, 0.0013, Figure 3.13B) with a significant reduction when cells were co-treated with CsA (Figure 3.13B). Interestingly, there was an inverse effect on phosphorylated tau expression with EtOH treatment. Cells treated with 250 mM and 500 mM EtOH showed a significant decrease in p-tau protein expression (p≤ 0.0001 and ≤ 0.0001, Figure 3.13C) respectively.

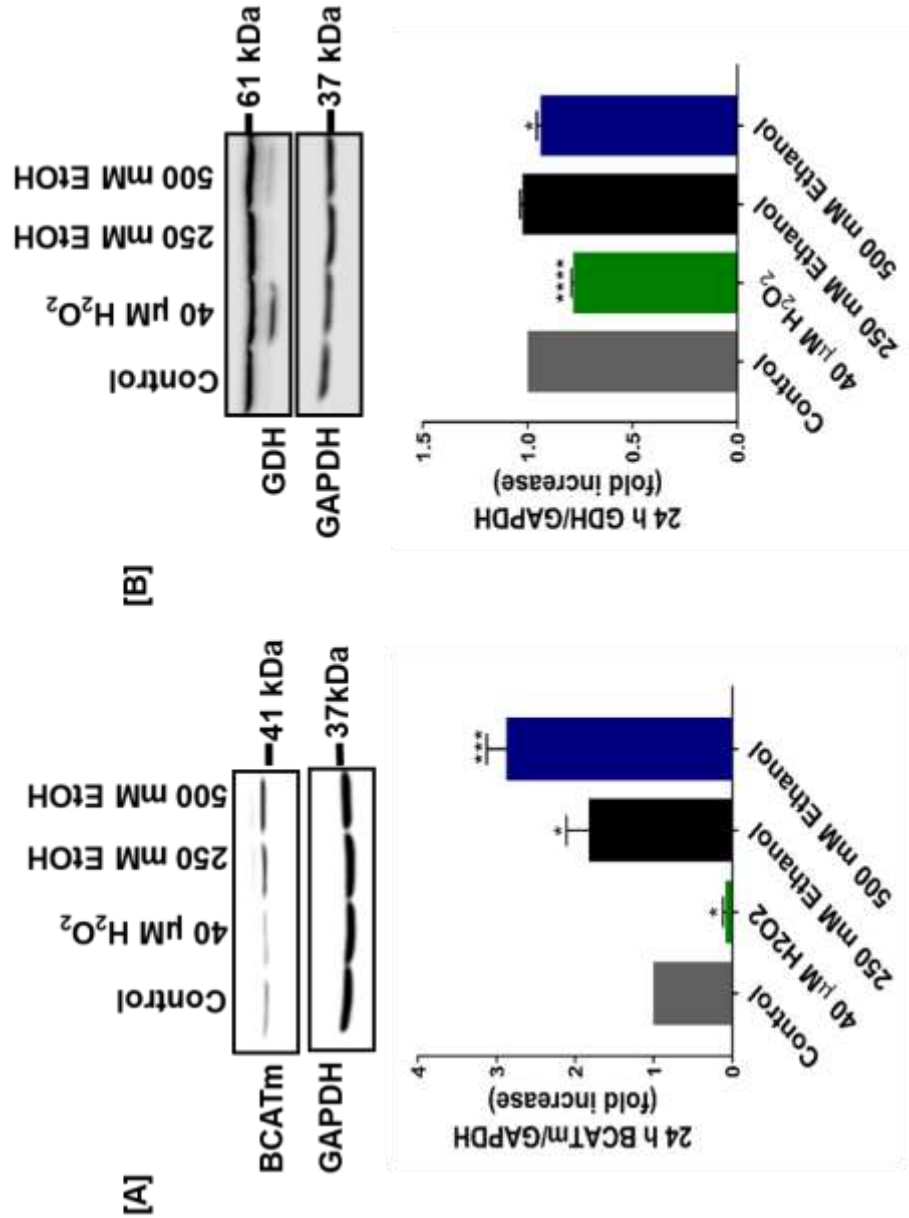

Figure 3.12. Metabolic proteins BCATm and GDH are upregulated in ethanol treated SH-SY5Y neuronal cells. Cells were treated as indicated relative to control cells for 24 h. Protein expression determined by Western blot analysis. Data is expressed relative to GAPDH and control samples. **Panel A:** Representative Western blot and densitometric analysis of BCATm relative to GAPDH expression. **Panel B:** Representative Western blot and densitometric analysis of GDH relative to GAPDH expression. Data are expressed as mean ± SEM of 3 independent experiments (n=3). *$p \leq 0.05$, ***$p \leq 0.001$

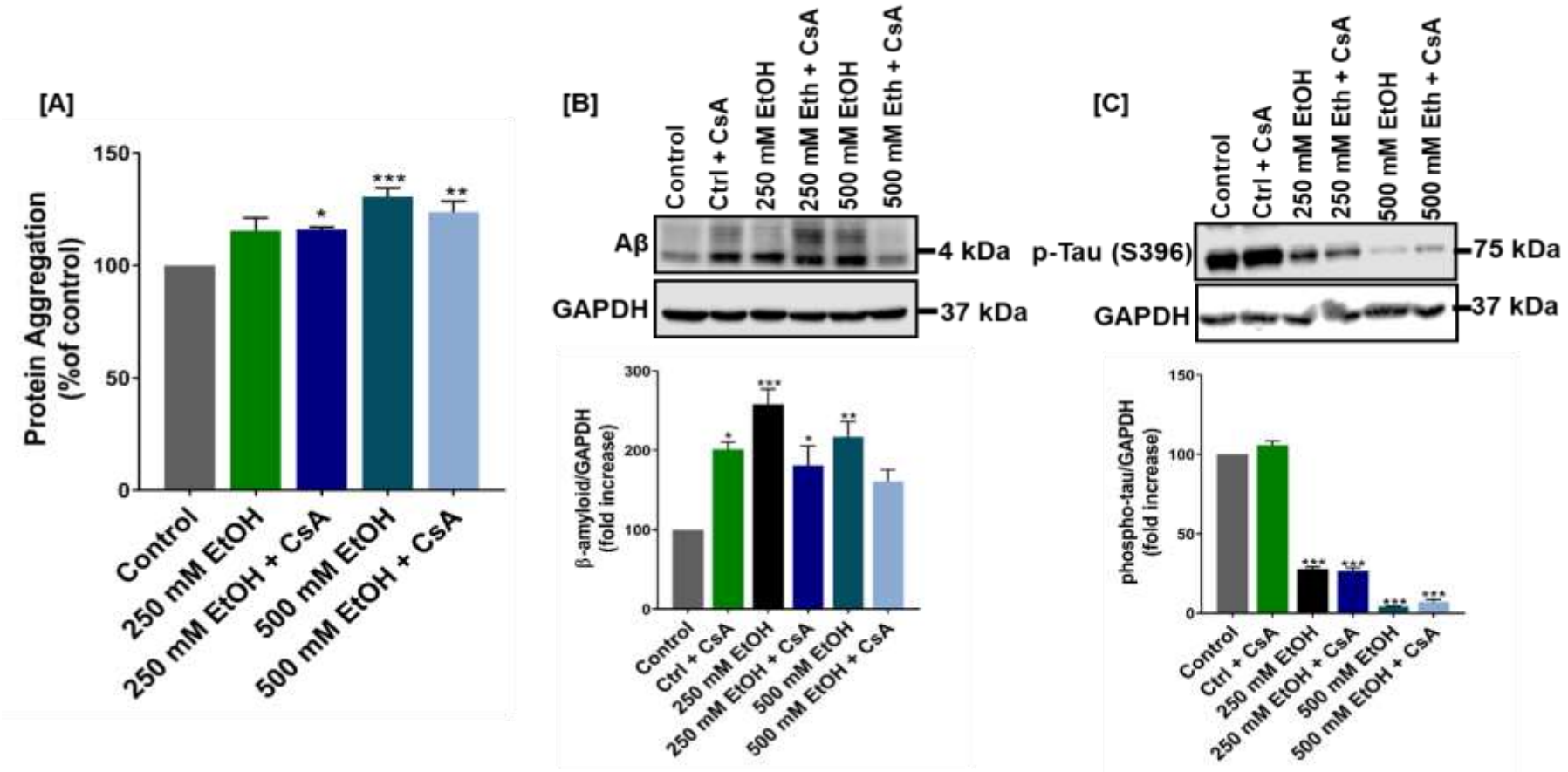

Figure 3.13. Protein aggregation is increased in EtOH treated in SH-SY5Y cells with an increase in Aβ but a concomitant decrease in pTau. Cells were treated as indicated relative to control cells for 24 h. Protein aggregation was determined using the Proteostat total protein aggregation assay. In a separate experiment, under the same conditions, the level of Aβ and pTau were assessed using Western blot analysis. **Panel A:** Histogram representing the percentage of aggresome formation relative to control. **Panel B:** Representative Western blot and densitometric analysis of Aβ relative to GAPDH expression. **Panel C:** Representative Western blot and densitometric analysis of p-Tau relative to GAPDH expression. Data are expressed as mean ± SEM of 3 independent experiments. *p ≤ 0.05, **p ≤ 0.01, ***p ≤ 0.001 compared to control.

3.4- DISCUSSION

Previous studies have established that EtOH and its toxic metabolite acetaldehyde, induces oxidative stress in neuronal cells and dysregulates intracellular redox balance (Yan *et al.,* 2016, Liu *et al.,* 2014, Hernandez *et al.,* 2016). Several studies in humans have tried to link alcohol consumption and AD pathology with competing outcomes and theories. Some studies propose a faster decline in cognitive function in heavy alcohol users while others suggest moderate alcohol consumption ameliorate Aβ accumulation as seen in AD. With some others reporting no association between EtOH consumption and AD (Huang *et al.,* 2016, Piazza-Gardner *et al.,* 2013, Heymann *et al.,* 2016). What remains unclear however is the mechanism underlying EtOH-induced neurotoxicty and the eventual manifestation of AD-like pathobiology. The impact of EtOH on mitochondrial fission/fusion dynamics, mitochondrial bioenergetics and cell metabolic signalling pathway with the possible protective role played by CsA is yet to be determined. This study has demonstrated that EtOH exposure to neuronal cells caused a significant decrease in cell viability and increased ROS production with a resultant dysregulation of the antioxidant system of the neuronal cell. Additionally, we observed an increase in autophagy and apoptosis with a resultant impairment of mitochondrial function. The mitophagy-regulating fusion/fission pathway was dysregulated leading to activation of Ras/ERK, PI3K/MAPK, key cellular metabolic signalling pathways necessary for cell survival, proliferation and function. Protein aggregation and Aβ formation both significant parts of AD hallmarks were also increased in response to EtOH treatment, however there was a decrease in hyperphosphorylated tau. We therefore propose EtOH could play dual role in relation to AD pathology. Finally, co-treatment with CsA has the potential to attenuate the damaging effect of increased fission but effecting a compensatory increase in fusion.

3.4.1- IMPACT OF ETHANOL ON CELL REDOX MECHANISM

Data from our study show an increase in oxidative stress and activation of the cell antioxidant system following EtOH exposure. ROS generation is increased in cells treated with 250 and 500 mM EtOH in a concentration and time

dependent manner (**Figure 3.2B**). This reflects in the subsequent loss in cell viability from EtOH exposure (**Figure 3.2A**). As a result, the predominant antioxidant response was facilitated by the Trx system (**Figure 3.3B**) as opposed to the glutaredoxin system. This may be in part due to reduced levels of GSR which would affect glutathione levels required by both glutaredoxin and GPx for optimal activity. Similar patterns were reported in response to acute ethanol posioning in mouse models (Zhong *et al.,* 2013). In humans, there is an age-related decrease in GSH, exaccerbated in neurodegenerative conditions (Vogt and Richie, 2007]. Levels reported in conditions such as Parkinsons disease have been shown to be decreased but supposedly remain unchanged in AD (Aoyama and Nakaki, 2013), however, this will depend on the overall cellular redox status. Morever, glutaredoxin system system has been suggested to be a thioredoxin backup system providing support and keeping Trx in a reduced state (Fernandes and Holmgren, 2004, Du *et al.,* 2010). SOD activity was also significantly increased in response to ethanol but only in response to moderate ethanol exposure over short time periods (**Figure 3.4A**). Increased SOD activity is considered an adaptive response to ethanol toxicity, however, prolonged exposure reduces this activity as reported in our model (Ledig *et al.,* 1981). Further consequence of increased ROS include increased lipid peroxidation and protein carbonylation which contribute to GSH decline resulting in MPTP opening and cytochrome C release triggering apoptosis (Latham *et al.,* 2001). Therefore in SH-SY5Y neuronal cells, ethanol-induced toxicity trigger a cell protective antioxidant mechanism that bypass decrease in glutathione levels but is upheld by the support of the thioredoxin system.

3.4.2- ETHANOL IMPAIR MITOCHONDRIAL BIOENERGETICS AND DYSREGULATES MITOCHONDRIAL FISSION/FUSION DYNAMICS IN SH-SY5Y CELLS

Ethanol exposure has also been implicated in reducing mitochondrial membrane integrity resulting in reduced MMP (Yang *et al.,* 2012). Here we show that mitochondrial dynamics were altered together with a global depression of mitochondrial bioenergetics parameters (Basal and maximal oxygen consumption rate, proton leak, spare respiratory capacity, coupling

efficiency and ATP production) in response to EtOH. There is paucity of studies on the impact of EtOH on mitochondrial bioenergetics in neuronal cells using the seahorse mitostress assay. Here, we have shown a decrease in maximal OCR in myoblasts exposed to chronic binge alcohol (Duplanty *et al.,* 2018). Hypoxic conditions resulting from chronic EtOH consumption have been shown to result in decreased mitochondrial ATP production (Young *et al.,* 2006). Mitochondrial fragmentation is another measure of oxidative stress induced toxicity in SH-SY5Y cells with an increase in Drp1 protein expression reported (Qi *et al.,* 2011, Bonet-Ponce *et al.,* 2015). Under normal physiological conditions, mitochondrial dynamics, i.e. fusion/fission are necessary for the maintenance, function and distribution of mitochondria (Berthelot *et al.,* 2016). We report an imbalance in the mitochondrial fusion/fission pathway, where we propose that acute exposure elicits a cytoprotective effect which becomes compromised with chronic ethanol exposure. In this study, increase in Drp1 is observed following EtOH treatment in SH-SY5Y cells (**Figure 3.7A**). Studies have shown a crosstalk between mitochondrial fission and oxidative stress. Paraquat-induced oxidative stress in mice alveolar cells showed that there is a resultant increase in Drp1 and decrease of fusion proteins (Zhao *et al.,* 2017). PKC-induced oxidative stress in SH-SY5Y cells also caused an increase in fragmentation hence the increase in Drp1 protein expression, with a PKC inhibitor resulting in decreased Drp1 expression levels (Qi *et al.,* 2011). Comparative studies using human retinal pigment eptithelial ARPE-19 cells treated with 600 mM EtOH also reported an increase in fission, however, this was sustained at these higher concentrations, which could reflect the sensitivity of neuronal cells to EtOH (Bonet-Ponce *et al.,* 2015). This explains that neuronal mitochondria respond to oxidative stress via increase in fragmentation to enable the removal of damaged mitochondria during high cellular stress levels. In this study, there was decrease in expression levels of Opa1 and Mfn1 proteins following 500 mM EtOH treatment. There was an opposite response of slight increase following 250 mM EtOH treatment (**Figure 3.7B**), supporting evidence from studies suggesting a neuroprotective effect from mild (1-3 and 1-7 U/week for women and men respectively) to moderate >3 and >7 U/week for women and men respectively) alcohol intake (Scott et al., 2008). Study of hepatocytes

isolated from EtOH chronically-fed rats show a decrease in fusion activity compared to normal hepatocytes. While there was mitochondrial matrix continuity and many fusion events going on in hepatocytes isolated from control rats, there was a suppressed mitochondrial matrix continuity and dynamics due to sensitivity to EtOH exposure (Das *et al.,* 2012). Moreso, cardiomyocytes chronically exposed to EtOH exhibited a 40% decrease in mitochondrial continuity and a 75% decrease in fusion activities (Eisner *et al.,* 2017). These data evidence the role of mitochondrial dynamics in maintaining balance and the role EtOH play in disrupting this fusion/fission dynamics similar to phenotype of neurodegeneration suggesting the potential for targeting this pathway providing insight into the amelioration of mitochondrial dysfunction-induced neurodegenerative manifestations.

3.4.3- ETHANOL ACTIVATES AUTOPHAGY AND MITOPHAGY IN SH-SY5Y CELLS

Autophagy is fundamental to maintaining brain health which has high metabolic activity and extensive oxygen consumption. Autophagy is thought to be scarce in a nutrient-rich neuronal environment, but studies have shown that it occurs physiologically in neurons at undetectable levels, with evidence to support that autophagy is very efficient at physiologic level hence the difficulty in its detection (Bland *et al.,* 2008, Lee *et al.,* 2011). On the other hand, excessive or imbalanced autophagy can lead to autophagosome or aggregate accumulation contributing to neurodegenerative conditions such as AD, Lewy body dementia and Parkinson's disease. Accumulation of autophagosomes may be due to an increase of autophagosome synthesis, disruption of autophagosome-lysosome fusion or both (Orr and Oddo, 2013). Under normal physiological conditions autophagy is responsible for the clearance of protein aggregates and indeed entire organelles. Here, we showed that increased autophagy in response to high EtOH load corresponded with an increase in LC3II-lipidation and p62/Sequestosome1 (SQSTM1) (**Figure 3.9A & B**), a multifunctional scaffold protein, which acts as a receptor that binds and delivers poly-ubiquitinated proteins to the UPS or to the autophagosome for degradation, playing a major role in recognition and selective autophagy (Komatsu and Ichimura, 2010). The increase in both these markers suggest

that accumulation is due to the increase in autophagosome synthesis rather than increased flux, as a decrease in p62 is characteristically associated with enhanced degradation of the autolysosome (Flores-Bellver *et al.,* 2014).

Together with autophagy, mitophagy a specialised form of autophagy, function to remove dysfunctional mitochondria. An accumulation of autophagosomes therefore signals the beginning of cell death i.e. identifying the stage by which autophagy moves from cytoprotective to cytotoxic. Aberrant mitophagy could accelerate the development of neurodegenerative diseases through the imbalanced MQC, mitochondrial dysfunction induced apoptosis, necrosis and axon degeneration (Liu *et al.,* 2017, Franco-Iborra *et al.,* 2018). Reports have indicated that p62 is required for the transportation of mitochondria via microtubules to a juxta-nuclear site forming mito-aggresomes, which is considered to precede autophagic clearance of mitochondria (Geisler *et al*., 2010; Lee *et al*., 2010; Okatsu *et al*., 2010). Here, aberrant p62 expression and a loss in autophagy regulation, could cause a defect in the transport of mitochondria and provoke synaptic loss through dysregulated mitophagy (Du *et al*., 2010). These together indicate a role for increased autophagycombating EtOH-induced toxicity in SH-SY5Y neuronal cells in a bid to enhance the clearance of damaged organelles and mitophagy stepping in to get rid of excessively fragmented mitochondria in a bid to restore balance and optimal function of the energy metabolic system of the cells.

3.4.4- CHRONIC ETHANOL EXPOSURE ENHANCE APOPTOSIS

The marked decrease in mitochondrial membrane potential was assocated with an increase in Bax, where in this instance it functions as a pro-apoptotic marker, as opposed to participating in mitochondrial fission, supported by the fact that Bax was not upregulated in repsonse to moderate levels of ethanol when mitophagy was at its highest but was upregulated at chronic alcohol level (**Figure 3.8A**). Bax is required for EtOH-induced neuronal apoptosis in developing mouse brain (Young *et al.,* 2003). Neurons exposed to EtOH undergo intrinsic apoptotic cell death program independent of p53 and caspase-3 activation (Nowoslawski *et al.,* 2005). Neuronal cells exposed to acetaldehyde, the toxic metabolite of EtOH activate apoptotic signalling via

downregulating the antiapoptotic proteins Bcl2 and Bcl-xL while upregulating the proapototic protein Bax (Yan *et al.,* 2016). Phosphatidylserine (PS) accumulation promotes neuronal cell protection from apoptosis. EtOH inhibits PS accumulation thereby enhancing apoptotic cell death (Akbar *et al.,* 2006). Disruption to PS-Akt interaction necessary for cell survival increases susceptibility to cell death (Huang *et al.,* 2011). Upregulation of the pro-apoptotic marker Bax following EtOH-induced toxicity indicates an activation of apoptosis which could potential lead to cell death in the absence of an effecient compensatory process equivalent to the ensuing damage.

3.4.5- RECOVERY EFFECT OF CSA ON ETHANOL-INDUCED DYSREGULATION OF MITOCHONDRIAL DYNAMICS IN SH-SY5Y CELLS

EtOH disruption of fusion/fission dynamics correlates with ROS-mediated injury. A level of recovery was also observed following EtOH co-treatment with CsA indicating the potential role for the toxic effects being superseded. This toxicity was associated with a decrease in MMP (**Figure 3.5A**) where CsA affords partial protection. This is comparable to previous studies carried out on mice cerebellar cells that have shown EtOH treatment resulting in decreased MMP, which was ameliorated by the use of antioxidant Vitamin E suggesting that the decrease in MMP is ROS induced (Heaton *et al.,* 2011). EtOH treatment has been implicated in reducing mitochondrial membrane integrity thereby resulting in reduced MMP (Yang *et al.,* 2012). Opening of the MPTP will result in loss of MMP as implicated by EtOH in pancreatic acinar cells. Here EtOH treatment sensitised cell mitochondria leading to MTPT activation and subsequent reduction of basal MMP. MPTP has been implicated also to induce mitochondrial injury in Huntington disease (Shalbueva *et al.,* 2013, Quintanilla *et al.,* 2013). In cultured rat hippocampal cells modelling AD, exposing cells to $A\beta_{1\text{-}42}$ alongside CsA improved cell death index compared to when exposed to $A\beta_{1\text{-}42}$ alone (Kravenska *et al.,* 2016) suggesting a role for MPTP in AD pathology. Similarly, genetic or chemical inhibition of CypD have been reported to confer protection on neuronal mitochondria (Du and Yan, 2010) with reduced dementia incidence observed in solid organ transplant patients exposed to the calcineurin inhibitor CsA when compared to the general

population (Taglialatela *et al.,* 2015) suggesting MPTP as a target for AD amelioration.

Under normal cell conditions, mitochondrial fusion/fission are necessary for the maintenance, function and distribution of the mitochondria (Berthelot *et al.,* 2016). Various disease models show that manipulation of this dynamics can partially rescue phenotype (Chen and Chan, 2009). In this study, increase in Drp1, a mitochondrial fission marker succeed EtOH treatment in SH-SY5Y cells (**Figure 3.7A**). Following fusion proteins (Mfn1 and Opa1) decrease from 500 mM EtOH treatment, there is a subsequent recovery and induced increase in the protein levels following 500 mM EtOH cotreatment with CsA (**Figure 3.7B & C**). Studies have shown that BGP-15 which protects against oxidative stress promotes mitochondrial fusion (Szabo *et al.,* 2018) with oxidative stress causes a reversal of stimulated mitochondrial hyperfusion in C2C12 murine models (Redpath *et al.,* 2013). This points to CsA being a potential target for regeneration of the disruption to the fission/fusion dynamic process in the SH-SY5Y neuronal cells and that MPTP play a role in maintaining the balance of both mitochondrial structural integrity and subsequently the bioenergetic functions of the cell.

3.4.4- ETHANOL-INDUCED ACTIVATION OF RAS/ERK AND MTOR CELL SIGNALLING PATHWAYS IN SH-SY5Y CELLS

The loss of mitochondrial dynamics and associated increase in autophagy was linked to changes in key signalling pathways, such as the Ras/ERK and P13/Akt/mTORC1 pathways. Using hepatocyte and rat models of EtOH-induced liver toxicity, various MAPKs have been shown to be differentially activated, dependent on the concentration and exposure time to EtOH. Moreover, administration of MAP kinase inhibitors was shown to decrease liver injury and suppress endotoxin-induced liver injury (Kaizu *et al*., 2008). In our study, moderate exposure to EtOH resulted in effective activation of pAKT(**Figure 3.14B**) but this repsonse was attenuated in SH-SY5Y cells exposed to high levels of alcohol. The effect on neuronal cells is important as the majority of studies focus on EtOH-induced liver toxicity, in particular with an emaphsis on binge drinking. In some hepatocyte models, outcomes were

reported where rats exposed to chronic levels of EtOH showed depressed activation of several MAPK including p38 MAPK and JNK1/2 suggesting these pathways were not involved in the liver injury reported in this model (Lee *et al*., 2002). Interestingly, ERK1/2 activation was considered anti-apoptotic in EtOH treated primary hepatocytes (Lee and Shukla, 2005). It is widely accepted that ERK1/2 regulate several neuronal functions including synaptic remodelling, differentiation and survival. Changes to its subcellular localisation and activation have been reported in human Parkinson disease brain tissue, where ERK1/2 was found to be colocalised with mitochondria and autophagosomes signalling a shift in its cellular role in pathogenic conditions (Zhu *et al.,* 2003). Using the neuronal cell model, SH-SY5Y, increased ERK expression increased toxin-induced mitochondrial autophagy, indicating that ERK is a modulator of mitophagy and autophagy (Dagda, 2008). Here, we propose that increased ERK activation is a pre-requisite step to autophagy-induced apoptosis.

Conversely, an increase in Akt/mTORC1 was observed in response to higher levels of EtOH exposure (**Figure 3.14B & C**). Although controversial, some studies have indicated that there is a role for insulin sensitization in neurocognitive recovery and psychosocial adaption in chronic alcoholics (Esler *et al*., 2001). Although light to moderate alcohol intake may reduce cardiovascular risk via triglyceride load and insulin sensitivity, chronic alcohol consumption is closely correlated with insulin resistance (Vernay, 2004). Using mice models Li and Ren established that chronic alcohol exposure caused glucose intolerance. Usually activated mTORC1 inhibits autophagy, so why does increased levels of EtOH induce autophagy yet show activated mTORC1. Interestingly, in senescent cells despite an active mTOR, the autophagy pathway is also active, which was potentially linked to cell cycle arrest (Carrol *et al.,* 2017). Indeed, under conditions where AD pathology persists, levels of Akt activation, mTORC1 phosphorylated at Ser248 only, together with phosphorylated 4EBP1, p70S6K and eIF4E were significantly increased in AD brain and correlated with Braak staging and tau pathology, indicating that protein translation is radicallly disordered. mTORC1 hyperactivation also correlated with cognitive decline in AD individuals (Shafei *et al.,* 2017).

Activation of Akt through phosphorylation can signal this kinase to migrate to the cytsol and the nucleus to regulate metabolism, cell proliferation or apoptosis (Ogita and Lorusso, 2011). Sterol regulatory element-binding protein-1 (SREBP-1) activation plays an important role in EtOH-induced fatty liver associated with the PI3K/Akt pathway (Zeng *et al*., 2012).The consequence of increased Akt activation was increased phosphorylation of GsKB. The activation of AKT and mTOR despite increased autophagy points to the fact that in the SH-SY5Y neuronal cells, there is a potential disorganisation of protein translation and a potential for the activation of a cell-cycle arrest in a bid to activate a repair mechanism capable of restoring balance to cell function.

3.4.5- IMPACT OF ETHANOL ON PROTEIN AGGREGATION, AB AND PHOSPHORYLATED TAU PRODUCTION IN SH-SY5Y CELLS

Ultimately, the consequence of EtOH exposure resulted in an overall increase in protein aggregation and Aβ accumulation at both EtOH concentrations indicating that EtOH-induced Aβ deposition precedes apoptosis. This study show first a significant increase in total protein aggregation with a minimal but significant reduction in aggregation levels following 500 mm EtOH and CsA co-treatment (**Figure 3.15A**). Experiments involving focal brain ischemia has shown the presence of persistent protein aggregation (Ge *et al.,* 2007). Formaldehyde a metabolite of EtOH has been shown to cause induced misfolding and aggregation of amyloid-like tau aggregates in SH-SY5Y cells (Nie *et al.,* 2007). Several studies support a contributory link between chronic alcohol consumption (or thiamine deficiency) and Aβ generation (Gong *et al.,* 2016), however, low concentrations of EtOH are considered protective (Munoz *et al.,* 2014). Not only are Aβ levels reported as increased but so too are the levels of the amyloid precursor protein (APP), BACE1 and presenillin 1, in the cerebellum, hippocampus, and striatum regions of rodent brain from the chronic alcohol-fed group (Kim *et al.,* 2010; Huang *et al.,* 2017). Using the 3xTgAD triple transgenic mouse model of AD, one study showed that primary hippocampal cultures exposed to co-treatment with Aβ and low EtOH levels (10-100 mM) showed a neuroprotective effect against Aβ toxicity, through direct action on Aβ oligomers (Munoz *et al.,* 2015). In a separate in vitro study,

EtOH levels at 10 mM was shown to reduce the formation of Aβ dimers. Using insilico modelling the authors suggest that EtOH alters the dynamics for assembling Aβ (Ormeno *et al.,* 2013).

The abnormal accumulation of Tau protein in intracellular aggregates is observed across a broad spectrum of neurodegenerative disorders collectively referred to as tauopathies. Phosphorylation of Tau are cruical for its physiological and pathological activities. An increase in the phosphorylation of Tau together with increased accumulation of NFT have long been described as a halmark of AD pathology. Despite this fact, these intraneuronal NFTs do not appear to be the main toxic entities and more soluble forms of Tau rather than fibrillar tangles are involved in toxicity and disease progression (Guo *et al.,* 2016). Reports of Tau inclusions in cell populations, such as microglia, that do not normally expressed Tau indicate that Tau is transferred between brain cell populations (Perea *et al.,* 2018). Interestingly, Tau dephosphorylation through tissue-non-specific alkaline phosphatase is required before secretion to the extracelular space (Diaz-Hernandez *et al.,* 2010). We show a dose-dependent decrease in the phosphorylation of Tau, uncharacteristic of AD pathology. However, male Sprague-Dawley rats exposed to low (6-48 mM EtOH) and high (96-768 mM EtOH), showed a biphasic response to the incorportaion of $\gamma^{32}P$ into microtubule preparations, where low concentrations showed an increase in phosphorylation and high concentrations decreased phosphorylation. There are several possible explanations to the decreased level of phosphorylated Tau reflected in this study: 1) a decrease in the amount of substrate available for phosphorylation 2) EtOH has a toxic effect on the catalytic activity of kinases (Ahluwalia *et al*., 2000) 3) Tau is dephosphoryated and exported or 4) Tau has formed aggregates and has been sequestered in atuophagosomes. When dephosphorylated, it behaves as a muscarinic receptor agonist, causing a sustained increase in intracellular calcium that finally leads to neuornal death. Moreover, npTau has devastating effects on the structural plasticity of hippocampal newborn neurons (Perea *et al*., 2018).

EtOH-treatment of mouse brains results in subsequent caspase-3 and GSK-3β activation which in turn leads to the elevation of phosphorylated tau measured by paired helical filament (PHF)-1 antibody (Saito *et al.,* 2010) with

GSK-3β inhibitor lithium blocking phospho-tau increase. GSK-3β has been linked as an integral molecule playing a role in multiple proliferation and differentiation signals in neuronal progenitor cells (Kim *et al.,* 2009) with several studies linking GSK-3β inhibitor to neuroprotection from different stress-induced injuries (Chin *et al.,* 2005, Chuang *et al.,* 2011). Experiments involving the inhibition of GSK-3 revealed an induction of proliferation, migration and differentiation of neural stem cells towards neuronal phenotype (Morales-Garcia *et al.,* 2012), however another study show that cells stably expressing GSK-3β isoform particularly using retroviral vectors inhibits neuronal differentiation of progenitor cells (Ahn *et al.,* 2014). Several studies in the treatment of acute myeloid leukaemia have found that instead of targeting to kill rapidly replicating cells, the enhancement of differentiation using GSK3 inhibitor, lithium and all-trans retinoic acid (ATRA) have been a clinical potential in ameliorating the disease (Gupta *et al.,* 2012). The increase in total protein aggregation and Aβ levels from EtOH-induced neurotoxicity indicate a similarity in neurodegenerative phenotype despite a decrease in phosphorylated tau suggesting a potential link between chronic alcohol consumption and AD-like phenotype which is independent of increased burden of phosphorylated tau. This also suggests a focus on anti-amyloid drug trials maybe the way forward towards combating AD phenotype.

3.4.6- SUMMARY

In this study the impact of EtOH on cell viability, ROS generation, autophagy and apoptosis were investigated. EtOH influence on mitochondrial bioenergetics, morphology and the fusion/fission pathway was also determined. The downstream effect of all these on the Ras/Erk pathways and AD hallmark, Aβ and phosphorylated tau were evaluated. The results indicate ethanol induces significant mitochondrial dysfunction shown by increased ROS, fission, suppressed fusion combined with increased autophagy and apoptosis through dysregulation of the Ras/ERK and PI3K-PDK-mTOR pathway ultimately leading to an increase in protein aggregation and Aβ build-up. Interestingly, phosphorylated tau was rather decreased and remains to be further investigated on its potentiality as targeted therapy against tauopathy.

Chapter 4

Dysregulated mitochondrial function and dynamics in AD pathology following zinc-induced oxidative stress

Contents

4.1- INTRODUCTION

As previously introduced, Zn is an essential micronutrient important for gene regulation, antioxidant enzyme synthesis and activity, neuronal cell growth, development, differentiation and cell signaling. (MacDonald, 2000; Pfaender *et al.,* 2016, Takeda, 2001). The link between Zn and AD hallmarks- increased Aβ peptide deposition and phosphorylated tau (Craddock *et al.,* 2012, Szutowicz *et al.,* 2017) and the unanswered questions regarding the underlying mechanisms involved is the premise of this study.

Although the physiologic level of total Zn in adult brain is estimated to be about 150-200 µM, the majority of it is bound to cytosolic proteins (Sensi *et al.,* 2011). Excessive amounts of Zn exogenously introduced to rat cerebellar neuronal cells at a concentration range of 100 µM to 500 µM were found to be neurotoxic and associated with early onset mitochondrial injury (Manev *et al.,* 1997). In mice cortical cells, the ED_{50} of Zn after 18-24-hour exposure was reported to be 225 µM with higher concentrations and longer exposure time enhancing glial and neuronal injury (Choi *et al.,* 1988). In SN cholinergic neuroblastoma cells, an acute elevation of Zn in cholinergic neuroblastoma cells (up to 200 µM) resulted in a decrease of cell viability. However, prolonged Zn treatment led to irreversible inhibition of pyruvate dehydrogenase (PD) activity indicating the ability of zinc neurotoxicity to impair the mitochondrial energy signalling and its associated pathways (Ronowska *et al.,* 2007). The link between Zn-induced neurotoxicity and its contribution to several neurodegenerative conditions is suggested to be mediated through the inhibition of various mitochondrial enzymes and glycolysis, via the production of ROS (Sensi *et al.,* 2003). In rat striatal tissue, Zn-induced oxidative stress induced the cell antioxidant system mediated by an increase in the levels of SOD and heme-oxygenase, both associated with increased oxidative stress (Singh *et al.,* 2011).

Whilst previous studies suggest a link between Zn toxicity and ROS generation, Aβ aggregation, enhanced neurofibrillary tau tangle formation, there is paucity of data on the impact of differential toxic Zn concentrations on associated pathways especially mitophagy. Furthermore, despite literature evidence of a link between dysregulation of mitochondrial dynamics-

fission/fusion and AD, there is no study linking dysregulated mitochondrial dynamics and impaired mitochondrial function following excessive Zn exposure related to Aβ aggregation and neurofibrillary tangle formation in neuronal cells.

In this thesis, differentiated SH-SY5Y cells were used to investigate the impact of 150 µM and 300 µM Zn on cell viability, ROS generation and modulation of the antioxidant system. Downstream effects on mitochondrial dynamics (mitophagy), mitochondrial respiration and energy production, autophagy and apoptosis were also determined. The response of the cell survival mediating Ras/Erk/MAPK, mTORC1 signalling pathways and Aβ, phosphorylated tau production to Zn exposure have been described. Here, we show that Zn exposure reduced cell viability over time in a concentration-dependent manner. This is correlated with an increase in ROS production which induced increased levels of the antioxidant proteins GRX and TRX, SOD especially at 150 µM Zn concentration. A dysregulation of mitochondrial dynamics by an increase in fission at 300 µM Zn with no corresponding fusion increase as compensation to maintain organelle integrity triggered mitophagy and even apoptosis. Zn also decreased MMP, depressing mitochondrial respiration and energy production. Additionally, Zn activated kinases of the Ras/Erk/MAPK, mTORC1 signalling pathways, increased Aβ generation tau phosphorylation. Taken together, these results suggest that Zn-induced increase in Aβ production and tau phosphorylation is potentially mediated by dysregulated mitophagy and impaired mitochondrial function.

The schematic diagram (Figure 4.1) highlights the processes and pathways impacted by exposure to excessive amount of exogenous Zn. They include ROS generation, antioxidant enzymes levels and activity, mitochondrial respiration, ATP production, mitochondrial fission/fusion dynamics, autophagy and apoptosis, protein synthesis and MAPK/PI3k/AKT signalling.

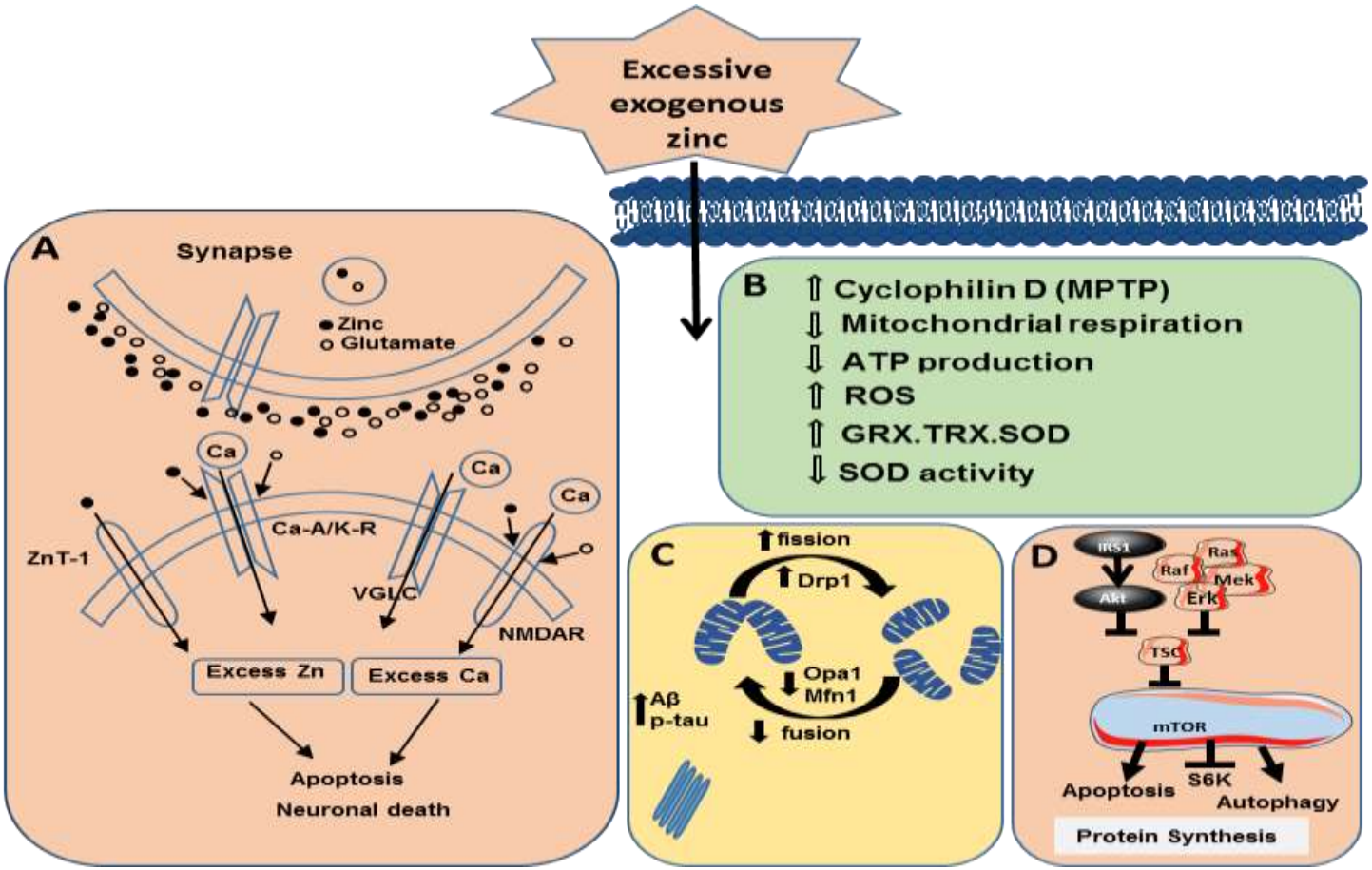

Figure 4.1: Pathways targeted in response to zinc neurotoxicity. Vesicular Zn is released following excitation of zincergic/glutamergic synapses causing a rise in Zn concentration at the synaptic cleft accompanied by excessive excitation of glutamate receptors. This results in impaired calcium homeostasis which is a key mediator of neuronal cell death (**A**). Exogenously applied excessive Zn mediate an increase in ROS generation, eliciting an increase in antioxidant protein levels, decreased MMP impairing mitochondrial respiration and ATP production (**B**). This results in a failure to maintain mitochondrial dynamics, thereby disrupting the fusion/fission cycle which contributes to increased Aβ production and tau phosphorylation (**C**), thereby activating the cell survival signalling pathways to combat Zn-induced neuronal cell oxidative stress (**D**).

4.2- AIMS AND OBJECTIVES

Hypothesis: Zn-induced tau phosphorylation and increased Aβ production is mediated by dysregulated fusion/fission dynamics and impaired mitochondrial function.

Specific aim 1: Investigate the impact of zinc-induced oxidative stress on the redox status of SH-SY5Y neuronal cells.

Specific aim 2: Determine the effect of zinc on neuronal cell mitophagy (fusion/fission dynamics) and protein folding.

Specific aim 3: Evaluate the impact of dysregulated mitochondrial function on cell survival signaling pathways as a result of zinc toxicity.

Specific aim 4: Assess Zn-mediated contribution to AD pathology using the SH SY5Y neuronal cell model.

4.3- RESULTS

4.3.1- ZINC DECREASES SH-SY5Y CELL VIABILITY, INCREASES ROS FORMATION AND MODULATES THE CELL ANTIOXIDANT SYSTEM

The uptake of Zn in neuronal cells at high concentrations caused a loss in cell viability and an increased production of ROS (Figure 4.2). SH-SY5Y cell viability was significantly decreased in a concentration (200-1600 µM) and time dependent manner (6 h, 24 h and 48 h) ($p< 0.0001$-0.03, Figure 4.2A). To better understand the mechanism that underpins the cytotoxic effects of Zn in SH-SY5Y cells, ROS generation following Zn exposure was investigated. SH-SY5Y cells were labelled with DCFDA which forms a highly fluorescent compound DCF in response to ROS oxidation. A significant increase in DCF intensity was measured in a dose dependent manner after 6- and 24-hour Zn exposure ($p\leq 0.001$-0.001, Figure 4.2B). In response to Zn-induced toxicity, there was also an increase in GRX levels ($p=0.0016$ and 0.0475) following exposure to 150 and 300 µM Zn for 24 h and an increase in thioredoxin (TRX) levels following exposure to 150 µM Zn for 24 h ($p=0.0164$) (Figure 4.3 B and C).

SOD activity, which plays an important role in ROS metabolism was also measured (Figure 4.4). At shorter exposure times (3 hour), there was a decrease in SOD activity at 300 µM concentrations of Zn ($p=0.0153$, Figure 4.4 A) and significant increase by comparing 300 µM Zn to 300 µM Zn + CsA treatments ($p=0.0280$, Figure 4.4 A) whereas an increase in SOD activity at longer exposure times (24 hour) in cells treated with 150 µM Zn was observed ($p=0.0377$, Figure 4.4 B). Cells co-treated with CsA suggested a boost to the protective role of the antioxidant system. Here, cells exposed to 300 µM Zn + CsA treatment showed significant increase in SOD activity after 24 h treatment ($p=0.0198$)

These results suggest that the GRX and TRX systems protect the cells from Zn-induced neurotoxicity and SOD activity is enhanced with persistent exposure to Zn as a coping mechanism to respond to induced oxidative stress.

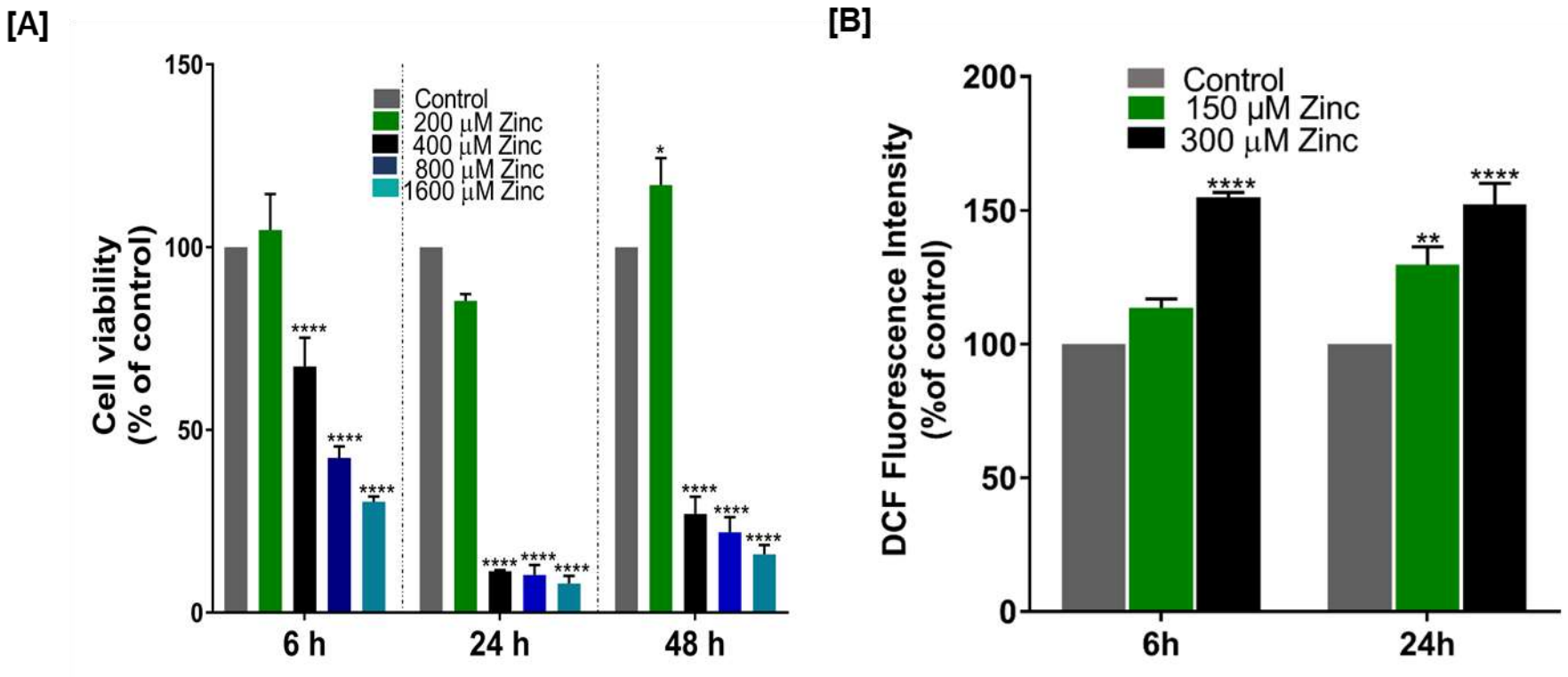

Figure 4.2: Loss of cell viability and an increase in ROS in SH-SY5Y cells in response to zinc toxicity. Cell viability/metabolic activity and intracellular ROS generation in zinc treated SH-SY5Y cells was determined by MTS reduction and DCFDA fluorescent dye staining, respectively. **Panel A:** Cells were treated with 200-1600 µM zinc, relative to control cells and incubated for 6 h, 24 h and 48 h, respectively. Cell viability was assessed using the MTS assay and the change in absorbance measured at 500 nm. **Panel B:** Cells were treated with 150 µM and 300 µM zinc, respectively, relative to control cells for 6 and 24 h. Intracellular ROS was assessed using DCFDA and DCF fluorescent intensity at 500 nm. Data are expressed as mean ± SEM of 3 independent experiments. *p < 0.05, **p < 0.01, ***p < 0.001, ****p < 0.0001 relative to control.

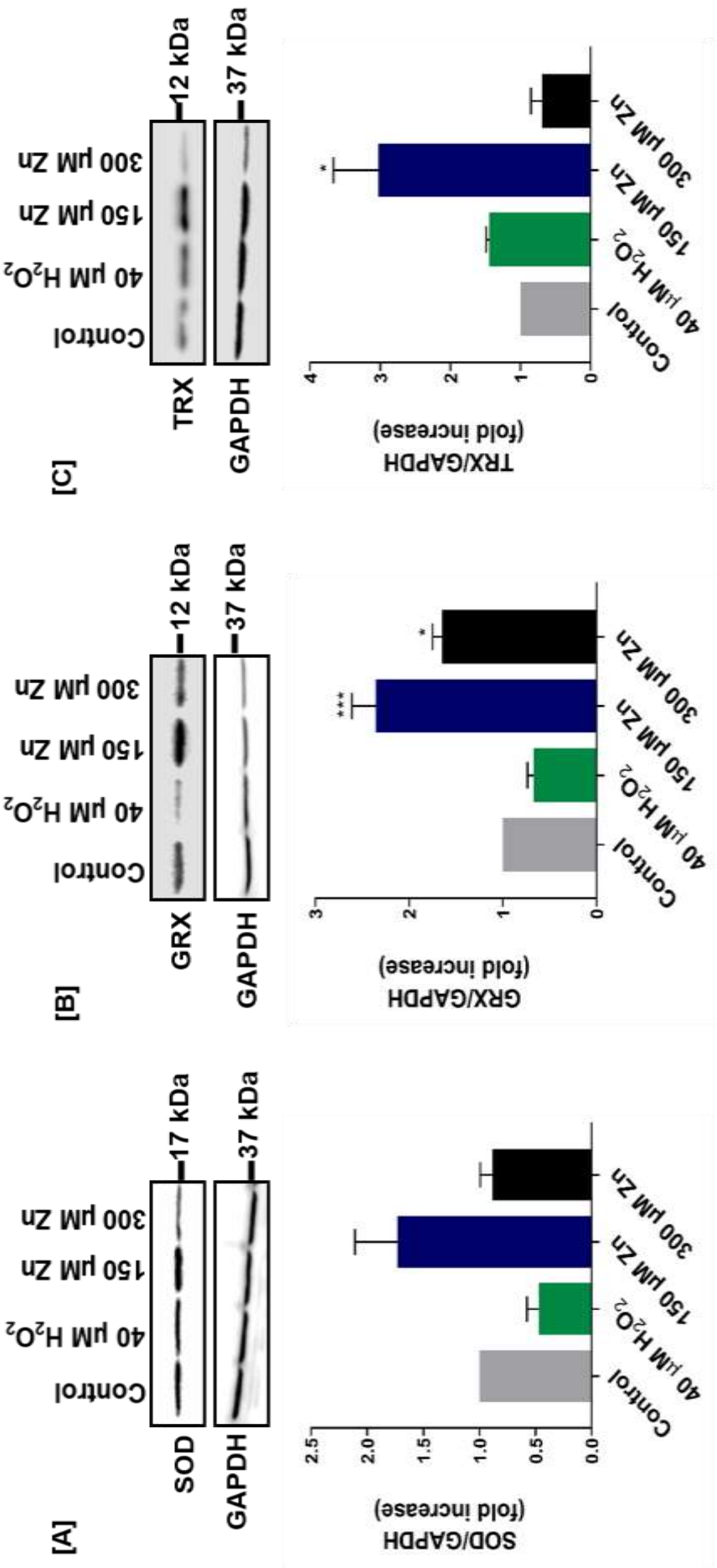

Figure 4.3. Differential protein expression of SOD, GRX and TRX in zinc treated SH-SY5Y neuronal cells. Cells were treated as indicated relative to control cells for 24 h. SOD, GRX and TRX protein expression were determined by Western blot analysis. Immunoblot of **Panel A:** SOD, **Panel B:** GRX, **Panel C**: TRX and their respective GAPDH expression. Data was normalized to respective GAPDH and the data are expressed as mean ± SEM of 3 independent experiments. *p < 0.05, **, ***p < 0.001 compared to control cells.

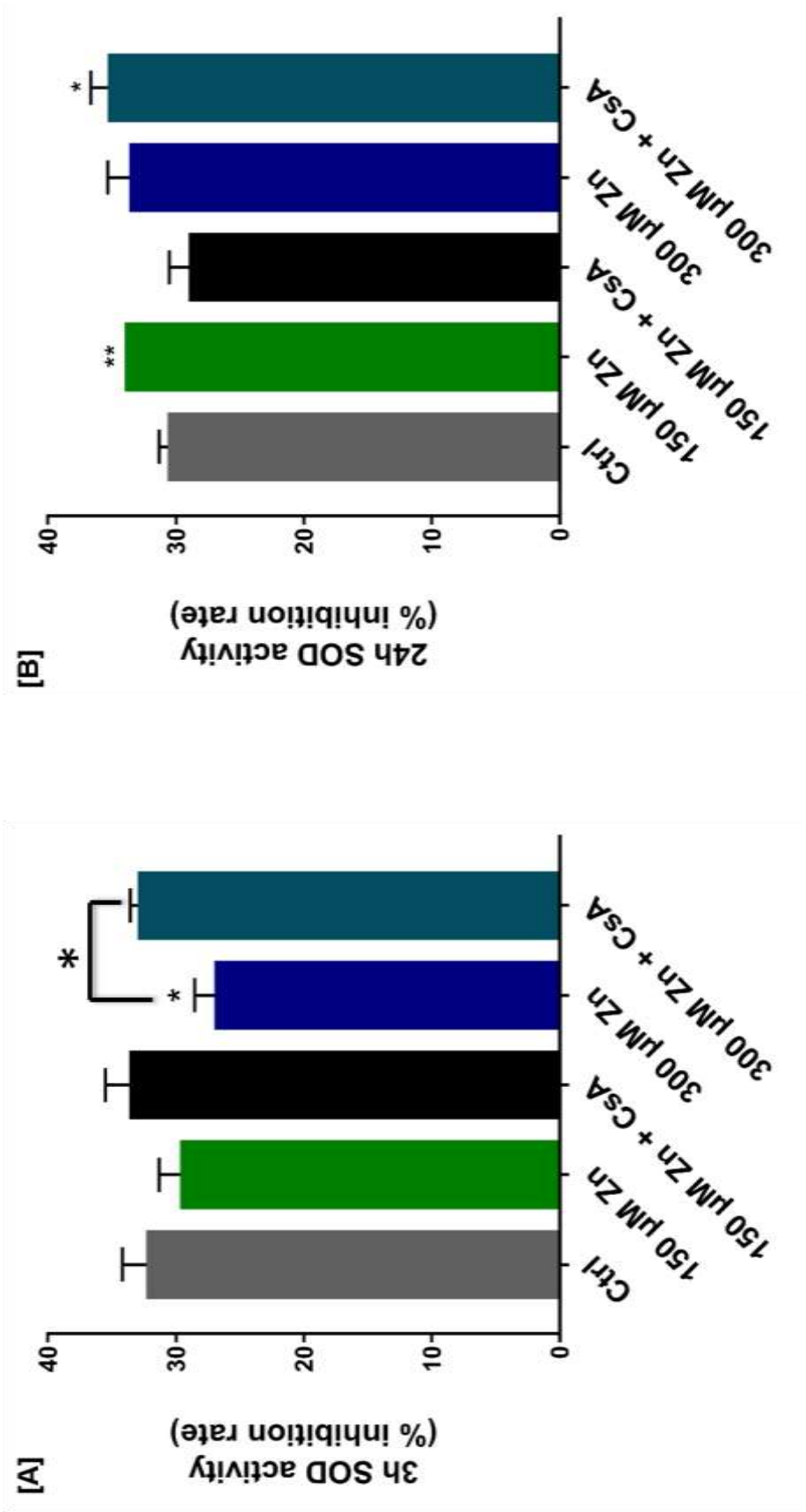

Figure 4.4. SOD activity in zinc treated SH-SY5Y neuronal cells. Cells were treated as indicated relative to control cells and assayed for SOD activity using the SOD enzyme activity assay kit. **Panel A:** SOD activity in response to varied zinc concentration incubated for 3 h and **Panel B:** SOD activity in response to varied zinc concentration incubated for 24 h. Data are expressed as mean ± SEM of 3 independent experiments. *$p < 0.05$, **$p < 0.01$.

4.3.2- ALTERED MITOCHONDRIAL MEMBRANE POTENTIAL AND BIOENERGETICS IN ZN-TREATED SH-SY5Y CELLS

In response to Zn treatment, mitochondrial membrane potential (MMP) was measured using the fluorogenic dye JC-1. A significant reduction of MMP was observed following Zn treatment at 150 µM and 300 µM ($p= 0.0401$ and 0.0370, respectively, Figure 4.5A), with no significant changes observed following CsA onlly and 300 µM Zn co-treatment with CsA.

The effect of Zn on mitochondrial bioenergetics using the Agilent seahorse XFe24 analyzer has not been previously examined. SH-SY5Y neuronal cells were treated with 150 µM and 300 µM Zn and control cells treated with 10 % FBS DMEM for 24 hours prior to performing the Mito Stress assay. This assay measures OCR, basal mitochondrial respiration, proton leak, spare respiratory capacity and ATP production (Figure 4.5 C, D and E). Zn treatment resulted in both increased and decreased basal mitochondrial respiration and oxygen consumption in a concentration dependent manner. There was a significant increase in basal mitochondrial respiration following 150 µM Zn and CsA treatment ($p=0.0048$) and significant decrease following 300 µM Zn and CsA treatment ($p=0.0004$). Similar trends were observed in proton leak ($p=0.00094$ and 0.0445), spare respiratory capacity ($p=0.0206$ and 0.0432) and ATP production ($p=0.0041$ and <0.0001), with an increase and decrease following 150 µM and 300 µM Zn treatments, respectively. This indicates the toxic extent of 150 µM Zn is not sufficient to elicit an impairment of mitochondrial function and ATP production whereas 300 µM Zn induces cell toxicity sufficient to diminish mitochondrial function and respiration overriding any recovery effect from CsA cotreatment.

The level of the mitochondrial matrix marker cyclophilin D was significantly increased in response to 300 µM Zn treatment ($p=0.0289$, Figure 4.6A) indicating also a possible disruption of calcium metabolism. There was also an increase in the mitochondrial chaperone Hsp60 level following Zn treatment (Figure 4.6B).

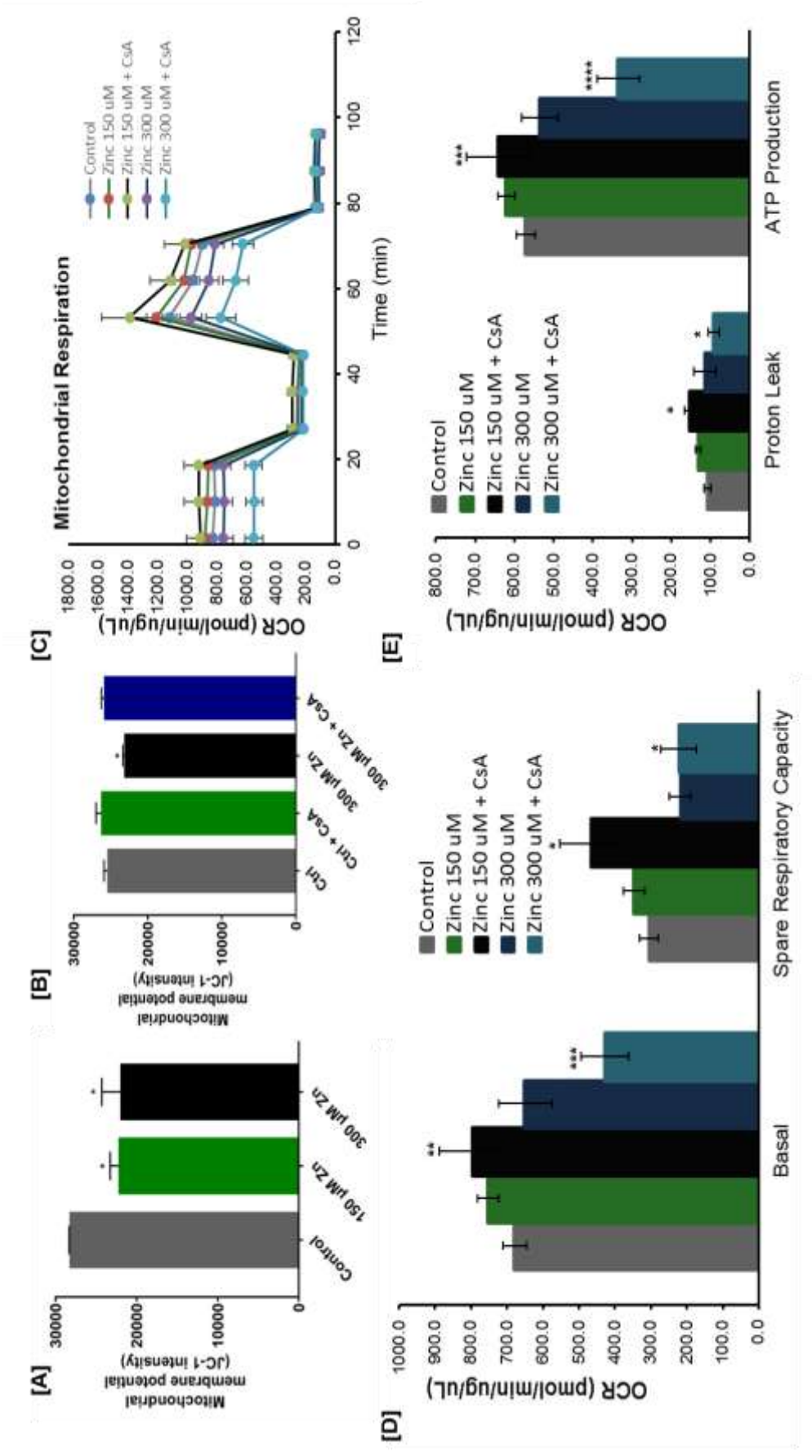

Figure 4.5- Zinc exposure decreased mitochondrial membrane potential and altered mitochondrial respiration in SH-SY5Y cells. Cells were treated as indicated relative to control cells for 24 h. **Panel A and B:** JC-1 assay measuring MMP. **Panel C:** Seahorse Mito Stress Test measuring oxygen consumption rate (OCR), **Panel D:** basal mitochondrial respiration and spare respiratory capacity, **Panel E:** mitochondrial proton leak and ATP production. Data are expressed as mean ± SEM of 3 independent experiments. *p < 0.05, **p < 0.01, ***p < 0.001, ****p < 0.0001.

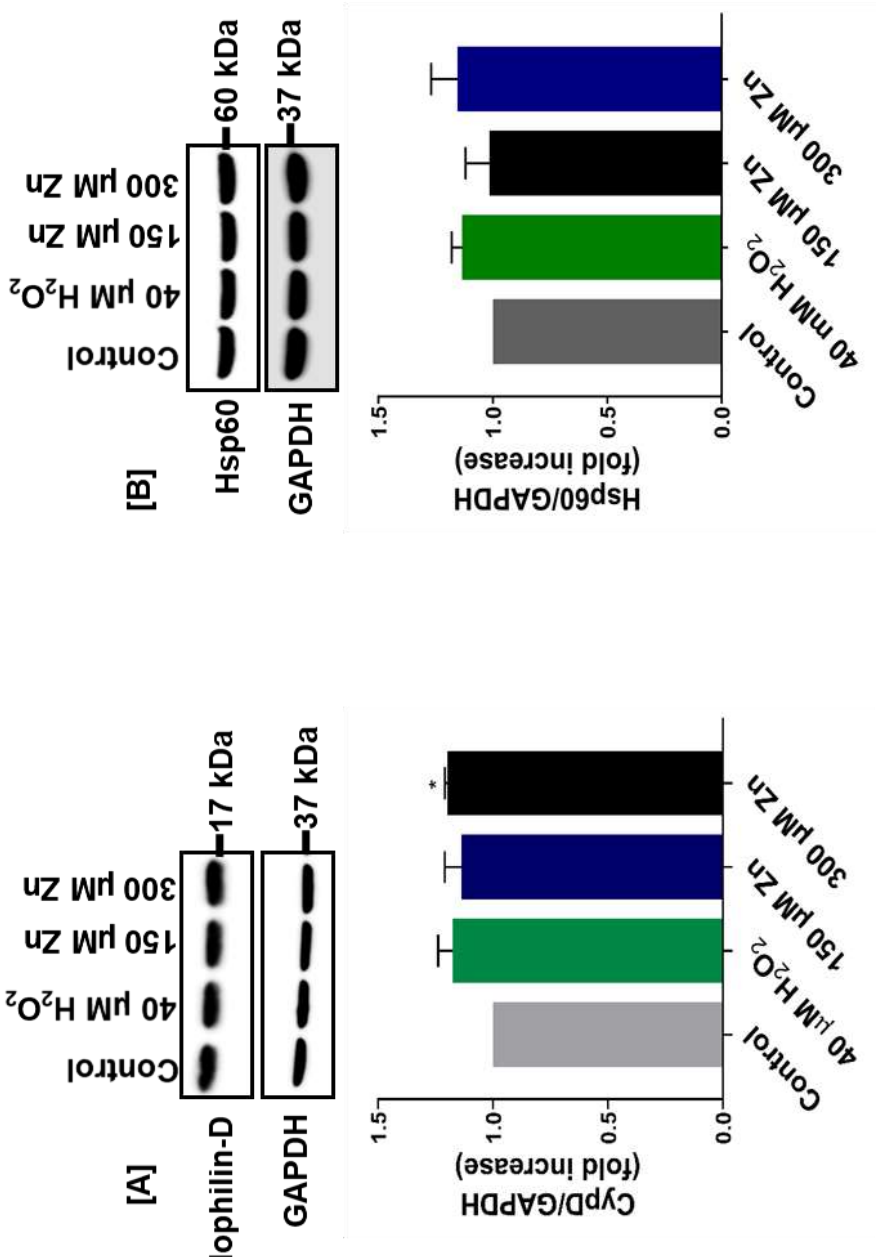

Figure 4.6. Expression of mitochondrial proteins Cyclophilin D and Hsp60 in zinc treated SH-SY5Y neuronal cells. Cells were treated as indicated relative to control cells for 24 h. Cyclophilin D/ Hsp60 protein expression was determined by Western blot analysis. Data is expressed relative to GAPDH and control. **Panel A: Representative** Western blot, and densitometric analysis of Cyclophilin D relative to GAPDH expression. **Panel B: Representative** Western blot and densitometric analysis of Hsp60 relative to GAPDH expression. Data are expressed as mean ± SEM of 3 independent experiments. *$p < 0.05$

4.3.3- MITOCHONDRIAL DYNAMICS DISRUPTION IN RESPONSE TO ZN TREATMENT

Cyclosporine A, an inhibitor of cyclophilin D responsible for MPTP opening and function was used to co-treat the Zn treated cells to determine whether it plays a protective role with reference to Zn-induced neurotoxicity. Furthermore, the mitochondrial fusion/fission cycle plays an important intracellular role in maintaining neuronal cell homeostasis. To determine the effect of Zn on mitochondrial dynamic complexes, the fission/fusion pathway protein levels were examined. The protein levels of dynamin-like GTPases Drp1, OPA1 and MFN1 were determined by Western blot analysis.

As shown in Figure 4.7A, cells exposed to 1 µM CsA showed significant increase ($p=0.0224$) in Drp1, significant increase in the level of the fission protein Drp1 ($p=0.0386$) in response to 300 µM Zn alone was observed with no significant change observed in response to 150 µM Zn. Incubating cells with CsA only caused a significant decrease in Opa1 ($p=0.013$). Both 150 µM and 300 µM Zn caused a decrease in Opa1 ($p=0.0002$, 0.0412, Figure 4.7B), with sustained decrease following co-treatment of 150 µM Zn with CsA ($p=0.0321$). The level of the fusion protein, MFN1, is decreased on exposure to 150 µM ($p=0.0003$) and 300 µM ($p=0.0265$) Zn where cells co-treated with CsA showed a protective effect ($p= 0.0453$, Figure 4.7C).

Using 300 µM Zn, mitophagy was increased as evidenced by the increase expression of Drp1, Mfn1. Morphological changes in mitochondria were also reported as monitored by the mitochondrial dye Mito Tracker (Figure 4.7D). Although there was increased fission in response to 300 µM Zn, there is no evidence of apoptosis, indicated by no change in the levels of the apoptotic marker Bax. Co-treatment with CsA in fact caused a significant decrease in Bax protein levels ($p= 0.0379$ and $p=0.0003$ respectively) (Figure 4.8A). It is also important to note that both Zn concentrations elicited an increase in the anti-apoptotic marker Bcl2, which was significant at 300 µM Zn ($p= 0.048$, Figure 4.8B) suggesting that despite zinc-induced toxicity, the apoptotic pathway is not activated..

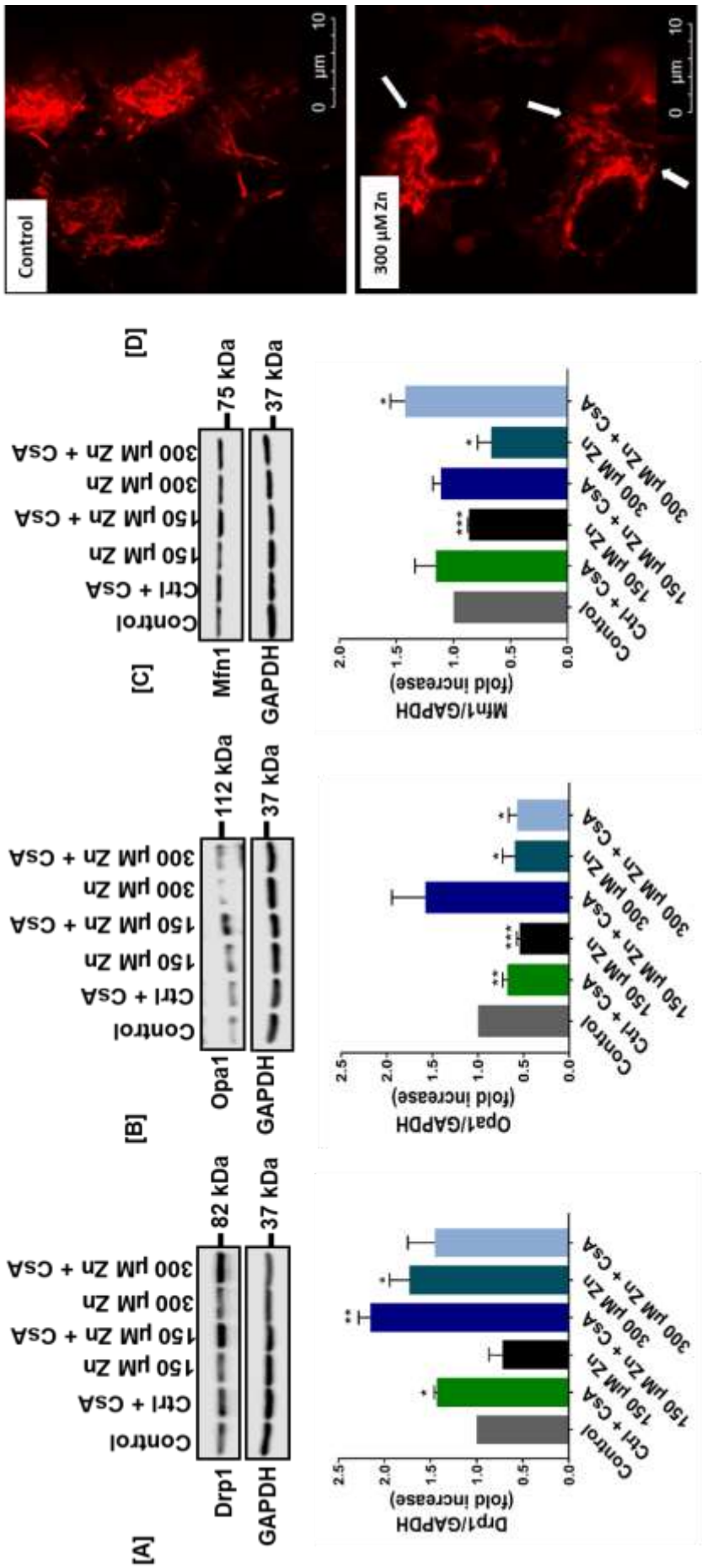

Figure 4.7. Differential expression of mitochondrial fission protein Drp1 and fusion proteins Opa1 and Mfn1 in zinc treated SH-SY5Y neuronal cells. Cells were treated as indicated relative to control cells for 24 h. Protein expression was determined by Western blot analysis. Data is expressed relative to GAPDH and control samples. **Panel A:** Representative Western blot and densitometric analysis of Drp1 relative to GAPDH expression **Panel B:** Representative Western blot and densitometric analysis of Mfn1 relative to GAPDH expression. **Panel C:** Representative Western blot and densitometric analysis of Opa1 relative to GAPDH expression. **Panel D:** Confocal analysis of Mitotracker red in control relative to zinc treated cells. Arrows indicate a fragmented mitochondrion typical of mitochondrial fission and an extensive breakdown of mitochondrial network. Data are expressed as mean ± SEM of 3 independent experiments. *$p < 0.05$, **$p < 0.01$, ***$p < 0.001$, compared to control.

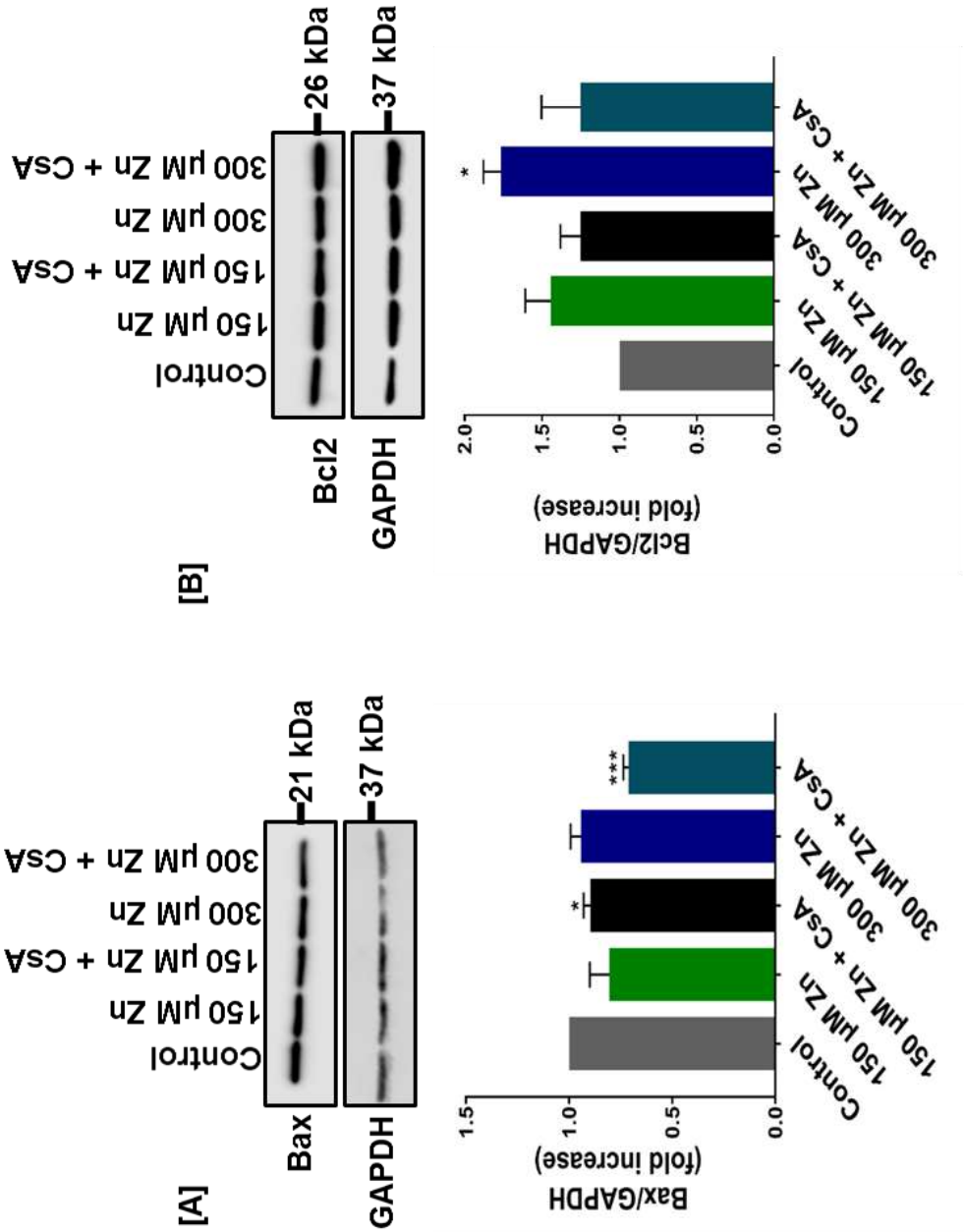

Figure 4.8- Apoptotic markers Bax and Bcl2 in zinc treated SH-SY5Y neuronal cells. Cells were treated as indicated relative to control cells for 24 h. Protein expression was determined by Western blot analysis. Data is expressed relative to GAPDH and control samples. **Panel A:** Representative Western blot and densitometric analysis of Bax relative to GAPDH expression **Panel B:** Representative Western blot and densitometric analysis of Bcl2 relative to GAPDH expression. Data are expressed as mean ± SEM of 3 independent experiments. *p < 0.05, **p < 0.01, ***p < 0.001, ****p < 0.0001.

4.3.4- ZN TREATMENT ELICITS AUTOPHAGY IN SH-SY5Y CELLS

Cells maintain homeostasis by recycling damaged organelles through the process of autophagy. To maintain cell homeostasis, autophagy is activated to allow for recycling of damaged cell organelles. This process is an adapted mechanism for cell survival. In this study, it has been shown that exposing SH-SY5Y cells to Zn caused an increase in autophagy evidenced by an increase in LC3I/II and p62. Results showed a significant increase in the conversion of LC3-I to its lipid-conjugated autophagosome-bound form LC3-II in 300 µM treatment (Figure 4.9A, p=0.0001). The levels of p62, the protein delivering ubiquinated autophagic cargo to the autophagosomes by interacting with LC3, was also increased at both concentrations of Zn treatment (Figure 4.9B, p=<0.0001 and 0.0005). Immunofluorescence confocal microscopy was also used to detect LC3 following Zn exposure showing an increased LC3 staining in cells exposed to Zn treatment after 24 h, with a unique feature of the autophagy marker concentrating in the nucleus is observed at 300 µM Zn (Figure 4.9C) suggesting a prominent role of nuclear LC3 pool to enable autophagic flux. The autophagic machinery is sometimes specifically targeted to a single organelle. Evaluation of autophagy using confocal microscope imaging of Zn-treated cells stained with Mitotracker Red and Lysotracker green. Results showed possible co-localization of Mitotracker Red and Lysotracker green (Figure 4.9D) in response to Zn treatment indicating disruption to mitochondrial biogenesis and cell attempt to restore mitochondrial integrity by degrading defective mitochondria.

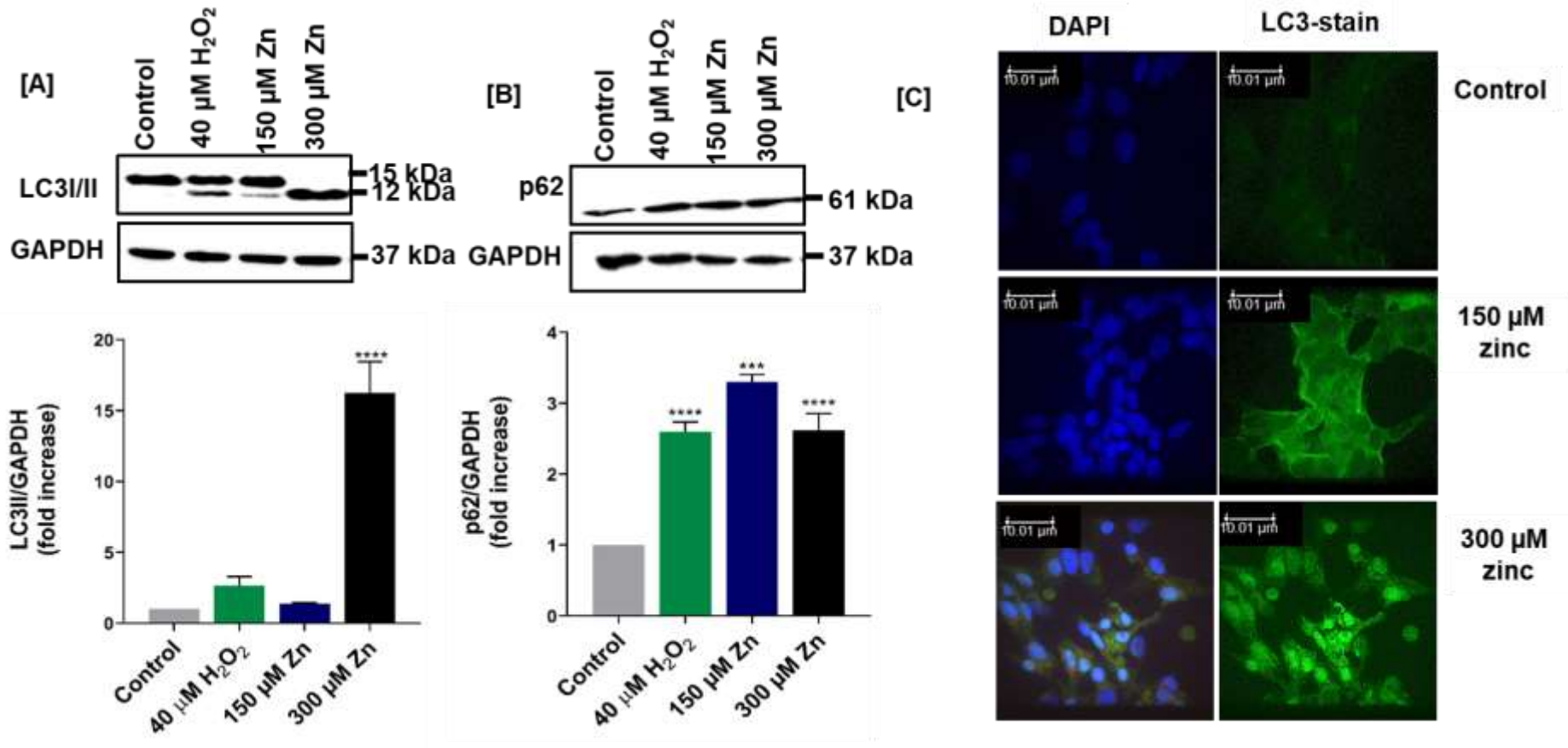

Figure 4.9- Autophagy is increased in zinc treated SH-SY5Y neuronal cells. Cells were treated as indicated relative to control cells for 24 h. Protein expression was determined by Western blot analysis. Data is expressed relative to GAPDH and control samples**. Panel A:** Representative Western blot and densitometric analysis of LC3I/II relative to GAPDH expression **Panel B:** Representative Western blot and densitometric analysis of p62 relative to GAPDH expression. **Panel C:** Using confocal microscopy LC3 expression was increased in zinc treated samples relative to controls. Arrow show membrane versus nuclear staining of the autophagy marker LC3. Cells treated with 300 μM zinc show an accumulation of LC3 in the nucleus. Data are expressed as mean ± SEM of 3 independent experiments (n=3). *p < 0.05,

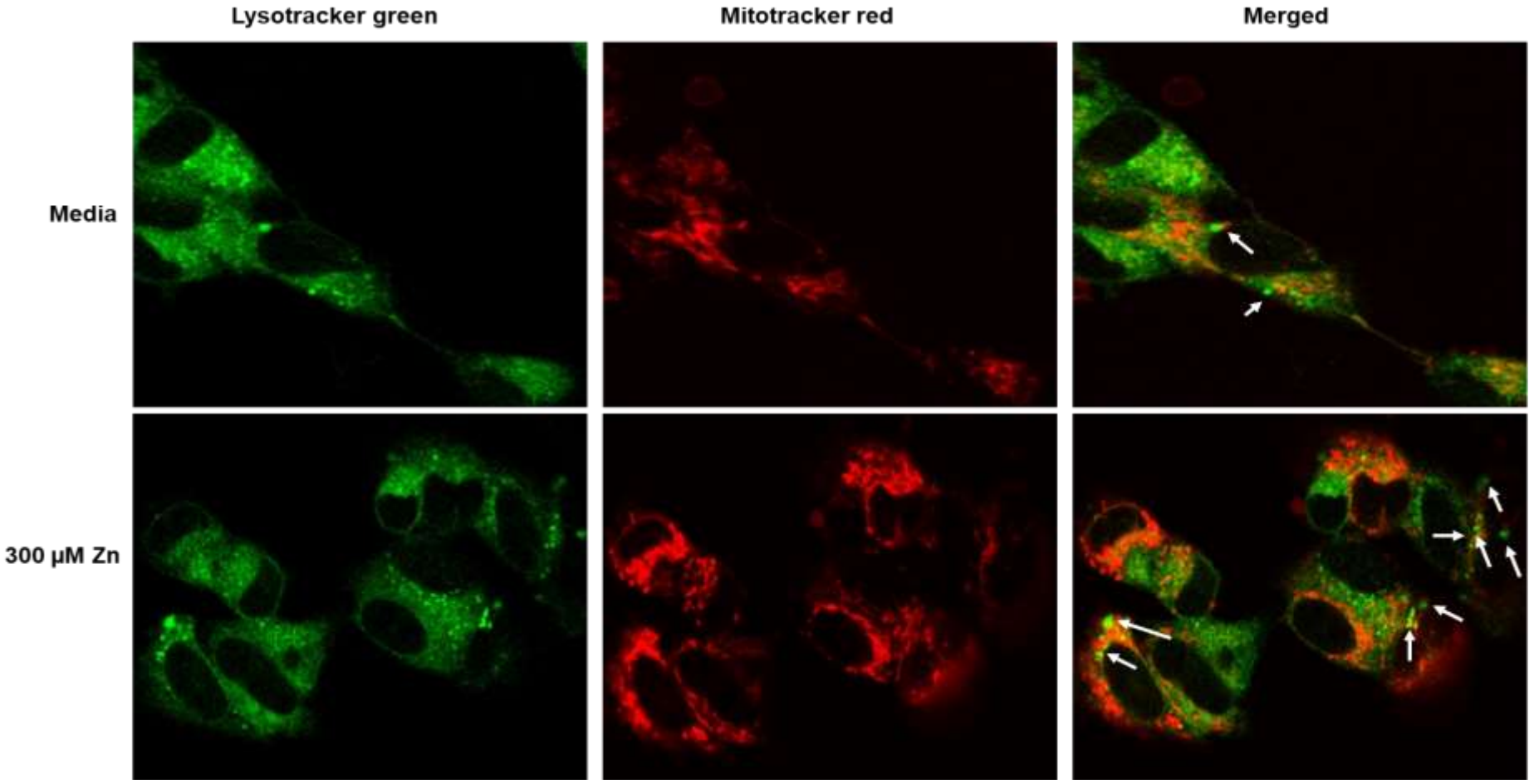

Figure 4.10- Representative confocal images of MitoTracker Red (MTR) and LysoTracker green (LTG) in SH-SY5Y cells treated with or without 300 µM Zn for 24 h. The morphology of the mitochondria in response to 300 µM Zn exposure was visualised using the MTR dye. Zn exposed cells show a more rounded morphology, arrow highlights increase in punctate formation following 300 µM Zn exposure for 24 h relative to untreated cells.

4.3.5- ZN EXPOSURE REGULATES THE ACTIVATION OF THE RAS/ERK AND PI3K/AKT, MTORC1/S6K PATHWAYS IN SH-SY5Y NEURONAL CELLS

The Ras/ERK and PI3K/Akt/mTORC1 pathway mediates cell survival and death and are implicated in the pathogenesis of many human diseases. Receptors to several growth factors are linked to the Ras/ERK and PI3K/Akt signalling pathways. The mTORC1 complex, an important regulator of growth and metabolism is regulated by the Ras/Erk signalling pathway. In this study, the effect of Zn exposure on ERK, AKT and mTORC1 activation was determined using Western blot analysis.

Activation of kinases of the Ras/Erk/MAPK pathway reflected by their respective phosphorylation was determined. Results showed cells exposed to 1 µM CsA manifested no significant change to phosphorylation of ERk, AKT and mTOR. There was a non-significant activation of ERK1/2 upon exposure to 150 µM and 300 µM Zn followed by inactivation from 150 µM and 300 µM Zn CsA cotreatment (Figure 4.11a). Similarly, 150 µM Zn exposure activated AKT kinase in a non-significant manner, however, upon exposure to 300 µM Zn, this activation is significantly lost ($p=0.0416$, Figure 4.11b) corresponding to decrease in cell metabolism and failed cell survival. There was no significant change to mTORC1 phosphorylation following both 150 µM and 300 µM Zn exposure (Figure 4.11c).

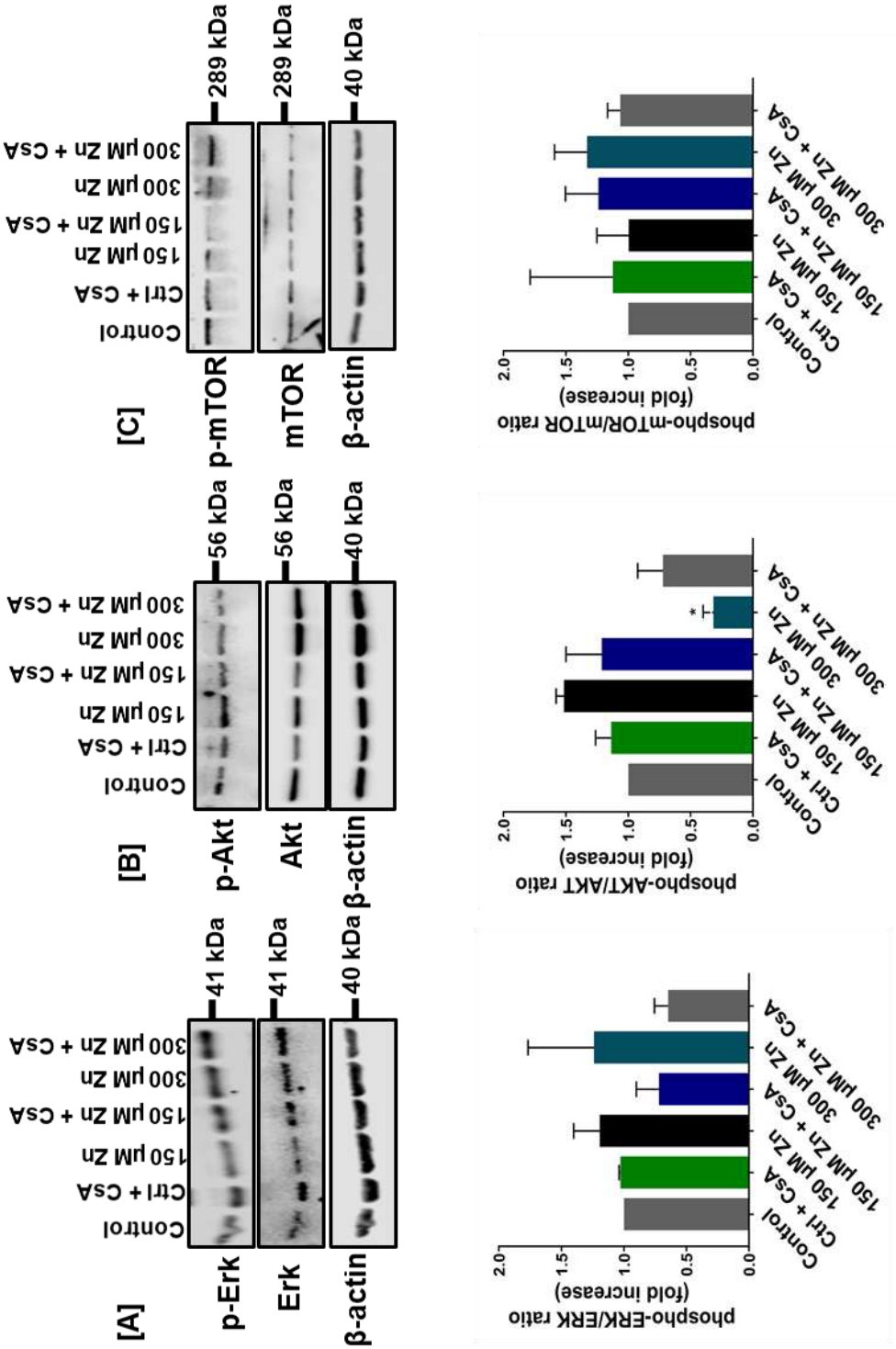

Figure 4.11. Phosphorylation of the Erk, Akt and mTOR signalling pathways are regulated by zinc in SH-SY5Y neuronal cells. Cells were treated as indicated relative to control cells for 24 h. Protein expression was determined by Western blot analysis. **Panel A:** Representative Western blot and densitometric analysis of pErk/ Erk ratio relative to actin expression **Panel B:** pAkt/ Akt ratio relative to actin expression. **Panel C:** p-mTOR/mTOR ratio relative to actin expression. Data are expressed as mean ± SEM of 3 independent experiments. *p < 0.05 compared to control.

4.3.6- ZN INCREASES METABOLIC PROTEINS BCATM AND GDH

The BCATm and GDH are both enzymes responsible for branched chain amino acids (BCAA) and glutamate catabolism. GDH is part of a protein complex formed by BCATm and BCKDC responsible for BCAA oxidation and cycling of nitrogen (Islam *et al.,* 2010). Using western blot analysis, the effect of Zn treatment on the expression of BCATm and GDH was investigated. Results show a significant increase in BCATm levels on exposure to 150 µM and 300 µM Zn (Figure 4.11A, p= 0.0047 and <0.0001) and a significant increase in GDH levels (Figure 4.11B, p= 0.0157 and 0.0009) with 40 µM H_2O_2 used as oxidative stress positive control significantly decreased (p= 0.0139) . This data suggests that key proteins involved in BCAA metabolism are regulated by micronutrients such as Zn.

4.3.7- CONCENTRATION-DEPENDENT EFFECT OF ZN ON PROTEIN AGGREGATION WHILE INCREASING Aβ LOAD

Protein misfolding is a hallmark of several neurodegenerative disorders including Alzheimer's disease. As a result of its association with increased oxidative stress, we investigated the impact of Zn treatment on total cell protein aggregation. There was a significant increase in aggregated protein following 150 µM Zn treatment (p= 0.0216, Figure 4.12A), which was prevented with CsA cotreatment (p=0.0021, Figure 4.12A). At higher concentrations of Zn, a decrease in aggregated proteins occurred when SH-SY5Y neuronal cells were treated with 300 µM Zn or with CsA co-treatment (p= 0.0057 and 0.0013, Figure 4.12A).

Finally, an increase in the levels of β-amyloid (Aβ) was observed in both Zn and CsA cotreated samples (p=0.0025, 0.0001, 0.0015 and 0.0199, Figure 4.12B). There was a significant increase in phosphorylated tau protein levels with 150 µM and 300 µM Zn exposure (p=0.0077, p=0.0032, Figure 4.12C). These results suggest that exposing differentiated SH-SY5Y neuronal cells to excessive Zn levels manifest a similar pattern of increased Aβ production and tau phosphorylation observed in AD.

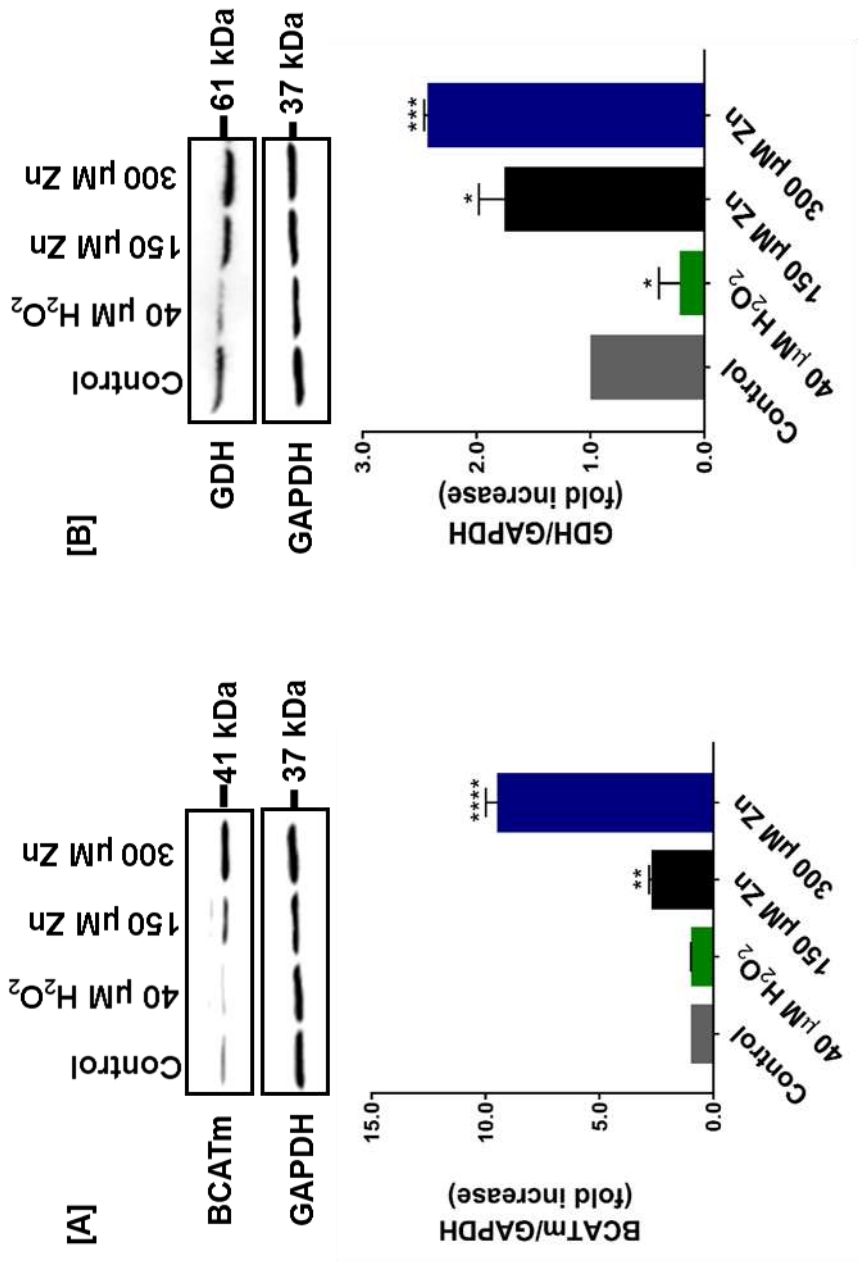

Figure 4.12. Metabolic proteins BCATm and GDH are upregulated in zinc treated SH-SY5Y neuronal cells. Cells were treated as indicated relative to control cells for 24 h. Protein expression determined by Western blot analysis. Data is expressed relative to GAPDH and control samples. **Panel A:** Representative Western blot and densitometric analysis of BCATm relative to GAPDH expression. **Panel B:** Representative Western blot and densitometric analysis of GDH relative to GAPDH expression. Data are expressed as mean ± SEM of 3 independent experiments. *p < 0.05, **p < 0.01, ***p < 0.001, ****p < 0.0001 compared to control.

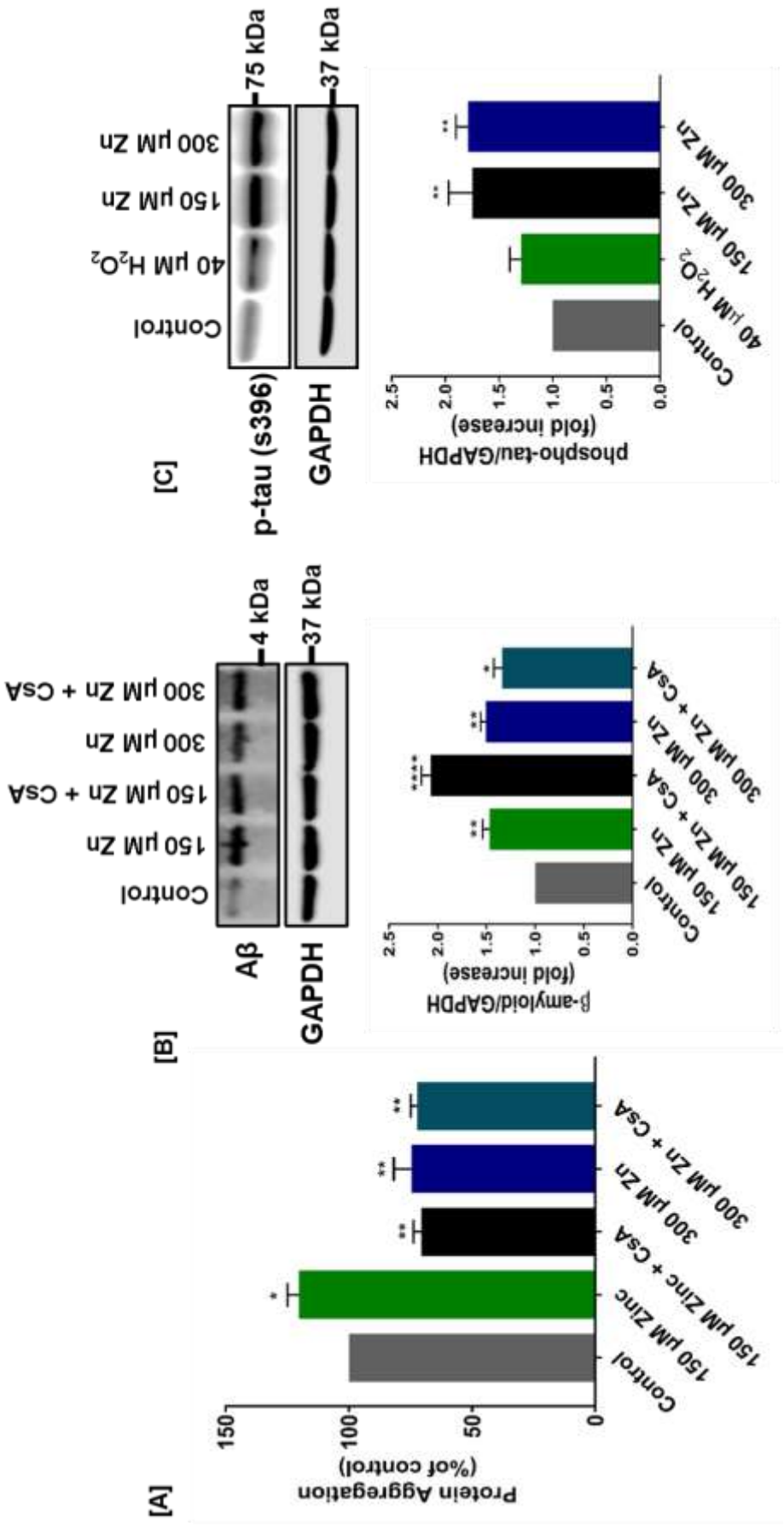

Figure 4.13. Protein aggregation in zinc treated in SH-SY5Y cells with an increase in Aβ but a concomitant decrease in pTau. Cells were treated as indicated relative to control cells for 24 h. Protein aggregation was determined using the Proteostat total protein aggregation assay. In a separate experiment, under the same conditions, the level of Aβ and pTau were assessed using Western blot analysis. **Panel A:** Histogram representing the percentage of aggresome formation relative to control following SH-SY5Y cell treatment. **Panel B:** Representative Western blot and densitometric analysis of Aβ relative to GAPDH expression. **Panel C:** Representative Western blot and densitometric analysis of p-Tau relative to GAPDH expression. Data are expressed as mean ± SEM of 3 independent experiments. *$p < 0.05$, **$p < 0.01$, ****$p < 0.0001$ compared to control.

4.4- DISCUSSION

Previous studies have established that the release of accumulated Zn in pre-synaptic vesicles in neuronal cells into the synaptic cleft induce neurotoxicity due to accompanying release of excessive glutamate which impact on calcium homeostasis eventually resulting in neuronal cell death (Zatta *et al.,* 2003). While this is thought to be the main source of Zn-mediated neuronal cell injury, there is evidence that exogenously acquired Zn can be transported into neurons. Mitochondria have been identified as targets for Zn induced toxicity, however, details of the underpinning mechanisms are limited. Previous evidence supports a role for Zn-induced mitochondrial damage through targeting of key mitochondrial enzymes including cytochrome C oxidase, succinate dehydrogenase, alpha-ketoglutarate and aconitase, which will ultimately affect ATP generation and lead to increased ROS generation (Lemire *et al.,* 2008). A link between Zn and AD pathology have been established (Huang *et al.,* 2000, Yuan *et al.,* 2014, Li *et al.,* 2016) as shown in Zn-induced Aβ peptide aggregation, colocalization of toxic Zn concentration (1055 µM) within amyloid plaque deposits (Miller *et al.,* 2006, Lim *et al.,* 2007), increased Zn staining in the hippocampus of AD brains (Danscher *et al.,* 1997). The aim of this study however, was to determine the possibility of a link between Zn-induced tau phosphorylation, increased Aβ production and dysregulation of the fusion/fission dynamics, impairment of mitochondrial function while exploring the potential protective role of CsA.

For the first time the impact of differential Zn concentrations- 150 µM and 300 µM have been investigated in differentiated SH-SY5Y neuroblastoma cell line. The findings suggested that Zn increased ROS generation, modulating the cell antioxidant system and decreasing mitochondrial respiration and energy production. This results in dysregulation of the fission/fusion dynamics eliciting autophagy-mediated anti-apoptotic response suggesting that activation of the MAPK/PI3K/AKT/mTORC1 signalling pathways mediated cell survival and recovery through an alternative non-apoptotic pathway.

4.4.1- IMPACT OF ZN ON CELL REDOX MECHANISM: PROOXIDANT OR ANTIOXIDANT

An increase in ROS generation was stimulated in response to Zn (**Figure 4.2b**). In similar studies, exposure of cultured cortical neurons (expressing Ca AMPA/Kainate channel) to 300 µM Zn resulted in increased mitochondrial permeability via the mitochondrial Ca^{2+} uniporter (MCU), sustaining ROS production, whereas blocking Zn entry into the mitochondria through the MCU decreased ROS generation (Sensi *et al.,* 1999, Clausen *et al.,* 2013) suggesting Zn-induced ROS generation is specifically as a result of its entry into the mitochondria. Similarly sympathetic neurons exposed to 400 µM Zn showed increased activation of NADPH oxidase in a PKC-dependent manner thereby increasing ROS generation (Noh and Koh, 2000). Here, a pivotal role of the MCU has been suggested and explains an observed increase or loss in cell viability from differential Zn levels (**Figure 4.2a**), where cell viability increase at 150 µM Zn levels and significantly decreased at 300 µM Zn and above. Zn has also been implicated in the upregulation of Nrf2 activity contributing to decreased oxidative stress (Ha *et al.,* 2006). The binding of Nrf2 to the antioxidant responsive element (ARE) regulates the gene expression of a number of antioxidant enzymes such as SOD, hemeoxygenase, GSH and glutathione transferase (Li *et al.,* 2014). ROS is a crucial signalling molecule regulating cell redox status via the GRX/TRX systems that act to protect against irreversible protein damage (Ren *et al.,* 2017) with glutathione peroxidase (GPx) catalysed H_2O_2 scavenging a first line defence (Trachootham *et al.,* 2008). We propose that our reported increase levels of SOD, GRX and TRX proteins following 150 µM Zn and a sustained increase in GRX levels at 300 µM Zn (**Figure 4.3a, b & c**) and GPx at 300 µM Zn is triggered through a ROS-Nrf pathway. In related studies of brown mussels and killfish systems, exposure to sublethal Zn concentration also activated the antioxidant response (Loro *et al.,* 2012)

The comparative response of SH-SY5Y cells to differential Zn levels in both acute and chronic conditions resulting in ROS-induced activation of the antioxidant proteins SOD, GRX, TRX and SOD activity as first line defence mechanisms is geared towards restoration of the cell redox balance. This is

also an indication of the involvement of calcium metabolism hence disruption of MPTP which inturn stimulates the response from the antioxidant system.

4.4.2- IMPACT OF ZN ON MITOCHONDRIAL RESPIRATION AND CELLULAR ENERGY METABOLISM IN SH-SY5Y CELLS

In addition to increased ROS generation, our data showed a concentration dependent impact on MMP, mitochondrial respiration and ATP production. (**Figures 4.5 a, c, d & e**). We suggest that Zn-induced dysregulation of mitochondrial parameters are due to MPTP opening allowing further impairment of mitochondrial respiration and energy metabolism. This is supported by observing an increase in Cyp D a regulator of MMP, also reported in retinal ganglion cells where MPT pore opening was reported (Kim *et al.,* 2014) supporting data from this study which showed a significant increase in CypD expression **(Figure 4.6a)**. Despite these findings, there is not sufficient evidence on the impact of differential Zn concentrations on energy metabolism in differentiated SH-SY5Y neuronal cells. In a related study in cortical neuronal cells, 100 µM Zn treatment caused mitochondrial hyperpolarisation and changes to MMP impacting cell energy production and metabolism (He and Aizeman, 2010). Supporting studies from Lemire *et al.,* 2008 demonstrated HepG2 cells exposed to toxic Zn levels showed impaired ATP production following inhibition of enzymes- succinate dehydrogenase cytochrome C oxidase, aconitase, alpha-ketoglutarate dehydrogenase and isocitrate. However, M17 neuroblastoma cells exposed to only 5 µM Zn for 24 h similarly impaired mitochondrial bioenergetics through decreased basal OCR/ECAR, ATP production, MMP (Sadli *et al.,* 2013, McGee *et al.,* 2011) implying the effect of Zn on mitochondrial function is both concentration and cell-specific. Zn-induced impairment of mitochondrial function have been suggested to be calcium-dependent. Rat hippocampal neurons exposed to exogenous 300 µM Zn in a Ca^{2+}-free media reported only depolarisation and ROS generation with no mitochondrial response which was only triggered in a Ca^{2+}-containing media, suggesting Zn-induced mitochondrial dysfunction is a Ca^{2+}-dependent process (Pivovarova *et al.,* 2014). Contrasting evidence from Sensi *et al.,* 2000 using Zn and Ca^{2+} as intracellular toxins reported that Zn-induced mitochondrial dysfunction were more potent and long-lasting than those from

Ca^{2+} as Zn toxicity persisted even after recovery from Ca^{2+}-induced toxicity (Sensi *et al.,* 2000). This indicated Zn-induced neurotoxicity is likely to act in synergy with Ca but also most likely involve intricate mechanisms independent of Ca^{2+}.

Interestingly, some studies that have suggested that Zn is capable of playing a protective role from varying compounds-induced toxicity and improve energy metabolism at low concentrations. In melanocytes, externally applied 50 µM Zn enhanced mitochondrial biogenesis, stabilised MMP and elevated ATP levels (Rudolf and Rudolf, 2017), while 50 µM Zn relieved HEK293 cells exposed to Ochratoxin A-induced toxicity of impaired energy metabolism (Yang *et al.,* 2017) indicating Zn at very low concentrations and in a cell-specific manner could play a protective role.

In retinal ganglion cells, mPTP opening was demonstrated to induce mitochondrial swelling, cytochrome C release, apoptotic cell death with all these effects ameliorated using the mPTP inhibitor CsA (Kim *et al.,* 2014, Tsujimoto and Shimizu, 2007) similar to recovery effect of CsA cotreatment with 300 µM Zn on MMP and CsA cotreatment with 150 µM Zn on basal respiration, spare respiratory capacity and ATP production evidenced in our data (**Figures 4.5 b, d & e**). The recovery effect on basal respiration, spare respiratory capacity and ATP production is however not demonstrated in CsA cotreatment with 300 µM Zn suggesting the impact of CsA treatment on Zn-induced toxicity is obscured by the overwhelming effect of Zn at this concentration. These findings taken together evidence the negative effect of toxic Zn levels on mitochondrial parameters and functioning is dependent on MPTP opening. The extent of impairment and protective potential of CsA is entirely concentration and cell-specific. A low Zn concentrations however is implicated in improving mitochondrial function and can be explored as targeted therapy in neurodegenerative conditions with mitochondrial dysfunction.

4.4.3- IMPACT OF ZN ON MITOCHONDRIAL FUSION/FISSION DYNAMICS IN SH-SY5Y CELLS

Data from this study reported a significant increase in mitochondrial fission protein Drp1 level and mitochondrial fragmentation following exposure to 300 µM Zn **(Figure 4.7a & d)** with a corresponding decrease in fusion proteins

Mfn1 and Opa1 **(Figure 4.7b & c)**. The impact of Zn toxicity on the fusion/fission dynamics in SH-SY5Y neuronal cells have not been reported. In related studies however, palmitate-induced ROS generation in pancreatic β-cells and high glucose-induced ROS in endothelial cells activated transient receptor potential melastatin (TRPM)-2 channel responsible for mitochondrial Zn and Ca uptake which led to Zn-dependent recruitment of Drp1 catalysing mitochondrial fission and fragmentation (Li *et al.,* 2017, Abuarab *et al.,* 2017) with Zn chelator TPEN attenuating mitochondrial fission in both studies. In human olfactory neurosphere (hON) culture, exposure to 100 µM Zn was toxic to cells and induced an increase in mitochondrial fragmentation which was prevented upon cell treatment with IBMX, a fusion promoting agent (Park *et al.,* 2014) supporting our data which showed an increase in Drp1 with toxic 300 µM Zn level with a simultaneous decrease in fusion markers Opa1 and Mfn1. Increase in ROS levels are known to play a key role in mitochondrial damage thereby enhancing mitochondrial fission. Zn-induced mitochondrial fission in our cells were likely mediated by Zn-induced ROS generation. Given the link between a MMP dissipation, enhanced mitochondrial fission and mitochondrial fusion inhibition (Ishihara *et al.,* 2003), the observed mitochondrial fission at 300 µM Zn level together with decreased mitochondrial fusion was caused by decreased MMP. Furthermore, cotreatment with CsA, an MPTP inhibitor did not attenuate mitochondrial fission, implying that decrease in MMP is responsible for mitochondrial fission increase. However, cotreatment-enhanced level of fusion protein Mfn1 indicates MPTP opening play a role in Zn-induced mitochondrial fusion. Exploring the neuroprotective role of zinc at low concentrations in SH-SY5Y cells is enabled due to an evidence of decreased fragmentation despite not being accompanied by a corresponding increase in fusion regardless of an evidence of decreased MMP. This can be suggested to reflect that despite a disruption of MPTP and corresponding decrease decreased membrane potential, this effect is not enough to elicit mitochondrial fission indicating the need to explore zinc exposure at low concentration as a possible therapeutic mechanism to attenuate mitochondrial dysfunction related phenotypes.

.

4.4.4- IMPACT OF ZN ON AUTOPHAGY AND MITOPHAGY IN SH-SY5Y CELLS

Evidence from this study demonstrates that a toxic Zn concentration (300 µM) results in overt activation of autophagy (**Figure 4.9a & c**) indicated by a significant increase in LC3-II protein expression and LC3 puncta. There is a further increase in mitophagy as shown by a possible colocalisation between the mitochondria and lysosome (**Figure 4.10**). Incubation with Zn has been shown to direct a dual role for autophagy to be either pro-cell death or cell survival. Studies have shown that depending on the concentration of intracellular Zn, autophagy is activated and could either be detrimental or enhance cell survival (Lee and Koh, 2010). As reported, accumulation of Zn in autophagic vacoules (AV) with accompanying lysosomal membrane permeabilisation (LMP) in astrocytes exposed to H_2O_2-induced oxidative stress enhanced autophagy and cell death with Zn chelator TPEN attenuated astrocytic cell death (Lee *et al.,* 2009) suggesting a role for a Zn-induced pro-cell death autophagic mechanism. Clioquinol, an anti-amyloid drug used in AD patients, upon exposure to astrocytes increased intracellular Zn levels and induced autophagy and enhance clearance of aggregated proteins with a reversal induced by Zn chelation by TPEN (Park *et al.,* 2011) suggesting a Zn-dependent pro-cell survival autophagic role. This supports our data that demonstrated increased autophagy/mitophagy that corresponded with a decrease in aggregated proteins (**Figure 4.13a**) which led to loss in cell viability (**Figure 4.2a**). Taken together, these results suggest that during Zn-induced toxicity, autophagy is activated as a possible pro-cell survival mechanism however, this attempt is not sustained and will possibly result in eventual cell death most likely through a non-apoptotic mechanism therefore the need for future study distinguishing pro-cell survival from pro-cell death mediated autophagy.

4.4.5- IMPACT OF ZN ON APOPTOSIS

In this report, we show no significant change in the pro-apoptotic marker Bax but a significant increase of the anti-apoptotic marker Bcl2 (**Figure 4.8a & b**). As previously discussed, growing evidence supports a dual role for Zn in

regulating cell homeostasis, with very low concentrations conferring a protective role whereas at very high concentrations and at longer exposure time, neurotoxic effects are observed. Very low level of Zn (1.5 µM) in IMR-32 cells and primary cortical culture have been reported to activate cyt c mediated apoptosis (Adamo *et al.,* 2010). Similarly, CA1 neuronal cells exposed to 30-35 µM Zn showed DNA fragmentation and slowly occurring apoptotic cell death whereas exposure to ≥ 40 µM Zn levels showed indicative features for necrotic cell death which was completely attenuated using Trolox implicating ROS generation as a contributory mechanism to both apoptotic and necrotic cell death (Kim *et al.,* 1999).

In a related study, SH-SY5Y cells exposed to ≥ 400 µM Zn demonstrated increased cell membrane permeability, DNA fragmentation, decreased MMP and an anti-apoptotic response possibly via ERK1/2 activation suggested to be necrotic rather than apoptotic cell death (An *et al.,* 2005). Furthermore, in C6 rat glioma cells, Zn levels (150-200 µM) resulted in DNA fragmentation and apoptosis with necrotic cell death shown to prevail in elevated Zn levels beyond 200 µM (Watjen *et al.,* 2002). Opening of the MPTP is a crucial step in the initiation of apoptotic and necrotic neuronal cell death and is suggested to be the principal mechanism involved (Zamzami and Kroemer, 2001). The fact that toxic zinc levels has no effect on apoptosis in SH-SY5Y neuronal cells suggests a possible bypassing of the apoptotic pathway and may involve a necrotic cell death mechanism in response to increased ROS generation and decreased MMP.

4.4.6- IMPACT OF ZN ON THE RAS/ERK AND MTOR CELL SIGNALLING PATHWAYS IN SH-SY5Y CELLS

Findings from this study demonstrate a non-significant activation of ERK and mTOR following 150 µM and 300 µM Zn exposure with a non-significant activation of AKT in 150 µM Zn treated cells and inactivation of AKT in 300 µM Zn treated cells (**Figure 4.11a, b & c**). Using phosphor-protein arrays, Zn transporter-mediated Zn release was shown to drive the PI3K-AKT, mTOR, and MAPK pathways (Nimmanon *et al.,* 2017). In a similar study, SH-SY5Y cells exposed to 100 µM Zn treatment have been shown to activate various kinases of the PI3K/MAPK pathways by inducing phosphorylation of ERK1/2,

p70S6K, GSK-3β with a knock-on effect on tau phosphorylation (An *et al.,* 2005). Similarly in PC12 neuronal cells, there is Zn-induced ERK1/2 phosphorylation and subsequent neuronal cell death (Seo *et al.,* 2001). Findings from investigating the effect of Zn in epithelial cells show that Zn mediates the activation of ERK1/2, AKT and mTOR/p70S6K with attenuation of these pathways following ZnR silencing or Zn chelation strongly linking the role of Zn in the activation of these pathways (Cohen *et al.,* 2014). Related study on Zn impact on mTOR/p70S6K pathway reported their activation in rat adipocytes, showing mTOR activity increase up to 2-5 fold in the presence of 10-300 µM Zn. This activity was maximally stimulated at about 100 µM Zn concentration but was decreased at higher concentrations (Lynch *et al.,* 2001). Extracellular Zn (100 µM) has been shown also to activate AKT and p70S6K in a biphasic manner (activation of AKT peaked at 5 & 60 minutes post exposure and decreased with increased exposure time) independent of extraellular calcium and PKC through a PI3K dependent signalling pathway (Kim *et al.,* 2000). The loss of AKT activation in response to 300 µM Zn indicates that despite zinc-induced toxicity reflected by increased ROS generation, this is not signal for the activation of the ERK/AKT pathway also supported by a failure to activate apoptosis suggesting an alternative pathway for any zinc related toxicity.

4.4.7- IMPACT OF ZN ON Aβ AND TAU PHOSPHORYLATION IN SH-SY5Y CELLS

Findings from our data show an increase in total protein aggregation following 150 µM Zn treatment which decline as the concentration of Zn exposure increased (**Figure 4.12a**). Both Aβ and phospho-tau protein expression were significantly increased in 150 and 300 µM Zn exposure (**Figure 4.12b & c**). As previously introduced, Zn toxicity have been linked to AD pathology. Zn have been reported to enhance Aβ aggregation and is a substantive component of the amyloid plaque (Butterfield *et al.,* 2001). *In vitro* studies using NMR analysis have shown rapid aggregation of Aβ peptides in the presence of Zn (Lim *et al.,* 2007). The post-synaptic release of Zn in transgenic mice have been shown to induce amyloid production (Maynard *et al.,* 2005) and increase the production of aggregate-prone Aβ43 found in AD brain senile plaques

(Gerber *et al.,* 2017). A study to determine how Aβ-Zn coordination promotes aggregation reported Zn shift the relative population of the pre-existing amyloid polymorphism causing a stabilisation of less structured assemblies thereby promoting Aβ42 aggregation. It was further shown that increasing Zn concentration slowed down the aggregation rate (Miller *et al.,* 2010), supporting findings from this study where increasing Zn concentration from 150 µM to 300 µM caused a decrease in protein aggregation (**Figure 4.13a**). Tauopathy is thought to result from tau phosphorylation, where a role for Zn has been implicated. In Drosophila tauopathy model, tau phosphorylation was dependent on Zn binding both mediating its toxicity (Huang *et al.,* 2014) specifically Zn-mediated phosphorylation of tau at Ser262 in rat cortical neuronal cells (Kwon *et al.,* 2015). Isothermal titration calorimetry suggested 5- 10 µM Zn mediated fibrillary tau formation whereas 50- 100 µM Zn formed granular aggregates (Mo *et al.,* 2009). Report from human tau transfected cells suggested that phospho-tau accumulation is Zn concentration dependent as cells exposed to 100 µM Zn showed tau dephosphorylation whereas increasing Zn concentration enhanced tau phosphorylation (Boom *et al.,* 2009). The response of zinc to tau phosphorylation suggests it involves a concentration-dependent mechanism.

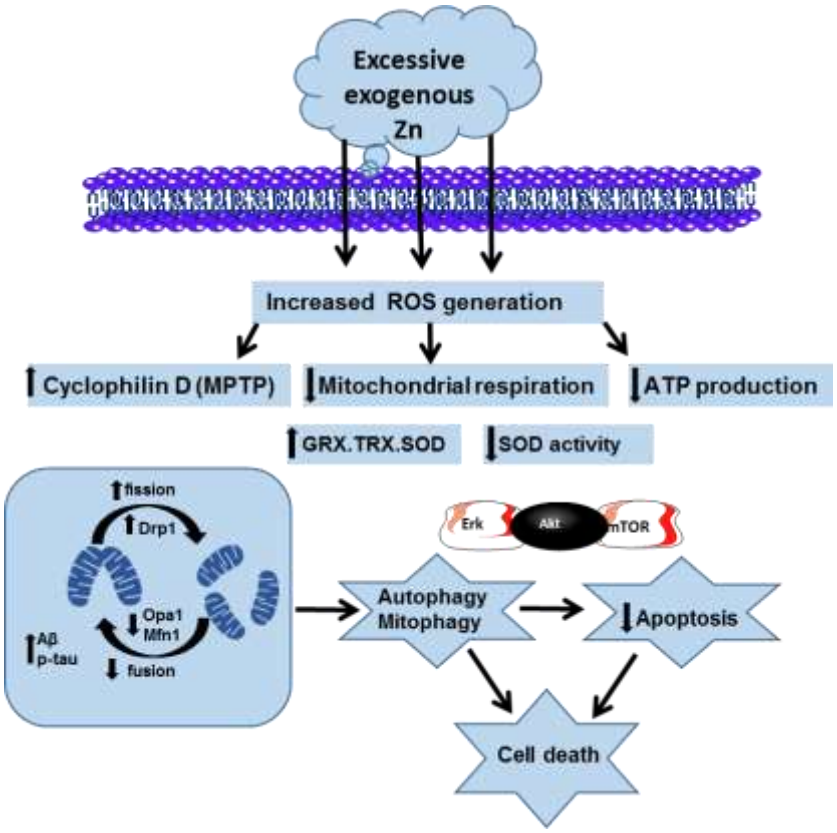

Figure 4.14- Schematic diagram representing the pathways impacted by excessive zinc exposure to SH-SY5Y neuronal cells. Increase in ROS open MPTP, dissipate MMP, impair mitochondrial respiration and ATP production resulting in mitochondrial fission and fragmentation while inhibiting fusion with a simultaneous increase in Aβ and phospho-tau. Autophagy and mitophagy is activated to enhance clearance of fragmented mitochondria, activating possible restoration from cell survival signalling PI3K/AKT/mTOR pathways. Non-apoptotic cell death mechanism likely necrotic is activated.

Chapter 5

Dysregulated mitochondrial function/association with AD pathology in manganese-induced oxidative stress

Contents

5.1- INTRODUCTION

Mn has been identified as the second most abundant metal next to iron and has many physiological roles beneficial to cellular function. Homeostatic dysregulation of Mn can be neurotoxic, giving rise to a condition sharing pathological similarities with Parkinson's disease known as manganism (Neal and Guilarte, 2013, Milatovic *et al.,* 2007). In the nervous system, transporters such as DMT1, transferrin (Tf) and ZIP8/14 mediate Mn entry into the brain (Itoh *et al.,* 2008, Fujishiro *et al.,* 2013, Fujishiro *et al.,* 2014). Although previous studies have highlighted the impact of excessive Mn on abnormalities in movement, new insights have revealed that cognitive functions and cortical structures are also affected by levels of Mn (reviewed in Prakash *et al.,* 2017). The physiological and pathophysiological threshold levels of Mn in the brain have been estimated to be 20-52.8 µM and 60.1-158.4 µM, respectively with similar sub-threshold and toxic levels suggested to apply for cells in *in vitro* studies (Bowman and Aschner, 2014). Similarly, comparing SH-SY5Y cellular content to literature values for human brain Mn content reported Mn dose ≤10 µM as comparable to normal human brain content while values ≥50 µM correlated with brain from toxic Mn exposure (Fernandes *et al.,* 2017). The extent and mode of Mn neurotoxicity have been shown to be tissue specific, with different regions of the brain targeted and damaged to varying degrees. In the human brain, the distribution of Mn levels are highest in the putamen and globus pallidus, with the lowest levels found in the medulla which correlate with age (Ramos *et al.,* 2014). At the cellular level, excessive Mn accumulation in the mitochondria has been implicated in Mn-induced neurotoxicity (Gavin *et al.,* 1999) and have been reported to accumulate in the mitochondria via the mitochondrial calcium uniporter (MCU) (Morello *et al.,* 2008). Similar to Zn-induced toxicity, elevated Mn levels induced mitochondrial dysfunction resulting in excessive production of ROS, loss of MMP, opening of the mitochondrial transition pores, mitochondrial swelling and oxidative phosphorylation impairment, results in decreased ATP synthesis (Milatovic *et al.,* 2007 and Yin *et al.,* 2008). This effect is linked to its incorporation into MnSOD involved in redox status signalling, as a result, Mn accumulation

impact on oxidative phosphorylation by inhibiting the formation of complex I of the electron transport chain, thereby generating ROS, causing mitochondrial dysfunction (Milatovic *et al.,* 2007) and depleting glutathione levels and glutathione peroxidase activities in the process (Desole *et al.,* 1997, Prabhakaran *et al.,* 2008). The impact of Mn neurotoxicity is suggested to be partly mediated through deregulation of neurotransmitters- glutamate, dopamine and GABA resulting in excitotoxicity and cell death (Erikson and Aschner, 2003, Fitsanakis and Aschner, 2005). Dopaminergic neurodegeneration as a result of dopamine depletion and downregulation of its transporters trigger motor dysfunction and neuronal loss, pointing to a possible interaction between oxidative stress and the resulting neurodegeneration in the substantia nigra (Deng *et al.,* 2015). Mn have been implicated in increasing the Aβ-like precursor-like protein 1 (APLP1) gene in the frontal cortex of macaques exposed to Mn treatment for 10 months, additionally, increased APLP1 labelling have been reported in the white matter of exposed cells, with Aβ plaque deposition reported in rat frontal cortex (Guilarte *et al.,* 2008) suggesting a role for Mn accumulation and AD pathology, however, reported studies with link between excessive Mn and AD is limited.

Despite Mn weak binding affinity to Aβ (Wallin *et al.,* 2016), neurodegenerative features resulting from cellular stress response such as dysregulated autophagy in memory-impaired mice (Wang *et al.,* 2017), activation of inflammatory pathway and glutamate excitotoxicity thereby apoptosis in excessive Mn are suggested as mechanisms mediating Mn-induced neurotoxicity. In addition to these mechanisms mediating Mn neurotoxicity, the link between dysregulated fission/fusion dynamics, impaired mitochondrial function and its contribution to AD hallmarks- Aβ and phospho-tau in SH-SY5Y cells is yet to be explored.

The schematic diagram highlights the pathways affected by Mn neurotoxicity and the underlying mechanisms involved. Exposure to toxic Mn concentration increased ROS generation, impaired mitochondrial respiration and ATP production while modulating antioxidant enzymes to combat ensuing oxidative stress. As a result, there is dysregulation of the mitochondrial fission/fusion

dynamics and a non-functional autophagy which activates the MAPK/PI3k/AKT signalling pathway triggering apoptosis.

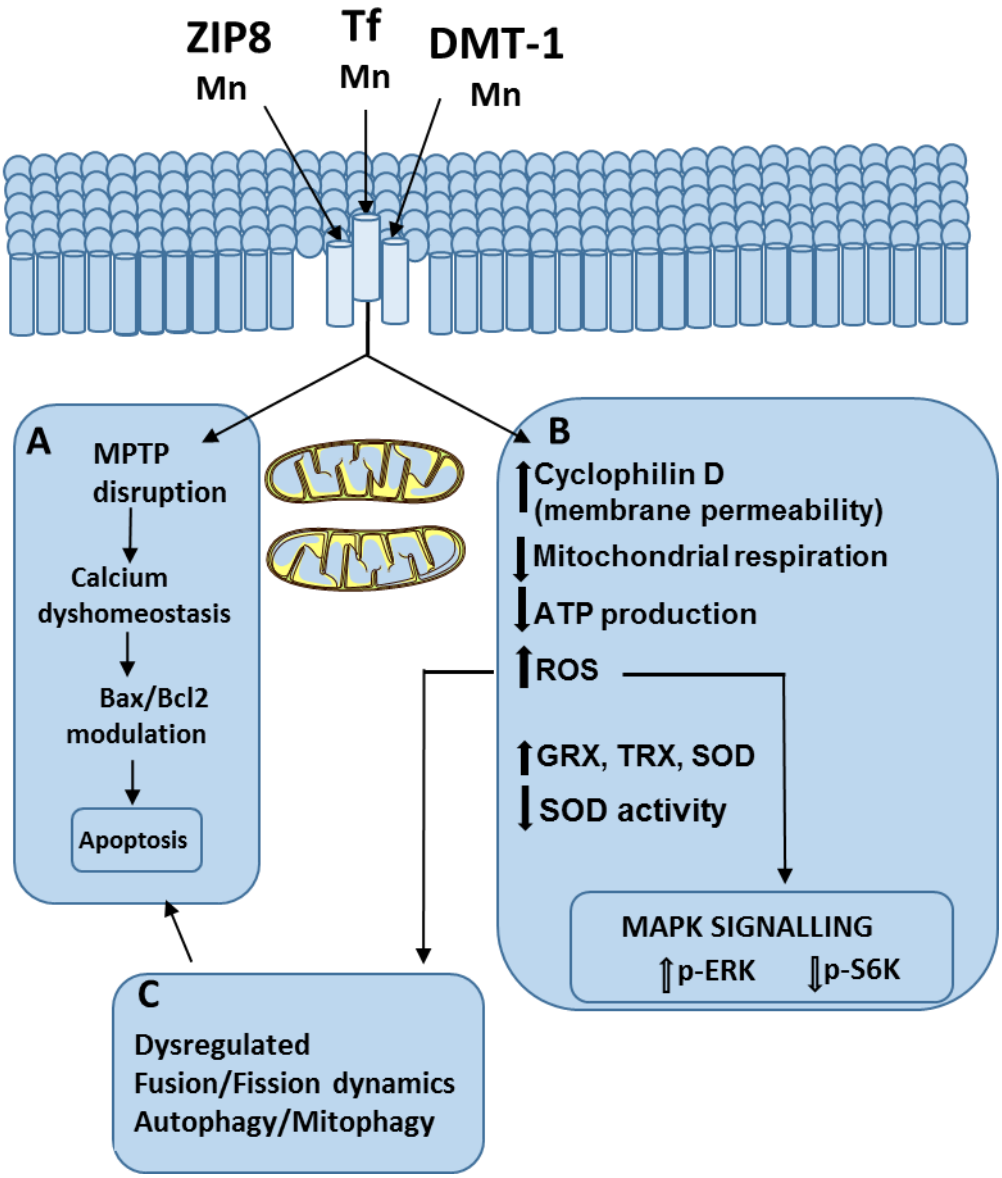

Figure 5.1: Targeted pathways in manganese-induced neurotoxicity. Accumulation of Mn in the mitochondria results in MPTP disruption mediating calcium dyshomeostasis, a key mediator of apoptotic cell death (**A**). Excessive Mn mediate increase in ROS generation also associated with MPTP opening, impairing mitochondrial respiration and ATP production. Increase in ROS generation elicits a response from the MAPK/ERK signalling pathway by activating ERK, a contributor to apoptotic cell death and mediating decrease in protein synthesis which play a role in neuronal cell death (**B**). Increased ROS from excessive Mn accumulation dysregulates mitochondrial dynamics, thereby disrupting the fusion/fission cycle which contributes to tau phosphorylation (**C**).

5.2- AIMS AND OBJECTIVES

Hypothesis: Manganese-induced neurotoxicity impairs mitochondrial function through disruption of the fusion/fission dynamics.

Specific Aim 1: To investigate the impact of Mn-induced oxidative stress on the redox state of SH-SY5Y neuronal cells.

Specific Aim 2: To determine the impact of Mn on neuronal cell mitophagy (fusion/fission dynamics) and protein folding

Specific Aim 3: To evaluate the impact of dysregulated mitochondrial function on metabolic signaling pathways.

Specific Aim 4: To understand the role of cyclosporine A in regulating mitophagy.

Specific Aim 5: To determine how Mn-induced toxicity contribute to AD pathology using the SH- SY5Y cell model.

5.3- RESULTS

5.3.1- Manganese decreases SH-SY5Y cell viability, increases ROS formation and modulates the cell antioxidant system

Exposure of neuronal cells to Mn beyond physiological threshold impact on the cell redox status thereby resulting in ROS production. To understand the oxidative stress impact of excessive Mn in SH-SY5Y cells, ROS generation following exposure to 200 µM and 400 µM Mn at 6 h and 24 h was investigated. The intensity of highly fluorescent DCF produced by ROS oxidation of DCFDA was measured. Results show a significant increase in DCF intensity in a dose dependent manner after 6 and 24 h ethanol exposure ($p= 0.0001-0.0013$, Figure 5.2B). The impact of increased ROS production on cell viability was measured using MTS assay. SH-SY5Y cells were exposed to 200 µM, 400 µM, 800 µM and 1600 µM Mn concentrations at time points 6 h, 24 h and 48 h. Results from this investigation show cell viability was significantly decreased in a concentration and time dependent manner ($p< 0.0001-0.01$, Figure 5.2A). Following an increase in ROS generation, modulation of proteins SOD, GRX and TRX involved in the cell's antioxidant system was determined. In response to 400 µM Mn exposure, there was significant increase in the levels of SOD ($p= 0.0088$), GRX ($p=0.0286$) proteins and TRX ($p=0.0257$, 0.0442) following 200 µM and 400 µM Mn exposure (Figure 5.3 A, B and C), respectively with 40 µM H_2O_2 used as oxidative stress positive control. In addition to the proteins, the activity of SOD enzyme, a mediator of ROS metabolism was also determined in acute and chronic exposure times (Figure 5.4). At 3h time point, 200 µM Mn treatment and 200 µM Mn + CsA cotreatment cause a significant decrease in SOD activity ($p=0.009$, 0.0034, Figure 5.4A). At 24 h time point, 400 µM Mn treatment caused a marginal decrease, with 400 µM Mn + CsA cotreatment resulting in a significant decrease in SOD activity ($p=0.0334$, Figure 5.4B).

These results suggests the SOD, GRX and TRX activation is a cellular response to ROS-induced stress signal to compensate for Mn-induced oxidative stress where an increase in protein expression with decreased SOD activity results from very toxic Mn levels and sustained ROS generation thereby overwhelming the antioxidant system resulting in loss of cell viability .

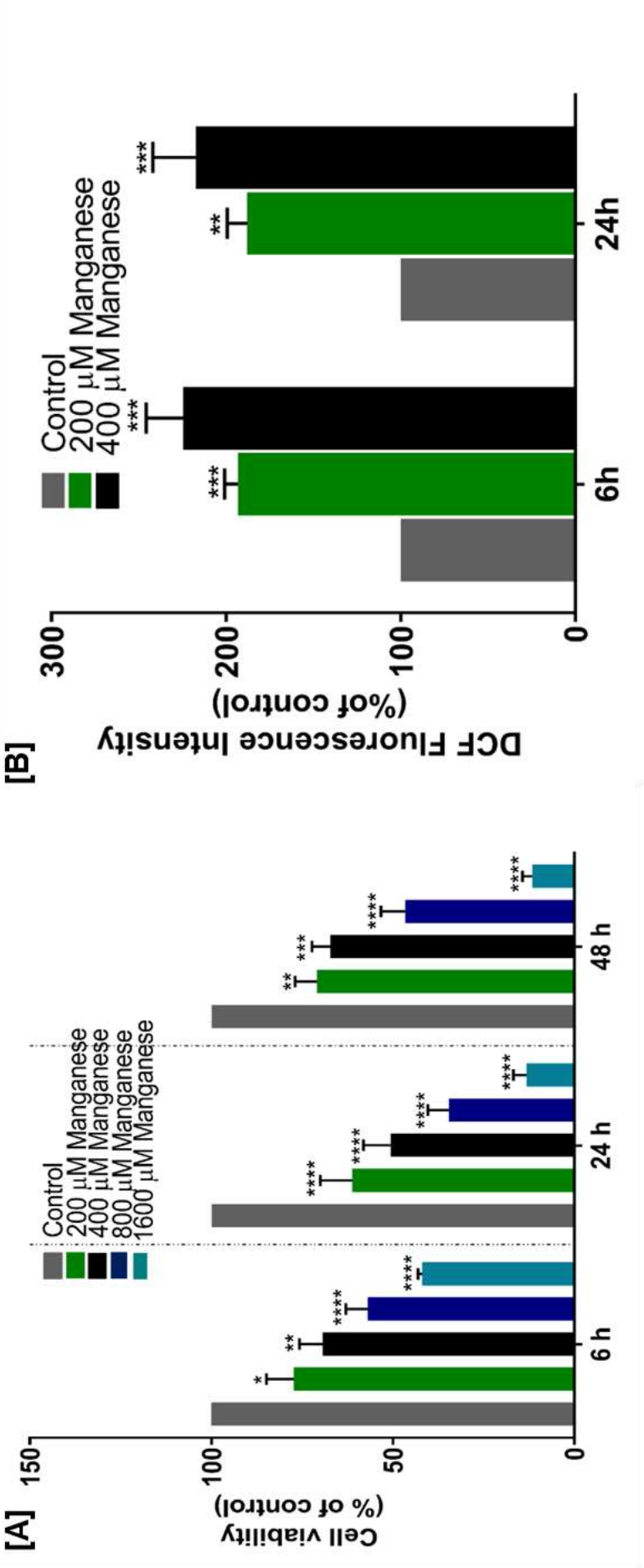

Figure 5.2 – Loss of cell viability and an increase in ROS in SH-SY5Y cells in response to manganese toxicity. Cell viability/metabolic activity and intracellular ROS generation in manganese treated SH-SY5Y cells determined by MTS reduction and DCFDA fluorescent dye staining, respectively. **Panel A:** Cells were treated with 200-1600 µM manganese, relative to control cells and incubated for 6 h, 24 h and 48 h, respectively. Cell viability was assessed using the MTS assay and the change in absorbance measured at 500 nm. **Panel B:** Cells were treated with 200 µM and 400 µM manganese, respectively, relative to control cells for 6 h and 24 h. Intracellular ROS was assessed using DCFDA with DCF fluorescent intensity at 500 nm. Data are expressed as mean ± SEM of 3 independent experiments. *p < 0.05, **p < 0.01, ***p < 0.001, ****p< 0.0001 compared to control.

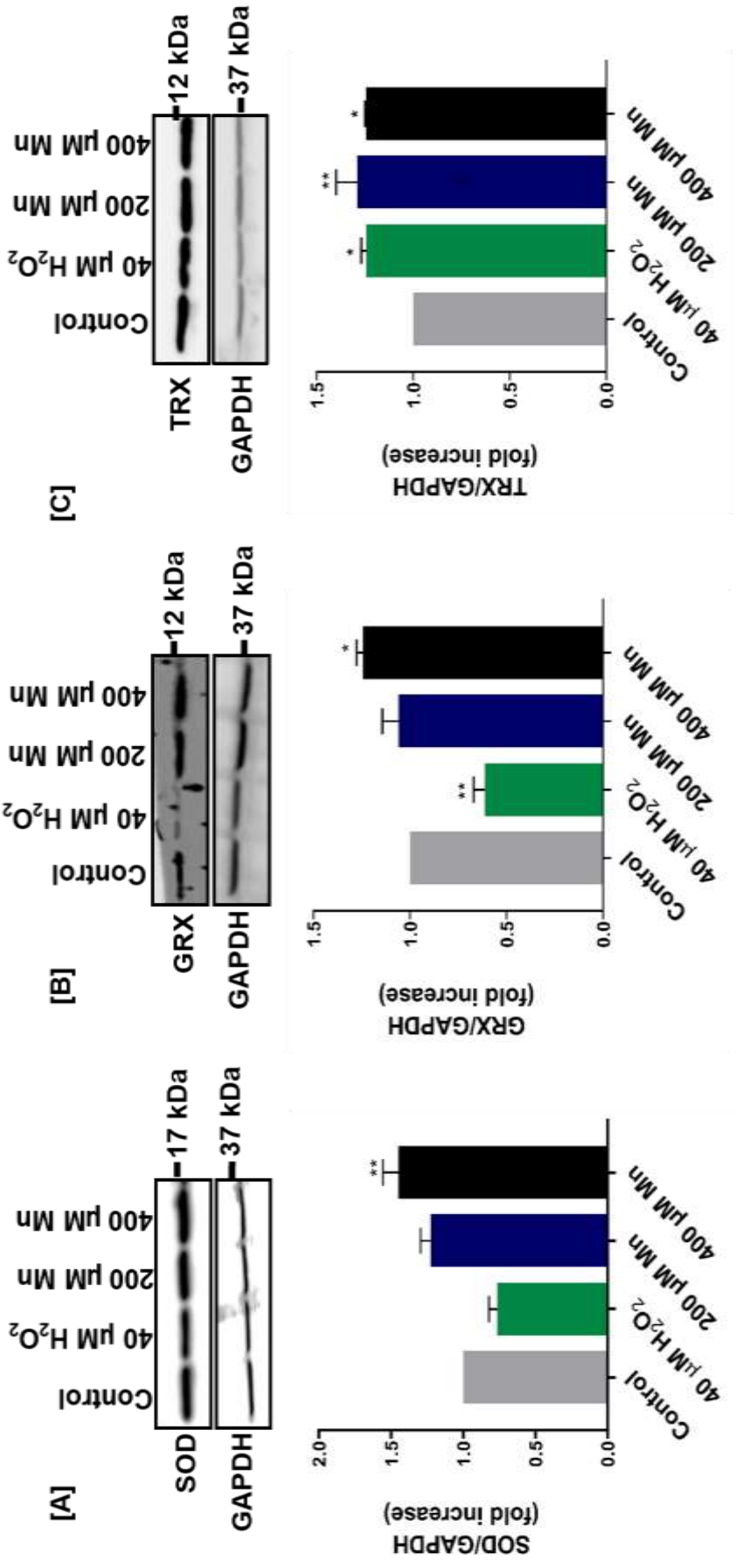

Figure 5.3. Differential protein expression of SOD, GRX and TRX in manganese treated SH-SY5Y neuronal cells. Cells were treated as indicated relative to control cells for 24 h. SOD, GRX and TRX protein expression were determined by Western blot analysis. Immunoblot of **Panel A:** SOD, **Panel B:** TRX, **Panel C**: GRX and their respective GAPDH expression. Data was normalized to respective GAPDH and expressed as mean ± SEM of 3 independent experiments. *$p < 0.05$, **$p < 0.01$ compared to control.

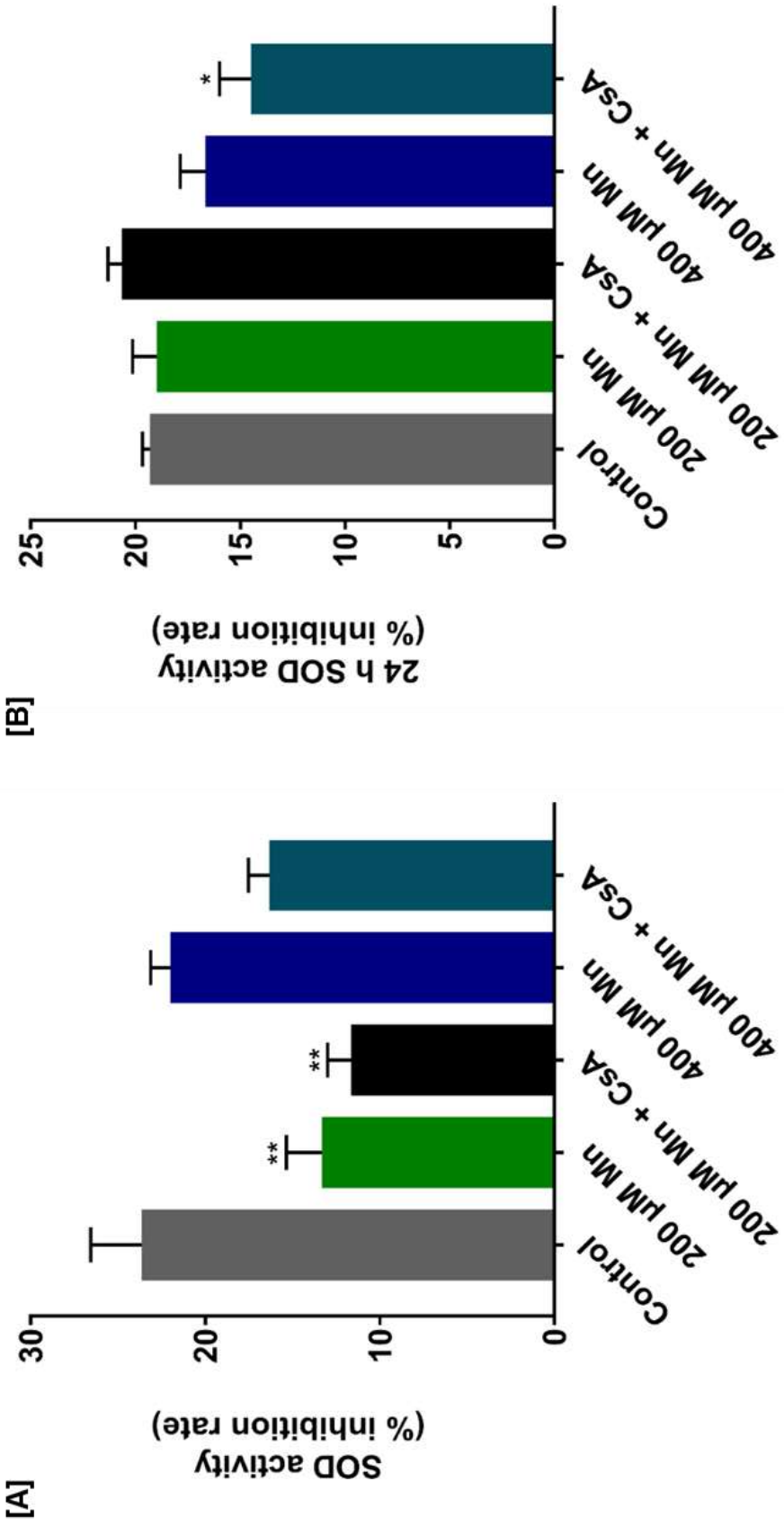

Figure 5.4. SOD activity in manganese treated SH-SY5Y neuronal cells. Cells were treated as indicated relative to control cells and assayed for SOD activity using the SOD enzyme activity assay kit. **Panel A:** SOD activity in response to varied manganese concentration incubated for 3 h and **Panel B:** SOD activity in response to varied manganese concentration incubated for 24 h. Data are expressed as mean ± SEM of 3 independent experiments. *p < 0.05, **p < 0.01, ***p < 0.001, ****p< 0.0001 compared to control.

5.3.2- Altered mitochondrial membrane potential and bioenergetics in manganese-treated SH-SY5Y cells

Using the fluorogenic dye JC-1, mitochondrial membrane potential was measured in response to Mn treatment. Presented data show a significant reduction of MMP following Mn treatments (Figure 5.5A, p= 0.0004 and 0.0003). Further investigation to determine the effect of Mn treatment on mitochondrial bioenergetics was carried out using the Agilent seahorse XFe24 analyzer MitoStress assay following cell treatment with 200 µM and 400 µM Mn and control cells treated with 10 % FBS DMEM for 24 hours prior to performing the Mito Stress assay. This assay directly measures OCR, basal mitochondrial respiration, proton leak, spare respiratory capacity and ATP production (Figure 5.5B, C and D). Exposing SH-SY5Y neuronal cells to 200 µM, 400 µM Mn and CsA cotreatments significantly decreased basal mitochondrial respiration following (p=0.0239, 0.0028, 0.0017 and <0.0001, Figure 5.5B & C). A similar trend was observed for ATP production with a significant decrease in 200 µM Mn, 400 µM Mn and CsA co-treated cells (p=0.0061, 0.0009, 0.0023 and <0.0001, Figure 5.5D). Spare respiratory capacity was significantly increased in 200 µM Mn + CsA treated cells (p=0.0014, Figure 5.5C) and proton leak was significantly decreased following 400 µM Mn and 400 µM Mn + CsA treated cells (p=0.0436 and 0.0049, Figure 5.5E), respectively. These results together suggest that in SH-SY5Y neuronal cells, 200 and 400 µM Mn dysregulates mitochondrial bioenergetics by disrupting both mitochondrial respiration and ATP production.

There was a significant increase in the level of the mitochondrial matrix marker cyclophilin D upon 200 µM and 400 µM Mn treatment (p= 0.0213 and 0.0069, Figure 5.6B) and 40 µM H_2O_2 exposure showing a non-significant increase in CypD levels indicating a possible disruption of calcium metabolism and MPTP involvement. There was a significant increase in the mitochondrial chaperone Hsp60 level following 400 µM Mn treatment (p= 0.03021, Figure 5.6A) with with 40 µM H_2O_2 used as oxidative stress positive control showing no significant change to Hsp60 protein levels.

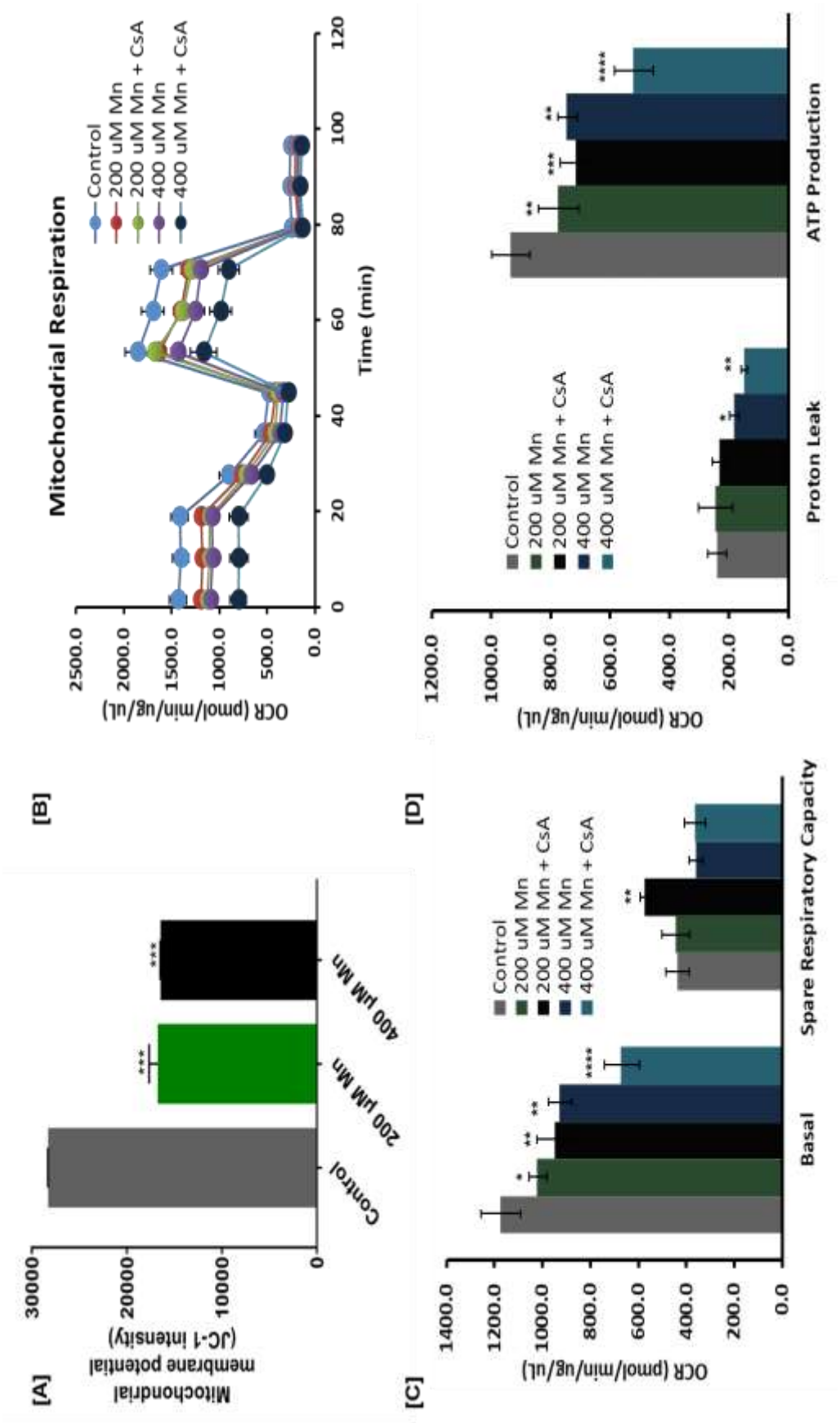

Figure 5.5- Manganese exposure decreased mitochondrial membrane potential and improved mitochondrial respiration and ATP production in SH-SY5Y cells. Cells were treated as indicated relative to control cells for 24 h. **Panel A and B:** JC-1 assay measuring MMP. **Panel C:** Seahorse Mito Stress Test measuring oxygen consumption rate (OCR), **Panel D:** basal mitochondrial respiration and spare respiratory capacity, **Panel E:** mitochondrial proton leak and ATP production. Data are expressed as mean ± SEM of 3 independent experiments. *p < 0.05, **p < 0.01, ***p < 0.001, p< 0.0001 compared to control.

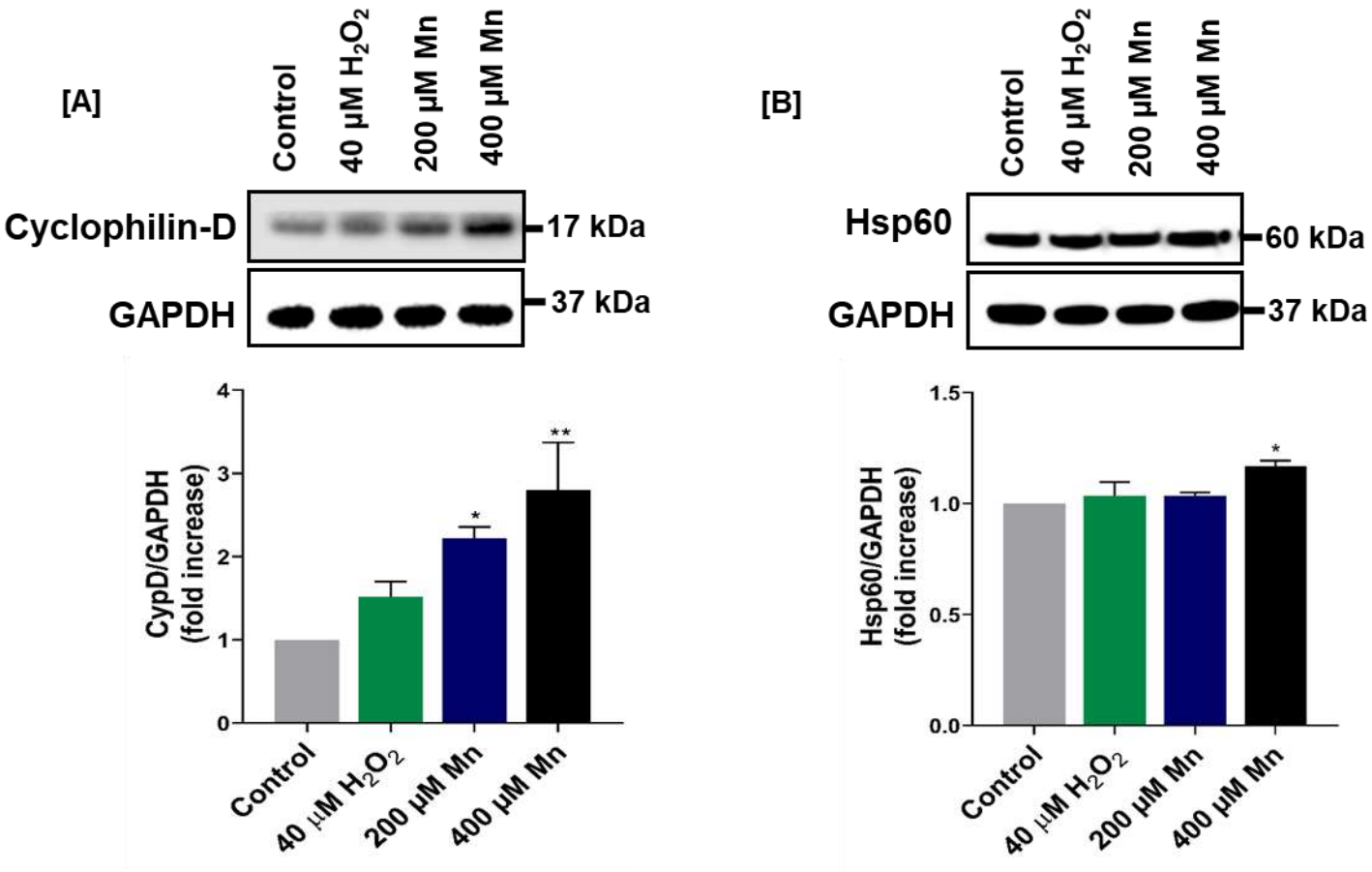

Figure 5.6. Expression of mitochondrial proteins Cyclophilin D and Hsp60 in manganese treated SH-SY5Y neuronal cells. Cells were treated as indicated relative to control cells for 24 h. Cyclophilin D /Hsp60 protein expression was determined by Western blot analysis. Data is expressed relative to GAPDH and control. **Panel A:** Representative Immunoblot blot and densitometric analysis of Cyclophilin D relative to GAPDH expression. **Panel B:** Representative Immunoblot blot and densitometric analysis of Hsp60 relative to GAPDH expression. Data are expressed as mean ± SEM of 3 independent experiments. *p < 0.05. **p < 0.01compared to control.

5.3.3- Mitochondrial dynamics disruption in response to manganese treatment

Cyclophilin D, a mediator of MPTP opening linked to MMP can be inhibited by CsA. Due to the important role the fission/fusion cycle play in maintaining mitochondrial morphology and integrity, the impact of exposing SH-SY5Y cells to 200 µM and 400 µM Mn were determined. CsA cotreatments were carried out to ascertain the possibility of a protective role to restore dysregulation of mitochondrial dynamics.

To ascertain this effect, Drp1, OPA1 and MFN1 were determined by Western blot analysis. As shown in Figure 5.7A, there was a significant increase in Drp1 level in response to 400 µM Mn ($p=0.0170$) and a non-significant decrease in Drp1 expression in 200 µM and 400 µM Mn cells cotreated with CsA. For fusion proteins Opa1 and MFN1, there was a significant decrease in Opa1 levels at 400 µM Mn exposure ($p=0.012$, Figure 5.7B). However, co-treating 200 µM Mn with CsA showed a significant increase in Opa-1 ($p= 0.047$, Figure 5.7B). The level of the fusion protein, MFN1, was significantly decreased on exposure to 200 µM and 400 µM Mn treatment ($p=0.0028$ and 0.0009, Figure 5.7C), with 400 µM Mn +CsA co-treated cells not showing any protective effect as it remained significantly decreased ($p= 0.0007$, Figure 5.7C).

These results together suggest that Mn exposure to neuronal cells cause an increase in mitochondrial fission with no corresponding increase in fusion to compensate for damage to mitochondrial morphology. With an increase in mitochondrial fission, cells were exposed to 400 µM Mn and stained with MitoTracker Red to monitor the morphological changes in mitochondria using confocal microscopy (Figure 5.7D). The image represented show that upon Mn exposure, there was an increase in mitochondrial fragmentation.

These results suggest that Mn-induced toxicity disrupts the fission/fusion dynamics in SH-SY5Y neuronal cells. The response is an increase in mitochondrial fission with a simultaneous depression of the fusion process causing a failure to balance out the organelle dyshomeostasis thereby eliciting apoptosis and mitophagy, with CsA conferring some protective effect.

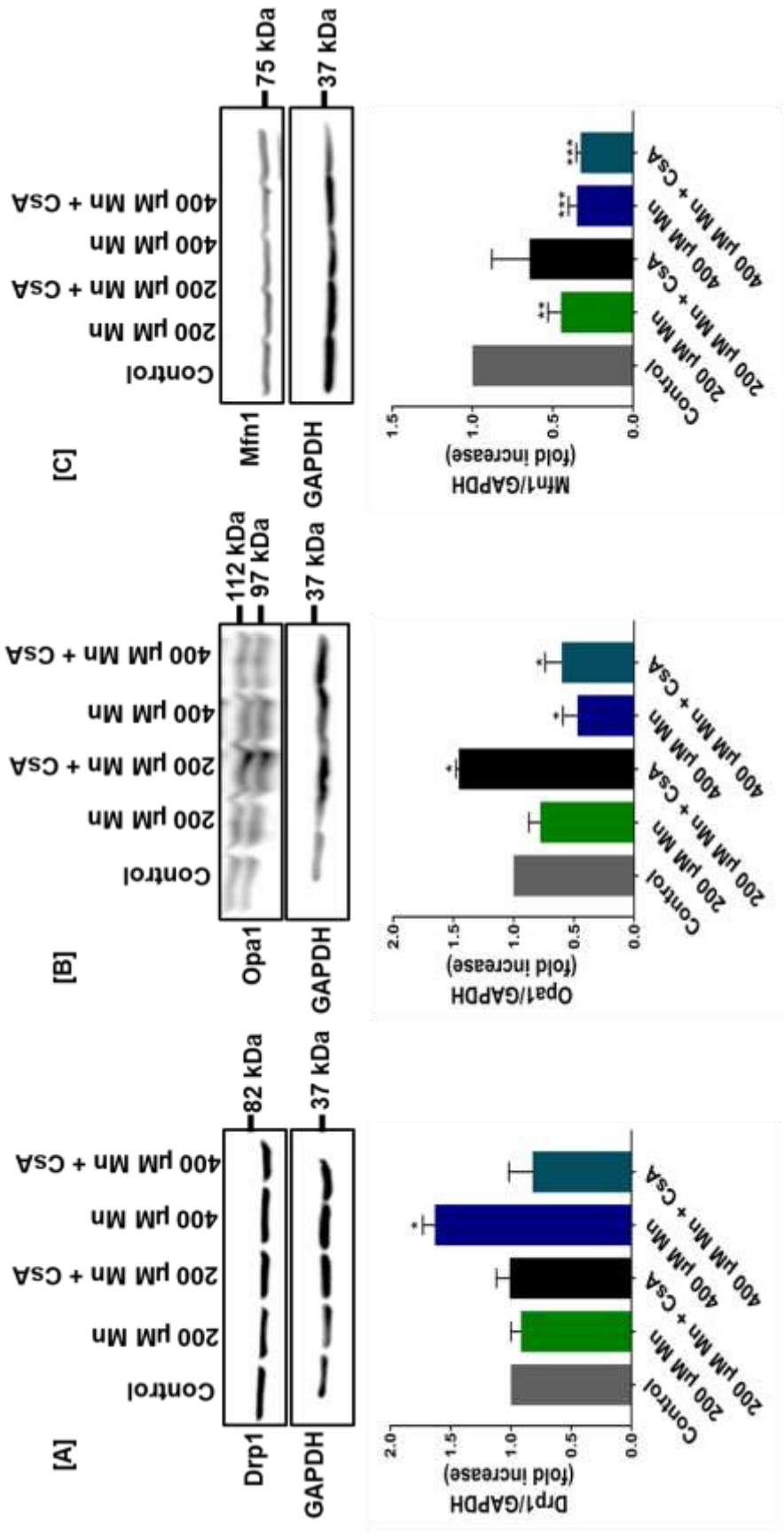

Figure 5.7. Differential expression of mitochondrial fission protein Drp1 and fusion proteins Opa1 and Mfn1 in manganese treated SH-SY5Y neuronal cells. Cells were treated as indicated relative to control cells for 24 h. Protein expression was determined by Western blot analysis. Data is expressed relative to GAPDH and control samples. **Panel A:** Representative Immunoblot and densitometric analysis of Drp1 **Panel B:** Opa1 **Panel C:** Mfn1 relative to GAPDH expression. Data are expressed as mean ± SEM of 3 independent experiments (n=3). *p < 0.05, **p < 0.01, ***p < 0.001, ****p<0.0001 compared to control.

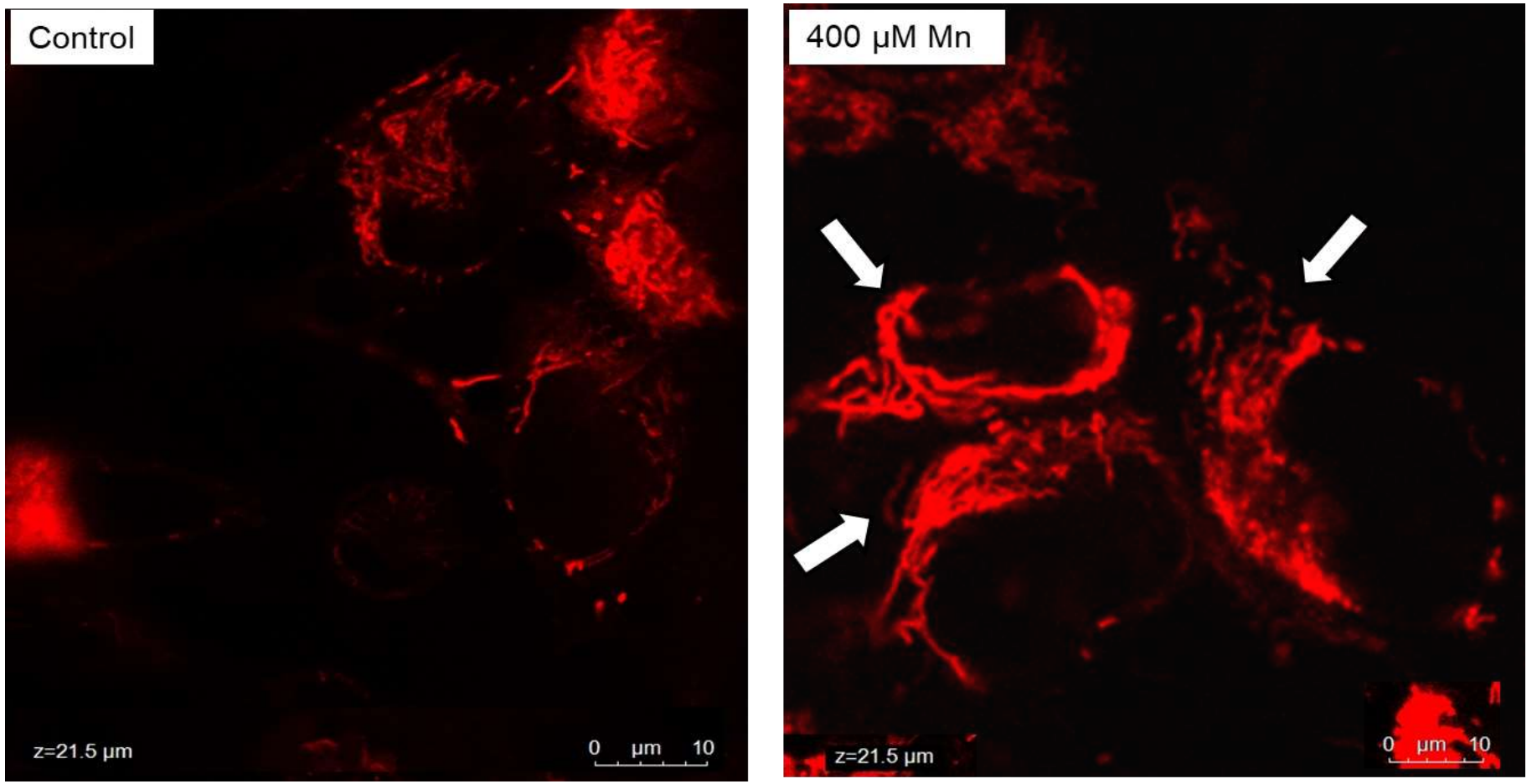

Figure 5.8. Representative confocal images of MitoTracker Red (MTR)-stained mitochondria in SH-SY5Y cells treated with or without 400 µM Mn for 24 h. The morphology of the mitochondria in response to 400 µM Mn exposure was visualised using the MTR dye. Mn exposed cells show fragmentation typical of mitochondrial fission, arrow highlights increase in punctate formation following 400 µM Mn exposure for 24 h relative to untreated cells.

5.3.4- Manganese treatment in SH-SY5Y cells activates autophagy and apoptosis

To maintain cell functioning and homeostasis, the autophagic pathway enable the degradation and recycling of damaged cell components. This process is an adapted cell survival mechanism in response to stress. Autophagic response following Mn exposure measured by changes in LC3 and p62 levels was determine using Western blot analysis. Following 24 h exposure of SH-SY5Y cells to 200 µM and 400 µM Mn, there was an increase in autophagy evidenced by increased expression of LC3I/II and p62. Results show a significant increase in the conversion of LC3-I to its lipid-conjugated autophagosome-bound form LC3-II in 400 µM Mn treatment ($p=0.0006$, Figure 5.9A). The levels of p62, the protein delivering ubiquinated autophagic cargo to the autophagosomes by interacting with LC3 was also increased following 200 µM and 400 µM Mn treatment ($p=0.0207$ and <0.0001, Figure 5.9B). Exposure to 40 µM H_2O_2 caused a significant increased in both LC3II and p62 levels ($p=0.0106$ and 0.0303). This suggests that Mn-induced toxicity in neuronal cells mediates autophagy which is either protective or detrimental suggested by potential downstream effect of eliciting apoptosis.

Following an increase in mitochondrial fragmentation in response to 400 µM Mn triggering the autophagy/ mitophagy machinery, the apoptosis pathway was activated. Result presented show a significant increase in the level of apoptotic marker Bax ($p=0.0456$, Figure 5.10A) upon exposure of SH-SY5Y cells to 400 µM Mn and a simultaneous decrease in anti-apoptotic marker Bcl2 level ($p=0.0278$, Figure 5.10B). Cotreatment with CsA attenuated Bax level ($p= 0.001$, Figure 5.10A) suggestive of a protective effect.

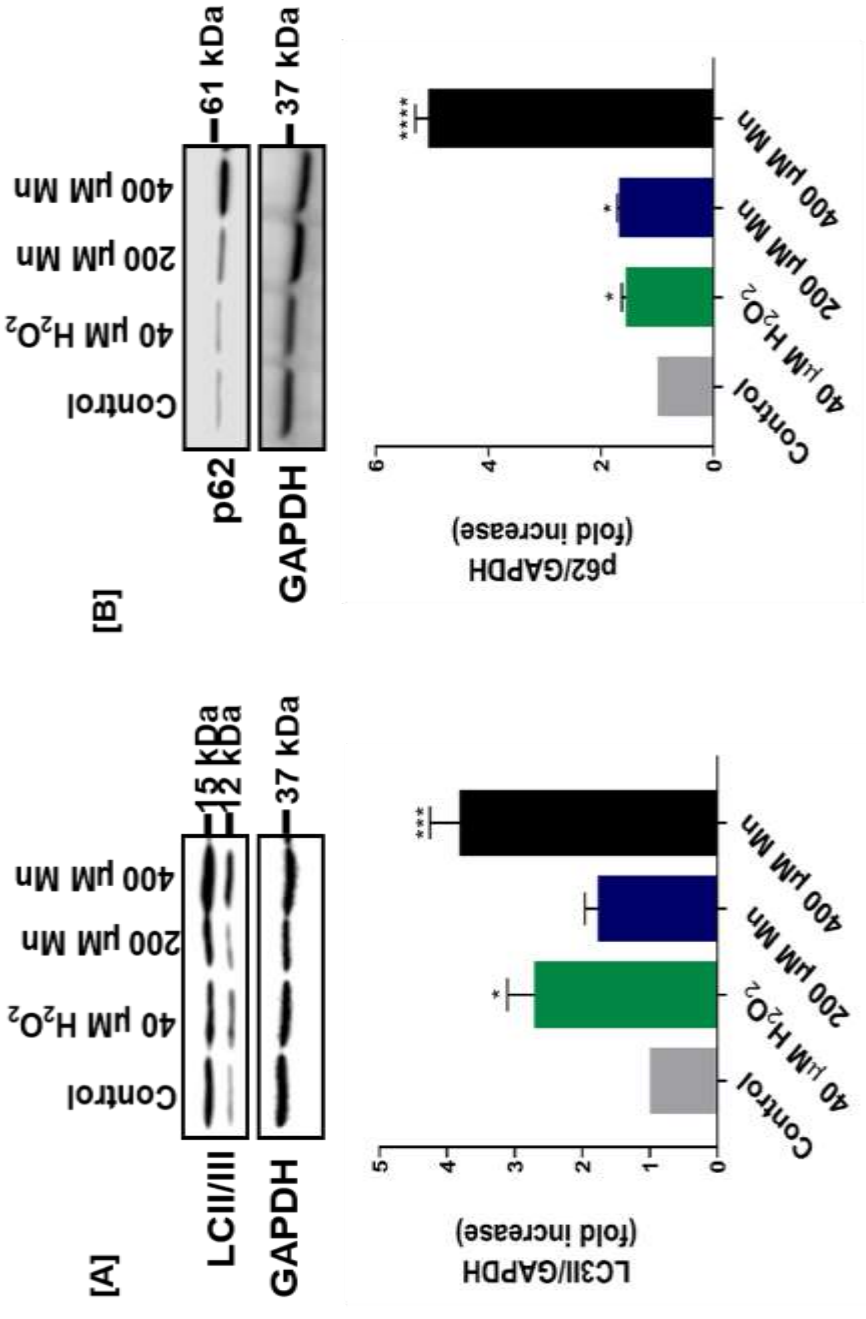

Figure 5.9 Autophagy is increased in manganese treated SH-SY5Y neuronal cells. Cells were treated as indicated relative to control cells for 24 h. Protein expression was determined by Western blot analysis. Data is expressed relative to GAPDH and control samples. **Panel A:** Representative Immunoblot and densitometric analysis of LC3I/II **Panel B:** p62 relative to GAPDH expression. Data are expressed as mean ± SEM of 3 independent experiments. *$p < 0.05$, ***$p < 0.001$ compared to control.

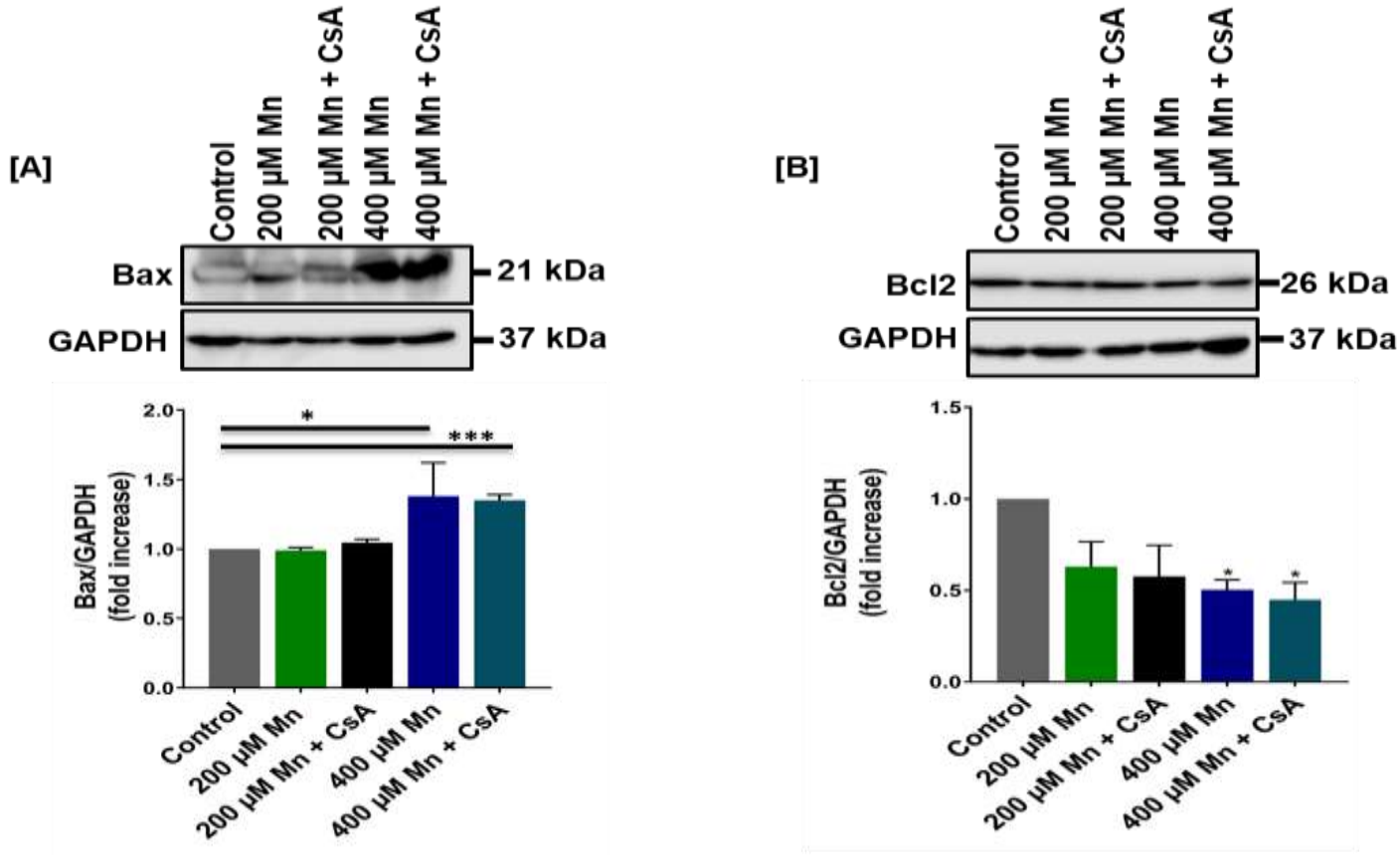

Figure 5.10 Apoptotic markers Bax and Bcl2 in manganese treated SH-SY5Y neuronal cells. Cells were treated as indicated relative to control cells for 24 h. Protein expression was determined by Western blot analysis. Data is expressed relative to GAPDH and control samples. **Panel A:** Representative Immunoblot and densitometric analysis of Bax **Panel B:** Bcl2 relative to GAPDH expression. Data are expressed as mean ± SEM of 3 independent experiments (n=3). *p < 0.05, ***p < 0.001compared to control.

5.3.5- Manganese exposure regulates the phosphorylation of the Ras/Erk and PI3K/Akt, mtorc1/S6K pathways in SH-SY5Y neuronal cells

The Ras/ERK, PI3K/Akt/mTORC1 and MAPK signalling pathways are involved in the regulation of processes mediating cell survival such as proliferation and apoptosis. ROS-mediated dysregulation of this signalling cascade is implicated in the pathogenesis of several neurodegenerative disease conditions. The mTORC1 complex, an important regulator of growth and metabolism is regulated by the Erk/Akt signalling pathway. This study investigated the effect of Mn exposure on kinases of the above-mentioned pathways. The activation of Erk, Akt, mTORC1, and S6k indicated by their respective phosphorylation was measured using Western blot analysis and a ratio of the phosphorylated to total kinase level determined. Results showed a general increase in Erk activation following 200 µM Mn + CsA, 400 µM Mn and 400 µM Mn +CsA cotreatment ($p=0.0056$, 0.0287, <0.0001, Figure 5.11A) respectively. Akt activation was significantly increased following 400 µM Mn exposure ($p= 0.0014$, $p=0.0015$ Figure 5.11B) however, was significantly decreased in response to 200 µM Mn + CsA and 400 µM Mn + CsA cotreatments ($p= 0.0014$, $p=0.0015$ Figure 5.11B) respectively. Downstream kinases of the Ras/Erk signalling pathway (S6K and mTOR) were also assessed. Result from this study reported an overall significant decrease in S6K activation in response to all Mn exposures and CsA cotreatments ($p=$ <0.0001, <0.0001, <0.0001 and <0.0001, Figure 5.11C), respectively. Following exposure to 200 µM 400 µM Mn treatments, there was no change in mTORC1 activation, with an albeit non-significant decrease seen when cells are exposed to 200 µM Mn + CsA (Figure 5.11D).

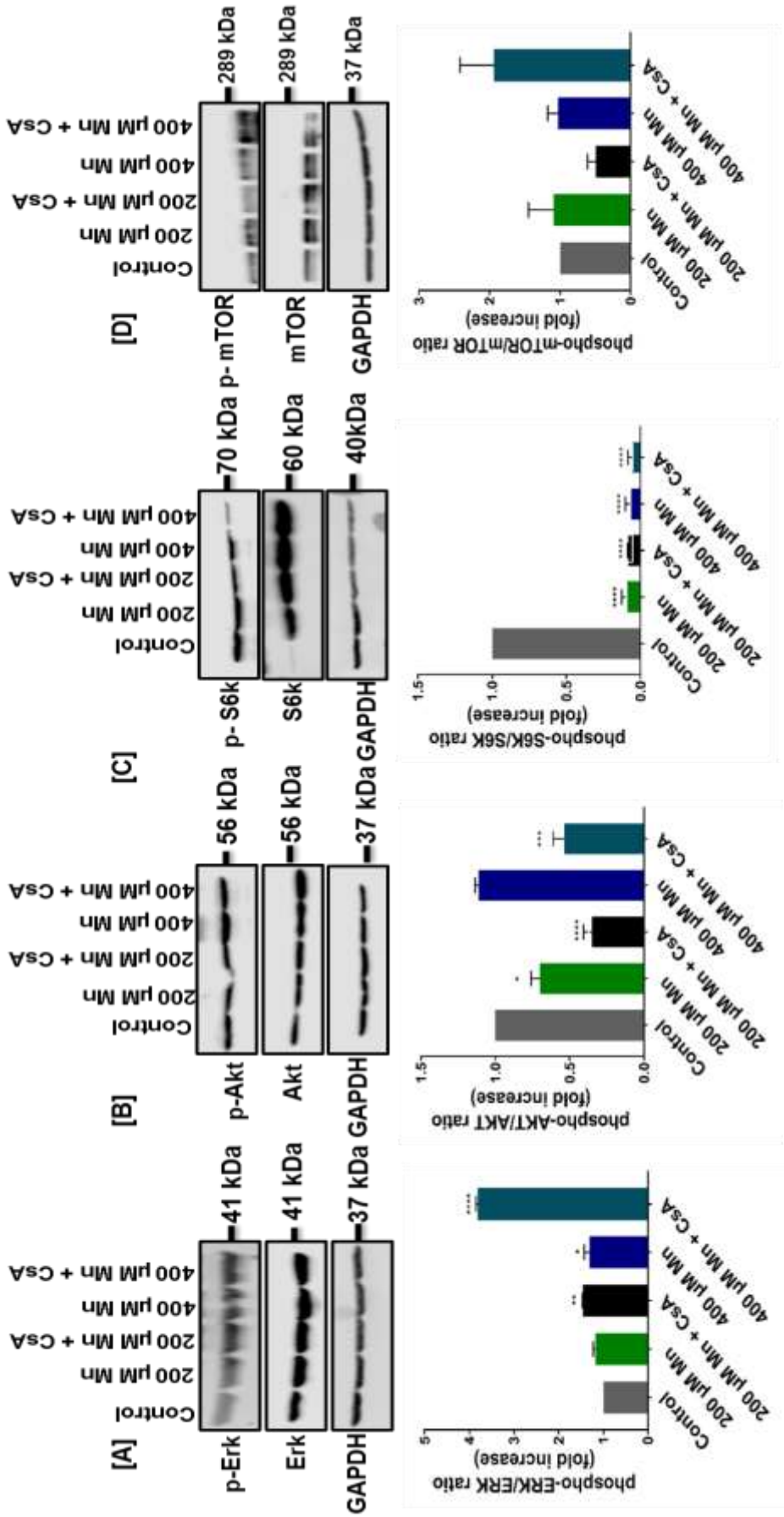

Figure 5.11. Phosphorylation of the Ras/Erk and P13K/Akt/mTOR signalling pathways are regulated by manganese in SH-SY5Y neuronal cells. Cells were treated as indicated relative to control cells for 24 h. Protein expression was determined by Western blot analysis. **Panel A:** Representative Immunoblot and densitometric analysis of pErk/Erk ratio **Panel B:** pAkt/Akt ratio. **Panel C:** pmTOR/mTOR ratio **Panel D:** pS6K/S6K ratio relative to GAPDH. Data are expressed as mean ± SEM of 3 independent experiments. *p < 0.05, **p < 0.01, ***p < 0.001, ****p< 0.0001 compared to control.

5.3.6- Manganese increases metabolic proteins BCATm and GDH

The impact of Mn exposure on both BCATm and GDH proteins, responsible for branched chain amino acids (BCAA) and glutamate catabolism were determined in this study. Using western blot analysis, the effect of 200 µM Mn and 400 µM Mn treatment on the BCATm and GDH reported a significant increase in BCATm following 200 µM Mn exposure for 24 h (p= 0.0021, Figure 5.12A) with 40 µM H_2O_2 an oxidative stress-inducingpositive control significantly decreased (p= 0.0189). Following cell exposure to 400 µM Mn there was a significant increase in GDH levels (p= 0.0419, Figure 5.12B).

5.3.7- Mn decreases protein aggregation while increasing Aβ load

Protein misfolding and aggregation is a common in neurodegenerative disorders including Alzheimer's disease. Protein aggregation is associated with increased oxidative stress, therefore we determined the impact of Mn exposure on total cell protein aggregation. Results showed a general decrease in aggregated proteins in response to 200 µM and 400 µM Mn with a significant decrease seen at 400 µM Mn concentration (p= 0.0031, Figure 5.13A) with further decrease in protein aggregation following 200 µM and 400 µM Mn CsA co-treatment (p=0.0224 and 0.0068, Figure 5.13A) respectively. Finally, this study report a significant increase in β-amyloid (Aβ) protein level in response to 200 µM Mn, 200 µM Mn + CsA and 400 µM Mn + CsA cotreated cells (p=0.0026, 0.008 and Figure 5.13B). However, in 400 µM Mn treated cells, there was a significant decrease in Aβ levels (p=0.0107, Figure 5.13B) suggesting a correlation between decrease in protein aggregation and the amount of Aβ produced. Regardless of a decline in the amount of aggregated protein, phosphorylated tau protein level was significantly increased in response to 200 µM Mn and 400 µM Mn treatment. These results together suggest that following Mn-induced toxicity, tau phosphorylation as a hallmark of AD will increase despite an observed decline in protein aggregation.

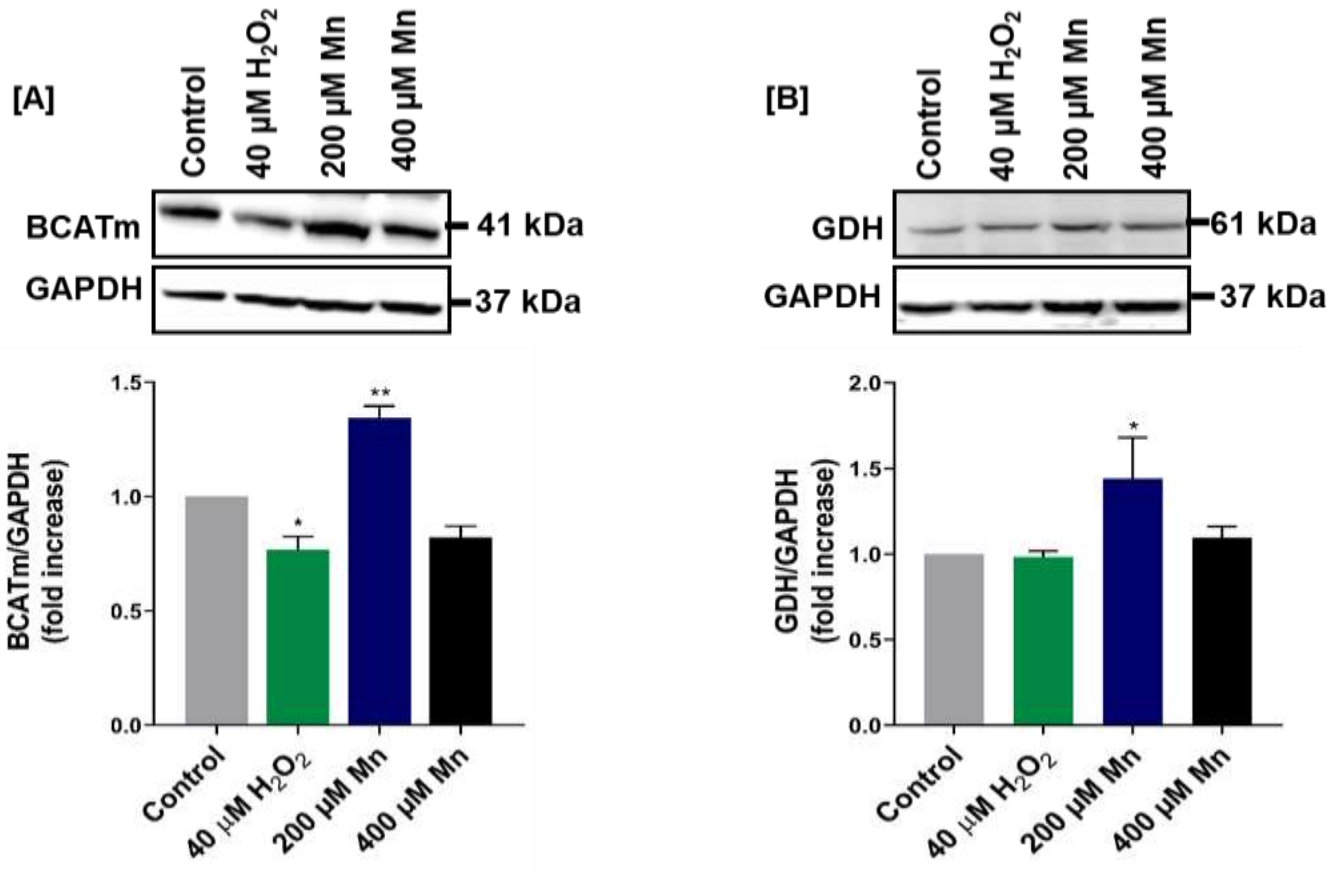

Figure 5.12. Increased expression of metabolic proteins BCATm and GDH in manganese treated SH-SY5Y neuronal cells. Cells were treated as indicated relative to control cells for 24 h. Protein expression determined by Western blot analysis. Data is expressed relative to GAPDH and control samples**. Panel A:** Representative Immunoblot and densitometric analysis of BCATm **Panel B:** GDH relative to GAPDH expression. Data are expressed as mean ± SEM of 3 independent experiments. *p < 0.05, **p < 0.01compared to control.

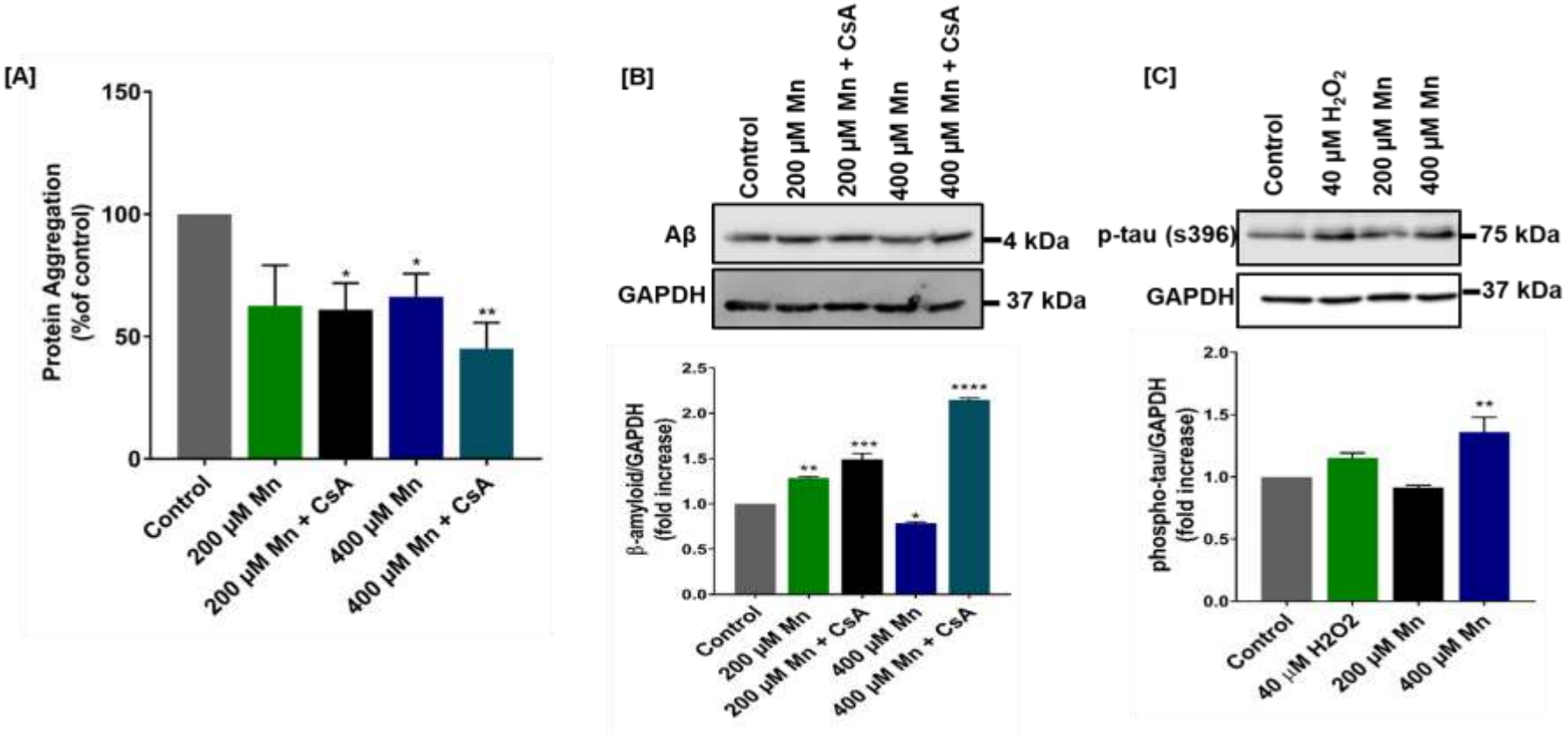

Figure 5.13. Protein aggregation decrease in manganese treated in SH-SY5Y cells with an increase in Aβ and pTau. Cells were treated as indicated relative to control cells for 24 h. Protein aggregation was determined using the Proteostat total protein aggregation assay. In a separate experiment, under the same conditions, the level of Aβ and pTau were assessed using Western blot analysis. **Panel A:** Histogram representing the percentage of aggresome formation following indicated treatment. **Panel B:** Representative Immunoblot and densitometric analysis of Aβ. **Panel C:** phospho-Tau relative to GAPDH expression. Data are expressed as mean ± SEM of 3 independent experiments. *p < 0.05, **p < 0.01, ***p < 0.001, ****p<0.0001 compared to control.

5.4- DISCUSSION

Previous studies clearly demonstrate the toxic effect that arises from excessive accumulation of Mn. Mn neurotoxicity commonly refered to as manganism is thought to be caused by overexposure and accumulation of Mn in neuronal cells. Excessive Mn exposure have been associated with an increase in ROS production, diminshed antioxidant defense mechanism, toxic metabolite accumulation (Wan *et al.,* 2014), altered bioenergetics and ATP production (Chen and Liao, 2002, Sarkar *et al.,* 2018). Manganism, a Parkinson disease-like condition poses questions as to why there is a narrow window between dietary adequacy and toxicity and the role it plays as a mitochondrial life-death switch (Smith *et al.,* 2017).

Although there are limited reports linking excessive Mn accumulation to AD, the impact of Mn-induced oxidative stress through ROS generation on mitochondrial dynamics and bioenergetics and how this contributes to modulation of AD hallmarks- Aβ and tau phosphorylation in SH-SY5Y cells was investigated in this study. This study also aimed at understanding the impact ROS-dand the role of CsA in ameliorating dysregulated mitochondrial dynamics and bioenergetics.

5.4.1- Manganese-induced modulation of SH-SY5Y cellular redox

Results from this study showed a concentration-dependent increase in ROS generation (**Figure 5.2b**) preceeding antioxidant response of increase in the levels of antioxidant proteins SOD, GRX and TRX (**Figure 5.3a, b & c**). In response to 200 µM and 400 µM Mn exposures for 3h and 24h, there was a decrease in SOD acivity (**Figure 5.4a & b**).

In related studies, primary cortical neuronal cells exposed to 500 µM Mn treatment reported an increase in oxidative injury indicated by lipid peroxidation biomarker F_2- isoprostanes and increased ROS production (Milatovic *et al.,* 2007, Milatovic *et al.,* 2009) together with decreased SOD activity in rat astrocytes exposed to 50 µM Mn treatment for 3h (Latronico *et al.,* 2013). Similarly, a decrease in SOD and catalase activity and increased levels of lipid peroxidation was reported in rat hippocampus exposed to 3.9 mM Mn over a 6-week period (Cheng *et al.,* 2018, Szpetnar *et al.,* 2016)

consistent with data from this study. Taken together, our results are consistent with the suggestion that Mn-induced neurotoxicity is linked to enhanced ROS generation, increased cellular oxidative stress, and a depleted cell defense system (Fernandes *et al.,* 2017, Martinez-Finley *et al.,* 2013) beyond physiological brain Mn concentration. In this neuronal cell model, response to manganese-induced ROS generation is mediated by the GRX and TRX systems to counteract this effect in a bid to restore redox balance and not SOD suggesting a possible role for manganese catalysing thiol modifications. The significant rise in TRX levels following hydrogen peroxide exposure indicate the involvement of this system in peroxide resuction as opposed to SOD.

5.4.2- Excessive Mn impair mitochondrial respiration and cellular energy metabolism in SH-SY5Y cells

Mn accumulation in neuronal mitochondria have been described to be persistent as a result of its poor efflux rate (Gavin *et al.,* 1999, Qin and Zhong, 2018) implicating it in dysfunction of the mitochondrial metabolic pathways. A significant decrease in mitochondrial OCR, basal mitochondrial respiration, and ATP production following 200 and 400 µM Mn exposure for 24 h which was not attenuated by CsA cotreatment was reported (**Figures 5.5 c, d & e**).
In a similar study, SH-SY5Y cells exposed to a range of Mn concentrations for 5h, reported an increase in basal OCR and ATP production at concentrations ≤50 µM hence a beneficial effect, however with increase Mn exposure to 100 µM, there was a 6% decrease in basal OCR and no difference in ATP production relative to control cells (Fernandes *et al.,* 2017). This suggests that although in the SH-SY5Y cell model Mn concentration ≥ 50 µM is reported as being in the toxicological range, 100 µM Mn exposure for a shorter duration (5h) signifies the acute phase of disruption of mitochondrial OCR, basal mitochondrial respiration and ATP production. In our study however where SH-SY5Y cells were exposed to 200 and 400 µM Mn for 24 h depicting Mn concentration at the higher toxicological range and a more chronic exposure time, result shows a 14%, 26% and 12%, 17% decrease in basal OCR and ATP production. This suggest a more profound outcome implying that in this cell model Mn exposure in the toxicological range will result in a decline in

mitochondrial respiration, OCR and energy production irrespective of exposure time.

In related studies, mouse astrocytes and microglial cells exposed to 100 µM Mn for 24 h showed a significant decrease in oxygen consumption, basal mitochondrial respiration and ATP production (Sarkar *et al.,* 2018, Sarkar *et al.,* 2019). Inhibition of the activity of the mitochondrial enzyme aconitase and ATP production have been reported following Mn exposure in rat brain (Zheng *et al.,* 1998, Gunter *et al.,* 2010, Roth *et al.,* 2002). Taken together, these findings suggests that in neuronal cells, Mn exposure beyond the physiological range matched with that observed in the human brain, results in increased ROS generation impairing mitochondrial oxygen consumption rate and the overall cell bioenergetic system leading to the inability of the cell to thrive.

5.4.3- Manganese-induced dysregulation of mitochondrial dynamics and the protective role of CsA in SH-SY5Y cells

The MPT pore (MPTP) largely controlled by cyclophilin D (CypD) is inhibited by CsA (Kim *et al.,* 2014). Results from this study show a significant increase in CypD expression **(Figure 5.6a)** with a simultaneous loss of MMP **(Figure 5.5a)** indicating Mn exposure and its impact on mitochondrial fission/fusion dynamics is mediated by MPT. Also shown is a significant increase in mitochondrial fission following 400 µM Mn exposure for 24h which was however attenuated by cotreatment with 1 µM CsA (**Figure 5.7a**) and significant decrease in expression of fusion proteins Mfn1 and Opa1. Mfn1 was significantly upregulated in 200 µM Mn cells cotreated with CsA with no impact on Opa1. (**Figure 5.7b & c**).

Mn-treated C6 astrocytoma cells exposed to 750 µM Mn for 24h reported marked decrease in fusion protein Opa-1 and ~43 fold increased level of fission protein Drp1 with CsA pre-incubation preventing MPTP opening hence MMP disruption, mitochondrial dysregulation and apoptosis (Alaimo *et al.,* 2014). Similar findings in Gli36 astrocytic cells treated with 350 µM Mn for 24h reported decrease in fusion proteins Opa-1 and Mfn-2, increase in mitochondrial fission protein Drp-1 and a resultant disruption in mitochondrial network evidenced by punctuated structure and loss of mitochondrial mass (Alaimo *et al.,* 2013). In related studies, 1 µM CsA pre-incubation prior to 10-

100 µM Mn exposure prevented MMP dissipation and mitochondrial swelling in astrocytes (Rao and Norenberg, 2004, Rama Rao *et al.,* 2007) and MES 23.5 cells exposed to 600 µM for 2h (Prabhakaran *et al.,* 2009).

Similar to findings in Alaimo *et al.,* 2014 that recorded up to a ~43 fold increase in Drp1 levels, our findings showed a ~2 fold increase suggesting a concentration and cell model-based difference. Overall this signifies that in different cell models, Mn exposure exceeding the physiological range favours an increase in ROS generation and also rise in mitochondrial fission with no corresponding increase in mitochondrial fusion to counter this imbalance. In this cell model, CsA attenuation of Drp1 increase coupled with its known role for preventing MPTP opening and MMP dissipation suggests that dysregulation of the mitochondrial fission/fusion dynamics following toxic Mn exposure is likely regulated by MMP disruption also suggesting it is the mechanism mediating the disruption of mitochondrial bioenergetic functions.

5.4.4- Manganese-induced toxicity activates autophagy and apoptosis in SH-SY5Y cells

Results from our findings reported a significant increase in both autophagy **(Figure 5.8a & b)** and apoptosis indicated by an increase in Bax expression and simultaneous decreased Bcl-2 expression **(Figure 5.9a & b)** following 400 µM Mn exposure in SH-SY5Y cells. Mn-induced neurotoxicity elicit various response in cells in a bid to ameliorate the harmful cellular environment resulting from its excessive accumulation, one of such response being autophagic flux activation. Several studies have reported autophagy activation as a protective response to Mn-induced cell damage as well as an apoptotic cell death response. In a related study, PC12 neuronal cells exposed to 300 µM Mn for 12h resulted in an increase in LC3-II and p62 accumulation signifying that despite autophagosome formation, subsequent degradation in the lysosome is inhibited hence an inhibition of the autophagic flux whereas when cells were pre-treated with rapamycin and exposed to 300 µM Mn, autophagic flux induction and significant reduction in cell death was reported evidenced by an increase in LC3-II and decrease p62 level suggesting autophagy play a protective role in Mn-induced toxicity while exposure to (Zhou *et al.,* 2018). The initial response is consistent with results from our study suggesting that 200 µM and 400 µM Mn exposure for 24h in SH-SY5Y cells

activate autophagosome accumulation which is possibly not degradation as shown by a simultaneous accumulation of p62 hence an inhibition of autophagic flux. Should this be the case, this could be a cell model and duration of exposure specific response, however, there is the need to confirm whether or not the autophagic flux is functional by measuring LC3-II levels in the presence of Baf A1, measure Beclin levels or use tandem fluorescence plasmid RFP-GFP-LC3 double tag assay to monitor autophagic activity in real time. Also considering that p62 is a multifunctional molecule which could be initially degraded by autophagy but restored following long starvation periods (Sahani *et al.,* 2014) also indicates the need to measure p62 in a time-based manner to observed its modulation pattern. Astrocytoma C6 cells exposed to 750 µM Mn for 6 and 24h showed autophagic activation indicated by pronounced increase in LC3-II following pre-incubation with Baf A1 which counteracts the harmful effects of Mn-mediated toxicity thereby conferring a protective role (Gorojod *et al.,* 2015). A compensatory activation of autophagy have been reported following short term (4-12 h) 1 M Mn exposure to rat striatum reflected by an increase in LC3-II/LC3-I ratio, (Zhang *et al.,* 2013). These findings taken together suggest that 24h Mn exposure in SH-SY5Y cells activate autophagosome formation and accumulation, but is unable to complete the autophagic flux hence failure for autophagy activation to play a protective role against cytotoxic cell death hence as reported there is apoptosis.

Apoptotic cell death has been reported as a response to Mn-induced toxicity. In Gli36 cells, 350 µM Mn exposure for 24 h was shown to trigger apoptotic cell death evidenced by an increase in Bax protein and concomitant decrease in Bcl2 protein while increased Bax and decreased Bcl2 mRNA levels were reported in rat hippocampus exposed to 3.9 mM Mn over 6 weeks (Alaimo *et al.,* 2013, Cheng *et al.,* 2018) consistent with findings from this study which showed an increase in Bax with a simultaneous decrease in Bcl2 protein levels. Features such as increased inter-nucleosomal DNA fragmentation indicative of apoptosis have been reported in PC12 neuronal cells and condensed chromatin and shrunk nuclei in SK-N-MC neuroblastoma cells after 24 h Mn exposure (Hirata, 2002, Bahar *et al.,* 2017). SK-N-MC neuronal cells exposed to a 1000 µM Mn were seen to exhibit increased apoptotic nuclear

shrinkage similar to cell shrinkage, condensed chromatin, cytochrome c release and caspase activation seen in neural stem cells (Yoon *et al.,* 2011, Wang *et al.,* 2015) suggested to be mediated by dysfunctional mitochondria and endoplasmic reticulum stress with ROS generation and loss of MMP as the mechanism involved (Tamm *et al.,* 2018, Zhang *et al.,* 2016).

Collectively, these findings suggest that despite evidence of autophagy activation after 24h, it is not clear whether there is a complete autophagic activity hence the inability for an autophagy-mediated cell protection hence activation of apoptosis.

5.4.5- Manganese dysregulates the Ras/Erk and PI3K/Akt/mTOR signalling pathways in SH-SY5Y cells

Downstream kinases of the MAPK pathway important for cell proliferation, differentiation, survival and apoptosis have been implicated in neurodegenerative conditions (Cordova *et al.,* 2012). Our findings show Erk activation and Akt activation, especially following 400 µM Mn exposure (**Figure 5.10a & b**). In related studies, exposure to both 500 and 1000 µM Mn reported an ERK activation in PC12 neuronal cells similar to BV2 microglial cells exposed to 500 µM Mn (Bae *et al.,* 2006, Cai *et al.,* 2011). Furthermore, Mn exposure of 100 and 500 µM to neonatal rat astrocytes led to a concentration and time-dependent ERK activation with antioxidant resveratrol reversing ERK phosphorylation suggesting an oxidative stress-mediated mechanism (Exil *et al.,* 2014, Latronico *et al.,* 2013). Similarly, in rat striatum exposed to 10/20 mg/kg Mn from post-natal days 8-12 results reported ERK and AKT activation as a result of increased ROS production which was reversed with antioxidant, Trolox also supporting the role of ROS generation in activation of these pathways (Cordova *et al.,* 2012). These findings are consistent with data from this study and suggest that exposing neuronal cells to toxic concentration of Mn increasing ROS generation possibly acts as signal for the activation of ERK and AKT both necessary to mediate cell survival through different mechanisms, which could include autophagy or apoptosis activation geared at maintaining cell homeostasis.

In PC12 neuronal cells, Mn-induced oxidative stress resulted in p70 S6K phosphorylation at Ser411 and Thr421/Ser424 (Hirata *et al.,* 1998). *In vitro*

assessment of immature female rat brain tissue reported chronic exposure to low dose Mn led to an increased expression of mTORC1 (Srivastava *et al.,* 2016). Similarly, in U87 glioblastoma cells, there was an increased activation of mTORC1 only at 100 µM Mn exposure. Further increase in Mn concentration from 400-1000 µM resulted in decreased mTORC1 phosphorylation (Puli *et al.,* 2006) supporting our findings where 200 µM and 400 µM Mn exposure had no effect on mTORC1 activation necessary for synaptic plasticity, memory and learning while significantly decreasing S6K activation. Consistent with loss in cell viability and increased ROS generation following Mn exposure at both 6 and 24h in our data (**Figure 5.2a&b**), it is evident that both transient and sustained Mn exposure, alongside a dysregulation of energy metabolism of the cell, induce stress stimuli which persistently overpowers any cell survival instinct resulting in severe neuronal damage and apoptosis.

5.4.6- Manganese upregulate Aβ and phosphorylated tau production and decrease protein aggregation, in SH-SY5Y cells

Findings from previous research suggested no correlation between Mn and AD due to a non-significant observation of Mn accumulation in control versus AD brain (Markesbery *et al*. 1984). Recent studies seek to answer questions regarding the role excessive Mn plays in the pathogenesis of AD and how this relate to Aβ and phosphorylated tau production. In a study of 40 men with different cognitive statuses significant correlation between increased plasma Mn levels and Aβ peptides accumulation as well as cognitive decline was reported (Tong *et al.,* 2014). Supporting this, chronic Mn exposure in non-human primate has been shown to cause an increase in the expression of APLP1 and Aβ plaques with silver grains indicating ongoing neurodegeneration which contributes to the cognitive deficiency (Guilarte *et al.,* 2008, Guilarte, 2010). Post-mortem CSF samples show a significant inverse correlation between Mn levels and Aβ concentration, the higher the concentration of Mn present! in CSF, the lower the Aβ levels (Strozyk *et al.,* 2009) consistent with our findings where despite a significant increase in Aβ protein level at 200 µM Mn exposure, 400 µM Mn exposure resulted in decreased Aβ level. Induction of tau hyperphosphorylation following 100- 500

µM Mn exposure for 6h in PC12 neuronal cells mediated by MAPK/ERK activation which was attenuated by ERK inhibition have been reported (Cai *et al.,* 2011) consistent with findings from our study suggesting that in our cell model, a similar response of increase in tau phosphorylation is mediated by ERK activation was also observed (**Figure 5.12b**). Taken together, this implies that Mn-induced tau hyperphosphorylation possibly mediated by ERK activation is a potential stress stimuli response to exposure to toxic Mn concentrations.

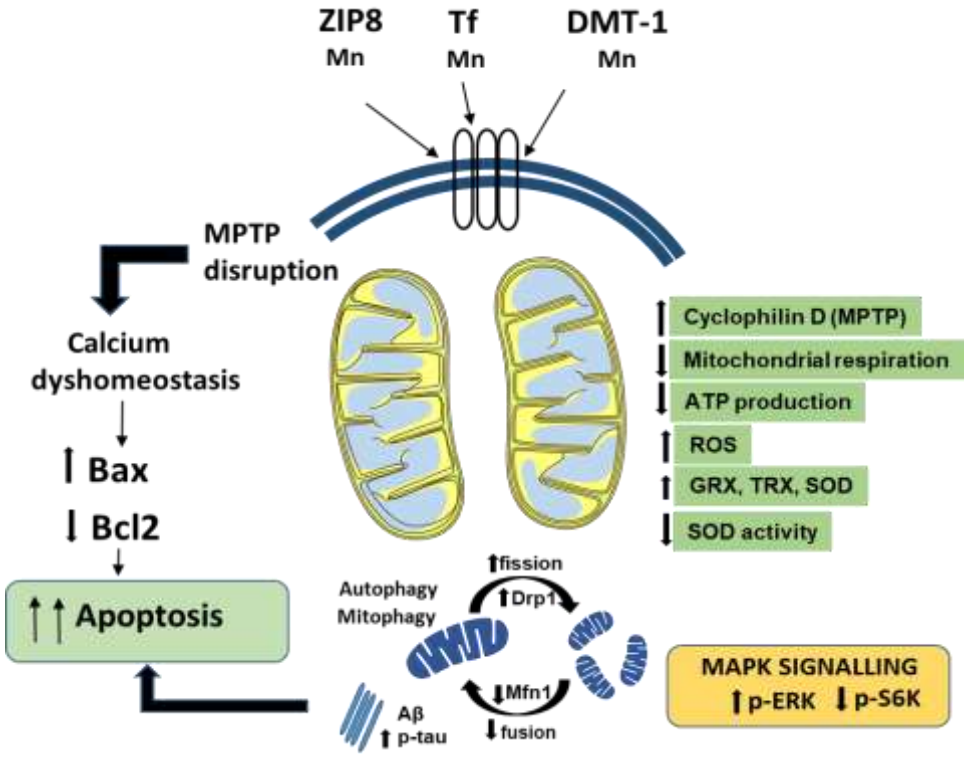

Figure 5.14- Schematic diagram representing the pathways impacted by excessive manganese exposure to SH-SY5Y neuronal cells. Increase in ROS open MPTP, dissipate MMP, impair mitochondrial respiration and ATP production resulting in mitochondrial fission and fragmentation while inhibiting fusion with a simultaneous increase in Aβ and phospho-tau. Autophagy and mitophagy is activated to enhance clearance of fragmented mitochondria, however it appears dysfunctional mitochondrial metabolism activates a response from cell survival signalling PI3K/AKT/mTOR pathways triggering apoptosis.

Chapter 6

6.0- SYNOPSIS AND CONCLUSION

This thesis had three main objectives and areas of interest. i) Investigate the underlying mechanisms and role of ethanol-induced mitophagy on neuronal cell Aβ and tau expression, ii) Determine the dual role of Zn in a-neuroprotective or neurotoxic capacity and its impact on the fusion/fission dynamics and mitochondrial function, iii) Evaluate the impact of Mn-induced toxicity on mitochondrial bioenergetics and dynamics.

ETHANOL

It was hypothesized in this thesis that ethanol-induced neurotoxicity plays a major role in dysregulating mitochondrial fusion/fission dynamics and bioenergetics and that targeting this pathway has the possibility to ameliorate the neurodegenerative phenotype. For the first time we show that chronic ethanol exposure induced atypical mitochondrial fission while inhibiting fusion-mediated repair and impaired mitochondrial function in SH-SY5Y neuronal cells. We also show CsA has the potential to restore fusion following chronic ethanol exposure to neuronal cells (**Chapter 3.3**). Evidence from previous studies with a focus on the underlying mechanisms of ethanol-mediated neurotoxicity suggests that autophagic pre-conditioning ameliorates ethanol-induced neuroapoptosis while autophagy inhibition exacerbates this through increased ROS generation and that therapeutic approach targeting this pathway confer neuroprotection (Chen *et al.,* 2012). Oxidative stress generation and a deficit in antioxidant capacity has also been hypothesised as the mechanism underlying ethanol-induced neurotoxicity in rat models (Heaton *et al.,* 2000, Ramezani *et al.,* 2012). Additionally and more recently, ethanol has been proposed to play a role in the initiation and sustenance of AD pathology via neuroinflammatory processes (Venkataraman *et al.,* 2017).

Based on the findings from our current study, an updated and alternative mechanism is proposed. In addition to a deficit in antioxidant response enough to combat ethanol-mediated ROS generation and the activation of autophagy and apoptosis, the disruption of the mitochondrial homeostatic system,

fusion/fission dynamics results in an impairment in the mitochondrial bioenergetics system likely to contribute to neuronal cell loss.

ZINC

In neuronal cells, Zn have been previously proposed to play a neurotoxic role alongside glutamate excitotoxicity following its excessive post-synaptic release during synaptic excitation (Takeda, 2011). Zn has also been previously proposed as capable of playing a dual role as both a prooxidant and antioxidant in a concentration-dependent manner (Lee, 2018). As an antioxidant, it is suggested to maintain cell redox balance through its involvement with glutathione metabolism and general protein thiol redox metabolism (Oteiza, 2012). As a prooxidant when present intracellularly in high concentrations, Zn is proposed to enhance neuronal cell death by cell energy production inhibition (Dineley *et al.,* 2003).

In this thesis we show for the first time that the protective role exerted by Zn although involves the upregulation of antioxidant marker proteins SOD, TRX and GRX at low Zn concentration as previously reported, additionally inhibits excessive mitochondrial fission at similar concentration, also reflected by enhanced ATP production. On the other hand neurotoxic Zn concentrations exogenously introduced into neuronal cells was shown to contribute to neuronal cell death through promotion of excessive mitochondrial fission, impairment of cell energy metabolism and dysregulation of cell signalling pathways necessary for cell survival (**Chapter 4.3**).

Using data from this thesis, we therefore propose a new and novel findings that help to understand the mechanisms involved in Zn neuroprotection. At low concentrations, Zn acts as a neuroprotective agent by inhibiting excessive mitochondrial fission in neuronal cells transcending to improved cell energy metabolism. On the other hand, at high Zn concentrations, there is aberrant mitochondrial fragmentation, impaired energy metabolism and an increase in Aβ and tau production eventually resulting in neuronal cell death in a non-apoptotic manner.

MANGANESE

Finally, Mn accumulation and neurotoxicity is frequently associated with Parkinson's disease, a condition with visible motor dysfunction, there need to be an increasing awareness and study about the impact of Mn exposure on cognitive functions and the mechanisms that mediate this. In addition to motor function problems, Mn have been proposed to induce AD-like pathology by accumulating in the hippocampus and cortex of the brain (Qin and Yuan-Zhong, 2018), however, there is the need to still ascertain the underlying mechanisms responsible for its associated AD-like pathology. Mn has been proposed to play a role in both cell survival and cell death through regulation of Mn-containing enzymes like MnSOD or increasing the activity of caspase enzyme. Despite its importance for mitochondrial functioning, accumulation at an excessive level leads to cell death (Smith *et al.,* 2017). A dysregulation and impairment of mitochondrial energy metabolism has been proposed in mouse and human astrocytes at neurotoxic levels specific to those cell types (Sarkar *et al.,* 2018, Sarkar *et al.,* 2019).

Smilar to our observations with respect to Zn neurotoxicity, we report that Mn-mediated neurotoxicity is through the alteration of mitochondrial fission/fusion dynamics and impaired mitochondrial respiration and ATP production. This mechanism involves an increase in ROS generation, which results in an antioxidant response with increased antioxidant markers SOD, GRX and TRX. Autophagy and apoptosis pathways were activated followed by an activation of the cell survival pathways at very high concentrations of Mn. Despite its proposed contribution to AD pathology, in this study, there does seem not to be a corresponding increase in protein aggregation or Aβ levels, however there is a consistent increase in phosphorylated tau expression with increasing Mn concentration (**Chapter 5.3**). Together this data indicates that although excessive Mn accumulation contributes to AD pathology, this is through the hyperphosphorylation of tau rather than Aβ accumulation. This is proposed to be as a result of increased fission and impairment of neuronal cell's energy metabolism.

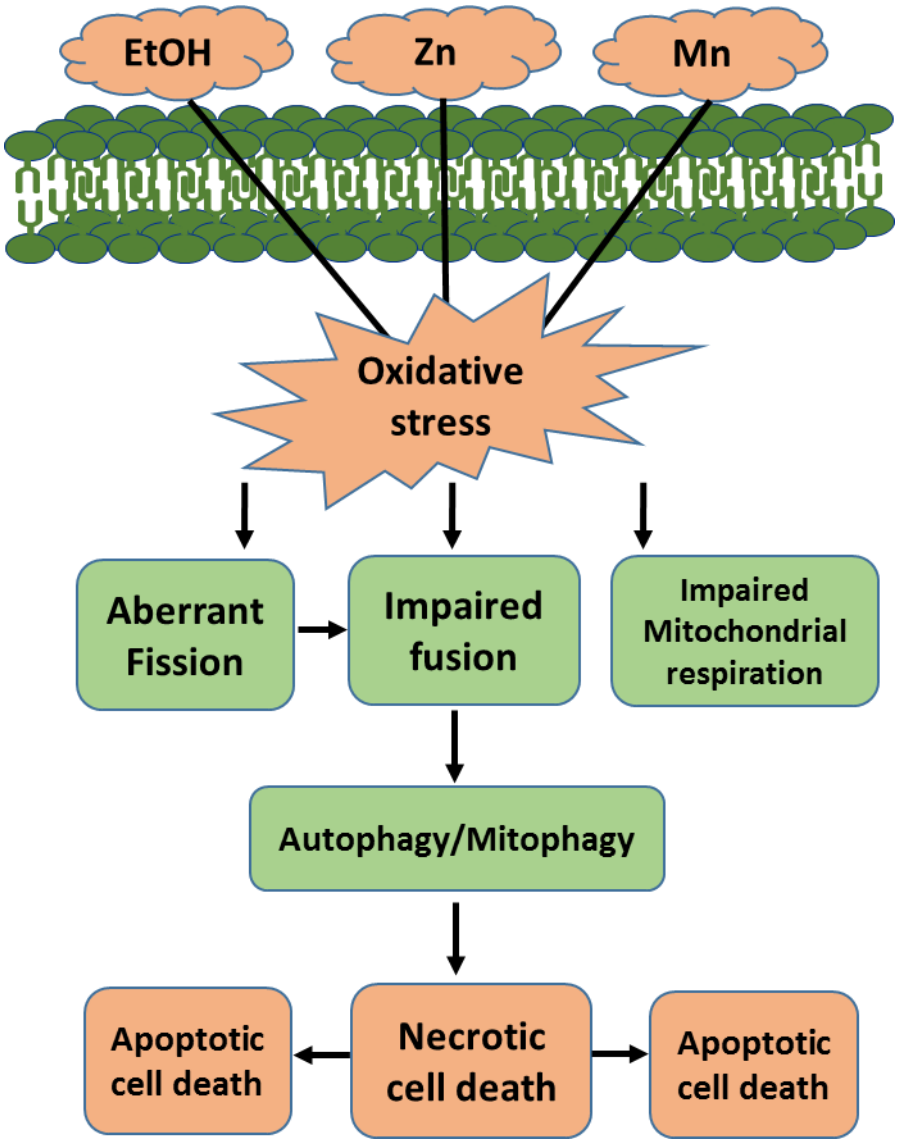

Figure 6.1- Proposed mechanism for ethanol, zinc and manganese-mediated neurotoxicity and contribution to AD pathology. Increase in ROS generation results in MMP dissipation affecting mitochondrial respiration and function likely due to opening of the MPTP. This results in increased mitochondrial fission and fragmentation while inhibiting mitochondrial fusion, subsequently regulating Aβ and phosphorylated tau production. Consequently, autophagy/mitophagy is activated to remove damaged cells in a bid to maintain cell homeostasis, however, the toxicity overwhelms the cells leading to neuronal cell death and loss either through the apoptotic or necrotic pathway.

6.1- FUTURE WORK

This thesis provides evidence that ethanol and micronutrients- Zn and Mn when exposed to neuronal cells at toxic concentrations, will result in dysregulation of otherwise tightly regulated pathways through mechanisms highlighted in this study. The recurring underlying mechanism that is affected in response to ethanol and these micronutrients is a dysregulation of mitochondrial fission/fusion mechanism and impairment of cell energy metabolism. It is important to understand these pathways as there is the potential for developing a targeted therapeutic approach to allow for neurodegenerative phenotype rescue. To further investigate this, the following experiments would be considered:

Manipulation of the fission/fusion pathway to determine their impact on other mitochondrial parameters. Suggested modifications include:

- Overexpression of the fusion gene Mfn1/2 and Opa 1 to ascertain if there is a different response to ethanol/Zn/Mn-mediated impairment of cell energy metabolism
- Knockdown of the fission gene Drp1 while overexpressing mitochondrial fusion. This will determine whether enhanced fusion in the absence of fission play a role in improving mitochondrial respiration and ATP production.
- Use of fission inhibitors- Dynasore and P110 to determine the potential of this inhibition on mitochondrial morphology and the extent to which this improves mitochondrial respiration.
- Investigate the impact of fission inhibition and enhanced fusion on Aβ accumulation and tau hyperphosphorylation.

High Zn concentrations have been implicated as a cause of copper deficiency by increasing metallothionein synthesis, which binds copper thereby preventing its absorption. Experiments to consider include:

- Determine if mechanisms of Zn-induced toxicity is as a result of copper deficiency.

- Use TPEN to chelate Zn while enhancing copper absorption to determine if this improves mitochondrial dynamics.

Manipulation of the mitochondrial protein hBCATm will be explored to:

- Determine the impact its knockdown or overexpression play in ethanol/Zn/Mn-mediated excessive increase in fission.
- Investigate the impact of hBCATm overexpression on mitochondrial fusion and overall function as a targeted therapeutic approach to resolve mitochondrial dynamics dysfunction and AD-like pathology.

References

Abraham, A.G. and O'Neill, E. (2014) PI3K/Akt-mediated regulation of p53 in cancer. *Biochemical Society Transactions* [online]. 42 (4), pp.798-803.

Abrahao, K.P., Salinas, A.G. and Lovinger, D.M. (2017) Alcohol and the Brain: Neuronal Molecular Targets, Synapses, and Circuits. *Neuron* [online]. 96 (6), pp.1223-1238.

Abuarab, N., Munsey, T.S., Jiang, L.H., Li, J. and Sivaprasadarao, A. (2017) High glucose-induced ROS activates TRPM2 to trigger lysosomal membrane permeabilization and Zn(2+)-mediated mitochondrial fission. *Science Signaling* [online]. 10 (490), pp.10.1126/scisignal.aal4161.

Adamo, A.M., Zago, M.P., Mackenzie, G.G., Aimo, L., Keen, C.L., Keenan, A. and Oteiza, P.I. (2010) The role of zinc in the modulation of neuronal proliferation and apoptosis. *Neurotoxicity Research* [online]. 17 (1), pp.1-14.

Ahluwalia, B., Ahmad, S., Adeyiga, O., Wesley, B. and Rajguru, S. (2000) Low levels of ethanol stimulate and high levels decrease phosphorylation in microtubule-associated proteins in rat brain: an in vitro study. *Alcohol and Alcoholism (Oxford, Oxfordshire)* [online]. 35 (5), pp.452-457.

Ahn, J., Jang, J., Choi, J., Lee, J., Oh, S.H., Lee, J., Yoon, K. and Kim, S. (2014) GSK3Î², but not GSK3Î±, inhibits the neuronal differentiation of neural progenitor cells as a downstream target of mammalian target of rapamycin complex1. *Stem Cells and Development* [online]. 23 (10), pp.1121-1133.

Akbar, M., Baick, J., Calderon, F., Wen, Z. and Kim, H.Y. (2006) Ethanol promotes neuronal apoptosis by inhibiting phosphatidylserine accumulation. *Journal of Neuroscience Research* [online]. 83 (3), pp.432-440.

Alaimo, A., Gorojod, R.M., Beauquis, J., Munoz, M.J., Saravia, F. and Kotler, M.L. (2014) Deregulation of mitochondria-shaping proteins Opa-1 and Drp-1 in manganese-induced apoptosis. *PloS One* [online]. 9 (3), pp.e91848.

Alaimo, A., Gorojod, R.M., Miglietta, E.A., Villarreal, A., Ramos, A.J. and Kotler, M.L. (2013) Manganese induces mitochondrial dynamics impairment and apoptotic cell death: A study in human Gli36 cells. *Neuroscience Letters* [online]. 554 pp.76-81.

Alano, C.C., Ying, W. and Swanson, R.A. (2004) Poly(ADP-ribose) polymerase-1-mediated cell death in astrocytes requires NAD+ depletion and mitochondrial permeability transition. *The Journal of Biological Chemistry* [online]. 279 (18), pp.18895-18902.

An, W.L., Pei, J.J., Nishimura, T., Winblad, B. and Cowburn, R.F. (2005) Zinc-induced anti-apoptotic effects in SH-SY5Y neuroblastoma cells via the extracellular signal-regulated kinase 1/2. *Brain Research.Molecular Brain Research* [online]. 135 (1-2), pp.40-47.

Anantharaman, M., Tangpong, J., Keller, J.N., Murphy, M.P., Markesbery, W.R., Kiningham, K.K. and St Clair, D.K. (2006) Beta-amyloid mediated nitration of manganese superoxide dismutase: implication for oxidative stress in a APPNLH/NLH X PS-1P264L/P264L double knock-in mouse model of Alzheimer's disease. *The American Journal of Pathology* [online]. 168 (5), pp.1608-1618.

Aoyama, K. and Nakaki, T. (2013) Impaired glutathione synthesis in neurodegeneration. *International Journal of Molecular Sciences* [online]. 14 (10), pp.21021-21044.

Ashrafi, G. and Schwarz, T.L. (2015) PINK1- and PARK2-mediated local mitophagy in distal neuronal axons. *Autophagy* [online]. 11 (1), pp.187-189.

Avila, D.S., Puntel, R.L. and Aschner, M. (2013) Manganese in health and disease. *Metal Ions in Life Sciences* [online]. 13 pp.199-227.

Axe, E.L., Walker, S.A., Manifava, M., Chandra, P., Roderick, H.L., Habermann, A., Griffiths, G. and Ktistakis, N.T. (2008) Autophagosome formation from membrane compartments enriched in phosphatidylinositol 3-phosphate and dynamically connected to the endoplasmic reticulum. *The Journal of Cell Biology* [online]. 182 (4), pp.685-701.

Ayton, S., Lei, P. and Bush, A.I. (2013) Metallostasis in Alzheimer's disease. *Free Radical Biology & Medicine* [online]. 62 pp.76-89.

Azriel-Tamir, H., Sharir, H., Schwartz, B. and Hershfinkel, M. (2004) Extracellular zinc triggers ERK-dependent activation of Na+/H+ exchange in colonocytes mediated by the zinc-sensing receptor. *The Journal of Biological Chemistry* [online]. 279 (50), pp.51804-51816.

Bae, J., Jang, B., Suh, S., Ha, E., Baik, H. H., Kim, S., Lee, M. and Shin, D. (2006) Manganese induces inducible nitric oxide synthase (iNOS) expression via activation of both MAP kinase and PI3K/Akt pathways in BV2 microglial cells. *Neuroscience Letters* [online]. 398(1), pp. 151-154.

Bahar, E., Kim, J.Y. and Yoon, H. (2017) Quercetin Attenuates Manganese-Induced Neuroinflammation by Alleviating Oxidative Stress through Regulation of Apoptosis, iNOS/NF-ÎºB and HO-1/Nrf2 Pathways. *International Journal of Molecular Sciences* [online]. 18 (9), pp.1989. doi: 10.3390/ijms18091989. eCollection 2017 Sep.

Balog, J., Mehta, S.L. and Vemuganti, R. (2016) Mitochondrial fission and fusion in secondary brain damage after CNS insults. *Journal of Cerebral Blood Flow and Metabolism : Official Journal of the International Society of Cerebral Blood Flow and Metabolism* [online]. 36 (12), pp.2022-2033.

Beckley, J.T., Laguesse, S., Phamluong, K., Morisot, N., Wegner, S.A. and Ron, D. (2016) The First Alcohol Drink Triggers mTORC1-Dependent Synaptic Plasticity in Nucleus Accumbens Dopamine D1 Receptor Neurons. *The*

Journal of Neuroscience : The Official Journal of the Society for Neuroscience [online]. 36 (3), pp.701-713.

Behl, C. and Ziegler, C. (2017) Beyond Amyloid - Widening the View on Alzheimer's Disease. *Journal of Neurochemistry* [online]. 143 (4), pp.394-395.

Bejanin, A., Schonhaut, D.R., La Joie, R., Kramer, J.H., Baker, S.L., Sosa, N., Ayakta, N., Cantwell, A., Janabi, M., Lauriola, M., O'Neil, J.P., Gorno-Tempini, M.L., Miller, Z.A., Rosen, H.J., Miller, B.L., Jagust, W.J. and Rabinovici, G.D. (2017) Tau pathology and neurodegeneration contribute to cognitive impairment in Alzheimer's disease. *Brain : A Journal of Neurology* [online]. 140 (12), pp.3286-3300.

Belmadani, A., Kumar, S., Schipma, M., Collins, M.A. and Neafsey, E.J. (2004) Inhibition of amyloid-beta-induced neurotoxicity and apoptosis by moderate ethanol preconditioning. *Neuroreport* [online]. 15 (13), pp.2093-2096.

Bertholet, A. M., Delerue, T., Millet, A. M., Moulis, M. F., David, C., Daloyau, M., Arnauné-Pelloquin, L., Davezac, N., Mils, V., Miquel, M. C., Rojo, M. and Belenguer, P. (2016) Mitochondrial fusion/fission dynamics in neurodegeneration and neuronal plasticity. *Neurobiology of Disease* [online]. 90pp. 3-19.

Boland, B., Kumar, A., Lee, S., Platt, F.M., Wegiel, J., Yu, W.H. and Nixon, R.A. (2008) Autophagy induction and autophagosome clearance in neurons: relationship to autophagic pathology in Alzheimer's disease. *The Journal of Neuroscience : The Official Journal of the Society for Neuroscience* [online]. 28 (27), pp.6926-6937.

Bonet-Ponce, L., Saez-Atienzar, S., da Casa, C., Flores-Bellver, M., Barcia, J.M., Sancho-Pelluz, J., Romero, F.J., Jordan, J. and Galindo, M.F. (2015) On the mechanism underlying ethanol-induced mitochondrial dynamic disruption and autophagy response. *Biochimica Et Biophysica Acta* [online]. 1852 (7), pp.1400-1409.

Boom, A., Authelet, M., Dedecker, R., Frederick, C., Van Heurck, R., Daubie, V., Leroy, K., Pochet, R. and Brion, J.P. (2009) Bimodal modulation of tau protein phosphorylation and conformation by extracellular Zn2+ in human-tau transfected cells. *Biochimica Et Biophysica Acta* [online]. 1793 (6), pp.1058-1067.

Bordi, M., Berg, M.J., Mohan, P.S., Peterhoff, C.M., Alldred, M.J., Che, S., Ginsberg, S.D. and Nixon, R.A. (2016) Autophagy flux in CA1 neurons of Alzheimer hippocampus: Increased induction overburdens failing lysosomes to propel neuritic dystrophy. *Autophagy* [online]. 12 (12), pp.2467-2483.

Bowman, A.B. and Aschner, M. (2014) Considerations on manganese (Mn) treatments for in vitro studies. *Neurotoxicology* [online]. 41 pp.141-142.

Boyadjieva, N.I. and Sarkar, D.K. (2013) Microglia play a role in ethanol-induced oxidative stress and apoptosis in developing hypothalamic neurons. *Alcoholism, Clinical and Experimental Research* [online]. 37 (2), pp.252-262.

Bozym, R.A., Thompson, R.B., Stoddard, A.K. and Fierke, C.A. (2006) Measuring picomolar intracellular exchangeable zinc in PC-12 cells using a ratiometric fluorescence biosensor. *ACS Chemical Biology* [online]. 1 (2), pp.103-111.

Braak, H., Alafuzoff, I., Arzberger, T., Kretzschmar, H. and Del Tredici, K. (2006) Staging of Alzheimer disease-associated neurofibrillary pathology using paraffin sections and immunocytochemistry. *Acta Neuropathologica* [online]. 112 (4), pp.389-404.

Brown, A.M., Kristal, B.S., Effron, M.S., Shestopalov, A.I., Ullucci, P.A., Sheu, K.F., Blass, J.P. and Cooper, A.J. (2000) Zn2+ inhibits alpha-ketoglutarate-stimulated mitochondrial respiration and the isolated alpha-ketoglutarate dehydrogenase complex. *The Journal of Biological Chemistry* [online]. 275 (18), pp.13441-13447.

Brown, S. and Taylor, N.L. (1999) Could mitochondrial dysfunction play a role in manganese toxicity? *Environmental Toxicology and Pharmacology* [online]. 7 (1), pp.49-57.

Bubber, P., Haroutunian, V., Fisch, G., Blass, J.P. and Gibson, G.E. (2005) Mitochondrial abnormalities in Alzheimer brain: mechanistic implications. *Annals of Neurology* [online]. 57 (5), pp.695-703.

Bush, A.I. (2013) The metal theory of Alzheimer's disease. *Journal of Alzheimer's Disease : JAD* [online]. 33 Suppl 1 pp.S277-81.

Bush, A.I., Pettingell, W.H., Multhaup, G., d Paradis, M., Vonsattel, J.P., Gusella, J.F., Beyreuther, K., Masters, C.L. and Tanzi, R.E. (1994) Rapid induction of Alzheimer A beta amyloid formation by zinc. *Science (New York, N.Y.)* [online]. 265 (5177), pp.1464-1467.

Cai, T., Che, H., Yao, T., Chen, Y., Huang, C., Zhang, W., Du, K., Zhang, J., Cao, Y., Chen, J. and Luo, W. (2011) Manganese induces tau hyperphosphorylation through the activation of ERK MAPK pathway in PC12 cells. *Toxicological Sciences : An Official Journal of the Society of Toxicology* [online]. 119 (1), pp.169-177.

Carroll, B., Nelson, G., Rabanal-Ruiz, Y., Kucheryavenko, O., Dunhill-Turner, N.A., Chesterman, C.C., Zahari, Q., Zhang, T., Conduit, S.E., Mitchell, C.A., Maddocks, O.D.K., Lovat, P., von Zglinicki, T. and Korolchuk, V.I. (2017) Persistent mTORC1 signaling in cell senescence results from defects in amino acid and growth factor sensing. *The Journal of Cell Biology* [online]. 216 (7), pp.1949-1957.

Cederbaum, A.I. (2012) Alcohol Metabolism. *Clinics in Liver Disease* [online]. 16 (4), pp.667-685.

Chandler, L.J. and Sutton, G. (2005) Acute ethanol inhibits extracellular signal-regulated kinase, protein kinase B, and adenosine 3':5'-cyclic monophosphate response element binding protein activity in an age- and brain region-specific manner. *Alcoholism, Clinical and Experimental Research* [online]. 29 (4), pp.672-682.

Chen, C.J. and Liao, S.L. (2002) Oxidative stress involves in astrocytic alterations induced by manganese. *Experimental Neurology* [online]. 175 (1), pp.216-225.

Chen, C.J. and Liao, S.L. (2002) Oxidative stress involves in astrocytic alterations induced by manganese. *Experimental Neurology* [online]. 175 (1), pp.216-225.

Chen, H. and Chan, D.C. (2009) Mitochondrial dynamics--fusion, fission, movement, and mitophagy--in neurodegenerative diseases. *Human Molecular Genetics* [online]. 18 (R2), pp.R169-76.

Cheng, H., Xia, B., Su, C., Chen, K., Chen, X., Chen, P., Zou, Y. and Yang, X. (2018) PI3K/Akt signaling pathway and Hsp70 activate in hippocampus of rats with chronic manganese sulfate exposure. *Journal of Trace Elements in Medicine and Biology* [online]. 50pp. 332-338.

Chevallet, M., Gallet, B., Fuchs, A., Jouneau, P.H., Um, K., Mintz, E. and Michaud-Soret, I. (2016) Metal homeostasis disruption and mitochondrial dysfunction in hepatocytes exposed to sub-toxic doses of zinc oxide nanoparticles. *Nanoscale* [online]. 8 (43), pp.18495-18506.

Chin, P.C., Majdzadeh, N. and D'Mello, S.R. (2005) Inhibition of GSK3beta is a common event in neuroprotection by different survival factors. *Brain Research.Molecular Brain Research* [online]. 137 (1-2), pp.193-201.

Choi, D. W., Yokoyama, M. and Koh, J. (1988) Zinc neurotoxicity in cortical cell culture. *Neuroscience* [online]. 24(1), pp. 67-79.

Chouraki, V. and Seshadri, S. (2014) Genetics of Alzheimer's disease. *Advances in Genetics* [online]. 87 pp.245-294.

Chtourou, Y., Garoui el, M., Boudawara, T. and Zeghal, N. (2014) Protective role of silymarin against manganese-induced nephrotoxicity and oxidative stress in rat. *Environmental Toxicology* [online]. 29 (10), pp.1147-1154.

Chuang, D.M., Wang, Z. and Chiu, C.T. (2011) GSK-3 as a Target for Lithium-Induced Neuroprotection Against Excitotoxicity in Neuronal Cultures and Animal Models of Ischemic Stroke. *Frontiers in Molecular Neuroscience* [online]. 4 pp.15.

Clausen, A., McClanahan, T., Ji, S.G. and Weiss, J.H. (2013) Mechanisms of rapid reactive oxygen species generation in response to cytosolic Ca2+ or Zn2+ loads in cortical neurons. *PloS One* [online]. 8 (12), pp.e83347.

Cohen, L., Sekler, I. and Hershfinkel, M. (2014) The zinc sensing receptor, ZnR/GPR39, controls proliferation and differentiation of colonocytes and thereby tight junction formation in the colon. *Cell Death & Disease* [online]. 5 pp.e1307.

Cohen-Kerem, R. and Koren, G. (2003) Antioxidants and fetal protection against ethanol teratogenicity. I. Review of the experimental data and implications to humans. *Neurotoxicology and Teratology* [online]. 25 (1), pp.1-9.

Comporti, M., Signorini, C., Leoncini, S., Gardi, C., Ciccoli, L., Giardini, A., Vecchio, D. and Arezzini, B. (2010) Ethanol-induced oxidative stress: basic knowledge. *Genes & Nutrition* [online]. 5 (2), pp.101-109.

Cordova, F.M., Aguiar, A.S.,Jr, Peres, T.V., Lopes, M.W., Goncalves, F.M., Remor, A.P., Lopes, S.C., Pilati, C., Latini, A.S., Prediger, R.D., Erikson, K.M., Aschner, M. and Leal, R.B. (2012) In vivo manganese exposure modulates Erk, Akt and Darpp-32 in the striatum of developing rats, and impairs their motor function. *PloS One* [online]. 7 (3), pp.e33057.

Craddock, T.J., Tuszynski, J.A., Chopra, D., Casey, N., Goldstein, L.E., Hameroff, S.R. and Tanzi, R.E. (2012) The zinc dyshomeostasis hypothesis of Alzheimer's disease. *PloS One* [online]. 7 (3), pp.e33552.

Crittenden, P.L. and Filipov, N.M. (2011) Manganese modulation of MAPK pathways: effects on upstream mitogen activated protein kinase kinases and mitogen activated kinase phosphatase-1 in microglial cells. *Journal of Applied Toxicology : JAT* [online]. 31 (1), pp.1-10.

Crossgrove, J. and Zheng, W. (2004) Manganese toxicity upon overexposure. *NMR in Biomedicine* [online]. 17 (8), pp.544-553.

Cuajungco, M.P., Goldstein, L.E., Nunomura, A., Smith, M.A., Lim, J.T., Atwood, C.S., Huang, X., Farrag, Y.W., Perry, G. and Bush, A.I. (2000) Evidence that the beta-amyloid plaques of Alzheimer's disease represent the redox-silencing and entombment of abeta by zinc. *The Journal of Biological Chemistry* [online]. 275 (26), pp.19439-19442.

Dagda, R.K., Zhu, J., Kulich, S.M. and Chu, C.T. (2008) Mitochondrially localized ERK2 regulates mitophagy and autophagic cell stress: implications for Parkinson's disease. *Autophagy* [online]. 4 (6), pp.770-782.

Danscher, G., Jensen, K. B., Frederickson, C. J., Kemp, K., Andreasen, A., Juhl, S., Stoltenberg, M. and Ravid, R. (1997) Increased amount of zinc in the hippocampus and amygdala of Alzheimer's diseased brains: A proton-induced

X-ray emission spectroscopic analysis of cryostat sections from autopsy material. *Journal of Neuroscience Methods* [online]. 76(1), pp. 53-59.

Das, S., HajnÃ³czky, N., Antony, A.N., CsordÃ¡s, G., Gaspers, L.D., Clemens, D.L., Hoek, J.B. and HajnÃ³czky, G. (2012) Mitochondrial morphology and dynamics in hepatocytes from normal and ethanol-fed rats. *Pflugers Archiv : European Journal of Physiology* [online]. 464 (1), pp.101-109.

Day, E., Bentham, P.W., Callaghan, R., Kuruvilla, T. and George, S. (2013) Thiamine for prevention and treatment of Wernicke-Korsakoff Syndrome in people who abuse alcohol. *The Cochrane Database of Systematic Reviews* [online]. (7):CD004033. doi (7), pp.CD004033.

de la Monte, S.M. and Kril, J.J. (2014) Human alcohol-related neuropathology. *Acta Neuropathologica* [online]. 127 (1), pp.71-90.

Deng, Y., Jiao, C., Mi, C., Xu, B., Li, Y., Wang, F., Liu, W. and Xu, Z. (2015) Melatonin inhibits manganese-induced motor dysfunction and neuronal loss in mice: involvement of oxidative stress and dopaminergic neurodegeneration. *Molecular Neurobiology* [online]. 51 (1), pp.68-88.

Diaz, G., Liu, S., Isola, R., Diana, A. and Falchi, A.M. (2003) Mitochondrial localization of reactive oxygen species by dihydrofluorescein probes. *Histochemistry and Cell Biology* [online]. 120 (4), pp.319-325.

Diaz-Hernandez, M., Gomez-Ramos, A., Rubio, A., Gomez-Villafuertes, R., Naranjo, J.R., Miras-Portugal, M.T. and Avila, J. (2010) Tissue-nonspecific alkaline phosphatase promotes the neurotoxicity effect of extracellular tau. *The Journal of Biological Chemistry* [online]. 285 (42), pp.32539-32548.

Dineley, K.E., Votyakova, T.V. and Reynolds, I.J. (2003) Zinc inhibition of cellular energy production: implications for mitochondria and neurodegeneration. *Journal of Neurochemistry* [online]. 85 (3), pp.563-570.

Dorn, G.W.,2nd, Vega, R.B. and Kelly, D.P. (2015) Mitochondrial biogenesis and dynamics in the developing and diseased heart. *Genes & Development* [online]. 29 (19), pp.1981-1991.

Du, H. and ShiDu Yan, S. (2010) Unlocking the Door to Neuronal Woes in Alzheimer's Disease: AÎ² and Mitochondrial Permeability Transition Pore. *Pharmaceuticals (Basel, Switzerland)* [online]. 3 (6), pp.1936-1948.

Du, K., Liu, M., Pan, Y., Zhong, X. and Wei, M. (2017) AssociationÂ ofÂ SerumÂ ManganeseÂ LevelsÂ withÂ AlzheimerÂ sÂ Diseas eÂ andÂ MildÂ CognitiveÂ Impairment:Â AÂ SystematicÂ ReviewÂ andÂ Me ta-Analysis. *Nutrients* [online]. 9 (3), pp.231. doi: 10.3390/nu9030231. eCollection 2017 Mar.

Dumont, M., Wille, E., Stack, C., Calingasan, N.Y., Beal, M.F. and Lin, M.T. (2009) Reduction of oxidative stress, amyloid deposition, and memory deficit

by manganese superoxide dismutase overexpression in a transgenic mouse model of Alzheimer's disease. *FASEB Journal : Official Publication of the Federation of American Societies for Experimental Biology* [online]. 23 (8), pp.2459-2466.

Duplanty, A.A., Siggins, R.W., Allerton, T., Simon, L. and Molina, P.E. (2018) Myoblast mitochondrial respiration is decreased in chronic binge alcohol administered simian immunodeficiency virusâ€• infected antiretroviralâ€• treated rhesus macaques. *Physiological Reports* [online]. 6 (5), pp.e13625. doi:10.1002/(ISSN)2051-817X 10.14814/phy2.13625.

Eisner, V., Cupo, R.R., Gao, E., CsordÃ¡s, G., Slovinsky, W.S., Paillard, M., Cheng, L., Ibetti, J., Chen, S.R.W., Chuprun, J.K., Hoek, J.B., Koch, W.J. and HajnÃ³czky, G. (2017) Mitochondrial fusion dynamics is robust in the heart and depends on calcium oscillations and contractile activity. *Proceedings of the National Academy of Sciences of the United States of America* [online]. 114 (5), pp.E859-68.

Elrod, J.W. and Molkentin, J.D. (2013) Physiologic functions of cyclophilin D and the mitochondrial permeability transition pore. *Circulation Journal : Official Journal of the Japanese Circulation Society* [online]. 77 (5), pp.1111-1122.

Erikson, K. M. and Aschner, M. (2003) Manganese neurotoxicity and glutamate-GABA interaction. *Neurochemistry International* [online]. 43(4), pp. 475-480.

Esler, M., Rumantir, M., Wiesner, G., Kaye, D., Hastings, J. and Lambert, G. (2001) Sympathetic nervous system and insulin resistance: from obesity to diabetes. *American Journal of Hypertension* [online]. 14 (11 Pt 2), pp.304S-309S.

Exil, V., Ping, L., Yu, Y., Chakraborty, S., Caito, S.W., Wells, K.S., Karki, P., Lee, E. and Aschner, M. (2014) Activation of MAPK and FoxO by manganese (Mn) in rat neonatal primary astrocyte cultures. *PloS One* [online]. 9 (5), pp.e94753.

Fadda, F. and Rossetti, Z. L. (1998) Chronic ethanol consumption:from neuroadaptation to neurodegeneration. *Progress in Neurobiology* [online]. 56(4), pp. 385-431.

Fernandes, A.P. and Holmgren, A. (2004) Glutaredoxins: glutathione-dependent redox enzymes with functions far beyond a simple thioredoxin backup system. *Antioxidants & Redox Signaling* [online]. 6 (1), pp.63-74.

Fernandes, J., Hao, L., Bijli, K.M., Chandler, J.D., Orr, M., Hu, X., Jones, D.P. and Go, Y.M. (2017) From the Cover: Manganese Stimulates Mitochondrial H2O2 Production in SH-SY5Y Human Neuroblastoma Cells Over Physiologic as well as Toxicologic Range. *Toxicological Sciences : An Official Journal of the Society of Toxicology* [online]. 155 (1), pp.213-223.

Fitsanakis, V. A. and Aschner, M. (2005) The importance of glutamate, glycine, and γ-aminobutyric acid transport and regulation in manganese, mercury and lead neurotoxicity. *Toxicology and Applied Pharmacology* [online]. 204(3), pp. 343-354.

Flores-Bellver, M., Bonet-Ponce, L., Barcia, J.M., Garcia-Verdugo, J.M., Martinez-Gil, N., Saez-Atienzar, S., Sancho-Pelluz, J., Jordan, J., Galindo, M.F. and Romero, F.J. (2014) Autophagy and mitochondrial alterations in human retinal pigment epithelial cells induced by ethanol: implications of 4-hydroxy-nonenal. *Cell Death & Disease* [online]. 5 pp.e1328.

Franco-Iborra, S., Vila, M. and Perier, C. (2018) Mitochondrial Quality Control in Neurodegenerative Diseases: Focus on Parkinson's Disease and Huntington's Disease. *Frontiers in Neuroscience* [online]. 12 pp.342.

Franklin, J.L. (2011) Redox Regulation of the Intrinsic Pathway in Neuronal Apoptosis. *Antioxidants & Redox Signaling* [online]. 14 (8), pp.1437-1448.

Frederickson, C.J., Koh, J.Y. and Bush, A.I. (2005) The neurobiology of zinc in health and disease. *Nature Reviews.Neuroscience* [online]. 6 (6), pp.449-462.

Fujishiro, H., Ohashi, T., Takuma, M. and Himeno, S. (2013) Suppression of ZIP8 expression is a common feature of cadmium-resistant and manganese-resistant RBL-2H3 cells. *Metallomics : Integrated Biometal Science* [online]. 5 (5), pp.437-444.

Fujishiro, H., Yoshida, M., Nakano, Y. and Himeno, S. (2014) Interleukin-6 enhances manganese accumulation in SH-SY5Y cells: implications of the up-regulation of ZIP14 and the down-regulation of ZnT10. *Metallomics : Integrated Biometal Science* [online]. 6 (4), pp.944-949.

Galanis, D.J., Joseph, C., Masaki, K.H., Petrovitch, H., Ross, G.W. and White, L. (2000) A longitudinal study of drinking and cognitive performance in elderly Japanese American men: the Honolulu-Asia Aging Study. *American Journal of Public Health* [online]. 90 (8), pp.1254-1259.

Galvani, P., Fumagalli, P. and Santagostino, A. (1995) Vulnerability of mitochondrial complex I in PC12 cells exposed to manganese. *European Journal of Pharmacology* [online]. 293 (4), pp.377-383.

Gavin, C.E., Gunter, K.K. and Gunter, T.E. (1999) Manganese and calcium transport in mitochondria: implications for manganese toxicity. *Neurotoxicology* [online]. 20 (2-3), pp.445-453.

Gavin, C.E., Gunter, K.K. and Gunter, T.E. (1999) Manganese and calcium transport in mitochondria: implications for manganese toxicity. *Neurotoxicology* [online]. 20 (2-3), pp.445-453.

Ge, P., Luo, Y., Liu, C.L. and Hu, B. (2007) Protein aggregation and proteasome dysfunction after brain ischemia. *Stroke* [online]. 38 (12), pp.3230-3236.

Geisler, S., Holmstrom, K.M., Skujat, D., Fiesel, F.C., Rothfuss, O.C., Kahle, P.J. and Springer, W. (2010) PINK1/Parkin-mediated mitophagy is dependent on VDAC1 and p62/SQSTM1. *Nature Cell Biology* [online]. 12 (2), pp.119-131.

Gerber, H., Wu, F., Dimitrov, M., Garcia Osuna, G.M. and Fraering, P.C. (2017) Zinc and Copper Differentially Modulate Amyloid Precursor Protein Processing by gamma-Secretase and Amyloid-beta Peptide Production. *The Journal of Biological Chemistry* [online]. 292 (9), pp.3751-3767.

Gerhardsson, L., Lundh, T., Minthon, L. and Londos, E. (2008) Metal concentrations in plasma and cerebrospinal fluid in patients with Alzheimer's disease. *Dementia and Geriatric Cognitive Disorders* [online]. 25 (6), pp.508-515.

Getachew, B., Hudson, T., Heinbockel, T., Csoka, A.B. and Tizabi, Y. (2018) Protective Effects of Donepezil Against Alcohol-Induced Toxicity in Cell Culture: Role of Caspase-3. *Neurotoxicity Research* [online]. 34 (3), pp.757-762.

Gibbs, P.N., Gore, M.G. and Jordan, P.M. (1985) Investigation of the effect of metal ions on the reactivity of thiol groups in human 5-aminolaevulinate dehydratase. *The Biochemical Journal* [online]. 225 (3), pp.573-580.

Glenner, G.G. and Wong, C.W. (1984) Alzheimer's disease: initial report of the purification and characterization of a novel cerebrovascular amyloid protein. *Biochemical and Biophysical Research Communications* [online]. 120 (3), pp.885-890.

Glick, D., Barth, S. and Macleod, K.F. (2010) Autophagy: cellular and molecular mechanisms. *The Journal of Pathology* [online]. 221 (1), pp.3-12.

Gong, C. -., Grundke-Iqbal, I. and Iqbal, K. (1994) Dephosphorylation of Alzheimer's disease abnormally phosphorylated tau by protein phosphatase-2A. *Neuroscience* [online]. 61(4), pp. 765-772.

Gonzalez, H.F. and Visentin, S. (2016) Micronutrients and neurodevelopment: An update. *Archivos Argentinos De Pediatria* [online]. 114 (6), pp.570-575.

Gorojod, R.M., Alaimo, A., Porte Alcon, S., Pomilio, C., Saravia, F. and Kotler, M.L. (2015) The autophagic- lysosomal pathway determines the fate of glial cells under manganese- induced oxidative stress conditions. *Free Radical Biology & Medicine* [online]. 87 pp.237-251.

Grenett, H.E., Aikens, M.L., Tabengwa, E.M., Davis, G.C. and Booyse, F.M. (2000) Ethanol downregulates transcription of the PAI-1 gene in cultured human endothelial cells. *Thrombosis Research* [online]. 97 (4), pp.247-255.

Grimm, A. and Eckert, A. (2017) Brain aging and neurodegeneration: from a mitochondrial point of view. *Journal of Neurochemistry* [online]. 143 (4), pp.418-431.

Guadagnoli, T., Caltana, L., Vacotto, M., Gironacci, M. M. and Brusco, A. (2016) Direct effects of ethanol on neuronal differentiation: An in vitro analysis of viability and morphology. *Brain Research Bulletin* [online]. 127pp. 177-186.

Guilarte, T.R. (2013) Manganese neurotoxicity: new perspectives from behavioral, neuroimaging, and neuropathological studies in humans and non-human primates. *Frontiers in Aging Neuroscience* [online]. 5 pp.23.

Guilarte, T.R., Burton, N.C., Verina, T., Prabhu, V.V., Becker, K.G., Syversen, T. and Schneider, J.S. (2008) Increased APLP1 expression and neurodegeneration in the frontal cortex of manganese-exposed non-human primates. *Journal of Neurochemistry* [online]. 105 (5), pp.1948-1959.

Gunter, T.E., Gerstner, B., Lester, T., Wojtovich, A.P., Malecki, J., Swarts, S.G., Brookes, P.S., Gavin, C.E. and Gunter, K.K. (2010) An analysis of the effects of Mn2+ on oxidative phosphorylation in liver, brain, and heart mitochondria using state 3 oxidation rate assays. *Toxicology and Applied Pharmacology* [online]. 249 (1), pp.65-75.

Guo, J.L., Buist, A., Soares, A., Callaerts, K., Calafate, S., Stevenaert, F., Daniels, J.P., Zoll, B.E., Crowe, A., Brunden, K.R., Moechars, D. and Lee, V.M. (2016) The Dynamics and Turnover of Tau Aggregates in Cultured Cells: INSIGHTS INTO THERAPIES FOR TAUOPATHIES. *The Journal of Biological Chemistry* [online]. 291 (25), pp.13175-13193.

Gupta, S., Pramanik, D., Mukherjee, R., Campbell, N.R., Elumalai, S., de Wilde, R.F., Hong, S.M., Goggins, M.G., De Jesus-Acosta, A., Laheru, D. and Maitra, A. (2012) Molecular determinants of retinoic acid sensitivity in pancreatic cancer. *Clinical Cancer Research : An Official Journal of the American Association for Cancer Research* [online]. 18 (1), pp.280-289.

Ha, K.N., Chen, Y., Cai, J. and Sternberg, P.,Jr (2006) Increased glutathione synthesis through an ARE-Nrf2-dependent pathway by zinc in the RPE: implication for protection against oxidative stress. *Investigative Ophthalmology & Visual Science* [online]. 47 (6), pp.2709-2715.

Halestrap, A. P. and Pasdois, P. (2009) The role of the mitochondrial permeability transition pore in heart disease. *Biochimica Et Biophysica Acta (BBA) - Bioenergetics* [online]. 1787(11), pp. 1402-1415.

Han, X.J., Hu, Y.Y., Yang, Z.J., Jiang, L.P., Shi, S.L., Li, Y.R., Guo, M.Y., Wu, H.L. and Wan, Y.Y. (2017) Amyloid Î²-42 induces neuronal apoptosis by targeting mitochondria. *Molecular Medicine Reports* [online]. 16 (4), pp.4521-4528.

Handing, E.P., Andel, R., Kadlecova, P., Gatz, M. and Pedersen, N.L. (2015) Midlife Alcohol Consumption and Risk of Dementia Over 43 Years of Follow-Up: A Population-Based Study From the Swedish Twin Registry. *The Journals of Gerontology.Series A, Biological Sciences and Medical Sciences* [online]. 70 (10), pp.1248-1254.

Hardy, J. and Selkoe, D.J. (2002) The amyloid hypothesis of Alzheimer's disease: progress and problems on the road to therapeutics. *Science (New York, N.Y.)* [online]. 297 (5580), pp.353-356.

Harwood, D.G., Kalechstein, A., Barker, W.W., Strauman, S., St George-Hyslop, P., Iglesias, C., Loewenstein, D. and Duara, R. (2010) The effect of alcohol and tobacco consumption, and apolipoprotein E genotype, on the age of onset in Alzheimer's disease. *International Journal of Geriatric Psychiatry* [online]. 25 (5), pp.511-518.

He, J., de la Monte, S. and Wands, J.R. (2007) Acute ethanol exposure inhibits insulin signaling in the liver. *Hepatology (Baltimore, Md.)* [online]. 46 (6), pp.1791-1800.

He, K. and Aizenman, E. (2010) ERK signaling leads to mitochondrial dysfunction in extracellular zinc-induced neurotoxicity. *Journal of Neurochemistry* [online]. 114 (2), pp.452-461.

Heaton, M.B., Paiva, M. and Siler-Marsiglio, K. (2011) Ethanol influences on Bax translocation, mitochondrial membrane potential, and reactive oxygen species generation are modulated by vitamin E and brain-derived neurotrophic factor. *Alcoholism, Clinical and Experimental Research* [online]. 35 (6), pp.1122-1133.

Heppner, F.L., Ransohoff, R.M. and Becher, B. (2015) Immune attack: the role of inflammation in Alzheimer disease. *Nature Reviews.Neuroscience* [online]. 16 (6), pp.358-372.

Hernandez, J.A., Lopez-Sanchez, R.C. and Rendon-Ramirez, A. (2016) Lipids and Oxidative Stress Associated with Ethanol-Induced Neurological Damage. *Oxidative Medicine and Cellular Longevity* [online]. 2016 pp.1543809.

Hernandez, R.B., Farina, M., Esposito, B.P., Souza-Pinto, N.C., Barbosa, F.,Jr and Sunol, C. (2011) Mechanisms of manganese-induced neurotoxicity in primary neuronal cultures: the role of manganese speciation and cell type. *Toxicological Sciences : An Official Journal of the Society of Toxicology* [online]. 124 (2), pp.414-423.

Heurtaux, T., Michelucci, A., Losciuto, S., Gallotti, C., Felten, P., Dorban, G., Grandbarbe, L., Morga, E. and Heuschling, P. (2010) Microglial activation depends on beta-amyloid conformation: role of the formylpeptide receptor 2. *Journal of Neurochemistry* [online]. 114 (2), pp.576-586.

Heymann, D., Stern, Y., Cosentino, S., Tatarina-Nulman, O., Dorrejo, J.N. and Gu, Y. (2016) The Association Between Alcohol Use and the Progression of Alzheimer's Disease. *Current Alzheimer Research* [online]. 13 (12), pp.1356-1362.

Hirata, Y., Adachi, K. and Kiuchi, K. (1998) Phosphorylation and activation of p70 S6 kinase by manganese in PC12 cells. *Neuroreport* [online]. 9 (13), pp.3037-3040.

Hirata, Y. (2002) Manganese-induced apoptosis in PC12 cells. *Neurotoxicology and Teratology* [online]. 24(5), pp. 639-653.

Hoek, J.B., Cahill, A. and Pastorino, J.G. (2002) Alcohol and mitochondria: a dysfunctional relationship. *Gastroenterology* [online]. 122 (7), pp.2049-2063.

Huang, B.X., Akbar, M., Kevala, K. and Kim, H.Y. (2011) Phosphatidylserine is a critical modulator for Akt activation. *The Journal of Cell Biology* [online]. 192 (6), pp.979-992.

Huang, X., Cuajungco, M.P., Atwood, C.S., Moir, R.D., Tanzi, R.E. and Bush, A.I. (2000) Alzheimer's disease, beta-amyloid protein and zinc. *The Journal of Nutrition* [online]. 130 (5S Suppl), pp.1488S-92S.

Huang, Y., Wu, Z., Cao, Y., Lang, M., Lu, B. and Zhou, B. (2014) Zinc Binding Directly Regulates Tau Toxicity Independent of Tau Hyperphosphorylation. *Cell Reports* [online]. 8 (3), pp.831-842.

Huang, Y. A., Zhou, B., Wernig, M. and Südhof, T. C. (2017) ApoE2, ApoE3, and ApoE4 Differentially Stimulate APP Transcription and Aβ Secretion. *Cell* [online]. 168(3), pp. 427-441.e21.

Igic, P.G., Lee, E., Harper, W. and Roach, K.W. (2002) Toxic effects associated with consumption of zinc. *Mayo Clinic Proceedings* [online]. 77 (7), pp.713-716.

Imam, I. (2010) Alcohol and the central nervous system. *British Journal of Hospital Medicine (London, England : 2005)* [online]. 71 (11), pp.635-639.

Ishihara, N., Jofuku, A., Eura, Y. and Mihara, K. (2003) Regulation of mitochondrial morphology by membrane potential, and DRP1-dependent division and FZO1-dependent fusion reaction in mammalian cells. *Biochemical and Biophysical Research Communications* [online]. 301 (4), pp.891-898.

Islam, M.M., Nautiyal, M., Wynn, R.M., Mobley, J.A., Chuang, D.T. and Hutson, S.M. (2010) Branched-chain amino acid metabolon: interaction of glutamate dehydrogenase with the mitochondrial branched-chain aminotransferase (BCATm). *The Journal of Biological Chemistry* [online]. 285 (1), pp.265-276.

Itoh, K., Sakata, M., Watanabe, M., Aikawa, Y. and Fujii, H. (2008) The entry of manganese ions into the brain is accelerated by the activation of N-methyl-D-aspartate receptors. *Neuroscience* [online]. 154 (2), pp.732-740.

Ittner, L.M. and Gotz, J. (2011) Amyloid-beta and tau--a toxic pas de deux in Alzheimer's disease. *Nature Reviews.Neuroscience* [online]. 12 (2), pp.65-72.

Jackson, K.A., Valentine, R.A., Coneyworth, L.J., Mathers, J.C. and Ford, D. (2008) Mechanisms of mammalian zinc-regulated gene expression. *Biochemical Society Transactions* [online]. 36 (Pt 6), pp.1262-1266.

Jahani-Asl, A., Cheung, E.C., Neuspiel, M., MacLaurin, J.G., Fortin, A., Park, D.S., McBride, H.M. and Slack, R.S. (2007) Mitofusin 2 protects cerebellar granule neurons against injury-induced cell death. *The Journal of Biological Chemistry* [online]. 282 (33), pp.23788-23798.

Jin, S., Kedia, N., Illes-Toth, E., Haralampiev, I., Prisner, S., Herrmann, A., Wanker, E.E. and Bieschke, J. (2016) Amyloid-beta(1-42) Aggregation Initiates Its Cellular Uptake and Cytotoxicity. *The Journal of Biological Chemistry* [online]. 291 (37), pp.19590-19606.

Kaizu, T., Ikeda, A., Nakao, A., Tsung, A., Toyokawa, H., Ueki, S., Geller, D.A. and Murase, N. (2008) Protection of transplant-induced hepatic ischemia/reperfusion injury with carbon monoxide via MEK/ERK1/2 pathway downregulation. *American Journal of Physiology.Gastrointestinal and Liver Physiology* [online]. 294 (1), pp.G236-44.

Kambe, T., Tsuji, T., Hashimoto, A. and Itsumura, N. (2015) The Physiological, Biochemical, and Molecular Roles of Zinc Transporters in Zinc Homeostasis and Metabolism. *Physiological Reviews* [online]. 95 (3), pp.749-784.

Kametani, F. and Hasegawa, M. (2018) Reconsideration of Amyloid Hypothesis and Tau Hypothesis in Alzheimer's Disease. *Frontiers in Neuroscience* [online]. 12 pp.25.

Karuppagounder, S.S., Pinto, J.T., Xu, H., Chen, H.L., Beal, M.F. and Gibson, G.E. (2009) Dietary supplementation with resveratrol reduces plaque pathology in a transgenic model of Alzheimer's disease. *Neurochemistry International* [online]. 54 (2), pp.111-118.

Kawahara, M., Mizuno, D., Koyama, H., Konoha, K., Ohkawara, S. and Sadakane, Y. (2014) Disruption of zinc homeostasis and the pathogenesis of senile dementia. *Metallomics : Integrated Biometal Science* [online]. 6 (2), pp.209-219.

Kawahara, M., Mizuno, D., Koyama, H., Konoha, K., Ohkawara, S. and Sadakane, Y. (2014) Disruption of zinc homeostasis and the pathogenesis of senile dementia. *Metallomics : Integrated Biometal Science* [online]. 6 (2), pp.209-219.

Kayed, R. and Lasagna-Reeves, C.A. (2013) Molecular mechanisms of amyloid oligomers toxicity. *Journal of Alzheimer's Disease : JAD* [online]. 33 Suppl 1 pp.S67-78.

Kelley, B.J. and Petersen, R.C. (2007) Alzheimer's disease and mild cognitive impairment. *Neurologic Clinics* [online]. 25 (3), pp.577-609, v.

Kelley, B.J. and Petersen, R.C. (2007) Alzheimer's disease and mild cognitive impairment. *Neurologic Clinics* [online]. 25 (3), pp.577-609, v.

Kerr, J.S., Adriaanse, B.A., Greig, N.H., Mattson, M.P., Cader, M.Z., Bohr, V.A. and Fang, E.F. (2017) Mitophagy and Alzheimer's Disease: Cellular and Molecular Mechanisms. *Trends in Neurosciences* [online]. 40 (3), pp.151-166.

Kidd, P.M. (2008) Alzheimer's disease, amnestic mild cognitive impairment, and age-associated memory impairment: current understanding and progress toward integrative prevention. *Alternative Medicine Review : A Journal of Clinical Therapeutic* [online]. 13 (2), pp.85-115.

Kim, E. K. and Choi, E. (2010) Pathological roles of MAPK signaling pathways in human diseases. *Biochimica Et Biophysica Acta (BBA) - Molecular Basis of Disease* [online]. 1802(4), pp. 396-405.

Kim, I., Rodriguez-Enriquez, S. and Lemasters, J.J. (2007) Selective degradation of mitochondria by mitophagy. *Archives of Biochemistry and Biophysics* [online]. 462 (2), pp.245-253.

Kim, J., Basak, J.M. and Holtzman, D.M. (2009) The role of apolipoprotein E in Alzheimer's disease. *Neuron* [online]. 63 (3), pp.287-303.

Kim, J., Onstead, L., Randle, S., Price, R., Smithson, L., Zwizinski, C., Dickson, D.W., Golde, T. and McGowan, E. (2007) Abeta40 inhibits amyloid deposition in vivo. *The Journal of Neuroscience : The Official Journal of the Society for Neuroscience* [online]. 27 (3), pp.627-633.

Kim, S., Jung, Y., Kim, D., Koh, H. and Chung, J. (2000) Extracellular zinc activates p70 S6 kinase through the phosphatidylinositol 3-kinase signaling pathway. *The Journal of Biological Chemistry* [online]. 275 (34), pp.25979-25984.

Kim, S.R., Jeong, H.Y., Yang, S., Choi, S.P., Seo, M.Y., Yun, Y.K., Choi, Y., Baik, S.H., Park, J.S., Gwon, A.R., Yang, D.K., Lee, C.H., Lee, S.M., Park, K.W. and Jo, D.G. (2011) Effects of chronic alcohol consumption on expression levels of APP and Abeta-producing enzymes. *BMB Reports* [online]. 44 (2), pp.135-139.

Kim, S.Y., Shim, M.S., Kim, K.Y., Weinreb, R.N., Wheeler, L.A. and Ju, W.K. (2014) Inhibition of cyclophilin D by cyclosporin A promotes retinal ganglion cell survival by preventing mitochondrial alteration in ischemic injury. *Cell Death & Disease* [online]. 5 (3), pp.e1105.

Kim, Y. -., Kim, E. Y., Gwag, B. J., Sohn, S. and Koh, J. -. (1999) Zinc-induced cortical neuronal death with features of apoptosis and necrosis: Mediation by free radicals. *Neuroscience* [online]. 89(1), pp. 175-182.

Komatsu, M. and Ichimura, Y. (2010) Physiological significance of selective degradation of p62 by autophagy. *FEBS Letters* [online]. 584 (7), pp.1374-1378.

Kopeikina, K.J., Hyman, B.T. and Spires-Jones, T.L. (2012) Soluble forms of tau are toxic in Alzheimer's disease. *Translational Neuroscience* [online]. 3 (3), pp.223-233.

Kozlov, S., Afonin, A., Evsyukov, I. and Bondarenko, A. (2017) Alzheimer's disease: as it was in the beginning. *Reviews in the Neurosciences* [online]. 28 (8), pp.825-843.

Kril, J.J., Halliday, G.M., Svoboda, M.D. and Cartwright, H. (1997) The cerebral cortex is damaged in chronic alcoholics. *Neuroscience* [online]. 79 (4), pp.983-998.

Kwon, K.J., Lee, E.J., Cho, K.S., Cho, D.H., Shin, C.Y. and Han, S.H. (2015) Ginkgo biloba extract (Egb761) attenuates zinc-induced tau phosphorylation at Ser262 by regulating GSK3beta activity in rat primary cortical neurons. *Food & Function* [online]. 6 (6), pp.2058-2067.

Latham, P., Lund, E.K., Brown, J.C. and Johnson, I.T. (2001) Effects of cellular redox balance on induction of apoptosis by eicosapentaenoic acid in HT29 colorectal adenocarcinoma cells and rat colon in vivo. *Gut* [online]. 49 (1), pp.97-105.

Latronico, T., Brana, M.T., Merra, E., Fasano, A., Di Bari, G., Casalino, E. and Liuzzi, G.M. (2013) Impact of manganese neurotoxicity on MMP-9 production and superoxide dismutase activity in rat primary astrocytes. Effect of resveratrol and therapeutical implications for the treatment of CNS diseases. *Toxicological Sciences : An Official Journal of the Society of Toxicology* [online]. 135 (1), pp.218-228.

Ledig, M., M'Paria, J.R. and Mandel, P. (1981) Superoxide dismutase activity in rat brain during acute and chronic alcohol intoxication. *Neurochemical Research* [online]. 6 (4), pp.385-390.

Lee, S., Sato, Y. and Nixon, R.A. (2011) Primary lysosomal dysfunction causes cargo-specific deficits of axonal transport leading to Alzheimer-like neuritic dystrophy. *Autophagy* [online]. 7 (12), pp.1562-1563.

Lee, S.J., Cho, K.S. and Koh, J.Y. (2009) Oxidative injury triggers autophagy in astrocytes: the role of endogenous zinc. *Glia* [online]. 57 (12), pp.1351-1361.

Lee, S.J. and Koh, J.Y. (2010) Roles of zinc and metallothionein-3 in oxidative stress-induced lysosomal dysfunction, cell death, and autophagy in neurons and astrocytes. *Molecular Brain* [online]. 3 (1), pp.30-6606-3-30.

Lee, S.R. (2018) Critical Role of Zinc as Either an Antioxidant or a Prooxidant in Cellular Systems. *Oxidative Medicine and Cellular Longevity* [online]. 2018 pp.9156285.

Lee, Y.J., Aroor, A.R. and Shukla, S.D. (2002) Temporal activation of p42/44 mitogen-activated protein kinase and c-Jun N-terminal kinase by acetaldehyde in rat hepatocytes and its loss after chronic ethanol exposure. *The Journal of Pharmacology and Experimental Therapeutics* [online]. 301 (3), pp.908-914.

Lee, Y.J. and Shukla, S.D. (2007) Histone H3 phosphorylation at serine 10 and serine 28 is mediated by p38 MAPK in rat hepatocytes exposed to ethanol and acetaldehyde. *European Journal of Pharmacology* [online]. 573 (1-3), pp.29-38.

Lei, H. and Kazlauskas, A. (2009) Growth factors outside of the platelet-derived growth factor (PDGF) family employ reactive oxygen species/Src family kinases to activate PDGF receptor alpha and thereby promote proliferation and survival of cells. *The Journal of Biological Chemistry* [online]. 284 (10), pp.6329-6336.

Lemasters, J.J. (2014) Variants of mitochondrial autophagy: Types 1 and 2 mitophagy and micromitophagy (Type 3). *Redox Biology* [online]. 2 pp.749-754.

Lemasters, J.J. (2014) Variants of mitochondrial autophagy: Types 1 and 2 mitophagy and micromitophagy (Type 3). *Redox Biology* [online]. 2 pp.749-754.

Lemire, J., Mailloux, R. and Appanna, V.D. (2008) Zinc toxicity alters mitochondrial metabolism and leads to decreased ATP production in hepatocytes. *Journal of Applied Toxicology : JAT* [online]. 28 (2), pp.175-182.

Leyns, C.E.G., Ulrich, J.D., Finn, M.B., Stewart, F.R., Koscal, L.J., Remolina Serrano, J., Robinson, G.O., Anderson, E., Colonna, M. and Holtzman, D.M. (2017) TREM2 deficiency attenuates neuroinflammation and protects against neurodegeneration in a mouse model of tauopathy. *Proceedings of the National Academy of Sciences of the United States of America* [online]. 114 (43), pp.11524-11529.

Li, B., Cui, W., Tan, Y., Luo, P., Chen, Q., Zhang, C., Qu, W., Miao, L. and Cai, L. (2014) Zinc is essential for the transcription function of Nrf2 in human renal tubule cells in vitro and mouse kidney in vivo under the diabetic condition. *Journal of Cellular and Molecular Medicine* [online]. 18 (5), pp.895-906.

Li, F., Munsey, T.S. and Sivaprasadarao, A. (2017) TRPM2-mediated rise in mitochondrial Zn(2+) promotes palmitate-induced mitochondrial fission and

pancreatic beta-cell death in rodents. *Cell Death and Differentiation* [online]. 24 (12), pp.1999-2012.

Li, J.Q., Tan, L., Wang, H.F., Tan, M.S., Tan, L., Xu, W., Zhao, Q.F., Wang, J., Jiang, T. and Yu, J.T. (2016) Risk factors for predicting progression from mild cognitive impairment to Alzheimer's disease: a systematic review and meta-analysis of cohort studies. *Journal of Neurology, Neurosurgery, and Psychiatry* [online]. 87 (5), pp.476-484.

Li, L. and Yang, X. (2018) The Essential Element Manganese, Oxidative Stress, and Metabolic Diseases: Links and Interactions. *Oxidative Medicine and Cellular Longevity* [online]. 2018 pp.7580707.

Li, L. and Yang, X. (2018) The Essential Element Manganese, Oxidative Stress, and Metabolic Diseases: Links and Interactions. *Oxidative Medicine and Cellular Longevity* [online]. 2018 pp.7580707.

Li, L.B. and Wang, Z.Y. (2016) Disruption of brain zinc homeostasis promotes the pathophysiological progress of Alzheimer's disease. *Histology and Histopathology* [online]. 31 (6), pp.623-627.

Liang, ,Jun-Hua and Jia, ,Jian-PingDysfunctional autophagy in Alzheimerâ€™s disease: pathogenic roles and therapeutic implications. [online].

Lim, K.H., Kim, Y.K. and Chang, Y.T. (2007) Investigations of the molecular mechanism of metal-induced Abeta (1-40) amyloidogenesis. *Biochemistry* [online]. 46 (47), pp.13523-13532.

Lin, A. M. Y., Fan, S. F., Yang, D. M., Hsu, L. L. and Yang, C. H. J. (2003) Zinc-induced apoptosis in substantia nigra of rat brain: neuroprotection by vitamin D3. *Free Radical Biology and Medicine* [online]. 34(11), pp. 1416-1425.

Lindberg, O., Walterfang, M., Looi, J.C., Malykhin, N., Ostberg, P., Zandbelt, B., Styner, M., Paniagua, B., Velakoulis, D., Orndahl, E. and Wahlund, L.O. (2012) Hippocampal shape analysis in Alzheimer's disease and frontotemporal lobar degeneration subtypes. *Journal of Alzheimer's Disease : JAD* [online]. 30 (2), pp.355-365.

Liu, C.C., Liu, C.C., Kanekiyo, T., Xu, H. and Bu, G. (2013) Apolipoprotein E and Alzheimer disease: risk, mechanisms and therapy. *Nature Reviews.Neurology* [online]. 9 (2), pp.106-118.

Liu, H., Dai, C., Fan, Y., Guo, B., Ren, K., Sun, T. and Wang, W. (2017) From autophagy to mitophagy: the roles of P62 in neurodegenerative diseases. *Journal of Bioenergetics and Biomembranes* [online]. 49 (5), pp.413-422.

Liu, L., Sun, T., Xin, F., Cui, W., Guo, J. and Hu, J. (2017) Nerve Growth Factor Protects Against Alcohol-Induced Neurotoxicity in PC12 Cells via

PI3K/Akt/mTOR Pathway. *Alcohol and Alcoholism (Oxford, Oxfordshire)* [online]. 52 (1), pp.12-18.

Liu, X., Sullivan, K.A., Madl, J.E., Legare, M. and Tjalkens, R.B. (2006) Manganese-induced neurotoxicity: the role of astroglial-derived nitric oxide in striatal interneuron degeneration. *Toxicological Sciences : An Official Journal of the Society of Toxicology* [online]. 91 (2), pp.521-531.

Liu, X., Yang, J., Lu, C., Jiang, S., Nie, X., Han, J., Yin, L. and Jiang, J. (2017) Downregulation of Mfn2 participates in manganese-induced neuronal apoptosis in rat striatum and PC12 cells. *Neurochemistry International* [online]. 108 pp.40-51.

Liu, X.F., Zhang, L.M., Guan, H.N., Zhang, Z.W. and Xu, S.W. (2013) Effects of oxidative stress on apoptosis in manganese-induced testicular toxicity in cocks. *Food and Chemical Toxicology : An International Journal Published for the British Industrial Biological Research Association* [online]. 60 pp.168-176.

Liu, Z., Liu, Y., Gao, R., Li, H., Dunn, T., Wu, P., Smith, R.G., Sarkar, P.S. and Fang, X. (2014) Ethanol suppresses PGC-1alpha expression by interfering with the cAMP-CREB pathway in neuronal cells. *PloS One* [online]. 9 (8), pp.e104247.

Loro, V.L., Jorge, M.B., Silva, K.R. and Wood, C.M. (2012) Oxidative stress parameters and antioxidant response to sublethal waterborne zinc in a euryhaline teleost Fundulus heteroclitus: protective effects of salinity. *Aquatic Toxicology (Amsterdam, Netherlands)* [online]. 110-111 pp.187-193.

Lynch, C.J., Patson, B.J., Goodman, S.A., Trapolsi, D. and Kimball, S.R. (2001) Zinc stimulates the activity of the insulin- and nutrient-regulated protein kinase mTOR. *American Journal of Physiology.Endocrinology and Metabolism* [online]. 281 (1), pp.E25-34.

Mairet-Coello, G., Courchet, J., Pieraut, S., Courchet, V., Maximov, A. and Polleux, F. (2013) The CAMKK2-AMPK kinase pathway mediates the synaptotoxic effects of Abeta oligomers through Tau phosphorylation. *Neuron* [online]. 78 (1), pp.94-108.

Manczak, M. and Reddy, P.H. (2012) Abnormal interaction between the mitochondrial fission protein Drp1 and hyperphosphorylated tau in Alzheimer's disease neurons: implications for mitochondrial dysfunction and neuronal damage. *Human Molecular Genetics* [online]. 21 (11), pp.2538-2547.

Manev, H., Kharlamov, E., Uz, T., Mason, R. P. and Cagnoli, C. M. (1997) Characterization of Zinc-Induced Neuronal Death in Primary Cultures of Rat Cerebellar Granule Cells. *Experimental Neurology* [online]. 146(1), pp. 171-178.

Maret, W. (2013) Zinc biochemistry: from a single zinc enzyme to a key element of life. *Advances in Nutrition (Bethesda, Md.)* [online]. 4 (1), pp.82-91.

Marik, S.A., Olsen, O., Tessier-Lavigne, M. and Gilbert, C.D. (2016) Physiological role for amyloid precursor protein in adult experience-dependent plasticity. *Proceedings of the National Academy of Sciences of the United States of America* [online]. 113 (28), pp.7912-7917.

Markesbery, W.R., Ehmann, W.D., Hossain, T.I. and Alauddin, M. (1984) Brain manganese concentrations in human aging and Alzheimer's disease. *Neurotoxicology* [online]. 5 (1), pp.49-57.

MartÃnez-Reyes, I., Diebold, L.P., Kong, H., Schieber, M., Huang, H., Hensley, C.T., Mehta, M.M., Wang, T., Santos, J.H., Woychik, R., Dufour, E., Spelbrink, J.N., Weinberg, S.E., Zhao, Y., DeBerardinis, R.J. and Chandel, N.S. (2016) TCA Cycle and Mitochondrial Membrane Potential Are Necessary for Diverse Biological Functions. *Molecular Cell* [online]. 61 (2), pp.199-209.

Martinez-Finley, E.J., Gavin, C.E., Aschner, M. and Gunter, T.E. (2013) Manganese neurotoxicity and the role of reactive oxygen species. *Free Radical Biology & Medicine* [online]. 62 pp.65-75.

Martinez-Galan, J.R., Diaz, C. and Juiz, J.M. (2003) Histochemical localization of neurons with zinc-permeable AMPA/kainate channels in rat brain slices. *Brain Research* [online]. 963 (1-2), pp.156-164.

Matheou, C.J., Younan, N.D. and Viles, J.H. (2016) The Rapid Exchange of Zinc(2+) Enables Trace Levels to Profoundly Influence Amyloid-beta Misfolding and Dominates Assembly Outcomes in Cu(2+)/Zn(2+) Mixtures. *Journal of Molecular Biology* [online]. 428 (14), pp.2832-2846.

Maynard, C.J., Bush, A.I., Masters, C.L., Cappai, R. and Li, Q.X. (2005) Metals and amyloid-Î² in Alzheimer's disease. *International Journal of Experimental Pathology* [online]. 86 (3), pp.147-159.

Mazan-Mamczarz, K., Peroutka, R.J., Steinhardt, J.J., Gidoni, M., Zhang, Y., Lehrmann, E., Landon, A.L., Dai, B., Houng, S., Muniandy, P.A., Efroni, S., Becker, K.G. and Gartenhaus, R.B. (2015) Distinct inhibitory effects on mTOR signaling by ethanol and INK128 in diffuse large B-cell lymphoma. *Cell Communication and Signaling : CCS* [online]. 13 pp.15-015-0091-0. eCollection 2015.

McCall, K.A., Huang, C. and Fierke, C.A. (2000) Function and mechanism of zinc metalloenzymes. *The Journal of Nutrition* [online]. 130 (5S Suppl), pp.1437S-46S.

McCall, K.A., Huang, C. and Fierke, C.A. (2000) Function and mechanism of zinc metalloenzymes. *The Journal of Nutrition* [online]. 130 (5S Suppl), pp.1437S-46S.

McGee, S.L., Sadli, N., Morrison, S., Swinton, C. and Suphioglu, C. (2011) DHA protects against zinc mediated alterations in neuronal cellular bioenergetics. *Cellular Physiology and Biochemistry : International Journal of*

Experimental Cellular Physiology, Biochemistry, and Pharmacology [online]. 28 (1), pp.157-162.

Mehta, D., Jackson, R., Paul, G., Shi, J. and Sabbagh, M. (2017) Why do trials for Alzheimer's disease drugs keep failing? A discontinued drug perspective for 2010-2015. *Expert Opinion on Investigational Drugs* [online]. 26 (6), pp.735-739.

Merlini, L., Angelin, A., Tiepolo, T., Braghetta, P., Sabatelli, P., Zamparelli, A., Ferlini, A., Maraldi, N.M., Bonaldo, P. and Bernardi, P. (2008) Cyclosporin A corrects mitochondrial dysfunction and muscle apoptosis in patients with collagen VI myopathies. *Proceedings of the National Academy of Sciences of the United States of America* [online]. 105 (13), pp.5225-5229.

Milatovic, D., Zaja-Milatovic, S., Gupta, R.C., Yu, Y. and Aschner, M. (2009) Oxidative damage and neurodegeneration in manganese-induced neurotoxicity. *Toxicology and Applied Pharmacology* [online]. 240 (2), pp.219-225.

Miller, L.M., Wang, Q., Telivala, T.P., Smith, R.J., Lanzirotti, A. and Miklossy, J. (2006) Synchrotron-based infrared and X-ray imaging shows focalized accumulation of Cu and Zn co-localized with beta-amyloid deposits in Alzheimer's disease. *Journal of Structural Biology* [online]. 155 (1), pp.30-37.

Miller, Y., Ma, B. and Nussinov, R. (2010) Zinc ions promote Alzheimer Abeta aggregation via population shift of polymorphic states. *Proceedings of the National Academy of Sciences of the United States of America* [online]. 107 (21), pp.9490-9495.

Miyamoto, Y., Koh, Y.H., Park, Y.S., Fujiwara, N., Sakiyama, H., Misonou, Y., Ookawara, T., Suzuki, K., Honke, K. and Taniguchi, N. (2003) Oxidative stress caused by inactivation of glutathione peroxidase and adaptive responses. *Biological Chemistry* [online]. 384 (4), pp.567-574.

Mizuno, D. and Kawahara, M. (2013) The molecular mechanisms of zinc neurotoxicity and the pathogenesis of vascular type senile dementia. *International Journal of Molecular Sciences* [online]. 14 (11), pp.22067-22081.

Mo, Z.Y., Zhu, Y.Z., Zhu, H.L., Fan, J.B., Chen, J. and Liang, Y. (2009) Low micromolar zinc accelerates the fibrillization of human tau via bridging of Cys-291 and Cys-322. *The Journal of Biological Chemistry* [online]. 284 (50), pp.34648-34657.

Mo, Z.Y., Zhu, Y.Z., Zhu, H.L., Fan, J.B., Chen, J. and Liang, Y. (2009) Low micromolar zinc accelerates the fibrillization of human tau via bridging of Cys-291 and Cys-322. *The Journal of Biological Chemistry* [online]. 284 (50), pp.34648-34657.

Moos, R.H., Schutte, K.K., Brennan, P.L. and Moos, B.S. (2009) Older adults' alcohol consumption and late-life drinking problems: a 20-year perspective. *Addiction (Abingdon, England)* [online]. 104 (8), pp.1293-1302.

Morello, M., Canini, A., Mattioli, P., Sorge, R.P., Alimonti, A., Bocca, B., Forte, G., Martorana, A., Bernardi, G. and Sancesario, G. (2008) Sub-cellular localization of manganese in the basal ganglia of normal and manganese-treated rats An electron spectroscopy imaging and electron energy-loss spectroscopy study. *Neurotoxicology* [online]. 29 (1), pp.60-72.

Morris, D.R. and Levenson, C.W. (2017) Neurotoxicity of Zinc. *Advances in Neurobiology* [online]. 18 pp.303-312.

Moselhy, H.F., Georgiou, G. and Kahn, A. (2001) Frontal lobe changes in alcoholism: a review of the literature. *Alcohol and Alcoholism (Oxford, Oxfordshire)* [online]. 36 (5), pp.357-368.

Munoz, G., Urrutia, J.C., Burgos, C.F., Silva, V., Aguilar, F., Sama, M., Yeh, H.H., Opazo, C. and Aguayo, L.G. (2015) Low concentrations of ethanol protect against synaptotoxicity induced by Abeta in hippocampal neurons. *Neurobiology of Aging* [online]. 36 (2), pp.845-856.

Nassir, F. and Ibdah, J.A. (2014) Role of mitochondria in alcoholic liver disease. *World Journal of Gastroenterology* [online]. 20 (9), pp.2136-2142.

Navarro, A. and Boveris, A. (2007) The mitochondrial energy transduction system and the aging process. *American Journal of Physiology.Cell Physiology* [online]. 292 (2), pp.C670-86.

Neal, A.P. and Guilarte, T.R. (2013) Mechanisms of lead and manganese neurotoxicity. *Toxicology Research* [online]. 2 (2), pp.99-114.

Neasta, J., Ben Hamida, S., Yowell, Q., Carnicella, S. and Ron, D. (2010) Role for mammalian target of rapamycin complex 1 signaling in neuroadaptations underlying alcohol-related disorders. *Proceedings of the National Academy of Sciences of the United States of America* [online]. 107 (46), pp.20093-20098.

Neugroschl, J. and Wang, S. (2011) Alzheimer's disease: diagnosis and treatment across the spectrum of disease severity. *The Mount Sinai Journal of Medicine, New York* [online]. 78 (4), pp.596-612.

Neznanova, O., BjÃ¶rk, K., Rimondini, R., Hansson, A.C., HyytiÃ¤, P., Heilig, M. and Sommer, W.H. (2009) Acute ethanol challenge inhibits glycogen synthase kinase-3beta in the rat prefrontal cortex. *The International Journal of Neuropsychopharmacology* [online]. 12 (2), pp.275-280.

Nie, C.L., Wang, X.S., Liu, Y., Perrett, S. and He, R.Q. (2007) Amyloid-like aggregates of neuronal tau induced by formaldehyde promote apoptosis of neuronal cells. *BMC Neuroscience* [online]. 8 pp.9-2202-8-9. eCollection 2007.

Nimmanon, T., Ziliotto, S., Morris, S., Flanagan, L. and Taylor, K.M. (2017) Phosphorylation of zinc channel ZIP7 drives MAPK, PI3K and mTOR growth and proliferation signalling. *Metallomics : Integrated Biometal Science* [online]. 9 (5), pp.471-481.

Nixon, R.A., Wegiel, J., Kumar, A., Yu, W.H., Peterhoff, C., Cataldo, A. and Cuervo, A.M. (2005) Extensive involvement of autophagy in Alzheimer disease: an immuno-electron microscopy study. *Journal of Neuropathology and Experimental Neurology* [online]. 64 (2), pp.113-122.

Noh, K.M. and Koh, J.Y. (2000) Induction and activation by zinc of NADPH oxidase in cultured cortical neurons and astrocytes. *The Journal of Neuroscience : The Official Journal of the Society for Neuroscience* [online]. 20 (23), pp.RC111.

Nowoslawski, L., Klocke, B.J. and Roth, K.A. (2005) Molecular regulation of acute ethanol-induced neuron apoptosis. *Journal of Neuropathology and Experimental Neurology* [online]. 64 (6), pp.490-497.

Nuttall, J.R. and Oteiza, P.I. (2012) Zinc and the ERK kinases in the developing brain. *Neurotoxicity Research* [online]. 21 (1), pp.128-141.

Ogita, S. and Lorusso, P. (2011) Targeting phosphatidylinositol 3 kinase (PI3K)-Akt beyond rapalogs. *Targeted Oncology* [online]. 6 (2), pp.103-117.

Okatsu, K., Saisho, K., Shimanuki, M., Nakada, K., Shitara, H., Sou, Y.S., Kimura, M., Sato, S., Hattori, N., Komatsu, M., Tanaka, K. and Matsuda, N. (2010) p62/SQSTM1 cooperates with Parkin for perinuclear clustering of depolarized mitochondria. *Genes to Cells : Devoted to Molecular & Cellular Mechanisms* [online]. 15 (8), pp.887-900.

Omata, Y., Salvador, G.A., Supasai, S., Keenan, A.H. and Oteiza, P.I. (2013) Decreased zinc availability affects glutathione metabolism in neuronal cells and in the developing brain. *Toxicological Sciences : An Official Journal of the Society of Toxicology* [online]. 133 (1), pp.90-100.

Onyango, I.G., Dennis, J. and Khan, S.M. (2016) Mitochondrial Dysfunction in Alzheimer's Disease and the Rationale for Bioenergetics Based Therapies. *Aging and Disease* [online]. 7 (2), pp.201-214.

Ormeno, D., Romero, F., Lopez-Fenner, J., Avila, A., Martinez-Torres, A. and Parodi, J. (2013) Ethanol reduces amyloid aggregation in vitro and prevents toxicity in cell lines. *Archives of Medical Research* [online]. 44 (1), pp.1-7.

Orr, M.E. and Oddo, S. (2013) Autophagic/lysosomal dysfunction in Alzheimer's disease. *Alzheimer's Research & Therapy* [online]. 5 (5), pp.53.

Pandya, C.D., Howell, K.R. and Pillai, A. (2013) Antioxidants as potential therapeutics for neuropsychiatric disorders. *Progress in Neuro-Psychopharmacology & Biological Psychiatry* [online]. 46 pp.214-223.

Park, J.S., Koentjoro, B., Veivers, D., Mackay-Sim, A. and Sue, C.M. (2014) Parkinson's disease-associated human ATP13A2 (PARK9) deficiency causes zinc dyshomeostasis and mitochondrial dysfunction. *Human Molecular Genetics* [online]. 23 (11), pp.2802-2815.

Park, M.H., Lee, S.J., Byun, H.R., Kim, Y., Oh, Y.J., Koh, J.Y. and Hwang, J.J. (2011) Clioquinol induces autophagy in cultured astrocytes and neurons by acting as a zinc ionophore. *Neurobiology of Disease* [online]. 42 (3), pp.242-251.

Parone, P.A., James, D. and Martinou, J.C. (2002) Mitochondria: regulating the inevitable. *Biochimie* [online]. 84 (2-3), pp.105-111.

Perea, J.R., Llorens-MartÃn, M., Ã• vila, J. and BolÃ³s, M. (2018) The Role of Microglia in the Spread of Tau: Relevance for Tauopathies. *Frontiers in Cellular Neuroscience* [online]. 12 pp.172.

Peres, T.V., Pedro, D.Z., de Cordova, F.M., Lopes, M.W., Goncalves, F.M., Mendes-de-Aguiar, C.B., Walz, R., Farina, M., Aschner, M. and Leal, R.B. (2013) In vitro manganese exposure disrupts MAPK signaling pathways in striatal and hippocampal slices from immature rats. *BioMed Research International* [online]. 2013 pp.769295.

Peres, T.V., Schettinger, M.R., Chen, P., Carvalho, F., Avila, D.S., Bowman, A.B. and Aschner, M. (2016) "Manganese-induced neurotoxicity: a review of its behavioral consequences and neuroprotective strategies". *BMC Pharmacology & Toxicology* [online]. 17 (1), pp.57-016-0099-0.

Pfaender, S., FÃ¶hr, K., Lutz, A.K., Putz, S., Achberger, K., Linta, L., Liebau, S., Boeckers, T.M. and Grabrucker, A.M. (2016) Cellular Zinc Homeostasis Contributes to Neuronal Differentiation in Human Induced Pluripotent Stem Cells. *Neural Plasticity* [online]. 2016 pp.3760702.

Pi, H., Xu, S., Zhang, L., Guo, P., Li, Y., Xie, J., Tian, L., He, M., Lu, Y., Li, M., Zhang, Y., Zhong, M., Xiang, Y., Deng, L., Zhou, Z. and Yu, Z. (2013) Dynamin 1-like-dependent mitochondrial fission initiates overactive mitophagy in the hepatotoxicity of cadmium. *Autophagy* [online]. 9 (11), pp.1780-1800.

Piazza-Gardner, A.K., Gaffud, T.J. and Barry, A.E. (2013) The impact of alcohol on Alzheimer's disease: a systematic review. *Aging & Mental Health* [online]. 17 (2), pp.133-146.

Pinsino, A., Roccheri, M.C., Costa, C. and Matranga, V. (2011) Manganese interferes with calcium, perturbs ERK signaling, and produces embryos with no skeleton. *Toxicological Sciences : An Official Journal of the Society of Toxicology* [online]. 123 (1), pp.217-230.

Pirscoveanu, D.F.V., Pirici, I., Tudorica, V., Balseanu, T.A., Albu, V.C., Bondari, S., Bumbea, A.M. and Pirscoveanu, M. (2017) Tau protein in neurodegenerative diseases - a review. *Romanian Journal of Morphology and*

Embryology = Revue Roumaine De Morphologie Et Embryologie [online]. 58 (4), pp.1141-1150.

Pitel, A.L., Chetelat, G., Le Berre, A.P., Desgranges, B., Eustache, F. and Beaunieux, H. (2012) Macrostructural abnormalities in Korsakoff syndrome compared with uncomplicated alcoholism. *Neurology* [online]. 78 (17), pp.1330-1333.

Pivovarova, N.B., Stanika, R.I., Kazanina, G., Villanueva, I. and Andrews, S.B. (2014) The interactive roles of zinc and calcium in mitochondrial dysfunction and neurodegeneration. *Journal of Neurochemistry* [online]. 128 (4), pp.592-602.

Powell, S.R. (2000) The antioxidant properties of zinc. *The Journal of Nutrition* [online]. 130 (5S Suppl), pp.1447S-54S.

Prabhakaran, K., Ghosh, D., Chapman, G.D. and Gunasekar, P.G. (2008) Molecular mechanism of manganese exposure-induced dopaminergic toxicity. *Brain Research Bulletin* [online]. 76 (4), pp.361-367.

Prabhakaran, K., Chapman, G. D. and Gunasekar, P. G. (2009) BNIP3 up-regulation and mitochondrial dysfunction in manganese-induced neurotoxicity. *Neurotoxicology* [online]. 30(3), pp. 414-422.

Prakash, A., Dhaliwal, G.K., Kumar, P. and Majeed, A.B. (2017) Brain biometals and Alzheimer's disease - boon or bane? *The International Journal of Neuroscience* [online]. 127 (2), pp.99-108.

Puli, S., Lai, J.C., Edgley, K.L., Daniels, C.K. and Bhushan, A. (2006) Signaling pathways mediating manganese-induced toxicity in human glioblastoma cells (u87). *Neurochemical Research* [online]. 31 (10), pp.1211-1218.

Qi, X., Disatnik, M.H., Shen, N., Sobel, R.A. and Mochly-Rosen, D. (2011) Aberrant mitochondrial fission in neurons induced by protein kinase CÎ´ under oxidative stress conditions in vivo. *Molecular Biology of the Cell* [online]. 22 (2), pp.256-265.

Quintanar, L. (2008) Manganese neurotoxicity: A bioinorganic chemist's perspective. *Inorganica Chimica Acta* [online]. 361(4), pp. 875-884.

Quintanilla, R.,A., Jin, Y.,N., von Bernhardi, ,Rommy and Johnson, G.,V.W.Mitochondrial permeability transition pore induces mitochondria injury in Huntington disease. [online].

Rademakers, R., Cruts, M. and van Broeckhoven, C. (2004) The role of tau (MAPT) in frontotemporal dementia and related tauopathies. *Human Mutation* [online]. 24 (4), pp.277-295.

Rama Rao, K.V., Reddy, P.V., Hazell, A.S. and Norenberg, M.D. (2007) Manganese induces cell swelling in cultured astrocytes. *Neurotoxicology* [online]. 28 (4), pp.807-812.

Ramezani, A., Goudarzi, I., Lashkarboluki, T., Ghorbanian, M.T., Abrari, K. and Elahdadi Salmani, M. (2012) Role of Oxidative Stress in Ethanol-induced Neurotoxicity in the Developing Cerebellum. *Iranian Journal of Basic Medical Sciences* [online]. 15 (4), pp.965-974.

Ramlochansingh, C., Taylor, R.E. and Tizabi, Y. (2011) Toxic effects of low alcohol and nicotine combinations in SH-SY5Y cells are apoptotically mediated. *Neurotoxicity Research* [online]. 20 (3), pp.263-269.

Ramos, P., Santos, A., Pinto, N.R., Mendes, R., Magalhaes, T. and Almeida, A. (2014) Anatomical region differences and age-related changes in copper, zinc, and manganese levels in the human brain. *Biological Trace Element Research* [online]. 161 (2), pp.190-201.

Rao, K.V. and Norenberg, M.D. (2004) Manganese induces the mitochondrial permeability transition in cultured astrocytes. *The Journal of Biological Chemistry* [online]. 279 (31), pp.32333-32338.

Ravingerova, T., Barancik, M. and Strniskova, M. (2003) Mitogen-activated protein kinases: a new therapeutic target in cardiac pathology. *Molecular and Cellular Biochemistry* [online]. 247 (1-2), pp.127-138.

Rebrin, I., Forster, M.J. and Sohal, R.S. (2007) Effects of age and caloric intake on glutathione redox state in different brain regions of C57BL/6 and DBA/2 mice. *Brain Research* [online]. 1127 (1), pp.10-18.

Reddy, V.D., Padmavathi, P., Kavitha, G., Saradamma, B. and Varadacharyulu, N. (2013) Alcohol-induced oxidative/nitrosative stress alters brain mitochondrial membrane properties. *Molecular and Cellular Biochemistry* [online]. 375 (1-2), pp.39-47.

Redpath, C.J., Bou Khalil, M., Drozdzal, G., Radisic, M. and McBride, H.M. (2013) Mitochondrial Hyperfusion during Oxidative Stress Is Coupled to a Dysregulation in Calcium Handling within a C2C12 Cell Model. *Plos One* [online]. 8 (7), pp.e69165. doi:10.1371/journal.pone.0069165.

Rehm, J., Hasan, O.S.M., Black, S.E., Shield, K.D. and Schwarzinger, M. (2019) Alcohol use and dementia: a systematic scoping review. *Alzheimer's Research & Therapy* [online]. 11 (1), pp.1-018-0453-0.

Religa, D., Strozyk, D., Cherny, R.A., Volitakis, I., Haroutunian, V., Winblad, B., Naslund, J. and Bush, A.I. (2006) Elevated cortical zinc in Alzheimer disease. *Neurology* [online]. 67 (1), pp.69-75.

Ren, X., Zou, L., Zhang, X., Branco, V., Wang, J., Carvalho, C., Holmgren, A. and Lu, J. (2017) Redox Signaling Mediated by Thioredoxin and Glutathione

Systems in the Central Nervous System. *Antioxidants & Redox Signaling* [online]. 27 (13), pp.989-1010.

Roberson, E.D., Scearce-Levie, K., Palop, J.J., Yan, F., Cheng, I.H., Wu, T., Gerstein, H., Yu, G.Q. and Mucke, L. (2007) Reducing endogenous tau ameliorates amyloid beta-induced deficits in an Alzheimer's disease mouse model. *Science (New York, N.Y.)* [online]. 316 (5825), pp.750-754.

Robert, J., Button, E.B., Yuen, B., Gilmour, M., Kang, K., Bahrabadi, A., Stukas, S., Zhao, W., Kulic, I. and Wellington, C.L. (2017) Clearance of beta-amyloid is facilitated by apolipoprotein E and circulating high-density lipoproteins in bioengineered human vessels. *Elife* [online]. 6 pp.10.7554/eLife.29595.

Rojo, A.I., Innamorato, N.G., Martin-Moreno, A.M., De Ceballos, M.L., Yamamoto, M. and Cuadrado, A. (2010) Nrf2 regulates microglial dynamics and neuroinflammation in experimental Parkinson's disease. *Glia* [online]. 58 (5), pp.588-598.

Ron, D. and Messing, R.O. (2013) Signaling pathways mediating alcohol effects. *Current Topics in Behavioral Neurosciences* [online]. 13 pp.87-126.

Ronowska, A., Dys, A., Jankowska-Kulawy, A., Klimaszewska-Lata, J., Bielarczyk, H., Romianowski, P., Pawelczyk, T. and Szutowicz, A. (2010) Short-term effects of zinc on acetylcholine metabolism and viability of SN56 cholinergic neuroblastoma cells. *Neurochemistry International* [online]. 56 (1), pp.143-151.

Ronowska, A., Gul-Hinc, S., Bielarczyk, H., Pawelczyk, T. and Szutowicz, A. (2007) Effects of zinc on SN56 cholinergic neuroblastoma cells. *Journal of Neurochemistry* [online]. 103 (3), pp.972-983.

Roth, J.A., Horbinski, C., Higgins, D., Lein, P. and Garrick, M.D. (2002) Mechanisms of manganese-induced rat pheochromocytoma (PC12) cell death and cell differentiation. *Neurotoxicology* [online]. 23 (2), pp.147-157.

Rudolf, E. and Rudolf, K. (2017) Increases in Intracellular Zinc Enhance Proliferative Signaling as well as Mitochondrial and Endolysosomal Activity in Human Melanocytes. *Cellular Physiology and Biochemistry : International Journal of Experimental Cellular Physiology, Biochemistry, and Pharmacology* [online]. 43 (1), pp.1-16.

Sadli, N., Barrow, C.J., McGee, S. and Suphioglu, C. (2013) Effect of DHA and coenzymeQ10 against Abeta- and zinc-induced mitochondrial dysfunction in human neuronal cells. *Cellular Physiology and Biochemistry : International Journal of Experimental Cellular Physiology, Biochemistry, and Pharmacology* [online]. 32 (2), pp.243-252.

Sahani, M.H., Itakura, E. and Mizushima, N. (2014) Expression of the autophagy substrate SQSTM1/p62 is restored during prolonged starvation

depending on transcriptional upregulation and autophagy-derived amino acids. *Autophagy* [online]. 10 (3), pp.431-441.

Saito, M., Chakraborty, G., Mao, R.F., Paik, S.M., Vadasz, C. and Saito, M. (2010) Tau phosphorylation and cleavage in ethanol-induced neurodegeneration in the developing mouse brain. *Neurochemical Research* [online]. 35 (4), pp.651-659.

Salgueiro, M.J., Zubillaga, M.B., Lysionek, A.E., Caro, R.A., Weill, R. and Boccio, J.R. (2002) The role of zinc in the growth and development of children. *Nutrition (Burbank, Los Angeles County, Calif.)* [online]. 18 (6), pp.510-519.

Sanna, P.P., Simpson, C., Lutjens, R. and Koob, G. (2002) ERK regulation in chronic ethanol exposure and withdrawal. *Brain Research* [online]. 948 (1-2), pp.186-191.

Sarkar, S., Rokad, D., Malovic, E., Luo, J., Harischandra, D.S., Jin, H., Anantharam, V., Huang, X., Lewis, M., Kanthasamy, A. and Kanthasamy, A.G. (2019) Manganese activates NLRP3 inflammasome signaling and propagates exosomal release of ASC in microglial cells. *Science Signaling* [online]. 12 (563), pp.10.1126/scisignal.aat9900.

Sarkar, S., Malovic, E., Harischandra, D. S., Ngwa, H. A., Ghosh, A., Hogan, C., Rokad, D., Zenitsky, G., Jin, H., Anantharam, V., Kanthasamy, A. G. and Kanthasamy, A. (2018) Manganese exposure induces neuroinflammation by impairing mitochondrial dynamics in astrocytes. *Neurotoxicology* [online]. 64pp. 204-218.

Schinzel, A.C., Takeuchi, O., Huang, Z., Fisher, J.K., Zhou, Z., Rubens, J., Hetz, C., Danial, N.N., Moskowitz, M.A. and Korsmeyer, S.J. (2005) Cyclophilin D is a component of mitochondrial permeability transition and mediates neuronal cell death after focal cerebral ischemia. *Proceedings of the National Academy of Sciences of the United States of America* [online]. 102 (34), pp.12005-12010.

Schneider, J.S., Williams, C., Ault, M. and Guilarte, T.R. (2013) Chronic manganese exposure impairs visuospatial associative learning in non-human primates. *Toxicology Letters* [online]. 221 (2), pp.146-151.

Schonheit, B., Zarski, R. and Ohm, T.G. (2004) Spatial and temporal relationships between plaques and tangles in Alzheimer-pathology. *Neurobiology of Aging* [online]. 25 (6), pp.697-711.

Sensi, S.L., Paoletti, P., Koh, J.Y., Aizenman, E., Bush, A.I. and Hershfinkel, M. (2011) The neurophysiology and pathology of brain zinc. *The Journal of Neuroscience : The Official Journal of the Society for Neuroscience* [online]. 31 (45), pp.16076-16085.

Sensi, S.L., Ton-That, D., Sullivan, P.G., Jonas, E.A., Gee, K.R., Kaczmarek, L.K. and Weiss, J.H. (2003) Modulation of mitochondrial function by

endogenous Zn2+ pools. *Proceedings of the National Academy of Sciences of the United States of America* [online]. 100 (10), pp.6157-6162.

Sensi, S.L., Yin, H.Z., Carriedo, S.G., Rao, S.S. and Weiss, J.H. (1999) Preferential Zn2+ influx through Ca2+-permeable AMPA/kainate channels triggers prolonged mitochondrial superoxide production. *Proceedings of the National Academy of Sciences of the United States of America* [online]. 96 (5), pp.2414-2419.

Sensi, S.L., Yin, H.Z. and Weiss, J.H. (2000) AMPA/kainate receptor-triggered Zn2+ entry into cortical neurons induces mitochondrial Zn2+ uptake and persistent mitochondrial dysfunction. *The European Journal of Neuroscience* [online]. 12 (10), pp.3813-3818.

Seo, S.R., Chong, S.A., Lee, S.I., Sung, J.Y., Ahn, Y.S., Chung, K.C. and Seo, J.T. (2001) Zn2+-induced ERK activation mediated by reactive oxygen species causes cell death in differentiated PC12 cells. *Journal of Neurochemistry* [online]. 78 (3), pp.600-610.

Shafei, M.A., Harris, M. and Conway, M.E. (2017) Divergent Metabolic Regulation of Autophagy and mTORC1-Early Events in Alzheimer's Disease? *Frontiers in Aging Neuroscience* [online]. 9 pp.173.

Shalbueva, N., Mareninova, O.A., Gerloff, A., Yuan, J., Waldron, R.T., Pandol, S.J. and Gukovskaya, A.S. (2013) Effects of oxidative alcohol metabolism on the mitochondrial permeability transition pore and necrosis in a mouse model of alcoholic pancreatitis. *Gastroenterology* [online]. 144 (2), pp.437-446.e6.

Shamas-Din, A., Kale, J., Leber, B. and Andrews, D.W. (2013) Mechanisms of Action of Bcl-2 Family Proteins. *Cold Spring Harbor Perspectives in Biology* [online]. 5 (4), pp.a008714. doi:10.1101/cshperspect.a008714.

Sharma, A.K., Pavlova, S.T., Kim, J., Kim, J. and Mirica, L.M. (2013) The effect of Cu(2+) and Zn(2+) on the Abeta42 peptide aggregation and cellular toxicity. *Metallomics : Integrated Biometal Science* [online]. 5 (11), pp.1529-1536.

Shi, ,Qinghua, Zhu, ,Zhujun, Xu, ,Min, Qian, ,Qiongqiu and Yu, ,Jingquan [online].

Shi, Y., Yamada, K., Liddelow, S.A., Smith, S.T., Zhao, L., Luo, W., Tsai, R.M., Spina, S., Grinberg, L.T., Rojas, J.C., Gallardo, G., Wang, K., Roh, J., Robinson, G., Finn, M.B., Jiang, H., Sullivan, P.M., Baufeld, C., Wood, M.W., Sutphen, C., McCue, L., Xiong, C., Del-Aguila, J.L., Morris, J.C., Cruchaga, C., Alzheimer's Disease Neuroimaging Initiative, Fagan, A.M., Miller, B.L., Boxer, A.L., Seeley, W.W., Butovsky, O., Barres, B.A., Paul, S.M. and Holtzman, D.M. (2017) ApoE4 markedly exacerbates tau-mediated neurodegeneration in a mouse model of tauopathy. *Nature* [online]. 549 (7673), pp.523-527.

Shirihai, O.S., Song, M. and Dorn, G.W.,2nd (2015) How mitochondrial dynamism orchestrates mitophagy. *Circulation Research* [online]. 116 (11), pp.1835-1849.

Singh, M., Gupta, S., Singhal, U., Pandey, R. and Aggarwal, S. (2013) Evaluation of the Oxidative Stress in Chronic Alcoholics. *Journal of Clinical and Diagnostic Research : JCDR* [online]. 7 (8), pp.1568-1571.

Smith, M. R., Fernandes, J., Go, Y. and Jones, D. P. (2017) Redox dynamics of manganese as a mitochondrial life-death switch. *Biochemical and Biophysical Research Communications* [online]. 482(3), pp. 388-398.

Solfrizzi, V., D'Introno, A., Colacicco, A.M., Capurso, C., Del Parigi, A., Baldassarre, G., Scapicchio, P., Scafato, E., Amodio, M., Capurso, A., Panza, F. and Italian Longitudinal Study on Aging Working Group (2007) Alcohol consumption, mild cognitive impairment, and progression to dementia. *Neurology* [online]. 68 (21), pp.1790-1799.

Srivastava, V.K., Hiney, J.K. and Dees, W.L. (2016) Manganese-Stimulated Kisspeptin Is Mediated by the IGF-1/Akt/Mammalian Target of Rapamycin Pathway in the Prepubertal Female Rat. *Endocrinology* [online]. 157 (8), pp.3233-3241.

Stelmashook, E.V., Isaev, N.K., Genrikhs, E.E., Amelkina, G.A., Khaspekov, L.G., Skrebitsky, V.G. and Illarioshkin, S.N. (2014) Role of zinc and copper ions in the pathogenetic mechanisms of Alzheimer's and Parkinson's diseases. *Biochemistry.Biokhimiia* [online]. 79 (5), pp.391-396.

Stott, D.J., Falconer, A., Kerr, G.D., Murray, H.M., Trompet, S., Westendorp, R.G., Buckley, B., de Craen, A.J., Sattar, N. and Ford, I. (2008) Does low to moderate alcohol intake protect against cognitive decline in older people? *Journal of the American Geriatrics Society* [online]. 56 (12), pp.2217-2224.

Strozyk, D., Launer, L.J., Adlard, P.A., Cherny, R.A., Tsatsanis, A., Volitakis, I., Blennow, K., Petrovitch, H., White, L.R. and Bush, A.I. (2009) Zinc and copper modulate Alzheimer Abeta levels in human cerebrospinal fluid. *Neurobiology of Aging* [online]. 30 (7), pp.1069-1077.

Suen, D.F., Norris, K.L. and Youle, R.J. (2008) Mitochondrial dynamics and apoptosis. *Genes & Development* [online]. 22 (12), pp.1577-1590.

Swerdlow, R.H., Burns, J.M. and Khan, S.M. (2014) The Alzheimer's disease mitochondrial cascade hypothesis: progress and perspectives. *Biochimica Et Biophysica Acta* [online]. 1842 (8), pp.1219-1231.

Szabo, A., Sumegi, K., Fekete, K., Hocsak, E., Debreceni, B., Setalo, G., Kovacs, K., Deres, L., Kengyel, A., Kovacs, D., Mandl, J., Nyitrai, M., Febbraio, M. A., Gallyas, F. and Sumegi, B. (2018) Activation of mitochondrial fusion provides a new treatment for mitochondria-related diseases. *Biochemical Pharmacology* [online]. 150pp. 86-96.

Szewczyk, B., Pochwat, B., Rafalo, A., Palucha-Poniewiera, A., Domin, H. and Nowak, G. (2015) Activation of mTOR dependent signaling pathway is a necessary mechanism of antidepressant-like activity of zinc. *Neuropharmacology* [online]. 99 pp.517-526.

Szpetnar, ,Maria, Luchowska-Kocot, ,Dorota, Boguszewska-Czubara, ,Anna and Kurzepa, ,JacekThe Influence of Manganese and Glutamine Intake on Antioxidants and Neurotransmitter Amino Acids Levels in Ratsâ€™ Brain. [online].

Szutowicz, A., Bielarczyk, H., Zysk, M., Dys, A., Ronowska, A., Gul-Hinc, S. and Klimaszewska-Lata, J. (2017) Early and Late Pathomechanisms in Alzheimer's Disease: From Zinc to Amyloid-beta Neurotoxicity. *Neurochemical Research* [online]. 42 (3), pp.891-904.

Taglialatela, G., Rastellini, C. and Cicalese, L. (2015) Reduced Incidence of Dementia in Solid Organ Transplant Patients Treated with Calcineurin Inhibitors. *Journal of Alzheimer's Disease : JAD* [online]. 47 (2), pp.329-333.

Takahashi, M., Miyata, H., Kametani, F., Nonaka, T., Akiyama, H., Hisanaga, S. and Hasegawa, M. (2015) Extracellular association of APP and tau fibrils induces intracellular aggregate formation of tau. *Acta Neuropathologica* [online]. 129 (6), pp.895-907.

Takeda, A. (2001) Zinc homeostasis and functions of zinc in the brain. *Biometals : An International Journal on the Role of Metal Ions in Biology, Biochemistry, and Medicine* [online]. 14 (3-4), pp.343-351.

Takeda, A., Tamano, H., Imano, S. and Oku, N. (2010) Increases in extracellular zinc in the amygdala in acquisition and recall of fear experience and their roles in response to fear. *Neuroscience* [online]. 168(3), pp. 715-722.

Tamayev, R., Matsuda, S., Arancio, O. and D'Adamio, L. (2012) beta- but not gamma-secretase proteolysis of APP causes synaptic and memory deficits in a mouse model of dementia. *EMBO Molecular Medicine* [online]. 4 (3), pp.171-179.

Tamm, C., Sabri, F. and Ceccatelli, S. (2008) Mitochondrial-mediated apoptosis in neural stem cells exposed to manganese. *Toxicological Sciences : An Official Journal of the Society of Toxicology* [online]. 101 (2), pp.310-320.

Taniguchi, M., Fukunaka, A., Hagihara, M., Watanabe, K., Kamino, S., Kambe, T., Enomoto, S. and Hiromura, M. (2013) Essential role of the zinc transporter ZIP9/SLC39A9 in regulating the activations of Akt and Erk in B-cell receptor signaling pathway in DT40 cells. *PloS One* [online]. 8 (3), pp.e58022.

Taylor, K.M., Vichova, P., Jordan, N., Hiscox, S., Hendley, R. and Nicholson, R.I. (2008) ZIP7-mediated intracellular zinc transport contributes to aberrant growth factor signaling in antihormone-resistant breast cancer Cells. *Endocrinology* [online]. 149 (10), pp.4912-4920.

Tilokani, L., Nagashima, S., Paupe, V. and Prudent, J. (2018) Mitochondrial dynamics: overview of molecular mechanisms. *Essays in Biochemistry* [online]. 62 (3), pp.341-360.

Tilokani, L., Nagashima, S., Paupe, V. and Prudent, J. (2018) Mitochondrial dynamics: overview of molecular mechanisms. *Essays in Biochemistry* [online]. 62 (3), pp.341-360.

Tilokani, L., Nagashima, S., Paupe, V. and Prudent, J. (2018) Mitochondrial dynamics: overview of molecular mechanisms. *Essays in Biochemistry* [online]. 62 (3), pp.341-360.

Tong, Y., Yang, H., Tian, X., Wang, H., Zhou, T., Zhang, S., Yu, J., Zhang, T., Fan, D., Guo, X., Tabira, T., Kong, F., Chen, Z., Xiao, W. and Chui, D. (2014) High manganese, a risk for Alzheimer's disease: high manganese induces amyloid-beta related cognitive impairment. *Journal of Alzheimer's Disease : JAD* [online]. 42 (3), pp.865-878.

Topiwala, A. and Ebmeier, K.P. (2018) Effects of drinking on late-life brain and cognition. *Evidence-Based Mental Health* [online]. 21 (1), pp.12-15.

Trachootham, D., Lu, W., Ogasawara, M.A., Nilsa, R.D. and Huang, P. (2008) Redox regulation of cell survival. *Antioxidants & Redox Signaling* [online]. 10 (8), pp.1343-1374.

Tsujimoto, Y. and Shimizu, S. (2007) Role of the mitochondrial membrane permeability transition in cell death. *Apoptosis : An International Journal on Programmed Cell Death* [online]. 12 (5), pp.835-840.

Ulland, T.K., Song, W.M., Huang, S.C., Ulrich, J.D., Sergushichev, A., Beatty, W.L., Loboda, A.A., Zhou, Y., Cairns, N.J., Kambal, A., Loginicheva, E., Gilfillan, S., Cella, M., Virgin, H.W., Unanue, E.R., Wang, Y., Artyomov, M.N., Holtzman, D.M. and Colonna, M. (2017) TREM2 Maintains Microglial Metabolic Fitness in Alzheimer's Disease. *Cell* [online]. 170 (4), pp.649-663.e13.

Uo, T., Dworzak, J., Kinoshita, C., Inman, D.M., Kinoshita, Y., Horner, P.J. and Morrison, R.S. (2009) Drp1 levels constitutively regulate mitochondrial dynamics and cell survival in cortical neurons. *Experimental Neurology* [online]. 218 (2), pp.274-285.

Venkataraman, A., Kalk, N., Sewell, G., Ritchie, C.W. and Lingford-Hughes, A. (2017) Alcohol and Alzheimer's Disease-Does Alcohol Dependence Contribute to Beta-Amyloid Deposition, Neuroinflammation and Neurodegeneration in Alzheimer's Disease? *Alcohol and Alcoholism (Oxford, Oxfordshire)* [online]. 52 (2), pp.151-158.

Vernay, M., Balkau, B., Moreau, J., Sigalas, J., Chesnier, M., Ducimetiere, P. and the Desir Study Group, (2004) Alcohol consumption and insulin resistance syndrome parameters: associations and evolutions in a longitudinal analysis

of the French DESIR cohort. *Annals of Epidemiology* [online]. 14(3), pp. 209-214.

Vogt, B.L. and Richie, J.P.,Jr (2007) Glutathione depletion and recovery after acute ethanol administration in the aging mouse. *Biochemical Pharmacology* [online]. 73 (10), pp.1613-1621.

Volkow, N.D., Kim, S.W., Wang, G.J., Alexoff, D., Logan, J., Muench, L., Shea, C., Telang, F., Fowler, J.S., Wong, C., Benveniste, H. and Tomasi, D. (2013) Acute alcohol intoxication decreases glucose metabolism but increases acetate uptake in the human brain. *Neuroimage* [online]. 64 pp.277-283.

WÃ¤tjen, W., Haase, H., Biagioli, M. and Beyersmann, D. (2002) Induction of apoptosis in mammalian cells by cadmium and zinc. *Environmental Health Perspectives* [online]. 110 (Suppl 5), pp.865-867.

Wallin, C., Kulkarni, Y.S., Abelein, A., Jarvet, J., Liao, Q., Strodel, B., Olsson, L., Luo, J., Abrahams, J.P., Sholts, S.B., Roos, P.M., Kamerlin, S.C., Graslund, A. and Warmlander, S.K. (2016) Characterization of Mn(II) ion binding to the amyloid-beta peptide in Alzheimer's disease. *Journal of Trace Elements in Medicine and Biology : Organ of the Society for Minerals and Trace Elements (GMS)* [online]. 38 pp.183-193.

Wallner, M. and Olsen, R.W. (2008) Physiology and pharmacology of alcohol: the imidazobenzodiazepine alcohol antagonist site on subtypes of GABAA receptors as an opportunity for drug development? *British Journal of Pharmacology* [online]. 154 (2), pp.288-298.

Wan, C., Ma, X., Shi, S., Zhao, J., Nie, X., Han, J., Xiao, J., Wang, X., Jiang, S. and Jiang, J. (2014) Pivotal roles of p53 transcription-dependent and -independent pathways in manganese-induced mitochondrial dysfunction and neuronal apoptosis. *Toxicology and Applied Pharmacology* [online]. 281 (3), pp.294-302.

Wang, D., Zhang, J., Jiang, W., Cao, Z., Zhao, F., Cai, T., Aschner, M. and Luo, W. (2017) The role of NLRP3-CASP1 in inflammasome-mediated neuroinflammation and autophagy dysfunction in manganese-induced, hippocampal-dependent impairment of learning and memory ability. *Autophagy* [online]. 13 (5), pp.914-927.

Wang, D., Zhang, J., Jiang, W., Cao, Z., Zhao, F., Cai, T., Aschner, M. and Luo, W. (2017) The role of NLRP3-CASP1 in inflammasome-mediated neuroinflammation and autophagy dysfunction in manganese-induced, hippocampal-dependent impairment of learning and memory ability. *Autophagy* [online]. 13 (5), pp.914-927.

Wang, H., Lim, P.J., Karbowski, M. and Monteiro, M.J. (2009) Effects of overexpression of huntingtin proteins on mitochondrial integrity. *Human Molecular Genetics* [online]. 18 (4), pp.737-752.

Wang, T., Li, X., Yang, D., Zhang, H., Zhao, P., Fu, J., Yao, B. and Zhou, Z. (2015) ER stress and ER stress-mediated apoptosis are involved in manganese-induced neurotoxicity in the rat striatum in vivo. *Neurotoxicology* [online]. 48 pp.109-119.

Wei, Y., Pattingre, S., Sinha, S., Bassik, M. and Levine, B. (2008) JNK1-mediated phosphorylation of Bcl-2 regulates starvation-induced autophagy. *Molecular Cell* [online]. 30 (6), pp.678-688.

Wei, Y., Sinha, S. and Levine, B. (2008) Dual role of JNK1-mediated phosphorylation of Bcl-2 in autophagy and apoptosis regulation. *Autophagy* [online]. 4 (7), pp.949-951.

Weiss, B. (2010) Lead, manganese, and methylmercury as risk factors for neurobehavioral impairment in advanced age. *International Journal of Alzheimer's Disease* [online]. 2011 pp.607543.

Wu, S., Zhou, F., Zhang, Z. and Xing, D. (2011) Mitochondrial oxidative stress causes mitochondrial fragmentation via differential modulation of mitochondrial fission-fusion proteins. *The FEBS Journal* [online]. 278 (6), pp.941-954.

Yamada, K., Patel, T.K., Hochgrafe, K., Mahan, T.E., Jiang, H., Stewart, F.R., Mandelkow, E.M. and Holtzman, D.M. (2015) Analysis of in vivo turnover of tau in a mouse model of tauopathy. *Molecular Neurodegeneration* [online]. 10 pp.55-015-0052-5.

Yan, T., Zhao, Y. and Zhang, X. (2016) Acetaldehyde Induces Cytotoxicity of SH-SY5Y Cells via Inhibition of Akt Activation and Induction of Oxidative Stress. *Oxidative Medicine and Cellular Longevity* [online]. 2016 pp.10.1155/2016/4512309.

Yang, K.M., Lee, N.R., Woo, J.M., Choi, W., Zimmermann, M., Blank, L.M. and Park, J.B. (2012) Ethanol reduces mitochondrial membrane integrity and thereby impacts carbon metabolism of Saccharomyces cerevisiae. *FEMS Yeast Research* [online]. 12 (6), pp.675-684.

Yang, X., Wang, H., Huang, C., He, X., Xu, W., Luo, Y. and Huang, K. (2017) Zinc enhances the cellular energy supply to improve cell motility and restore impaired energetic metabolism in a toxic environment induced by OTA. *Scientific Reports* [online]. 7 (1), pp.14669-017-14868-x.

Yokoyama, M., Koh, J. and Choi, D. W. (1986) Brief exposure to zinc is toxic to cortical neurons. *Neuroscience Letters* [online]. 71(3), pp. 351-355.

Young, C., Klocke, B.J., Tenkova, T., Choi, J., Labruyere, J., Qin, Y.Q., Holtzman, D.M., Roth, K.A. and Olney, J.W. (2003) Ethanol-induced neuronal apoptosis in vivo requires BAX in the developing mouse brain. *Cell Death and Differentiation* [online]. 10 (10), pp.1148-1155.

Yu, Q. and Zhou, Y.Z. (2018) High level of Mn in brain is a risk for Alzheimer disease. *Sheng Li Xue Bao : [Acta Physiologica Sinica]* [online]. 70 (2), pp.193-200.

Yu, Q. and Zhou, Y.Z. (2018) High level of Mn in brain is a risk for Alzheimer disease. *Sheng Li Xue Bao : [Acta Physiologica Sinica]* [online]. 70 (2), pp.193-200.

Yuan, Y., Niu, F., Liu, Y. and Lu, N. (2014) Zinc and its effects on oxidative stress in Alzheimer's disease. *Neurological Sciences : Official Journal of the Italian Neurological Society and of the Italian Society of Clinical Neurophysiology* [online]. 35 (6), pp.923-928.

Zahr, N.M., Mayer, D., Vinco, S., Orduna, J., Luong, R., Sullivan, E.V. and Pfefferbaum, A. (2009) In vivo evidence for alcohol-induced neurochemical changes in rat brain without protracted withdrawal, pronounced thiamine deficiency, or severe liver damage. *Neuropsychopharmacology : Official Publication of the American College of Neuropsychopharmacology* [online]. 34 (6), pp.1427-1442.

Zakhari, S. (2013) Alcohol metabolism and epigenetics changes. *Alcohol Research : Current Reviews* [online]. 35 (1), pp.6-16.

Zakhari, S. (2006) Overview: how is alcohol metabolized by the body? *Alcohol Research & Health : The Journal of the National Institute on Alcohol Abuse and Alcoholism* [online]. 29 (4), pp.245-254.

Zamzami, N. and Kroemer, G. (2001) The mitochondrion in apoptosis: how Pandora's box opens. *Nature Reviews.Molecular Cell Biology* [online]. 2 (1), pp.67-71.

Zatta, P., Lucchini, R., van Rensburg, S.J. and Taylor, A. (2003) The role of metals in neurodegenerative processes: aluminum, manganese, and zinc. *Brain Research Bulletin* [online]. 62 (1), pp.15-28.

Zemirli, N., Morel, E. and Molino, D. (2018) Mitochondrial Dynamics in Basal and Stressful Conditions. *International Journal of Molecular Sciences* [online]. 19 (2), pp.10.3390/ijms19020564.

Zeng, T., Zhang, C., Song, F., Zhao, X., Yu, L., Zhu, Z. and Xie, K. (2012) PI3K/Akt pathway activation was involved in acute ethanol-induced fatty liver in mice. *Toxicology* [online]. 296(1), pp. 56-66.

Zhang, J., Cao, R., Cai, T., Aschner, M., Zhao, F., Yao, T., Chen, Y., Cao, Z., Luo, W. and Chen, J. (2013) The role of autophagy dysregulation in manganese-induced dopaminergic neurodegeneration. *Neurotoxicity Research* [online]. 24 (4), pp.478-490.

Zhang, J., Wang, X., Vikash, V., Ye, Q., Wu, D., Liu, Y. and Dong, W. (2016) ROS and ROS-Mediated Cellular Signaling. *Oxidative Medicine and Cellular Longevity* [online]. 2016 pp.4350965.

Zhang, L., Wang, L., Wang, R., Gao, Y., Che, H., Pan, Y. and Fu, P. (2017) Evaluating the Effectiveness of GTM-1, Rapamycin, and Carbamazepine on Autophagy and Alzheimer Disease. *Medical Science Monitor : International Medical Journal of Experimental and Clinical Research* [online]. 23 pp.801-808.

Zhao, Y., Hu, X., Liu, Y., Dong, S., Wen, Z., He, W., Zhang, S., Huang, Q. and Shi, M. (2017) ROS signaling under metabolic stress: cross-talk between AMPK and AKT pathway. *Molecular Cancer* [online]. 16 (1), pp.79-017-0648-1.

Zheng, W., Ren, S. and Graziano, J.H. (1998) Manganese inhibits mitochondrial aconitase: a mechanism of manganese neurotoxicity. *Brain Research* [online]. 799 (2), pp.334-342.

Zhong, W., Zhao, Y., Sun, X., Song, Z., McClain, C.J. and Zhou, Z. (2013) Dietary zinc deficiency exaggerates ethanol-induced liver injury in mice: involvement of intrahepatic and extrahepatic factors. *PloS One* [online]. 8 (10), pp.e76522.

Zhou, Q., Fu, X., Wang, X., Wu, Q., Lu, Y., Shi, J., Klaunig, J.E. and Zhou, S. (2018) Autophagy plays a protective role in Mn-induced toxicity in PC12 cells. *Toxicology* [online]. 394 pp.45-53.

Zhu, J.H., Guo, F., Shelburne, J., Watkins, S. and Chu, C.T. (2003) Localization of phosphorylated ERK/MAP kinases to mitochondria and autophagosomes in Lewy body diseases. *Brain Pathology (Zurich, Switzerland)* [online]. 13 (4), pp.473-481.

Zong, H., Ren, J.M., Young, L.H., Pypaert, M., Mu, J., Birnbaum, M.J. and Shulman, G.I. (2002) AMP kinase is required for mitochondrial biogenesis in skeletal muscle in response to chronic energy deprivation. *Proceedings of the National Academy of Sciences of the United States of America* [online]. 99 (25), pp.15983-15987.

Zuccala, G., Onder, G., Pedone, C., Cesari, M., Landi, F., Bernabei, R., Cocchi, A. and Gruppo Italiano di Farmacoepidemiologia nell'Anziano Investigators (2001) Dose-related impact of alcohol consumption on cognitive function in advanced age: results of a multicenter survey. *Alcoholism, Clinical and Experimental Research* [online]. 25 (12), pp.1743-1748.

APPENDIX

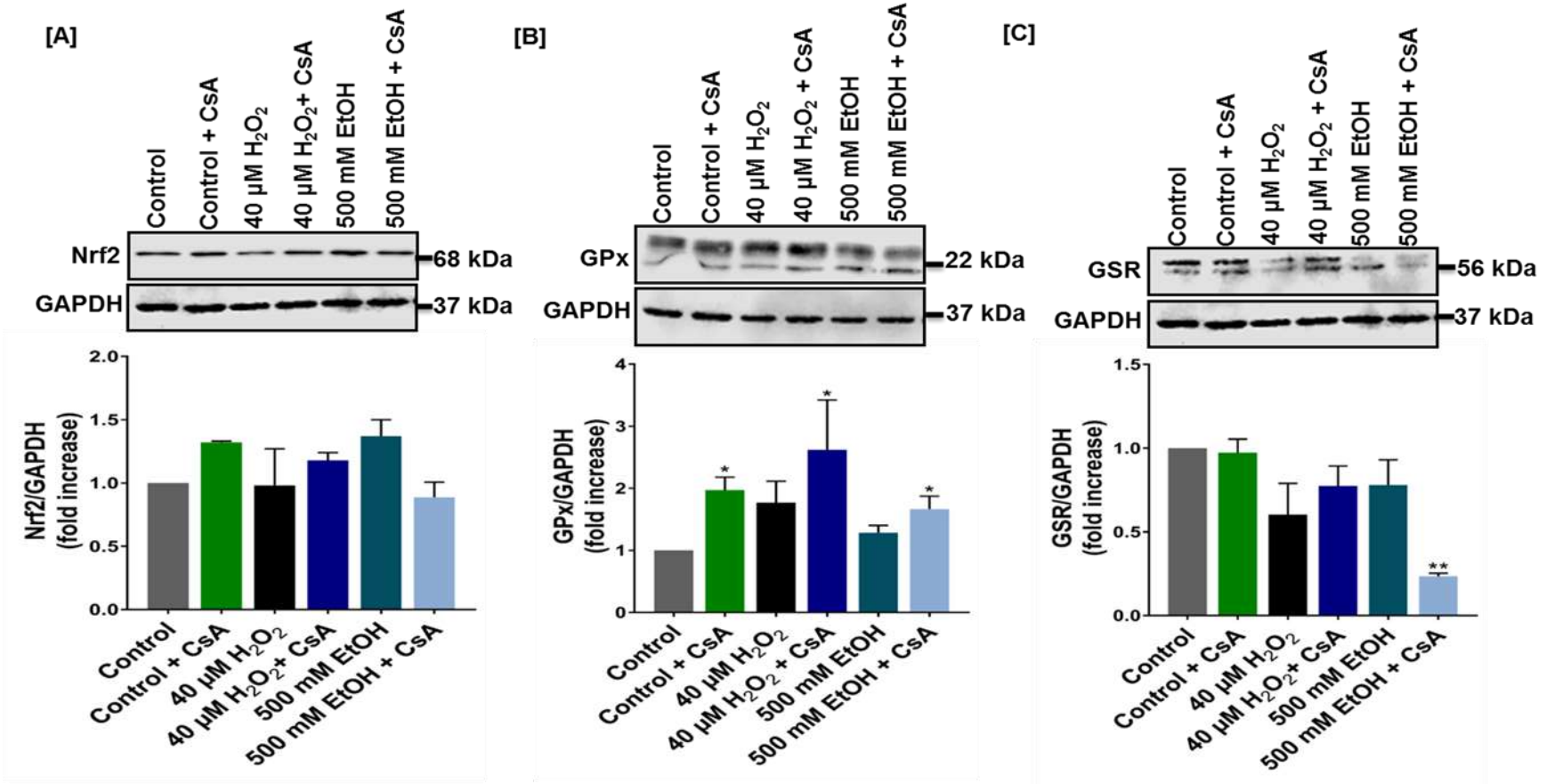

Differential protein expression of Nrf2, GSR and GPx in ethanol treated SH-SY5Y neuronal cells. Cells were treated as indicated relative to control cells for 24 h and Nrf2, GSR and GPx protein expression determined by Western blot analysis. Chemiluminescent blot of **Panel A:** Nrf2, **Panel B:** GPx**, Panel C**: GSR and their respective GAPDH expression. Normalized band intensity relative to GAPDH in standard culture cells**.** Data are expressed as mean ± SEM of 3 independent experiments (n=3). *p ≤ 0.05, **p ≤ 0.01, ***p ≤ 0.001.

Summary										
Image Gro	Score Nam	Score	Count							
Mitophagy	Colocalisa	2	0							
Mitophagy	Colocalisa	2.4	0							
Mitophagy	Colocalisa	2.5	3							
Mitophagy	Colocalisa	2.6	0							
All Results										
Image Gro	Colocalisa	File Name								
Mitophagy	2.5	F:\Grace export\Grace jan 2020\Grace 21.9.16_Control cells 21.9.18Snapshot2.jpg								
Mitophagy	2.5	F:\Grace export\Grace jan 2020\Grace 21.9.16_Control cells 21.9.18Snapshot4.jpg								
Mitophagy	2.5	F:\Grace export\Grace jan 2020\Grace 21.9.16_Control cells 21.9.18Snapshot3.jpg								
QC Results										
QC Images	3									
Image Gro	File Name	Duplicate S	Original Scores							
		Colocalisa	Colocalisation							
Mitophagy	F:\Grace e	2.5	2.5							
Mitophagy	F:\Grace e	2.5	2.5							
Mitophagy	F:\Grace e	2.5	2.5							

Summary									
Image Gro	Score Nam	Score	Count						
Ethanol tre	Colocalisa	2	0						
Ethanol tre	Colocalisa	2.4	0						
Ethanol tre	Colocalisa	2.5	3						
Ethanol tre	Colocalisa	2.6	0						
Mitophagy	Colocalisa	2	0						
Mitophagy	Colocalisa	2.4	0						
Mitophagy	Colocalisa	2.5	3						
Mitophagy	Colocalisa	2.6	0						
All Results									
Image Gro	Colocalisa	File Name							
Ethanol tre	2.5	F:\Grace export\Grace jan 2020\Grace 21.9.16_EtOH 21.9.18Snapshot4.jpg							
Ethanol tre	2.5	F:\Grace export\Grace jan 2020\Grace 21.9.16_EtOH 21.9.18Snapshot2.jpg							
Ethanol tre	2.5	F:\Grace export\Grace jan 2020\Grace 21.9.16_EtOH 21.9.18Snapshot3.jpg							
Mitophagy	2.5	F:\Grace export\Grace jan 2020\Grace 21.9.16_Control cells 21.9.18Snapshot3.jpg							
Mitophagy	2.5	F:\Grace export\Grace jan 2020\Grace 21.9.16_Control cells 21.9.18Snapshot4.jpg							
Mitophagy	2.5	F:\Grace export\Grace jan 2020\Grace 21.9.16_Control cells 21.9.18Snapshot2.jpg							
QC Results									
QC Images	6								
Image Gro	File Name	Duplicate S	Original Scores						
		Colocalisa	Colocalisation						
Ethanol tre	F:\Grace e	2.5	2.5						
Ethanol tre	F:\Grace e	2.5	2.5						
Ethanol tre	F:\Grace e	2.5	2.5						
Mitophagy	F:\Grace e	2.5	2.5						
Mitophagy	F:\Grace e	2.5	2.5						
Mitophagy	F:\Grace e	2.5	2.5						